SINGLE-CELL MOLECULAR CHARACTERIZATION FOR IMPROVING CANCER IMMUNOTHERAPY

EDITED BY: Qihui Shi, Wei Wei and Ziming Li

PUBLISHED IN: Frontiers in Immunology and Frontiers in Oncology

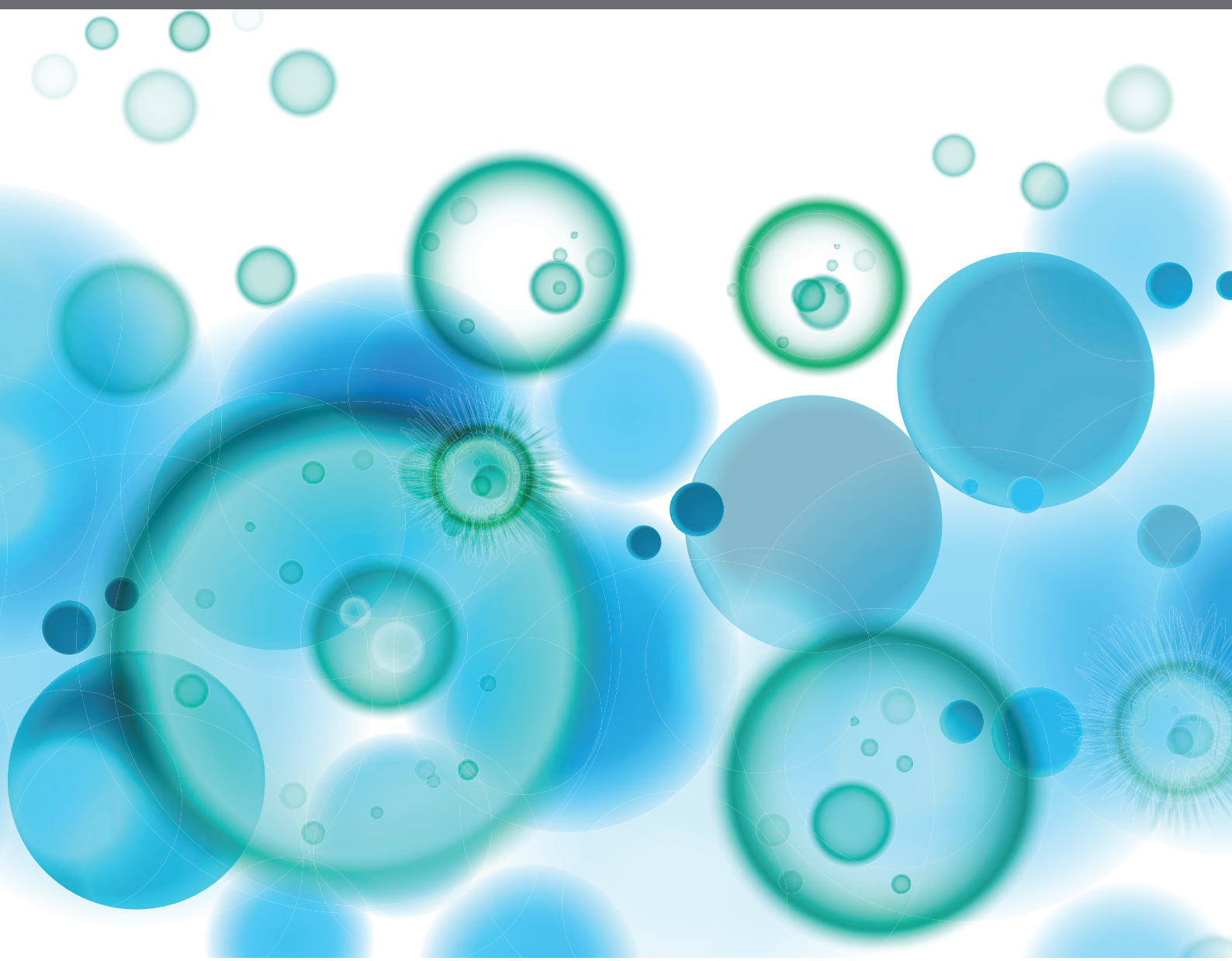

frontiers Research Topics

frontiers

ISSN 1664-8714
ISBN 978-2-88974-479-4
DOI 10.3389/978-2-88974-479-4

About Frontiers

Frontiers is more than just an open-access publisher of scholarly articles: it is a pioneering approach to the world of academia, radically improving the way scholarly research is managed. The grand vision of Frontiers is a world where all people have an equal opportunity to seek, share and generate knowledge. Frontiers provides immediate and permanent online open access to all its publications, but this alone is not enough to realize our grand goals.

Frontiers Journal Series

The Frontiers Journal Series is a multi-tier and interdisciplinary set of open-access, online journals, promising a paradigm shift from the current review, selection and dissemination processes in academic publishing. All Frontiers journals are driven by researchers for researchers; therefore, they constitute a service to the scholarly community. At the same time, the Frontiers Journal Series operates on a revolutionary invention, the tiered publishing system, initially addressing specific communities of scholars, and gradually climbing up to broader public understanding, thus serving the interests of the lay society, too.

Dedication to Quality

Each Frontiers article is a landmark of the highest quality, thanks to genuinely collaborative interactions between authors and review editors, who include some of the world's best academicians. Research must be certified by peers before entering a stream of knowledge that may eventually reach the public - and shape society; therefore, Frontiers only applies the most rigorous and unbiased reviews.
Frontiers revolutionizes research publishing by freely delivering the most outstanding research, evaluated with no bias from both the academic and social point of view. By applying the most advanced information technologies, Frontiers is catapulting scholarly publishing into a new generation.

What are Frontiers Research Topics?

Frontiers Research Topics are very popular trademarks of the Frontiers Journals Series: they are collections of at least ten articles, all centered on a particular subject. With their unique mix of varied contributions from Original Research to Review Articles, Frontiers Research Topics unify the most influential researchers, the latest key findings and historical advances in a hot research area! Find out more on how to host your own Frontiers Research Topic or contribute to one as an author by contacting the Frontiers Editorial Office: frontiersin.org/about/contact

SINGLE-CELL MOLECULAR CHARACTERIZATION FOR IMPROVING CANCER IMMUNOTHERAPY

Topic Editors:
Qihui Shi, Fudan University, China
Wei Wei, Institute for Systems Biology (ISB), United States
Ziming Li, Shanghai Jiaotong University, China

Topic Editor Qihui Shi is the scientific co-founder of JunHealth, a company aiming to developing single-cell sequencing technologies for clinical applications, and received research funding from BeiGene.

Citation: Shi, Q., Wei, W., Li, Z., eds. (2022). Single-cell Molecular Characterization for Improving Cancer Immunotherapy. Lausanne: Frontiers Media SA.
doi: 10.3389/978-2-88974-479-4

Table of Contents

frontiers in Immunology

ORIGINAL RESEARCH
published: 23 February 2021
doi: 10.3389/fimmu.2021.627072

Interferon Regulatory Factor 4 Regulates the Development of Polymorphonuclear Myeloid-Derived Suppressor Cells Through the Transcription of c-Myc in Cancer

Quan Yang[1,2†], Hongyan Xie[1†], Xing Li[3], Yuanfa Feng[1], Shihao Xie[1], Jiale Qu[1], Anqi Xie[1], Yiqiang Zhu[1], Lu Zhou[1], Jinxue Yang[1], Xiaohao Hu[1], Haixia Wei[1], Huaina Qiu[1], Wenjuan Qin[4*] and Jun Huang[1,2*]*

[1] The State Key Laboratory of Respiratory Disease, The First Affliated Hospital, Guangzhou Medical University, Guangzhou, China, [2] Sino-French Hoffmann Institute, Guangzhou Medical University, Guangzhou, China, [3] Department of Medical Oncology and Guangdong Key Laboratory of Liver Disease Research, The Third Affiliated Hospital, Sun Yat-Sen University, Guangzhou, China, [4] Department of Radiation Oncology, Zhongshan Hospital Affiliated, Xiamen University, Xiamen, China

The accumulation of myeloid-derived suppressor cells (MDSCs) is one of the major obstacles to achieve an appropriate anti-tumor immune response and successful tumor immunotherapy. MDSCs in tumor-bearing hosts are primarily polymorphonuclear (PMN-MDSCs). However, the mechanisms regulating the development of MDSCs remain poorly understood. In this report, we showed that interferon regulatory factor 4 (IRF4) plays a key role in the development of PMN-MDSCs, but not monocytic MDSCs. IRF4 deficiency caused a significant elevation of PMN-MDSCs and enhanced the suppressive activity of PMN-MDSCs, increasing tumor growth and metastasis in mice. Mechanistic studies showed that c-Myc was up-regulated by the IRF4 protein. Over-expression of c-Myc almost abrogated the effects of IRF4 deletion on PMN-MDSCs development. Importantly, the IRF4 expression level was negatively correlated with the PMN-MDSCs frequency and tumor development but positively correlated with c-Myc expression in clinical cancer patients. In summary, this study demonstrated that IRF4 represents a novel regulator of PMN-MDSCs development in cancer, which may have predictive value for tumor progression.

Keywords: interferon regulatory factor 4 (IRF4), myeloid-derived suppressor cells (MDSCs), c-Myc, immunosuppression, cancer

OPEN ACCESS

Edited by:
Wei Wei,
Institute for Systems Biology (ISB), United States

Reviewed by:
Jie Ma,
Jiangsu University, China
Xiaoyang Ye,
Institute for Systems Biology (ISB), United States

***Correspondence:**
Quan Yang
yquangy2015@gzhmu.edu.cn
Wenjuan Qin
proftomato@163.com
Jun Huang
hj165@sina.com

†These authors have contributed equally to this work

Specialty section:
This article was submitted to Cancer Immunity and Immunotherapy, a section of the journal Frontiers in Immunology

Received: *08 November 2020*
Accepted: *11 January 2021*
Published: *23 February 2021*

Citation:
Yang Q, Xie H, Li X, Feng Y, Xie S, Qu J, Xie A, Zhu Y, Zhou L, Yang J, Hu X, Wei H, Qiu H, Qin W and Huang J (2021) Interferon Regulatory Factor 4 Regulates the Development of Polymorphonuclear Myeloid-Derived Suppressor Cells Through the Transcription of c-Myc in Cancer. Front. Immunol. 12:627072. doi: 10.3389/fimmu.2021.627072

INTRODUCTION

The immunosuppressive state of individuals with tumors is a key factor in limiting the body's anti-tumor immune response. Immunosuppressive cells, including tumor-associated macrophages, marrow-derived suppressor cells, tumor-associated neutrophils, cancer-associated fibroblasts, and regulatory T cell interactions to actively promote tumorigenesis (1). Myeloid-derived suppressor cells (MDSCs) has well known roles in the suppression of anti-tumor immunity in tumor-bearing hosts (2, 3). Therefore, the key to anti-tumor immunotherapy is to design targeted therapy for the tumor immunosuppression mechanism, and targeting MDSCs has become a promising strategy for tumor immunotherapy (4, 5).

Mouse MDSCs, characterized by the co-expression of the myeloid markers CD11b and Gr1, are broadly classified into two distinct subsets, polymorphonuclear (PMN-MDSCs) and monocytic (M-MDSCs), based on the expression status of the Ly6G and Ly6C epitopes (6, 7). MDSCs are now defined as different subpopulations with specific phenotypes in human with clear immunosuppressive capacities, which have three subsets: M-MDSCs (HLA-DR$^-$CD11b$^+$CD33^{hi}), PMN-MDSCs (HLA-DR$^-$CD11b$^+$CD33^{low}), and e-MDSC (Lin$^-$HLA-DR$^-$CD33$^+$) (8, 9). These subsets differ with respect to their function, tissue distribution, and regulatory mechanism (8, 10, 11). Interestingly, most tumor-derived MDSCs are polymorphonuclear (12, 13). Although some important transcription factors and signaling pathways have been identified to regulate the differentiation of tumor-derived MDSCs (14–16), the concrete mechanisms remain to be fully elucidated.

IRF4, also known as LSIRF, ICSAT, Pip and Mum1, was first cloned independently as a member of the IRF gene family in 1996 (17). Under physiological conditions, IRF4 is a key regulator of the differentiation of lymphoid, myeloid and DC, including the differentiation of mature B cells into plasma cells (18). Recent studies have found that the abnormal expression of IRF4 is closely related to the occurrence of various malignant tumors (lymphoma, multiple myeloma, etc.) and autoimmune diseases (19, 20). Numerous studies suggest that IRF4 is an oncogene (21, 22), for instance, Weilemann et al. proposed that IRF4 is needed for the survival of anaplasia large cell lymphoma (21). Some studies also suggest that IRF4 is a tumor suppressor gene (23, 24). For example, Naresh et al. suggest that follicular lymphoma does not express or rarely expresses IRF4 (23). However, the function of IRF4 in tumor immunology is still poorly understood compared with the extensive studies on IRF4 in tumor biology (19). Recently, it has been reported that IRF4 can regulate differentiation in the myeloid system and DC cells (25, 26), the silencing of IRF4 could promote the development and function of MDSCs (27).

The c-Myc gene, a crucial member of the Myc gene family, is an adjustable gene, which could be regulated by a variety of substances. It regulates the transcription of thousands of genes required for a range of cellular processes, including proliferation, differentiation, and metabolism, which is closely related to the development of various tumors (28). In addition to the pivotal role in tumors, Myc is involved in physiological and pathological processes of many other immune diseases. Studies have confirmed that the expression of Myc family members in immune cells is strictly regulated during the development or activation of immune cells (29).

MATERIALS AND METHODS

Ethics Statement

This research was approved by the Ethics Review Board of Guangzhou Medical University; written informed consent was provided by the study participants. All experimental protocols using animals were approved by the Animal Care and Use Committee of Guangzhou Medical University. Animal experiments were performed in strict accordance with the regulations of the Administration of Affairs Concerning Experimental Animals, and all efforts were made to minimize suffering.

Mice and Cell Lines

IRF4 conditional (floxed) mutant mice (*IRF4$^{flox/flox}$*; Stock No. 009380) and *LysM-Cre* mice (B6N.129P2 (B6) Lyz2tm1(cre)Ifo/J; Stock No: 018956) were originally were purchased from the Jackson Laboratory (Bar Harbor, ME, USA) and maintained with a C57B/L6 background. All mice were housed in a specific pathogen-free facility. All cell lines, including B16-F10 (B16), 3T3, 293T, and 32D were purchased from American type culture collection (ATCC). Female C57BL/6 mice were purchased from the Animal Experimental Center of Sun Yat-Sen University (Guangzhou, China).

Generation of Interferon Regulatory Factor 4 KO Mice

IRF4 KO mice were generated as described previously (30). *LysM-Cre* mice were mated with *IRF4$^{flox/flox}$* mice, and cohorts were established by mating F1 *IRF4$^{flox/+}$*; *Cre$^+$* mice to littermate *IRF4$^{flox/+}$*; *Cre$^-$* mice. The mice were maintained under a 14-h light/10-h dark cycle at a constant temperature (22°C) with free access to food and water.

Reagents

The following reagents, including Concanavalin A (Con A), dimethyl sulfoxide and c-Myc inhibitor (10074-G5) were purchased from Sigma-Aldrich (St. Louis, MO). The recombinant mouse cytokines, including GM-CSF, IL-6, and IL-4 were obtained from Peprotech (Rocky Hill, NJ). The antibodies against IRF4, S100A9, c-Myc, and β-actin and HRP-conjugated secondary antibodies were purchased from Santa Cruz Biotechnology (Santa Cruz, CA). The following fluorescein-conjugated anti-mouse antibodies: Gr-1-PE-Cy7 (RB6-8C5), Gr-1-PE (RB6-8C5), Ly-6C-PerCP-Cyanine5.5 (HK1.4), CD11b-FITC (M1/70.15), CD11b-PE-Cy7 (M1/70.15), CD3e-FITC (145-2C11), CD4-PE (RM4-5),

Abbreviations: BM, bone marrow; CFSE, 5,6 carboxy fluorescein diacetate succinimidyl ester; ChIP, Chromatin immunoprecipitation assay; Con A, Concanavalin A; c-Myc, Cellular myelocytomatosis oncogene; HCC, Hepatocellular carcinoma; IRF, interferon regulatory factor; KO, knockout mice; LLC, Lewis lung carcinoma; M, monocytic; MDSCs, myeloid-derived suppressor cells; PMN, polymorphonuclear; PB, peripheral blood; SP, spleen; WT, wild-type C57BL/6 mice.

CD8a-PE-Cy5 (53-6.7), CD8a-PE-Cy7 (53-6.7), PD-L1–APC (MIH5), PD-L2–Brilliant Violet 421 (TY25), GM-CSF-PerCP-Cy5.5 (MP1-22E9), IL-1α–PE (ALF-161), IL-10–APC (JES5-16E3), and IL-6–APC (MP5-20F3) and the corresponding isotype antibodies as well as the anti-human antibodies CD33-PE (HIM3-4), CD11b-FITC (ICRF44), and HLA-DR-PE-Cy5 (L243) and their isotype control antibodies (QA16A12) were obtained from Biolegend (San Diego, CA). Fluorescein-conjugated anti-mouse antibody Ly-6G-PE (1A8) was purchased from BD Biosciences (San Jose, CA). Lipofectamine 2000, 5,6 carboxy fluorescein diacetate succinimidyl ester (CFSE) and the reagents for cell culture were purchased from Invitrogen (Carlsbad, CA). Mouse Ly6G microbeads were purchased from Miltenyi Biotec (Teterow, Germany).

Microarray Analysis

An aliquot of 0.1 μg of total RNA was used to synthesize double-stranded cDNA, then produce biotin-tagged cRNA using the MessageAmp™ Premier RNA Amplification Kit. The resulting bio-tagged cRNA were fragmented to strands of 35–200 bases in length according to the protocols from Affymetrix. Hybridization was performed at 45°Cwith rotation for 16 h (Affymetrix GeneChip Hybridization Oven 640). The GeneChip arrays were washed and then stained (streptavidin-phycoerythrin) on an Affymetrix Fluidics Station 450 followed by scanning on a GeneChip Scanner 3000. The hybridization data were analyzed using GeneChip Operating software (GCOS 1.4). The scanned images were first assessed by visual inspection then analyzed to generate raw data files saved as CEL files using the default setting of GCOS 1.4. An invariant set normalization procedure was performed to normalize the different arrays using DNA-chip analyzer.

Tumor Models and Analyses

To establish tumor growth models (31), B16-F10 tumor cells (1×10^5) were injected subcutaneously (s.c.) into the flanks of mice. The tumors were measured every 2–3 days with calipers, and the volumes were calculated as V = ½ (length [mm] × [width {mm}]^2). For tumor metastasis models (32), mice were injected intravenously with B16-F10 tumor cells (1×10^5). At 3–4 weeks post tumor injection, the lungs were inflated with formalin followed by nodule counts and hematoxylin/eosin (H&E) staining.

Myeloid-Derived Suppressor Cell Depletion

For PMN-MDSCs depletion (32, 33), anti-Ly6G antibodies (IA8; BD Biosciences) were injected (80 μg per injection) through the tail vein 3 days and 1 day before and 1 day after the injection of tumor cells. Depletion efficiency was evaluated by flow cytometry 3 weeks after the tumor injection. The anti-IgG antibody (BioLegend, San Diego, CA) was used as a control.

In Vitro Generation of Myeloid-Derived Suppressor Cell

To generate MDSCs, we followed previously described procedures (34). Mouse Bone marrow (BM) cells were obtained from the femurs and tibias of mice and cultured in 24-well plates in RPMI 1640 medium containing 10% FBS, 50 mM 2-mercaptoethanol, 10 ng/ml IL-6, and 20 ng/ml GM-CSF. After 5 days of culture, the level of MDSCs was analyzed by flow cytometry. For MDSCs cultured with supernatant from tumor cells or 3T3 cells: BM cells from naive mice were cultured with GM-CSF and IL-6 in the presence of 30% (vol/vol) 3T3 or B16-F10 tumor supernatants (TS), After 2 days of culture, IRF4 expression was evaluated by qRT-PCR or by WB.

Invasion Assay

Matrigel matrix solution (200 μg/ml, Matrigel™ Basement Membrane Matrix, BD Bioscience) was applied to each transwell (Falcon, Franklin Lakes, NJ, USA). B16 cells (5×10^4) were seeded on the upper chamber of the transwell, and the lower chamber was then filled with collagen matrix (5 μg/ml). Noninvading cells on top of the matrix were removed after 18 h, and invading cells on the lower surface of the Matrigel matrix were fixed with 4% PFA and stained with 0.2% crystal violet. The cells were counted using ImageJ software (version 1.46).

Cell Surface Staining

Cells were washed twice in sterile PBS (500 g, 8 min), and blocked in PBS containing 1% BSA for 30 min. Then, the cells were stained with conjugated antibodies that were specific for cell surface antigens for 30 min at 4°C in dark. These antigens included CD11b, Gr1, Ly6G, Ly6C, CD3e, CD4, CD8a, PD-L1, PD-L2, CD33, HLA-DR, CD14, and CD15. The stained cells were washed twice in in washing buffer (PBS containing 0.1% BSA), and re-suspended in 300ul washing buffer. Cells were analyzed by using flow cytometry (Beckman Coulter, Fullerton, CA), and the results were analyzed with use of the software CytoExpert 2.0 (Beckman Coulter). Isotype-matched cytokine controls were included in each staining protocol.

Cell Sorting

For sorting of the mouse PMN-MDSC cells, mouse splenocytes were stained with CD11b-PE-Cy7, Ly-6G-PE, and Ly-6C-PerCP-Cyanine5.5 antibodies by cell surface staining as described before, and $CD11b^+Ly6G^+Ly6C^{-/low}$ cells were isolated by cell sorting on a FACS Aria cell sorter (BD, Mountain View, CA). For sorting of the human PMN-MDSC cells, peripheral blood mononuclear cells were stained with CD33-PE, CD11b-FITC, and HLA-DR-PE-Cy5, and $HLA\text{-}DR^-CD11b^+CD33^{low}$ cells were isolated by cell sorting on a FACS Aria cell sorter (BD, Mountain View, CA). The purified cells were identified by FACS, the purification of sorted cells was above 90%.

Cell Intracellular Cytokine and Molecule Staining

Single-cell suspensions from the spleens of WT and IRF4 KO tumor bearing mice were stimulated with 20 ng/ml phorbol 12-myristate 13-acetate (PMA) plus 1 μg/ml ionomycin for 5 h at 37°C under a 5% CO2 atmosphere. Brefeldin A (10 g/ml, Sigma, Shanghai, China) was added during the last 4 h of incubation. Cells were washed twice in PBS, fixed with 4% paraformaldehyde, and permeabilized overnight at 4°C in PBS buffer containing 0.1% saponin (Sigma), 0.1% BSA, and 0.05% NaN3. Cells were then stained for 30 min at 4°C in the dark with conjugated antibodies

specific for the cell surface antigens CD11b, and Gr1 as well as the intracellular cytokines or proteins GM-CSF, IL-10, IL-1α, and IL-6. The expression phenotypes of the antibody-labeled lymphocytes were analyzed by flow cytometry (Beckman Coulter, Fullerton, CA), and the results were analyzed with the software CytoExpert 2.0 (Beckman Coulter). Isotype-matched cytokine controls were included in each staining protocol.

Lentivirus Transduction

The lentiviral stock preparation and viral transduction were performed as previously described (35). HEK 293T cells were transfected with lentiviral vectors and packaging plasmids (pCMV-ΔR8.2, pMD.G) using Lipofectamine 2000. The culture supernatants were collected, concentrated and stored at -80°C. BM cells were infected with a 30% volume of concentrated lentiviral stock solution (the virus titer was 2×10^8 TU/ml) with 8 μg/ml polybrene. The medium was replaced with fresh medium at 3 h postinfection. The efficiency of infection was about 70%.

Quantitative RT-PCR

The total RNA was extracted with an RNase Minikit, and cDNA was synthesized with SuperScript III reverse transcriptase (Qiagen, Valencia, CA). PCR was performed in triplicate using SYBR Green Mastermix (TaKaRa, Otsu, Japan) and was normalized to endogenous β-actin. The primer sequences used are listed in **Supplemental Table 1**.

Western Blotting

Cultured or purified cells were collected and lysed. The protein concentration was measured with a bicinchoninic acid protein assay kit (Beyotime). The protein sample was separated in 10% SDS-denatured polyacrylamide gel and transferred to a polyvinylidene difluoride membrane. The polyvinylidene difluoride membranes were blocked with 5% skim milk in TBST at room temperature for 2 h. The targeted molecules were probed using specifc primary Abs and HRP-conjugated secondary Abs and were detected with an ECL HRP chemiluminescent substrate reagent kit (Invitrogen, Carlsbad, CA).

Chromatin Immunoprecipitation Assay

The ChIP assay was performed following the instructions from Millipore (Billerica, MA, USA). In brief, cultured BM cells were fixed with a 1% formaldehyde solution, lysed and sheared by sonication. The cell lysates were precleared with protein-G-agarose and immunoprecipitated with specific antibodies or the anti-IgG control. The antibody-chromatin complexes were collected with protein-G-agarose. The DNA in the complex was recovered and quantitated with qPCR. As an input control, 10% of the lysate was used before immunoprecipitation. The amplification of cyclophilin from the input was used as a loading control.

T-Cell Proliferation Assay

To quantify T-cell proliferation, we followed previously described procedures (35). Briefly, T-cell proliferation was determined by CFSE dilution. $CD3^+$ T cells from BALB/c mice was Purified by flow cytometric sorting, and labeled with CFSE (1 μM) (Invitrogen), stimulated with concanavalin A (5 μg/ml) and cultured alone or co-cultured with allogeneic MDSCs (from WT or IRF4 KO mice) at different ratios for 3 days. The cells were then stained with CD4-PE or CD8-PE-Cy5 antibodies, and T-cell proliferation was analyzed by flow cytometry.

Plasmid Constructs and Transfection Assays

The 5'-regulatory sequence of the mouse c-Myc gene was amplified by PCR using the primers listed in **Supplemental Table 1**. The wild type or mutated c-Myc promoter fragments were cloned into a pGL3-Basic vector (Promega), and the recombinations were confirmed by DNA sequencing. Transient transfections of the reporter plasmid were performed on 32D cells using Lipofectamine 2000 following the manufacturer's instructions. The luciferase activity was measured at 48 h post transfection.

Patients

Hepatocellular carcinoma (HCC) patients (n=20), individuals with hepatic fibrosis (n=20), were recruited at the Third Affiliated Hospital of Sun Yat-sen University (Guangzhou, China). Patients who had recently been pyrexial, had clinical evidence of an active infection, had previous or secondary cancers, or had received corticosteroids or nonsteroidal anti-inflammatory drugs were excluded from the study. The basic characteristics of patients are outlined in **Supplemental Table II**.

Statistics

The data were analyzed using Mann-Whitney tests, χ^2 tests, or Student's t tests as appropriate. The correlations between different parameters were analyzed using a Spearman rank test. Statistical tests were performed using Graph Pad Prism version 5.0a and SPSS Statistics 17.0. P-values of less than 0.05 were considered significant.

RESULTS

Decreased Interferon Regulatory Factor 4 Expression in Tumor-Deriving Myeloid-Derived Suppressor Cells

To determine the potential regulatory mechanism of MDSCs in tumor, a melanoma B16-F10 (B16) was used to establish a tumor mouse model. Gene chips were analyzed and screened by using MDSCs (T-MDSCs) sorted from tumor-bearing mouse spleens with immature myeloid cells from normal mouse spleens (N-MDSCs) as a control. We found that the expression of interferon regulatory factor 4 (IRF4) in the MDSCs of the tumor group was significantly down-regulated (**Figure 1A**). This result was validated by qRT-PCR ($P<0.05$, **Figure 1B**). The western blot (WB) further confirmed that expression of IRF4 in T-MDSCs was clearly down-regulated compared with N-MDSCs (**Figure 1C**). A lower expression of IRF4 was found in $CD11b^+Gr1^+$cells (MDSC) compared with $CD11b^+Gr1^-$ cells (no-MDSC) in the

spleen of tumor-bearing mice (**Figure 1D**). *In vitro* cell culture showed that the expression of IRF4 in MDSCs induced by the supernatant of cultured tumor cells was significantly decreased compared with the MDSCs induced by the supernatant of cultured 3T3 cells ($P<0.05$, **Figures 1E, F**). These data demonstrated that lower level of IRF4 was expressed in the tumor-induced MDSCs. This finding suggested that IRF4 may be a key transcription factor regulating MDSCs differentiation and accumulation in tumor development.

Interferon Regulatory Factor 4 Deficiency Could Facilitate Tumor Growth and Metastasis

To investigate whether the IRF4 gene can affect tumor progression in mice, a tumor growth models and tumor metastasis models were established in mouse. 6–8 weeks old *IRF4*$^{flox/flox}$*/LysM-Cre*$^{+}$ (IRF4 KO) female mice were selected for experiments, *IRF4*$^{flox/flox}$*/LysM-Cre*$^{-}$ female mice (WT) of the same age as a control. To detect tumor metastasis, B16 cells were injected into the WT and IRF4 KO mice *via* the tail vein, and the status of the tumor metastasis was determined 3 weeks later. The number of lung tumor metastasized mice increased significantly compared with WT mice ($P<0.05$, **Figure 2A**). Moreover, the appearance of lung was imaged (**Figure 2D**), and the slice of lung tissues was stained by H&E staining and observed under microscope (**Figure 2E**). Result showed that the number of lung metastasis nodules in the mouse and the area of lung metastasis nodules in IRF4-deficient mice were significantly increased relative to the control ($P<0.05$, **Figures 2B, C**). These results indicated that absence of IRF4 could significantly promote lung tumor metastasis.

In addition, to detect the role of IRF4 in tumor growth, B16 tumor cells were injected into the WT and IRF4 KO mice subcutaneously. The diameter of tumor was recorded, and the

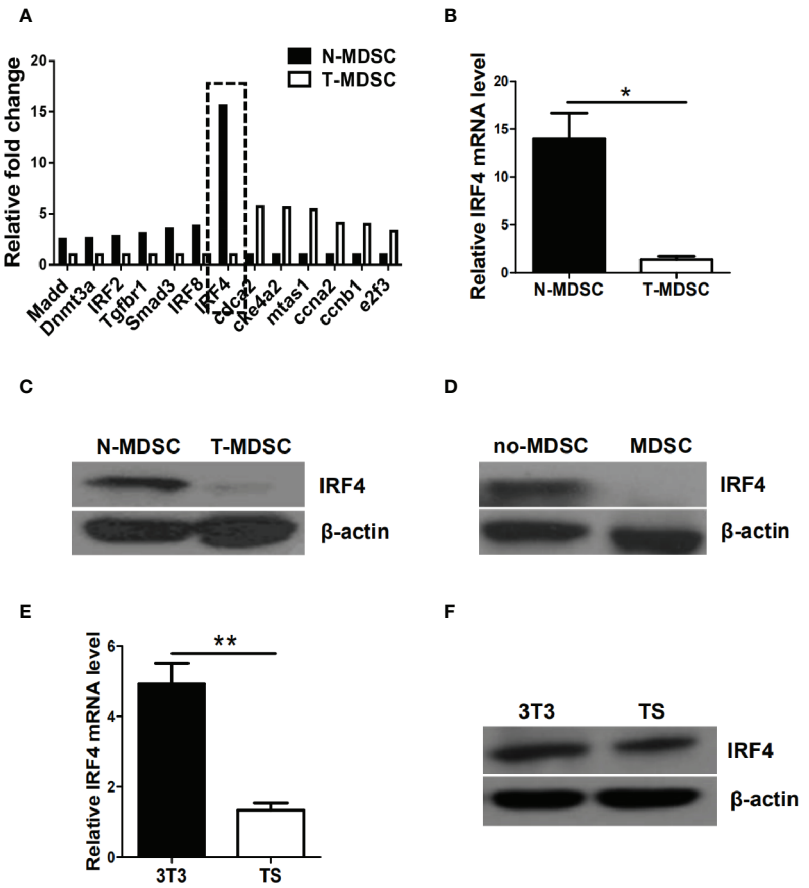

FIGURE 1 | Interferon regulatory factor 4 (IRF4) expression decreases in tumor-derived MDSCs. **(A)** Microarray analysis showing differentially expressed genes in splenic myeloid-derived suppressor cells (MDSCs) from tumor-bearing mice was injected with B16-F10 cells *via* the subcutaneously (T-MDSC) and the corresponding control cells from naive mice (N-MDSC). **(B)** Interferon regulatory factor 4 (IRF4) was evaluated by qRT-PCR with additional samples. **(C)** IRF4 expression in splenic MDSCs from tumor-bearing mice and control cells from naive mice was determined by a western blot (WB). **(D)** IRF4 expression in splenic CD11b^{+}Gr1^{+}cells and CD11b^{+}Gr1^{-}cells from tumor-bearing mice was determined by WB. **(E, F)** Bone marrow (BM) cells from naive mice were cultured with GM-CSF and IL-6 in the presence of 30% (vol/vol) 3T3 or B16-F10 tumor supernatants (TS); IRF4 expression was evaluated by qRT-PCR (e) and WB (f). **(B, E)** Data are shown as the mean ± SEM of six samples from three independent experiments. *$P < 0.05$, ** $P < 0.01$ compared with the corresponding controls in unpaired t tests.

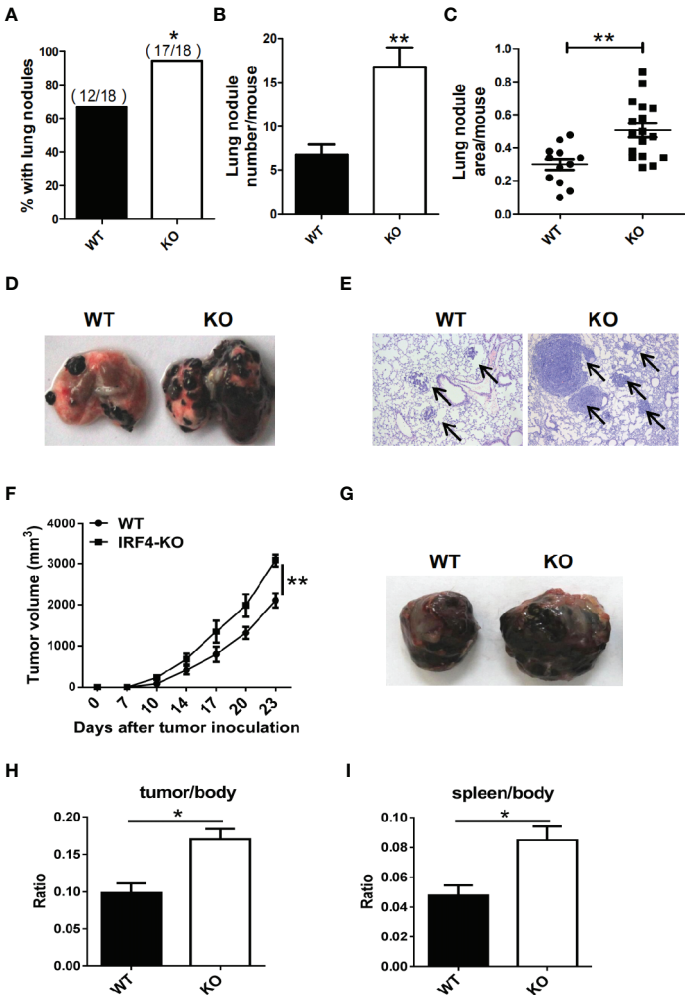

FIGURE 2 | Interferon regulatory factor 4 (IRF4) deficiency in the host facilitates tumor development. **(A–E)** WT (n=18) or IRF4 KO (n=18) mice were injected with B16-F10 cells *via* the tail vein; mice were sacrificed after 3 weeks. **(A)** Percentage of mice with lung nodules; $^*P < 0.05$, χ^2 test. **(B)** The number of lung nodules per mouse; $^*P < 0.05$, Student's *t* test. **(C)** Lung nodule area per mouse using NIH ImageJ; ***p < 0.001, Mann-Whitney test. **(D)** Representative images of lungs. **(E)** Representative images of lung H&E staining; arrows indicate metastases. **(F–I)** Tumor growth model; mice were subcutaneously injected with 1×10^5 B16-F10 tumor cells (n=6). Primary tumor growth was monitored **(F)**; $^*P < 0.05$, Mann-Whitney test. Representative images of tumor **(G)**. The ratio of tumor **(H)** or spleen **(I)** weight to mouse body weight; $^*P < 0.05$, Student's *t* test.

mean volume of tumor was calculated from day 7 to day 23, with 3–4 days interval. The results showed that the volume of tumor in the skin of IRF4 KO was bigger than that in the WT mice on day 17, day 20, and day 23 ($P<0.05$, **Figure 2F**). Furthermore, 3 weeks after B16 injection, the spleens and tumors tissue (**Figure 2G**) were picked out from mice, and weighed. The body weight of WT and IRF4 KO mice were also detected. The ratio of tumor-to-body weight and spleen-to-body weight were calculated, respectively. The results showed that the weight ratios of tumor/body and spleen/body were significantly increased in the IRF4 KO mice ($P<0.05$, **Figures 2H, I**). These results suggested that a deficiency of IRF4 in tumor-bearing mice not only promote lung tumor metastasis, but also promote tumor growth significantly.

Interferon Regulatory Factor 4 Inhibits the Effect of Primarily Polymorphonuclear-Myeloid-Derived Suppressor Cells on Tumor Growth and Metastasis

To detect the effect of PMN-MDSC on tumor growth and metastasis, B16 cells were injected to both WT and IRF4 KO mice from the vain of tail (tumor metastasis model) or subcutaneously (tumor growth models), respectively. Three weeks later, bone marrow (BM), spleen (SP), lung, peripheral blood (PB), and tumor tissue were picked out from B16-bearing WT and IRF4 KO mice. Mononuclear cells were isolated, respectively. The percentage of MDSCs ($CD11b^+$ $Gr1^+$) was analyzed by FACS. Results showed that the proportion and absolute number of MDSCs in samples from the IRF4 KO mice were significantly

increased in both the tumor metastasis models ($P<0.05$, **Figures 3A, B**) and tumor growth models ($P<0.05$, **Figures 3C, D**).

Moreover, the subsets of MDSCs in KO tumor-bearing WT and IRF4 mice were also explored by FACS. As showed in **Figure 3E**, the percentage of $CD11b^{+}Ly6G^{+}Ly6C^{-/low}$ PMN-MDSCs in the bone marrow and spleen of IRF4 KO tumor-bearing mice were increased significantly ($P<0.01$), whereas there was no significant change in the percentage of $CD11b^{+}Ly6G^{-}Ly6C^{high}$ M-MDSCs ($P>0.05$). These findings suggested that IRF4 deletion can specifically result in the accumulation of PMN-MDSCs in the bone marrow and spleen of tumor mice.

To determine whether tumor progression was mediated by PMN-MDSCs mice, B16 cells were injected to both WT and IRF4 KO mice through the vain of tail or subcutaneously. Anti-Ly6G antibodies were injected into mice through the tail vein 3 days and 1 day before and 1 day after the injection of B16 cells as described in materials and methods. Three weeks later, the radio of the tumor weight to the body weight was calculated, and the number of lung nodule was counted. The results showed that anti-Ly6G antibodies could decrease the value of these two detections in both WT and IRF4 KO mice ($P<0.05$, **Figures 3F–H**). More interesting is that the elimination of PMN-MDSCs can clearly reverse tumor growth (**Figure 3F**) and lung tumor metastasis (**Figures 3G, H**) in IRF4 KO mice. These data indicated that IRF4 mediates the effect of PMN-MDSCs on tumor growth and metastasis.

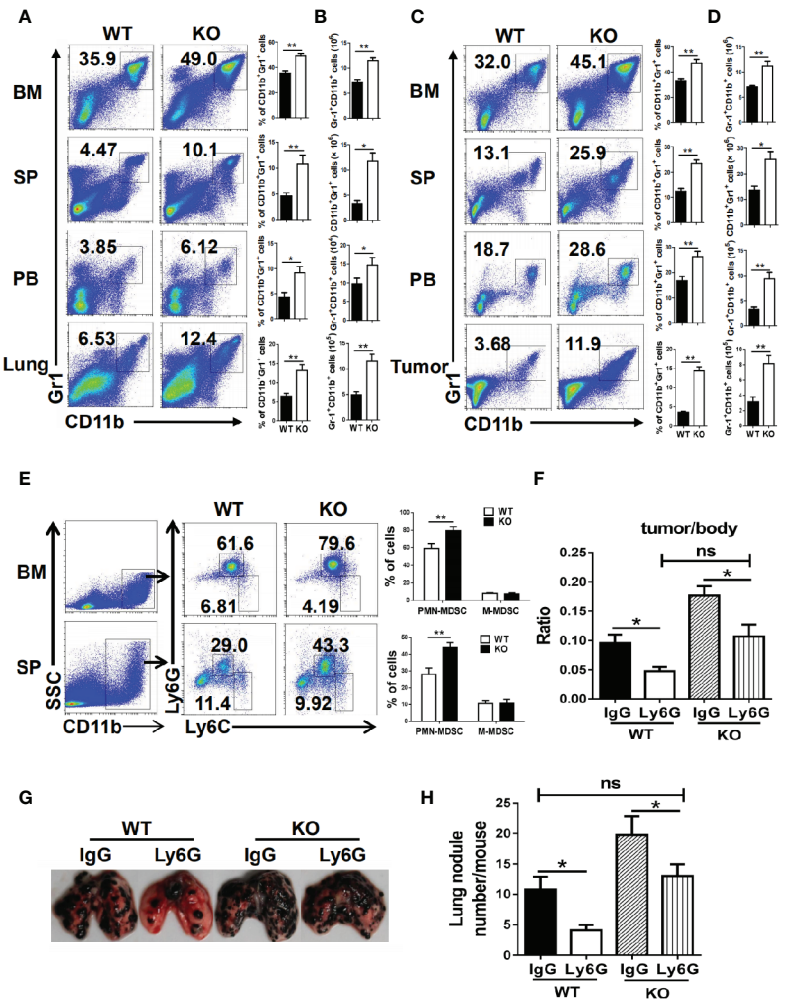

FIGURE 3 | Interferon regulatory factor 4 (IRF4) deficiency causes polymorphonuclear myeloid-derived suppressor cells (PMN-MDSCs) elevation in tumor-bearing mice. **(A–D)** B16-F10 tumor cells were injected into WT or KO mice (n=6) *via* the tail veil to establish tumor metastasis **(A, B)** or tumor-growth **(C, D)** models. Mice were sacrificed after 3 weeks. The percentages **(A, C)** and absolute numbers **(B, D)** of MDSCs were analyzed by flow cytometry; $^{*}P < 0.05$, $^{**}P < 0.01$, Student's t test. **(E)** The proportions of the MDSCs subtypes in the bone marrow (BM) and spleens from tumor-growth models were evaluated by flow cytometry. Each group included six mice; representative results (left) and the graphical representation (right) are shown; $^{**}P < 0.01$, Student's *t* test. **(F–H)** Mice (n=5) were injected intravenously with anti-Ly6G antibodies or an anti-IgG control before and after B16 tumor cell injection. **(F)** The ratio of tumor weight to mouse body weight; $^{*}P < 0.05$, Student's *t* test. **(G, H)** Lung transfer was evaluated 3 weeks after tumor injection. **(G)** Representative images of lung tissue. **(H)** The number of lung nodules per mouse; $^{**}P < 0.01$, Student's *t* test.

Interferon Regulatory Factor 4 Deficiency Enhance the Immunosuppressive Function of Primarily Polymorphonuclear-Myeloid-Derived Suppressor Cells

MDSCs are characterized by their immunosuppressive function, and we next investigated whether an IRF4 deficiency could influence the function of PMN-MDSCs. The splenic PMN-MDSCs from tumor-bearing WT and IRF4 KO mice were sorted by flow cytometry and mixed with T lymphocytes derived from allogeneic mice in different ratios (stimulated by ConA and labeled with CFSE). Three days later, the proliferation of T cells was detected by FACs. The results showed that PMN-MDSCs from the IRF4 KO group had a stronger ability to inhibit T cell proliferation than WT-derived PMN-MDSCs ($P<0.05$, **Figure 4A**). Simultaneously, a

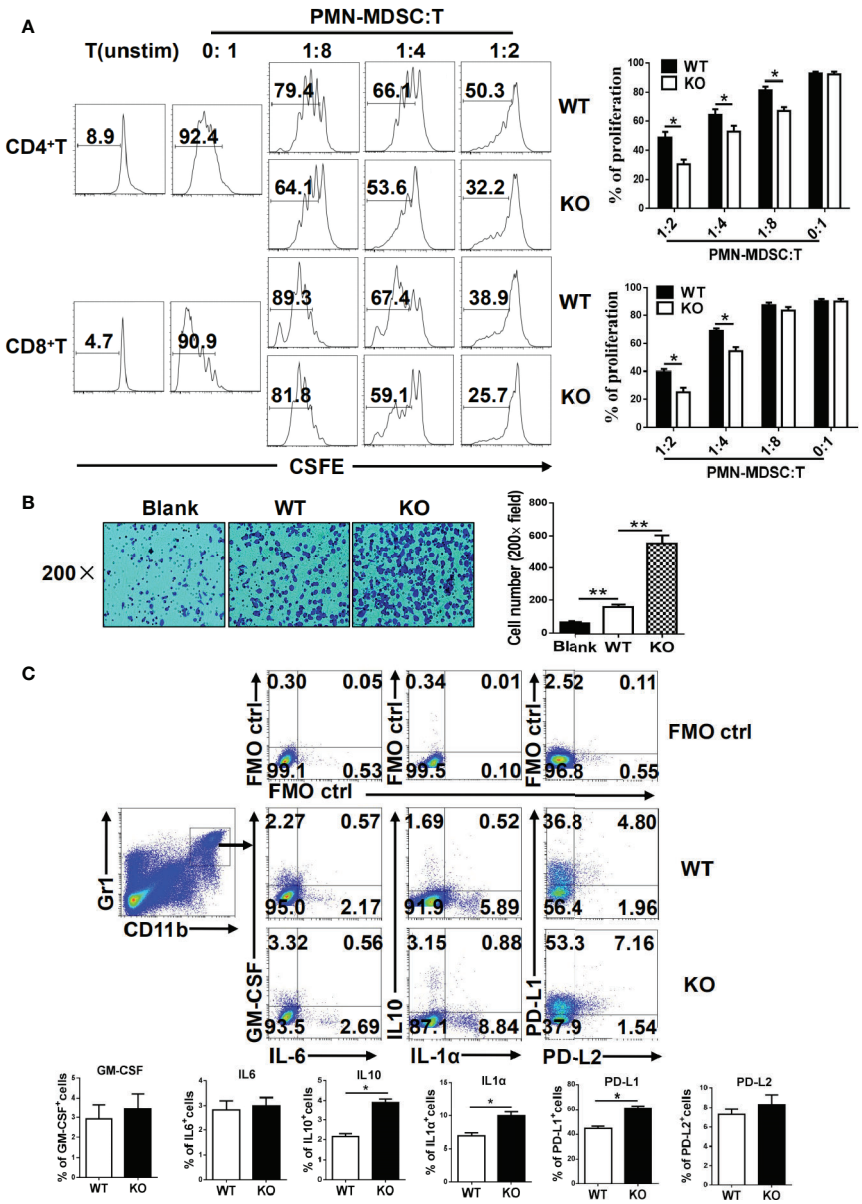

FIGURE 4 | Functional analysis of myeloid-derived suppressor cells (MDSCs). **(A)** Allogeneic mixed lymphocytes reaction. Allogeneic $CD3^+$ T cells were stimulated with concanavalin A (ConA) and then cocultured with splenic G-MDSCs that were purified with Ly6G beads from the spleen of tumor-bearing mice at different ratios for 3 days. T-cell proliferation was evaluated by CFSE dilution; unstimulated T cells were used as a negative control. Representative data from single experiment (left) and mean ± SEM from three independent experiments (right) are shown. **(B)** B16 cells were cocultured with polymorphonuclear (PMN)-MDSCs, and a cell invasion assay was performed with Matrigel (crystal violet). Left, representative from a single experiment; right, mean ± SEMs from three independent experiments, $^*P < 0.05$, $^{**}P < 0.01$, unpaired *t* test. **(C)** Single-cell suspensions of spleen cells from WT and IRF4 KO tumor-bearing mice were stimulated with PMA and ionomycin. The expression of PD-L1, PD-L2, GM-CSF, IL-1a, IL-6, and IL-10 were detected in MDSCs by FACS. Numbers in the quadrants are the percentages of cells in each expression phenotype (n = 5 mice per group). A representative of two independent experiments is shown.

difference in tumor metastasis was detected in WT and IRF4 KO tumor-bearing mice. In the tumor invasion experiment, B16 tumor cells were co-cultured with PMN-MDSCs derived from the spleens of both WT and IRF4 KO mice for 18 h. The results demonstrated that the PMN-MDSCs derived from IRF4 KO mice possessed a greater ability to promote tumor invasion compared with those from the WT group ($P < 0.01$, **Figure 4B**). The ability of MDSCs in producing inflammatory factors, including IL-1a, IL-6, IL-10, and GM-CSF, and the expression of PD-L1 and PD-L2 (programmed cell death 1 ligand 1/2) were detected by flow cytometry. As showed in **Figure 4C**, the significantly higher levels of IL-1a and IL-10 producing MDSCs were found in IRF4 KO mice ($P<0.05$) compared with the WT mice, whereas there was no clear difference in GM-CSF and IL-6 production ($P>0.05$). Additionally, the expression of PD-L1 on MDSCs derived from IRF4 KO mice was significantly higher than that from WT mice. There was also no difference between the groups in the expression of PD-L2 on MDSCs, (P>0.05, **Figure 4C**). These results revealed that an IRF4 deficiency could

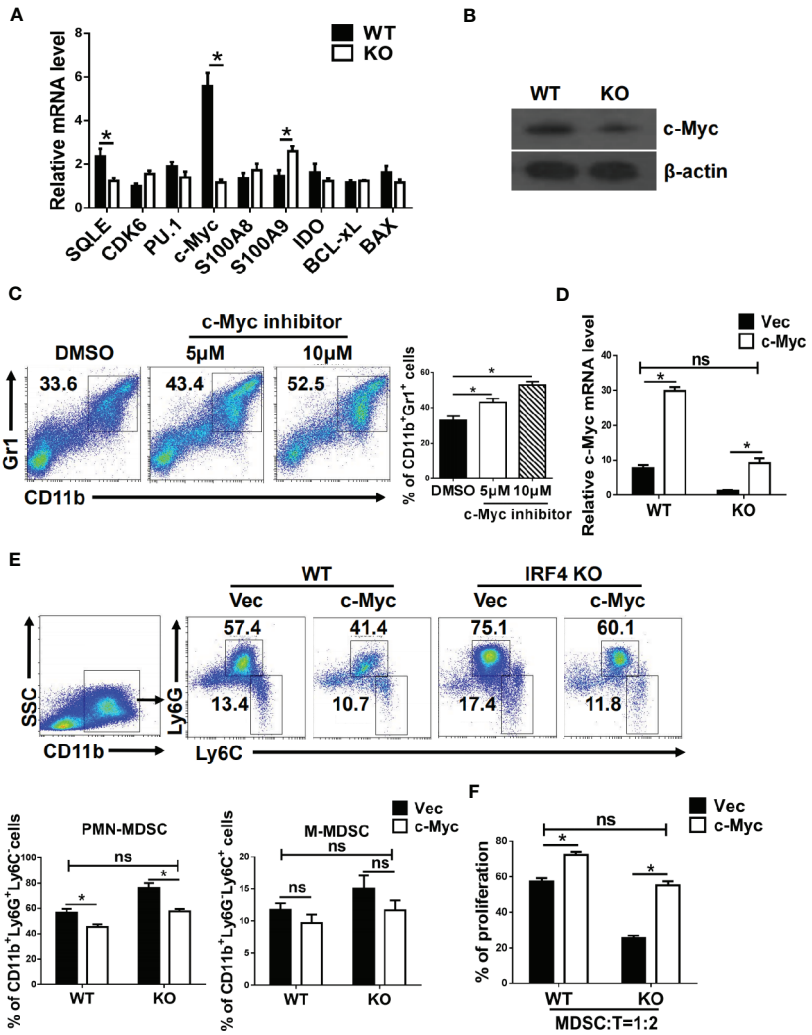

FIGURE 5 | c-Myc mediates the effects of interferon regulatory factor 4 (IRF4) on myeloid-derived suppressor cells (MDSCs) development. **(A, B)** Gene expression in sorted MDSCs was determined by quantitative RT-PCR (qRT-PCR) **(A)** and western blot **(B)**. **(C)** Mouse bone marrow (BM) cells from normal mice were cultured in medium containing GM-CSF and IL-6 with the different concentrations of c-Myc inhibitor (10074-G5). The proportions of the indicated populations were determined by flow cytometry after 5 days of culture. **(D–F)** BM cells from WT or KO mice were infected with lentivirus expressing c-Myc or an empty vector. **(D)** The c-Myc gene expression was determined by qRT-PCR after 48 h of culture. **(E)** The proportions of indicated populations were determined by flow cytometry after 5 days of culture. **(F)** MDSCs were purified by flow cytometric sorting. Allogeneic $CD3^+$ T cells (from BALB/c mice) were stimulated with Con A and then co-cultured with isolated PMN-MDSCs at 2:1 ratios for 3 days. T cell proliferation was evaluated by 5,6 carboxy fluorescein diacetate succinimidyl ester (CFSE) dilution. A comparison of the suppressive activity on $CD3^+$ T cells between MDSCs from WT or KO mice were infected with lentivirus expressing c-Myc or an empty vector. **(A, D, F)** Data are shown as the mean ± SEMs from three independent experiments. *$P < 0.05$, compared with the corresponding controls; unpaired t tests were used. **(C, E)** Representative results (left) and mean ± SEMs from 3 independent experiments; *$P < 0.05$, unpaired *t* tests.

enhance the immunosuppressive function of PMN-MDSCs in both tumor growth and tumor invasion, and enhance the ability of MDSCs to produce inflammatory factors.

c-Myc Mediate the Effects of Interferon Regulatory Factor 4 on Myeloid-Derived Suppressor Cell Development

To explore the mechanism by which IRF4 regulates PMN-MDSCs differentiation and tumor metastasis, the potential target genes of IRF4 in MDSCs and the genes related to the differentiation and survival of MDSCs were detected by gene expression. As showed in **Figure 5A**, the gene expression and protein expression levels of c-Myc in MDSCs derived from IRF4 KO mice were significantly down-regulated compared with the MDSCs derived from WT mice ($P<0.05$). Next, the expression of c-Myc protein in MDSCs was detected by the method of western blotting. Results showed that the expression of c-Myc protein in MDSCs derived from IRF4 KO mice was decreased significantly ($P<0.05$, **Figure 5B**). Moreover, different concentrations of c-Myc inhibitors were added to the cultured MDSCs *in vitro* to confirm the effects of c-Myc on the differentiation of MDSCs. The results indicated that c-Myc inhibitors increased the proportion of MDSCs in a concentration-dependent manner (**Figure 5C**). Additionally, a lentivirus containing a c-Myc over-expression plasmid was added to cultured bone marrow cells from both WT and IRF4 KO mice to induce MDSCs *in vitro* for 5 days. As showed in **Figures 5D–F**, results indicated that c-Myc over-expression in bone marrow cells (**Figure 5D**) and decreased percentage of MDSCs induced by IRF4 deletion could be produced by over-expression of c-Myc (**Figure 5D**). Furthermore, c-Myc over-expression significantly increased the suppressive activity of MDSCs derived from IRF4-deficient cells (**Figure 5F**). These results suggested that c-Myc may mediate the effects of IRF4 on MDSCs development and function.

c-Myc is a Transcriptional Target of Interferon Regulatory Factor 4 in Myeloid-Derived Suppressor Cells

The mechanism of c-Myc regulation by IRF4 in MDSCs was further investigated in the tumor microenvironment. First, a potential IRF4 binding site was identified in the regulatory region of c-Myc (near the region from −4,183 to −4,291 bp upstream of the transcription start site) after screening (**Figure 6A**). The chromatin immunoprecipitation experiments confirmed that the IRF4 protein can bind to these two sites (**Figure 6B**). Further experiments demonstrated that the over expression of IRF4 in the 32D myeloid cell line promoted the activity of c-Myc ($P<0.05$), but this effect disappeared when the potential binding site of IRF4 was deleted (**Figure 6C**). These results demonstrated that IRF4 regulates the expression of c-Myc at the level of transcription.

Clinical Significance of Interferon Regulatory Factor 4 Regulated Primarily Polymorphonuclear-Myeloid-Derived Suppressor Cells Development

To explore the clinical significance of IRF4-mediated differentiation of PMN-MDSCs, peripheral blood samples from patients with liver cancer (HCC) were collected, and peripheral blood samples from

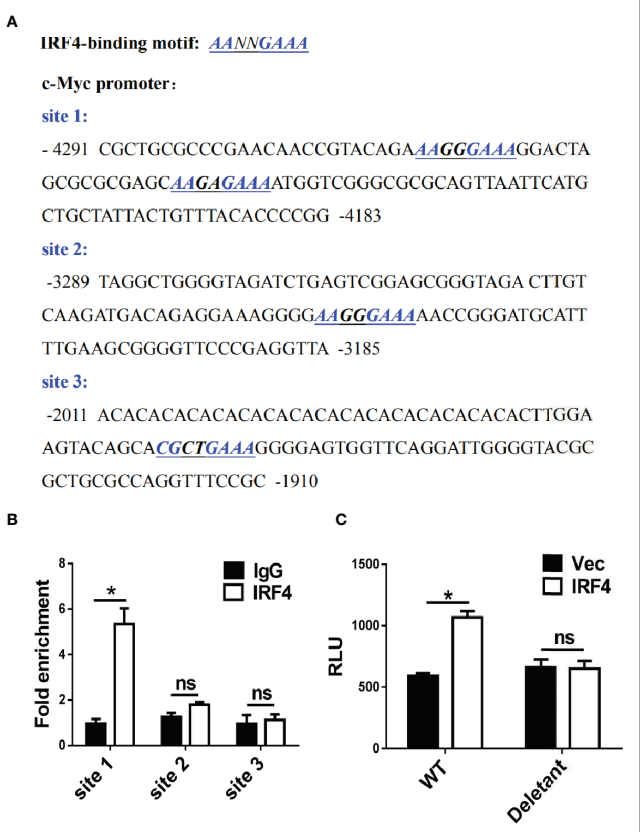

FIGURE 6 | c-Myc is a transcriptional target of interferon regulatory factor 4 (IRF4) in myeloid-derived suppressor cells (MDSCs). **(A)** Sequence analysis of c-Myc promoter; the potential IRF4-binding sites are underlined. **(B)** A chromatin immunoprecipitation (ChIP) assay was performed on a 3-day culture of bone marrow (BM) cells using anti-IRF4 or anti-IgG antibodies; the presence of the c-Myc promoter harboring the potential IRF4 binding sites (site 1: −4,291~−4,183) was measured by qPCR. Site 2 (−3,289~−3,185) and site 3 (−2,011~−1,910) were detected in parallel as controls. The data were normalized against input and presented as the fold increase over the IgG control. **(C)** 32D cells were co-transfected with the c-Myc reporter (WT, +157 ~−4,480) or deletant (+157 ~−3,573) and the plasmid expressing IRF4 or vector; luciferase activity was measured 48 h posttransfection. **(B, C)** Mean ± SEMs from three independent experiments; *$P < 0.05$, ns $P > 0.05$, unpaired t tests.

nontumor patients with liver fibrosis served as controls. The proportion of the M-MDSCs (HLA-DR$^-$CD11b$^+$CD33^{hi}CD14$^+$) and PMN-MDSCs (HLA-DR$^-$CD11b$^+$CD33^{low} CD15$^+$) in the peripheral blood of liver cancer patients was significantly increased ($P<0.01$, **Figure 7A**). Moreover, the expressions of IRF4 and c-Myc in PMN-MDSCs and M-MDSCs from tumor patients was explored. Results showed that the expressions of IRF4 and c-Myc were down-regulated in PMN-MDSCs from tumor patients compared with those in the controls ($P<0.05$), but no significant change was detected in expression of IRF4 in M-MDSCs (**Figures 7B, C**). Furthermore, the expression of IRF4 in PMN-MDSCs was inversely correlated with the proportion of PMN-MDSCs in liver cancer patients (**Figure 7D**). Consistent with the experimental results in mice, the expression of IRF4 was also positively

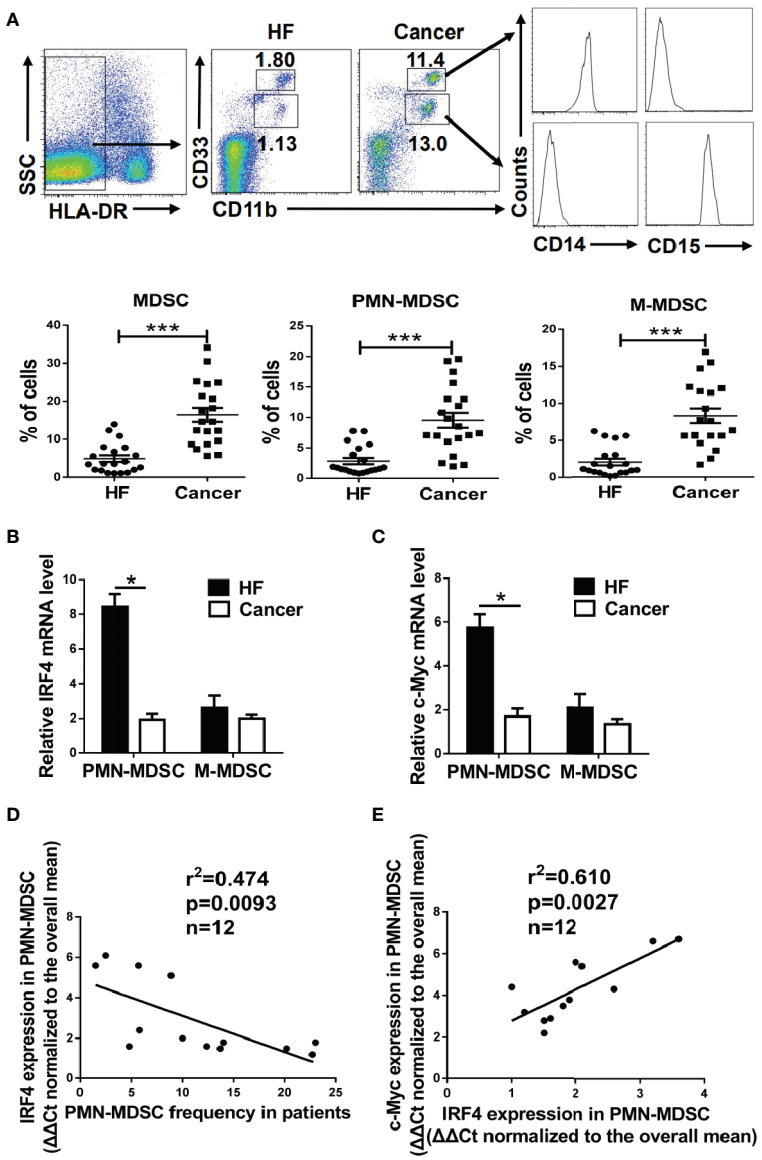

FIGURE 7 | Clinical significance of interferon regulatory factor 4 (IRF4)-mediated polymorphonuclear myeloid-derived suppressor cells (PMN-MDSCs) development. Peripheral blood samples were collected from hepatocellular carcinoma (HCC) patients (n=20); individuals with hepatic fibrosis (HF) (n=20) were used as a control. The levels of MDSCs and their subsets were determined by flow cytometry. **(A)** Representative results (upper) and mean ± SEMs (lower) are shown. **(B, C)** The expression of IRF4 **(B)** and c-Myc **(C)** in PMN-MDSCs and M-MDSCs were determined by qRT-PCR. Mean ± SEMs from 4 individuals are shown. **(D, E)** Correlations between IRF4 expression and PMN-MDSCs frequency (n=12) **(D)** and c-Myc expression in PMN-MDSCs (n=12) **(E)** are shown; Spearman rank test.

correlated with the gene expression of c-Myc in the PMN-MDSCs from tumor patients (**Figure 7E**). These results indicated that IRF4 mediated PMN-MDSCs differentiation has very important clinical significance during tumor progression.

DISCUSSION

Myeloid-derived suppressor cells (MDSCs) has well known roles in the suppression of anti-tumor immunity in tumor-bearing hosts (2, 3). However, few reports have focused on the mechanisms controlling the development and differentiation of MDSCs (33, 36, 37). Therefore, elucidation of the signaling events controlling MDSCs subsets will facilitate the development of an efficient MDSC-based clinical therapy.

It has been reported that IRF4 can regulate differentiation in the myeloid system and DC cells (25, 26), the silencing of IRF4 could promote the development and function of MDSCs (27). However, the role in the lineage determination of immune cells remains unknown. Despite the extensive studies on the roles of IRF4 in tumor biology, the function in tumor immunology remains poorly understood. Under physiological conditions,

the regulatory role of IRF4 in myeloid cell differentiation deserves further investigation. Here, we demonstrate that IRF4 represents a novel regulator of PMN-MDSCs, but not of M-MDSCs and IRF4 expression is also negatively correlated with PMN-MDSCs levels in clinical HCC patients. Thus, our results indicate that IRF4 may play an important role in MDSCs subset determination.

IRF4 has been shown to be important for efficient antigen cross-presentation of moDC (38), and IRF4 expression cloud induce macrophage by cytokines activation and polarization (39). Given the substantial reduction of moDC cells and induction of M2 cells, it seems more likely that this is due to an impaired sustained activation of anti-tumoral T cells than to the amplification and action of MDSC in IRF4-KO mice. We demonstrated that the PMN-MDSC frequency was correlated with tumor weight and metastasis in the B16 model. It suggested that the elevated levels of PMN-MDSC in the IRF4 KO mice could be a secondary effect of the increased tumor progress.

Valdez et al. reported that Prostaglandin E2 can suppress IRF4 expression in T cells (40). Meanwhile, Prostaglandin E2 promotes tumor progression by inducing myeloid-derived suppressor cells (41). These studies suggest a possibility that a high level of prostaglandin E2 in the tumor microenvironment induces MDSCs development by suppressing IRF4 expression. Here, we found that the expression of IRF4 was decreased in the MDSCs treated with supernatant from tumor cells compared with the supernatant from 3T3 cell. It implied that there might be some Prostaglandin E2 in the supernatant of cultured tumor cells which decreased the expression of IRF4 in MDSCs. Further experiment was needed to elucidate it.

Although the existing evidence suggests that Myc family members play a crucial role in regulating the development, differentiation and activation of immune cells (macrophages, dendritic cells, B cells and T cells, etc.) (42, 43), no studies have focused on the regulation of MDSCs differentiation and function by the c-Myc gene. In this study, the important role of the c-Myc gene in regulating the differentiation and function of MDSCs is elucidated and can be targeted for MDSCs treatment. These findings provide a new and important theoretical and experimental basis for improving the efficacy of current tumor immunotherapy.

MDSCs expansion in human tumors has also been extensively studied, revealing that MDSCs derived from distinct types of tumors vary with respect to both their phenotype and immune properties (8). Regardless, the significance of MDSCs subsets in clinical cancer patients is not well defined. In this study, we found that PMN-MDSCs, but not M-MDSCs, are associated with tumor metastasis in HCC patients. The negative correlation between IRF4 expression and PMN-MDSCs levels further supports the pathological significance of IRF4 in PMN-MDSCs development. However, we would like to note that the relationship between IRF4 and PMN-MDSCs in human tumors requires further detailed investigation in distinct tumor types before firm conclusions can be drawn.

In conclusion, our study demonstrates that IRF4 is a novel regulator of PMN-MDSCs in cancer and that c-Myc is the transcriptional target of IRF4 in MDSCs. IRF4 may have predictive value for determining the PMN-MDSCs level and tumor progression in cancer patients.

DATA AVAILABILITY STATEMENT

The raw data supporting the conclusions of this article will be made available by the authors, without undue reservation.

ETHICS STATEMENT

The studies involving human participants were reviewed and approved by the Ethics Review Board of Guangzhou Medical University. The patients/participants provided their written informed consent to participate in this study. The animal study was reviewed and approved by the Animal Care and Use Committee of Guangzhou Medical University. Written informed consent was obtained from the owners for the participation of their animals in this study. Written informed consent was obtained from the individual(s) for the publication of any potentially identifiable images or data included in this article.

AUTHOR CONTRIBUTIONS

QY and HX performed most of the experiments and analyzed the data with assistance from JH. XL collected the clinical samples, and YF, SX, JQ, AX, YZ, and LZ performed the animal experiment. JY, XH, and HW performed the selected immunoblots. HQ and WQ contributed to the scientific planning. QY and JH oversaw and designed the study. WQ, QY, and JH authored the manuscript. All authors contributed to the article and approved the submitted version.

FUNDING

This work was supported by a grant from the Natural Science Foundation of China (31800739, 81970771, 81771696), the Natural Science Foundation of Guangdong Province (2018A0303130317), the Guangdong Provincial Education Department (2017KTSCX157), the Medical Research Fund of Guangdong Province (A2019471), and the Youth Project Fund of the State Key Laboratory of Respiratory Diseases (SKLRDQN-201921).

SUPPLEMENTARY MATERIAL

The Supplementary Material for this article can be found online at: https://www.frontiersin.org/articles/10.3389/fimmu.2021.627072/full#supplementary-material

REFERENCES

1. Lu C, Rong D, Zhang B, Zheng W, Wang X, Chen Z, et al. Current perspectives on the immunosuppressive tumor microenvironment in hepatocellular carcinoma: challenges and opportunities. *Mol Cancer* (2019) 18:130. doi: 10.1186/s12943-019-1047-6
2. Bruger AM, Dorhoi A, Esendagli G, Barczyk-Kahlert K, van der Bruggen P, Lipoldova M, et al. How to measure the immunosuppressive activity of MDSC: assays, problems and potential solutions. *Cancer Immunol Immunother* (2019) 68:631–44. doi: 10.1007/s00262-018-2170-8
3. Li F, Zhao Y, Wei L, Li S, Liu J. Tumor-infiltrating Treg, MDSC, and IDO expression associated with outcomes of neoadjuvant chemotherapy of breast cancer. *Cancer Biol Ther* (2018) 19:695–705. doi: 10.1080/15384047.2018.1450116
4. Greene S, Robbins Y, Mydlarz WK, Huynh AP, Schmitt NC, Friedman J, et al. Inhibition of MDSC Trafficking with SX-682, a CXCR1/2 Inhibitor, Enhances NK-Cell Immunotherapy in Head and Neck Cancer Models. *Clin Cancer Res* (2020) 26:1420–31. doi: 10.1158/1078-0432.CCR-19-2625
5. Tesi RJ. MDSC; the Most Important Cell You Have Never Heard Of. *Trends Pharmacol Sci* (2019) 40:4–7. doi: 10.1016/j.tips.2018.10.008
6. Tumino N, Besi F, Di Pace AL, Mariotti FR, Merli P, Li PG, et al. PMN-MDSC are a new target to rescue graft-versus-leukemia activity of NK cells in haplo-HSC transplantation. *LEUKEMIA* (2020) 34:932–7. doi: 10.1038/s41375-019-0585-7
7. Yang F, Li Y, Zou W, Xu Y, Wang H, Wang W, et al. Adoptive transfer of IFN-gamma-induced M-MDSCs promotes immune tolerance to allografts through iNOS pathway. *Inflammation Res* (2019) 68:545–55. doi: 10.1007/s00011-019-01237-9
8. Solito S, Marigo I, Pinton L, Damuzzo V, Mandruzzato S, Bronte V. Myeloid-derived suppressor cell heterogeneity in human cancers. *Ann N Y Acad Sci* (2014) 1319:47–65. doi: 10.1111/nyas.12469
9. Bronte V, Brandau S, Chen SH, Colombo MP, Frey AB, Greten TF, et al. Recommendations for myeloid-derived suppressor cell nomenclature and characterization standards. *Nat Commun* (2016) 7:12150. doi: 10.1038/ncomms12150
10. Youn JI, Nagaraj S, Collazo M, Gabrilovich DI. Subsets of myeloid-derived suppressor cells in tumor-bearing mice. *J Immunol* (2008) 181:5791–802. doi: 10.4049/jimmunol.181.8.5791
11. Peranzoni E, Zilio S, Marigo I, Dolcetti L, Zanovello P, Mandruzzato S, et al. Myeloid-derived suppressor cell heterogeneity and subset definition. *Curr Opin Immunol* (2010) 22:238–44. doi: 10.1016/j.coi.2010.01.021
12. Chandra D, Gravekamp C. Myeloid-derived suppressor cells. *Oncoimmunology* (2013) 2(11):e26967. doi: 10.4161/onci.26967
13. Gabrilovich DI, Ostrand-Rosenberg S, Bronte V. Coordinated regulation of myeloid cells by tumours. *Nat Rev Immunol* (2012) 12:253–68. doi: 10.1038/nri3175
14. Dai H, Xu H, Wang S, Ma J. Connections between Metabolism and Epigenetic Modification in MDSCs. *Int J Mol Sci* (2020) 21:7356. doi: 10.3390/ijms21197356
15. Sanaei MJ, Salimzadeh L, Bagheri N. Crosstalk between myeloid-derived suppressor cells and the immune system in prostate cancer: MDSCs and immune system in Prostate cancer. *J Leukoc Biol* (2020) 107:43–56. doi: 10.1002/JLB.4RU0819-150RR
16. Huang M, Wu R, Chen L, Peng Q, Li S, Zhang Y, et al. S100A9 Regulates MDSCs-Mediated Immune Suppression via the RAGE and TLR4 Signaling Pathways in Colorectal Carcinoma. *Front Immunol* (2019) 10:2243. doi: 10.3389/fimmu.2019.02243
17. Yamagata T, Nishida J, Tanaka S, Sakai R, Mitani K, Yoshida M, et al. A novel interferon regulatory factor family transcription factor, ICSAT/Pip/LSIRF, that negatively regulates the activity of interferon-regulated genes. *Mol Cell Biol* (1996) 16:1283–94. doi: 10.1128/MCB.16.4.1283
18. Murphy TL, Tussiwand R, Murphy KM. Specificity through cooperation: BATF-IRF interactions control immune-regulatory networks. *Nat Rev Immunol* (2013) 13:499–509. doi: 10.1038/nri3470
19. Shaffer AL, Emre NC, Romesser PB, Staudt LM. IRF4: Immunity. Malignancy! Therapy? *Clin Cancer Res* (2009) 15:2954–61. doi: 10.1158/1078-0432.CCR-08-1845
20. Xu W, Pan H, Ye D, Xu Y. Targeting IRF4 in autoimmune diseases. *Autoimmun Rev* (2012) 11:918–24. doi: 10.1016/j.autrev.2012.08.011
21. Weilemann A, Grau M, Erdmann T, Merkel O, Lenz G. Essential role of IRF4 and MYC signaling for survival of anaplastic large cell lymphoma. *BLOOD* (2014) 125:124–32. doi: 10.1182/blood-2014-08-594507
22. So YL, Sookram R, Chaudhuri AA, Minisandram A, Cheng D, Xie C, et al. Dual mechanisms by which MiR-125b represses IRF4 to induce myeloid and B cell leukemias. *BLOOD* (2014) 124:1502–12. doi: 10.1182/blood-2014-02-553842
23. Naresh KN. MUM1 expression dichotomizes follicular lymphoma into predominantly, MUM1-negative low-grade and MUM1-positive high-grade subtypes. *HAEMATOLOGICA* (2007) 92:267–8. doi: 10.3324/haematol.10682
24. Carreras E, Turner S, Frank MB, Knowlton N, Osban J, Centola M, et al. Estrogen receptor signaling promotes dendritic cell differentiation by increasing expression of the transcription factor IRF4. *BLOOD* (2010) 115:238–46. doi: 10.1182/blood-2009-08-236935
25. Murphy TL, Grajales-Reyes GE, Wu X, Tussiwand R, Murphy KM. Transcriptional Control of Dendritic Cell Development. *Annu Rev Immunol* (2016) 34:239–67. doi: 10.1146/annurev-immunol-032713-120204
26. Metzger P, Kirchleitner SV, Boehmer D, Horth C, Eisele A, Ormanns S, et al. Systemic but not MDSC-specific IRF4 deficiency promotes an immunosuppressed tumor microenvironment in a murine pancreatic cancer model. *Cancer Immunol Immunother* (2020) 69:2101–12. doi: 10.1007/s00262-020-02605-9
27. Nam S, Kang K, Cha JS, Kim JW, Lee HG, Kim Y, et al. Interferon regulatory factor 4 (IRF4) controls myeloid-derived suppressor cell (MDSC) differentiation and function. *J Leukoc Biol* (2016) 100:1273–84. doi: 10.1189/jlb.1A0215-068RR
28. Pennanen M, Hagstrom J, Heiskanen I, Sane T, Mustonen H, Arola J, et al. C-myc expression in adrenocortical tumours. *J Clin Pathol* (2018) 71:129–34. doi: 10.1136/jclinpath-2017-204503
29. Casey SC, Baylot V, Felsher DW. MYC: Master Regulator of Immune Privilege. *Trends Immunol* (2017) 38:298–305. doi: 10.1016/j.it.2017.01.002
30. Eguchi J, Kong X, Tenta M, Wang X, Kang S, Rosen ED. Interferon Regulatory Factor 4 Regulates Obesity-Induced Inflammation Through Regulation of Adipose Tissue Macrophage Polarization. *DIABETES* (2013) 62:3394–403. doi: 10.2337/db12-1327
31. Capietto A, Kim S, Sanford DE, Linehan DC, Hikida M, Kumosaki T, et al. Down-regulation of PLCγ2–β-catenin pathway promotes activation and expansion of myeloid-derived suppressor cells in cancer. *J Exp Med* (2013) 210:2257–71. doi: 10.1084/jem.20130281
32. Yu LX, Yan L, Yang W, Wu FQ, Ling Y, Chen SZ, et al. Platelets promote tumour metastasis via interaction between TLR4 and tumour cell-released high-mobility group box1 protein. *Nat Commun* (2014) 5:5256. doi: 10.1038/ncomms6256
33. Yang Q, Li X, Chen H, Cao Y, Xiao Q, He Y, et al. IRF7 regulates the development of granulocytic myeloid-derived suppressor cells through S100A9 transrepression in cancer. *ONCOGENE* (2017) 36:2969–80. doi: 10.1038/onc.2016.448
34. Thevenot PT, Sierra RA, Raber PL, Al-Khami AA, Trillo-Tinoco J, Zarreii P, et al. The Stress-Response Sensor Chop Regulates the Function and Accumulation of Myeloid-Derived Suppressor Cells in Tumors. *IMMUNITY* (2014) 41:389–401. doi: 10.1016/j.immuni.2014.08.015
35. Yang Q, Wei J, Zhong L, Shi M, Zhou P, Zuo S, et al. Cross Talk between Histone Deacetylase 4 and STAT6 in the Transcriptional Regulation of Arginase 1 during Mouse Dendritic Cell Differentiation. *Mol Cell Biol* (2015) 35:63–75. doi: 10.1128/MCB.00805-14
36. Medina-Echeverz J, Haile LA, Zhao F, Gamrekelashvili J, Ma C, Métais J, et al. IFN-γ regulates survival and function of tumor-induced CD11b\r +\r Gr-1\r high\r myeloid derived suppressor cells by modulating the anti-apoptotic molecule Bcl2a1. *Eur J Immunol* (2014) 44:2457–67. doi: 10.1002/eji.201444497
37. Ioannou M, Alissafi T, Lazaridis I, Deraos G, Matsoukas J, Gravanis A, et al. Crucial role of granulocytic myeloid-derived suppressor cells in the regulation of central nervous system autoimmune disease. *J Immunol* (2012) 188:1136–46. doi: 10.4049/jimmunol.1101816
38. Briseño CG, Haldar M, Kretzer NM, Wu X, Theisen DJ, Kc W, et al. Distinct Transcriptional Programs Control Cross-Priming in Classical and Monocyte-Derived Dendritic Cells. *Cell Rep* (2016) 15:2462–74. doi: 10.1016/j.celrep.2016.05.025

39. Chistiakov DA, Myasoedova VA, Revin VV, Orekhov AN, Bobryshev YV. The impact of interferon-regulatory factors to macrophage differentiation and polarization into M1 and M2. *IMMUNOBIOLOGY* (2018) 223:101–11. doi: 10.1016/j.imbio.2017.10.005
40. Valdez PA, Vithayathil PJ, Janelsins BM, Shaffer AL, Williamson PR, Datta SK. Prostaglandin E2 suppresses antifungal immunity by inhibiting interferon regulatory factor 4 function and interleukin-17 expression in T cells. *IMMUNITY* (2012) 36:668–79. doi: 10.1016/j.immuni.2012.02.013
41. Finetti F, Travelli C, Ercoli J, Colombo G, Buoso E, Trabalzini L. Prostaglandin E2 and Cancer: Insight into Tumor Progression and Immunity. *Biol (Basel)* (2020) 9:434. doi: 10.3390/biology9120434
42. Yu L, Yu TT, Young KH. Cross-talk between Myc and p53 in B-cell lymphomas. *Chronic Dis Transl Med* (2019) 5:139–54. doi: 10.1016/j.cdtm.2019.08.001
43. Nepal RM, Martin A. Unmasking the Mysteries of MYC. *J Immunol* (2019) 202:2517–8. doi: 10.4049/jimmunol.1900186

Conflict of Interest: The authors declare that the research was conducted in the absence of any commercial or financial relationships that could be construed as a potential conflict of interest.

frontiers in Immunology

MINI REVIEW
published: 25 February 2021
doi: 10.3389/fimmu.2021.643692

Single-Cell Profiling to Explore Immunological Heterogeneity of Tumor Microenvironment in Breast Cancer

Xiao Yuan[1†], *Jinxi Wang*[2†], *Yixuan Huang*[3], *Dangang Shangguan*[4*] *and Peng Zhang*[3*]

[1] Changsha KingMed Center for Clinical Laboratory Co., Ltd, Changsha, China, [2] First Affiliated Hospital of Hunan University of Traditional Chinese Medicine, Changsha, China, [3] Division of Immunotherapy, Institute of Human Virology, University of Maryland School of Medicine, Baltimore, MD, United States, [4] Hunan Cancer Hospital, Changsha, China

Immune infiltrates in the tumor microenvironment (TME) of breast cancer (BRCA) have been shown to play a critical role in tumorigenesis, progression, invasion, and therapy resistance, and thereby will affect the clinical outcomes of BRCA patients. However, a wide range of intratumoral heterogeneity shaped by the tumor cells and immune cells in the surrounding microenvironment is a major obstacle in understanding and treating BRCA. Recent progress in single-cell technologies such as single-cell RNA sequencing (scRNA-seq), mass cytometry, and digital spatial profiling has enabled the detailed characterization of intratumoral immune cells and vastly improved our understanding of less-defined cell subsets in the tumor immune environment. By measuring transcriptomes or proteomics at the single-cell level, it provides an unprecedented view of the cellular architecture consist of phenotypical and functional diversities of tumor-infiltrating immune cells. In this review, we focus on landmark studies of single-cell profiling of immunological heterogeneity in the TME, and discuss its clinical applications, translational outlook, and limitations in breast cancer studies.

Keywords: single-cell sequencing, breast cancer, single cell mass cytometry, tumor microenviroment, immune cell

OPEN ACCESS

Edited by:
Wei Wei,
Institute for Systems Biology (ISB), United States

Reviewed by:
Yao Lu,
Chinese Academy of Sciences, China
Qiang Tian,
Shanghai Jiao Tong University, China

***Correspondence:**
Peng Zhang
Peng.Zhang@ihv.umaryland.edu
Dangang Shangguan
shangguandg@163.com

[†]These authors have contributed equally to this work

Specialty section:
This article was submitted to Cancer Immunity and Immunotherapy, a section of the journal Frontiers in Immunology

Received: *18 December 2020*
Accepted: *05 February 2021*
Published: *25 February 2021*

Citation:
Yuan X, Wang J, Huang Y, Shangguan D and Zhang P (2021) Single-Cell Profiling to Explore Immunological Heterogeneity of Tumor Microenvironment in Breast Cancer. Front. Immunol. 12:643692. doi: 10.3389/fimmu.2021.643692

INTRODUCTION

Born in 2009 (1), selected as the Method of the Year 2013 by Nature Methods (2), the single-cell sequencing technologies are revolutionizing the details of whole-transcriptome and proteome snapshots from a tissue to a cell (3–5). Compared with traditional bulk sequencing approaches, the single-cell sequencing technologies enable the identification of cellular heterogeneity in greater detail than conventional methods at the single-cell level. It shows unequaled strength in exploring cellular diversity especially immunological heterogeneity in the TME, which is an extremely subtle system and contains a variety of tumor cells and infiltrating immune cells (6, 7). Recently rapid developed single-cell RNA sequencing (scRNA-seq) methods have allowed for the identification of rare and novel cell types, simultaneous characterization of multiple different cell states, more accurate and integrated understanding of their roles in the tumor microenvironment. The workflow of scRNA-seq consists of single-cell capture, mRNA reverse transcription, cDNA amplification, library preparation, high-throughput sequencing, and data analysis. The number of sequenced reads, which represents the gene expression

level, has been counted as a digital gene expression matrix for bioinformatic analysis (8, 9). In this review, we will outline the recent findings on tumor-infiltrating immune cells based on scRNA-seq in human breast cancers, and their connections with immunotherapy and potential clinical applications. We also explore ways in which other single-cell approaches, such as single-cell mass cytometry (10), that deepen our understanding of immunological responses and resistance in the tumor microenvironment, and examine potential future innovations in the field.

DECOMPOSITION OF TUMOR IMMUNE MICROENVIRONMENT USING scRNA-seq

Although the tumor–immune ecosystem is highly complex and comprises a heterogeneous collection of cells, single-cell RNA sequencing technology has emerged as a powerful tool for the dissection of the tumor immune microenvironment that uncovers the mechanism of activation, regulation, and communication (**Figure 1**).

THE COMPLEXITY OF TUMOR-INFILTRATING LYMPHOCYTES (TILs)

A research group from Australia analyzed intratumoral T cells isolated from tumor tissues by using the multiparameter flow cytometry method, based on a prospective cohort of 123 breast cancer patients, and showed that significant heterogeneity existed in the infiltrating T lymphocytes populations (11). Then, they performed single-cell transcriptome analysis on 6,311 flow-sorted $CD3^+CD45^+$ T cells from two samples of human primary triple-negative breast cancer (TNBC) tumor. A total of 10 distinct cell clusters included 3 $CD8^+$ T cell clusters and 4 $CD4^+$ T cell clusters were identified. Of interest, among the $CD8^+$ T cell clusters, one cluster had the expression of

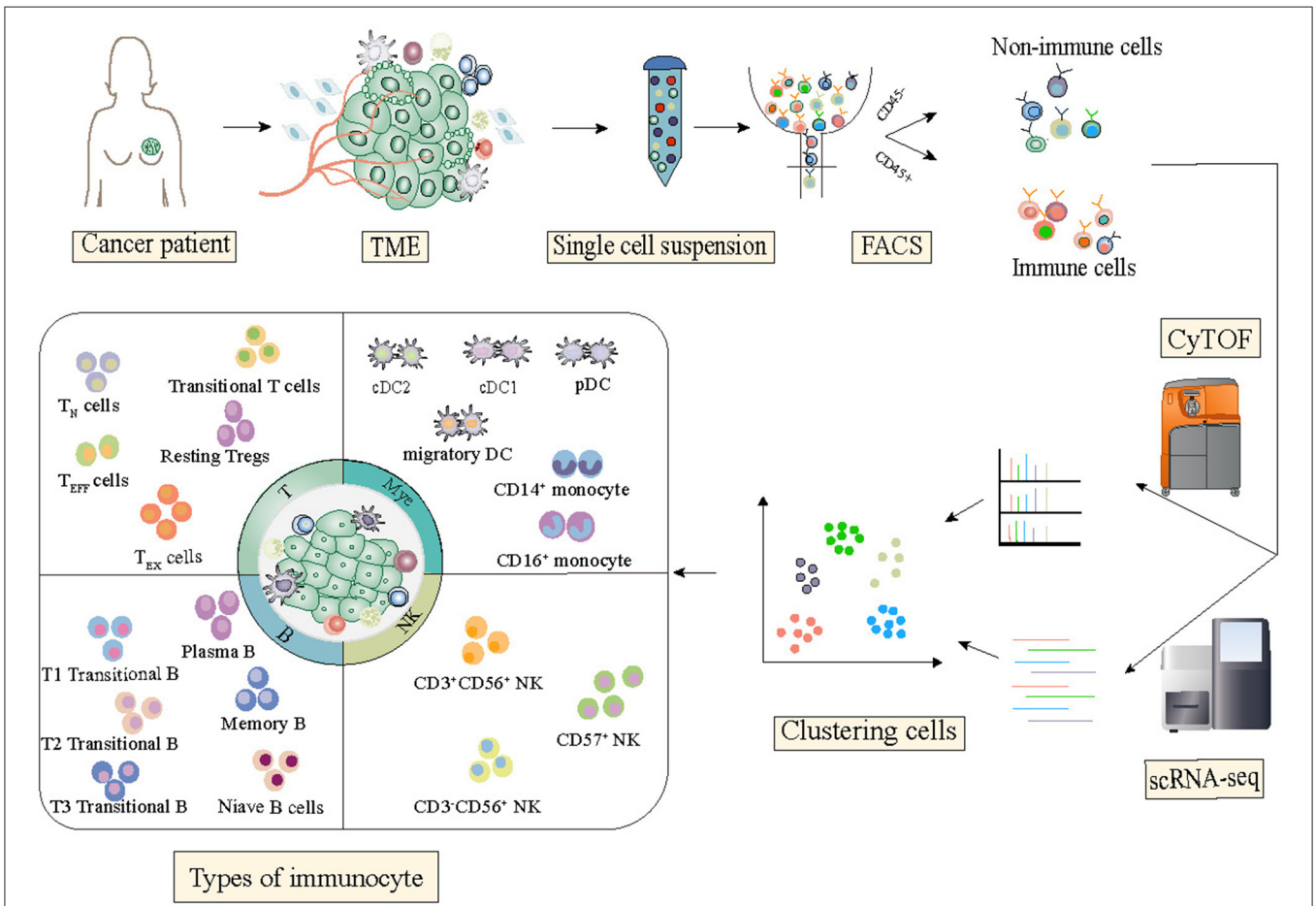

FIGURE 1 | State of the art of single-cell technology and its application in breast cancer studies. Single-cell sequencing technologies have been designed for almost all the molecular layers of genetic information flow from RNA to proteins. For each molecular layer, multiple technologies have been developed, all of which have specific advantages and disadvantages. Single-cell technologies are close to comprehensively depicting the state of the functional properties and dynamic changes of immune cells in the tumor microenvironment.

molecules suggestive of a tissue-resident memory T (T_{RM}) cell phenotype. This $CD8^+CD103^+$ T_{RM}-like cluster was highly distinct, with 400 genes including several hallmarks of T_{RM} differentiation that statistically differentially expressed when compared with the other T cell clusters, and highly expressed both immune checkpoint molecules (such as *PDCD1* and *CTLA4*) and cytotoxic effector proteins (such as *GZMB* and *PRF1*). Moreover, the gene signatures of the $CD8^+$ T_{RM} cluster that confirmed by using bulk RNA-seq data, were found to significantly correlate with favorable patient survival in early-stage TNBC. As indicated in this study, scRNA-seq enabled the discovery of minor subgroups of TILs that were related to immune-suppression or immune-surveillance, and biomarkers of these distinct immune cells may serve as prognostic factors or therapeutic targets for breast cancer. The main limitation of this study is that there were only two TNBC tumor samples profiled by scRNAseq.

It is clear that T cells have a dominant role in the tumor immune microenvironment, however, there is a growing appreciation of other components of TILs such as B cells may also contribute to anti-tumor immunity. Recently, Lu et al. (12) observed a phenotype switch of B cells during neoadjuvant chemotherapy that could enhance tumor-specific T cell responses. scRNA-seq of tumor-infiltrating B cells was performed in paired clinical samples of pre- (998 cells) and post-neoadjuvant chemotherapy (1,499 cells) collected from 4 breast cancer patients. The analytic result showed that a distinct B cell subset that expressed high levels of inducible T-cell co-stimulator ligand (*ICOSL*) significantly increased after neoadjuvant chemotherapy. Besides, the high expression of *CR2* and low expression of *IL-10* were also found in this special cell subset. The comparison between patients with stable diseases or progression and patients with partial or complete remission indicated that this cell subset was related to improved therapeutic efficacy. Further survival analyses indicated that $ICOSL^+$ B cell abundance was an independent positive prognostic factor. They also identified the *CD55*, expressed by tumor cells, as the key factor determining the subset switch and conflicting roles of tumor-infiltrating B cells during chemotherapy. It was proposed that this chemotherapy-associated subset of B cells could promote tumor-specific T cell proliferation and reduce regulatory T cells (Tregs). Collectively, this study uncovered a new role of complement in B-cell-dependent anti-tumor immunity and indicated that *CD55* induced chemo-resistance by impeding the induction of $ICOSL^+$ B cells and thus could be a potential therapeutic target to enhance the efficacy of immunogenic chemotherapy. However, their sub-stratified analysis and clinical conclusions should be validated in the future hypothesis-testing experimental investigation because of the small sample size examined in this study.

CHARACTERIZING IMMUNE CELL HETEROGENEITY

One of the most early-stage scRNA-seq studies for comprehensive profiling of breast cancer microenvironment was conducted by the Samsung Genome Institute (13). Researchers analyzed 515 cells from 11 patients representing the four subtypes of breast cancer: luminal A; luminal B; HER2; and triple-negative breast cancer (TNBC). The results revealed that after the separation of carcinoma cells via RNA-seq-inferred tumor-specific copy number variations, most of the non-cancer cells are immune cells because of their high scoring of the immune signatures. 175 tumor-associated immune cells were identified and further annotated as 3 distinct clusters including T lymphocytes, B lymphocytes, and macrophages by using immune cell type-specific gene sets. Interestingly, T cells and macrophages both display immunosuppressive characteristics: T cells with a regulatory or an exhausted phenotype and macrophages with an M2 phenotype. These immune cells with the expression of many immunosuppressive genes could promote tumorigenesis and restrain immune surveillance. Although the number of profiled cells was low and the sequencing depth was limited, this work demonstrated the feasibility of a comprehensive characterization of the heterogeneous immunological microenvironment of breast cancer samples by large-scale single-cell gene expression profiling protocol. Recently, Bao et al. (14) also described the molecular characteristics of M2-like TAM in the TME of breast cancer and identified the association of the immune landscape with clinical outcomes in TNBC by using an integrative analysis approach of combined single-cell and bulk tissue transcriptome profiling.

Another sophisticated TME profiling work provided by a team from the Memorial Sloan Kettering Cancer Center drew a single-cell atlas of diverse immune phenotypes of breast cancer samples and found the immune phenotype was associated with the tissue of residence (15). By assessing 45,000 cells captured from breast carcinomas, as well as matched normal breast tissue, blood, and lymph nodes of 8 treatment-naive patients, they identified 38 T cell, 27 myeloid lineage, 9 B cell, and 9 NK cell clusters, and observed several phenomena via data analysis: (1) T cells in blood and lymph node exhibited dissimilar phenotypes compared with T cells in breast tissue; (2) T and myeloid lineage cells exhibited considerable phenotypic overlap between tumor and normal tissue samples, but increased phenotypic heterogeneity and expansion of cell populations in the tumor was also observed; (3) Naive T cells were strongly enriched in 3 blood-specific clusters, while B cells were more prevalent in the lymph node than in other tissues; (4) A subset of T cell clusters was present in both tumor and normal tissue, but cytotoxic T cell clusters were more abundant in the tumor, as were Treg clusters; (5) Some myeloid clusters were shared between normal and tumor tissue, whereas clusters of more activated macrophages were specific to the tumor. Their results support a model of continuous activation and expansion (shaped by TCR specificity) in T cells and do not comport with the macrophage polarization model in the tumor microenvironment. Moreover, these findings offered a more nuanced view into the association between immune phenotypes and the tissues of residence and suggested that the immunological landscape based on the blood or normal samples may not reflect the functional and phenotypic diversity in the TME.

SPATIAL MAPPING OF SINGLE-CELL RNA-seq DATA

While scRNA-seq has mainly been used to delineate cell subpopulations and their lineage relationships, recently developed spatial transcriptomics technologies have been designed to infer cell-cell communications and spatial architecture in the tumor microenvironment. A research group from Sweden employed an in-house spatial transcriptomics method to resolve spatial immune cell distribution from tumor tissue sections of BRCA patients diagnosed with $HER2^+$ subtype (16, 17). The abundance and distribution of the infiltrated immune cells in different regions of the tumor tissue including invasive cancer regions were determined. Then the researchers combined the cross-sectioning and computational alignment to build three-dimensional images of the transcriptional map of the tumor microenvironment. This spatial transcriptomic landscape demonstrated the heterogeneous nature of tumor-immune interactions and reveal interpatient differences in TME patterns of breast cancer. To our knowledge, this is the first attempt to present a spatial map of comprehensive transcriptomics data from human breast cancer tissues and gain new insight into the immunological heterogeneity.

DISSECTING THE TUMOR MICROENVIRONMENT USING SINGLE-CELL MASS CYTOMETRY

Single-cell RNA-seq captures the expression of thousands of genes, but at the cost of sparse data. In comparison, although mass cytometry measures a limited number of pre-selected markers, these markers are backed with decades of experimental experience, which makes mass cytometry an effective and efficient way to define cellular heterogeneity and a key complement to scRNA-seq (2, 18, 19).

To investigate immunological features of TME and their associations with clinical characteristics of breast cancer, Wagner et al. (20) provided a large-scale single-cell atlas of the human breast cancer tumor microenvironment by analyzing 144 human BRCA tumors covering all clinical subtypes and 50 non-tumor tissue samples by using single-cell mass cytometry. Through tumor and immune cell-centric antibody panels, a total of 73 proteins in 26 million cells was evaluated. Researchers observed significant differences in the T cell landscape of ER^- and ER^+ tumors. In more than half of ER^- tumors but only 12% of ER^+ tumors, over 10% of T cells expressed PD-1. For cell level, distinct PD-1^+ phenotypes were separately enriched: PD-1^{high}CTLA-$4^+$$CD38^+$ T cells were more frequent in ER^- tumors, whereas PD-1^{int}CTLA-$4^-$$CD38^-$ T cells were enriched in ER^+ tumors. This observation support that patients with ER- tumors are more suitable candidates for immunotherapy (21). They also observed high frequencies of PD-$L1^+$ tumor-associated macrophages and exhausted T cells were found in high-grade ER^+ and ER^- tumors, suggesting a possible association between an immunosuppressed environment and poor-prognosis of high-grade tumors. This sophisticated work enhanced our comprehension of the immune ecosystem of human breast cancer and revealed that TME-based stratification will facilitate the identification of BRCA patients for precision medicine approaches targeting the tumor and its immune environment. However, there are still some limitations in this study, and the dominant one is a lack of correlation analysis between their ecosystem-based patient grouping and clinical outcome or treatment response of BRCA patients.

Another impressive research work performed by Jackson et.al depicted the first single-cell pathology landscape of breast cancer by using the imaging mass cytometry (IMC) technology (22, 23). By the use of a designed breast tissue-specific IMC histology panel, a total of 855,668 cells in 381 images (289 tumors, 87 healthy breasts, and 5 liver controls) were been investigated with 35 antibodies simultaneously quantified. Cellprofiler (24) was used for single-cell feature extraction to obtain the expression level of marker genes. And PhenoGraph (25) was employed to identify the 27 meta clusters which represented various immune, stromal, and epithelial cell types. "Community" which consists of interactions between one or more cell phenotypes, was introduced to describe the complex multicellular interaction pattern. The Louvain community detection algorithm (26) was applied to identify highly interconnected spatial subunits in the tissue graph. Researchers investigated how the organization of single cells into communities contributes to the tissue architecture of breast cancer and its subtypes, and found cells from multiple meta clusters appeared in each clinically defined breast cancer subtype, which indicated the general classification based on pathology had limitations in explicate inter-and intrapatient cellular heterogeneity. Then they re-grouped patients based on their tumor cell meta cluster composition and identified 18 novel single-cell pathologies (SCP) subgroups using unsupervised clustering. This higher-resolution classification was then proved to be associated with distinct clinical outcomes. This study revealed that complex single-cell phenotypes and their spatial context could be reflected in the histological stratification and provided a basis for future study on spatial and phenotypic tissue features' influence on disease outcome. But, currently, the high complexity of data analysis for imaging mass cytometry approaches presents a major obstacle to the broad use of these methods in the scientific basic research and potential clinical use.

PERSPECTIVES OF SINGLE-CELL TECHNOLOGIES IN BREAST CANCER RESEARCH

Although the heterogeneous cell populations in the TME stand out as the key barrier to delineate the tumor ecosystems, the advances in single-cell technologies, in particular scRNA-seq and mass cytometry, has revolutionized breast cancer research. The pioneering studies summarized in **Table 1** have covered the development and applications of single-cell RNA sequencing and mass cytometry to address a wide range of topics such as intra-tumor heterogeneity of tumor samples, the characteristics of tumor microenvironments, and the mechanism

TABLE 1 | Summary table for the hallmark breast cancer studies using single-cell technologies.

	Technology	Sample/data	Main findings	Clinical significance	References
The complexity of tumor-infiltrating lymphocytes (TILs)	scRNA-seq (10X Genomics)	6,311 flow-sorted CD3+CD45+ T cells from two samples of TNBC	Discovery of minor subgroups of TILs that were related to immune-suppression	Biomarkers of the minor distinct TILs may serve as prognostic factors or therapeutic targets	(11)
	scRNA-seq (10X Genomics)	Paired samples of pre- (998 cells) and post-neoadjuvant chemotherapy (1,499 cells) collected from 4 BRCA patients	$ICOSL^+$ B cells boost anti-tumor immunity by enhancing the effector to regulatory T cell ratio	The critical role of the B cell subset switch in chemotherapy response, which has implications in designing novel anti-cancer therapies.	(12)
Decomposition of tumor immune microenvironment using scRNA-seq	scRNA-seq (Fluidigm C1)	515 cells from 11 patients representing the four subtypes of breast cancer	T lymphocytes and macrophages both display immunosuppressive characteristics	The characteristics of different BRCA subtypes that are shaped by tumor cells and immune cells in TME	(13)
	scRNA-seq (inDrop); single-cell VDJ sequencing (10X Genomics)	45,000 cells captured in the normal and malignant breast tissues, lymph nodes, and peripheral blood of 8 treatment-naive patients	Despite the significant similarity between normal and tumor tissue-resident immune cells, continuous phenotypic expansions specific to the TME was observed	Support a model of continuous activation in T cells and do not comport with the macrophage polarization model in cancer	(15)
Spatial mapping of single-cell RNA-seq data	Spatial Transcriptomics (in-house)	Tumor tissue sections from BRCA patients diagnosed with HER2+ subtype	Demonstration of the heterogeneous nature of tumor-immune interactions and reveal interpatient differences in immune cell infiltration patterns	Potential for an improved stratification and description of the tumor-immune interplay, which is likely to be essential in treatment decisions	(16, 17)
Dissecting the tumor microenvironment using single-cell mass cytometry	Single-Cell Mass Cytometry	26 million cells from 144 human breast tumors including and 50 non-tumor tissue samples	Relationship analyses between tumor and immune cells revealed characteristics of TME related to immunosuppression and poor prognosis	TME-based classification of BRCA will facilitate the identification of individuals for precision medicine approaches	(20)
	Imaging mass cytometry	855,668 cells in 381 images (289 tumors, 87 healthy breasts, and 5 liver controls)	Multicellular features of TME and novel subgroups of breast cancer that are associated with distinct clinical outcomes	Spatially resolved, single-cell analysis can characterize intratumor phenotypic heterogeneity with the potential to inform patient-specific diagnosis	(23)

of immunotherapy resistance. Improvement of existing single-cell sequencing technologies and the integration of single-cell sequencing with other high throughput and experimental protocols have provided powerful toolsets to understand many of the remaining mysteries of breast cancers.

The advent of rapidly developing single-cell sequencing technologies are revolutionizing our ability to study tumor immunology, and these initial studies provided a proof of concept for the utility of single-cell profiling of TME. However, substantial limitations and challenges still exist in this approach. First, most single-cell technologies (such as single-cell RNA-sequencing) are very sensitive to the quality of sample collection and library construction, and therefore couldn't be applied to the profiling of sub-optimally preserved or handled clinical specimens (27, 28). Second, given the technological and throughput constraints of cellular captures, single-cell technologies usually profile only a partial sampling of tumor tissues. To what extent the sequenced cells represent the distribution of cells in the entire microenvironment is not clear. Third, high cost limits the ability to profile large cohorts of tumor samples, so most single-cell studies to date include a few patients, which limits the opportunity to investigate effects on clinical characteristics and outcomes. Spatial single-cell sequencing, single-cell proteomics, and single-cell epigenomics technologies are some of the major directions of single-cell sequencing technologies that will bring the second wave of revolutions of cancer research (29–31). Understanding the orchestrated organizations and interactions of cancer and immune cells in a spatial coordinate system will provide further insights into cancer progression and could provide clues for improving the efficiency of current immunotherapies.

Besides, the use of single-cell technologies in profiling the tumor microenvironment of breast cancers has been largely limited to basic research. Its potential for clinical utility including

disease diagnosis, dynamical monitoring, therapeutic efficacy, and prognostic prediction is yet to be realized (32–34). First, the standardized procedures of sample processing for clinical use of single-cell sequencing technologies are urgently required. It is important to set measurable criteria and establish practical protocols for the processing of tissue sampling from operations (such as resection, selection, and isolation from tissue to single cells). Second, the methodologies and procedures of single-cell sequencing data pre-processing, quality control, data analysis, and visualizations of results need to be simplified. Besides, the most important issue for potential clinical use is how to interpret analysis results to clinicians and patients, and provide valuable information for clinical decision-making. We believe, in the near future, the promising clinical use based on developed single-cell technologies will improve the understanding of molecular pathogenesis and pathophysiology, and facilitate the discovery and validation of biomarkers and targets for breast cancer.

AUTHOR CONTRIBUTIONS

XY and JW contributed equally to researching, writing of initial drafts, and assembling manuscripts with the help of YH. DS and PZ conceptualized, edited, and assembled the final submitted manuscript. All authors contributed to the article and approved the submitted version.

REFERENCES

1. Tang F, Barbacioru C, Wang Y, Nordman E, Lee C, Xu N, et al. mRNA-Seq whole-transcriptome analysis of a single cell. *Nat. Methods.* (2009) 6:377–82. doi: 10.1038/nmeth.1315
2. Method of the year 2013. *Nat. Methods.* (2014) 11:1. doi: 10.1038/nmeth.2801
3. Wang Y, Navin NE. Advances and applications of single-cell sequencing technologies. *Mol. Cell.* (2015) 58:598–609. doi: 10.1016/j.molcel.2015.05.005
4. van Dijk EL, Jaszczyszyn Y, Naquin D, Thermes C. The third revolution in sequencing technology. *Trends Genet.* (2018) 34:666–81. doi: 10.1016/j.tig.2018.05.008
5. Potter SS. Single-cell RNA sequencing for the study of development, physiology and disease. *Nat. Rev. Nephrol.* (2018) 14:479–92. doi: 10.1038/s41581-018-0021-7
6. Zhang Y, Zhang Z. The history and advances in cancer immunotherapy: understanding the characteristics of tumor-infiltrating immune cells and their therapeutic implications. *Cell Mol. Immunol.* (2020) 17:807–21. doi: 10.1038/s41423-020-0488-6
7. Ren X, Kang B, Zhang Z. Understanding tumor ecosystems by single-cell sequencing: promises and limitations. *Genome Biol.* (2018) 19:211. doi: 10.1186/s13059-018-1593-z
8. Dal Molin A, Di Camillo B. How to design a single-cell RNA-sequencing experiment: pitfalls, challenges and perspectives. *Brief Bioinform.* (2019) 20:1384–94. doi: 10.1093/bib/bby007
9. Forcato M, Romano O, Bicciato S. Computational methods for the integrative analysis of single-cell data. *Brief Bioinform.* (2021) 22:20–9. doi: 10.1093/bib/bbaa042
10. Spitzer MH, Nolan GP. Mass cytometry: single cells, many features. *Cell.* (2016) 165:780–91. doi: 10.1016/j.cell.2016.04.019
11. Savas P, Virassamy B, Ye C, Salim A, Mintoff CP, Caramia F, et al. Single-cell profiling of breast cancer T cells reveals a tissue-resident memory subset associated with improved prognosis. *Nat. Med.* (2018) 24:986–93. doi: 10.1038/s41591-018-0078-7
12. Lu Y, Zhao Q, Liao JY, Song E, Xia Q, Pan J, et al. Complement signals determine opposite effects of B cells in chemotherapy-induced immunity. *Cell.* (2020) 180:1081–97.e24. doi: 10.1016/j.cell.2020.02.015
13. Chung W, Eum HH, Lee HO, Lee KM, Lee HB, Kim KT, et al. Single-cell RNA-seq enables comprehensive tumour and immune cell profiling in primary breast cancer. *Nat. Commun.* (2017) 8:1–12. doi: 10.1038/ncomms15081
14. Bao X, Shi R, Zhao T, Wang Y, Anastasov N, Rosemann M, et al. Integrated analysis of single-cell RNA-seq and bulk RNA-seq unravels tumour heterogeneity plus M2-like tumour-associated macrophage infiltration and aggressiveness in TNBC. *Cancer Immunol. Immunother.* (2020) 70:189–202. doi: 10.1007/s00262-020-02669-7
15. Azizi E, Carr AJ, Plitas G, Cornish AE, Konopacki C, Prabhakaran S, et al. Single-cell map of diverse immune phenotypes in the breast tumor microenvironment. *Cell.* (2018) 174:1293–308.e36. doi: 10.1016/j.cell.2018.05.060
16. Andersson A, Larsson L, Stenbeck L, Salmén F, Ehinger A, Wu S, et al. Spatial deconvolution of HER2-positive breast tumors reveals novel intercellular relationships. *bioRxiv.* (2020) 2020.07.14.200600. doi: 10.1101/2020.07.14.200600
17. Salmén F, Vickovic S, Larsson L, Stenbeck L, Vallon-Christersson J, Ehinger A, et al. Multidimensional transcriptomics provides detailed information about immune cell distribution and identity in HER2+ breast tumors. *bioRxiv.* (2018) 358937. doi: 10.1101/358937
18. Karaayvaz M, Cristea S, Gillespie SM, Patel AP, Mylvaganam R, Luo CC, et al. Unravelling subclonal heterogeneity and aggressive disease states in TNBC through single-cell RNA-seq. *Nat. Commun.* (2018) 9:3588. doi: 10.1038/s41467-018-06052-0
19. Zhang F, Wei K, Slowikowski K, Fonseka CY, Rao DA, Kelly S, et al. Defining inflammatory cell states in rheumatoid arthritis joint synovial tissues by integrating single-cell transcriptomics and mass cytometry. *Nat. Immunol.* (2019) 20:928–42. doi: 10.1038/s41590-019-0378-1
20. Wagner J, Rapsomaniki MA, Chevrier S, Anzeneder T, Langwieder C, Dykgers A, et al. A single-cell atlas of the tumor and immune ecosystem of human breast cancer. *Cell.* (2019) 177:1330–45.e18. doi: 10.1016/j.cell.2019.03.005
21. Dieci MV, Griguolo G, Miglietta F, Guarneri V. The immune system and hormone-receptor positive breast cancer: is it really a dead end? *Cancer Treat. Rev.* (2016) 46:9–19. doi: 10.1016/j.ctrv.2016.03.011
22. Giesen C, Wang HAO, Schapiro D, Zivanovic N, Jacobs A, Hattendorf B, et al. Highly multiplexed imaging of tumor tissues with subcellular resolution by mass cytometry. *Nat. Methods.* (2014) 11:417–22. doi: 10.1038/nmeth.2869
23. Jackson HW, Fischer JR, Zanotelli VRT, Ali HR, Mechera R, Soysal SD, et al. The single-cell pathology landscape of breast cancer. *Nature.* (2020) 578:615–20. doi: 10.1038/s41586-019-1876-x
24. McQuin C, Goodman A, Chernyshev V, Kamentsky L, Cimini BA, Karhohs KW, et al. CellProfiler 3.0: next-generation image processing for biology. *PLoS Biol.* (2018) 16:e2005970. doi: 10.1371/journal.pbio.2005970
25. Levine JH, Simonds EF, Bendall SC, Davis KL, Amir ED, Tadmor MD, et al. Data-driven phenotypic dissection of AML reveals progenitor-like cells that correlate with prognosis. *Cell.* (2015) 162:184–97. doi: 10.1016/j.cell.2015.05.047
26. Blondel VD, Guillaume J-L, Lambiotte R, Lefebvre E. Fast unfolding of communities in large networks. *J. Stat. Mech. Theory Exp.* (2008) 2008:P10008. doi: 10.1088/1742-5468/2008/10/P10008
27. Lafzi A, Moutinho C, Picelli S, Heyn H. Tutorial: guidelines for the experimental design of single-cell RNA sequencing studies. *Nat. Protoc.* (2018) 13:2742–57. doi: 10.1038/s41596-018-0073-y
28. Ding J, Adiconis X, Simmons SK, Kowalczyk MS, Hession CC, Marjanovic ND, et al. Systematic comparison of single-cell and single-nucleus RNA-sequencing methods. *Nat. Biotechnol.* (2020) 38:737–46. doi: 10.1038/s41587-020-0465-8
29. Satija R, Farrell JA, Gennert D, Schier AF, Regev A. Spatial reconstruction of single-cell gene expression data. *Nat. Biotechnol.* (2015) 33:495–502. doi: 10.1038/nbt.3192

30. Papalexi E, Satija R. Single-cell RNA sequencing to explore immune cell heterogeneity. *Nat. Rev. Immunol.* (2018) 18:35–45. doi: 10.1038/nri.2017.76
31. Stuart T, Satija R. Integrative single-cell analysis. *Nat. Rev. Genet.* (2019) 20:257–72. doi: 10.1038/s41576-019-0093-7
32. Luecken MD, Theis FJ. Current best practices in single-cell RNA-seq analysis: a tutorial. *Mol. Syst. Biol.* (2019) 15:e8746. doi: 10.15252/msb.20188746
33. Lähnemann D, Köster J, Szczurek E, McCarthy DJ, Hicks SC, Robinson MD, et al. Eleven grand challenges in single-cell data science. *Genome Biol.* (2020) 21:31. doi: 10.1186/s13059-020-1926-6
34. Zhang J, Wang W, Huang J, Wang X, Zeng Y. How far is single-cell sequencing from clinical application? *Clin. Transl. Med.* (2020) 10:e117. doi: 10.1002/ctm2.117

Conflict of Interest: XY was employed by the Changsha KingMed Center For Clinical Laboratory Co., Ltd.

The remaining authors declare that the research was conducted in the absence of any commercial or financial relationships that could be construed as a potential conflict of interest.

frontiers in Immunology

ORIGINAL RESEARCH
published: 25 February 2021
doi: 10.3389/fimmu.2021.631483

Comprehensive Genomic Profiling of Rare Tumors in China: Routes to Immunotherapy

Shuhang Wang[1], Yuan Fang[2], Ning Jiang[2], Shujun Xing[2], Qin Li[3], Rongrong Chen[3], Xin Yi[3], Zhiqian Zhang[1] and Ning Li[2]**

[1] Key Laboratory of Carcinogenesis and Translational Research (Ministry of Education), Department of Cell Biology, Peking University Cancer Hospital and Institute, Beijing, China, [2] Clinical Cancer Center, National Cancer Center/National Clinical Research Center for Cancer/Cancer Hospital, Chinese Academy of Medical Sciences and Peking Union Medical College, Beijing, China, [3] Department of Medical Center, Geneplus-Beijing Institute, Beijing, China

OPEN ACCESS

Edited by:
Qihui Shi,
Fudan University, China

Reviewed by:
Zhuo Wang,
Fudan University, China
Ziming Li,
Shanghai Jiaotong University, China

***Correspondence:**
Zhiqian Zhang
zlzqzhang@bjmu.edu.cn
Ning Li
lining@cicams.ac.cn

Specialty section:
This article was submitted to Cancer Immunity and Immunotherapy, a section of the journal Frontiers in Immunology

Received: *20 November 2020*
Accepted: *18 January 2021*
Published: *25 February 2021*

Citation:
Wang S, Fang Y, Jiang N, Xing S, Li Q, Chen R, Yi X, Zhang Z and Li N (2021) Comprehensive Genomic Profiling of Rare Tumors in China: Routes to Immunotherapy. Front. Immunol. 12:631483. doi: 10.3389/fimmu.2021.631483

Treatment options for rare tumors are limited, and comprehensive genomic profiling may provide useful information for novel treatment strategies and improving outcomes. The aim of this study is to explore the treatment opportunities of patients with rare tumors using immune checkpoint inhibitors (ICIs) that have already been approved for routine treatment of common tumors. We collected immunotherapy-related indicators data from a total of 852 rare tumor patients from across China, including 136 programmed cell death ligand-1 (PD-L1) expression, 821 tumors mutational burden (TMB), 705 microsatellite instability (MSI) and 355 human leukocyte antigen class I (HLA-I) heterozygosity reports. We calculated the positive rates of these indicators and analyzed the consistency relationship between TMB and PD-L1, TMB and MSI, and HLA-I and PD-L1. The prevalence of PD-L1 positive, TMB-H, MSI-, and HLA-I -heterozygous was 47.8%, 15.5%, 7.4%, and 78.9%, respectively. The consistency ratio of TMB and PD-L1, TMB and MSI, and HLA-I and PD-L1 was 54.8% (78/135), 87.3% (598/685), and 47.4% (54/114), respectively. The prevalence of the four indicators varied widely across tumors systems and subtypes. The probability that neuroendocrine tumors (NETs) and biliary tumors may benefit from immunotherapy is high, since the proportion of TMB-H is as high as 50% and 25.4% respectively. The rates of PD-L1 positivity, TMB-H and MSI-H in carcinoma of unknown primary (CUP) were relatively high, while the rates of TMB-H and MSI-H in soft tissue tumors were both relatively low. Our study revealed the distribution of immunotherapeutic indicators in patients with rare tumors in China. Comprehensive genomic profiling may offer novel therapeutic modalities for patients with rare tumors to solve the dilemma of limited treatment options.

Keywords: rare tumors, immunotherapy, PD-L1, TMB, HLA-I

INTRODUCTION

Currently, there exists no consensus definition for the category of "rare tumors," either worldwide or in China. Because of the low incidence rate, it is difficult to carry out large-scale studies on these diseases. Due to this lack of study, patients with rare tumors are often unable to take advantage of therapeutic advances. In China, there is a lack of research on rare tumors, leading to limited options for effective treatment and poor survival and prognosis for these patients compared to those with common tumors.

Based on the definition of rare tumors by Food and Drug Administration (FDA), National Cancer Institute and European Society for Medical Oncology (1, 2), Professor Li Ning's team from Clinical Trial Canter, National Cancer Hospital, Chinese Academy of Medical Sciences and Peking Union Medical College, proposed the definition of rare tumors in China first time. This definition was based on data from the National Cancer Registration Office of China National Cancer Canter, combined with the incidence rate of cancer, the characteristics of the population in China, classification according to the International Classification of Diseases and the OncoTrees (http://oncotree.mskcc.org/). The incidence threshold for a "rare tumor" was initially set at 2.5/100,000. In a previous study, we compared the incidence of therapeutic targets in rare tumors in the cBioPortal database (https://www.cbioportal.org/datasets) and a Chinese population database (Geneplus database). We found that the incidence of therapeutic targets in rare tumors in the Chinese population was significantly higher than in the general population (53.43% vs. 20.40% respectively). Moreover, in the Chinese population, prevalence of targetable genomic alterations within those rare tumors (ALK, BRAF, BRCA2, CDKN2A, EGFR, HER2, KIT, MET, ROS1) was 32.4%, which is more than 3 times that which is found in the general population according to cBioPortal (3).

Using the National Comprehensive Cancer Network and Chinese Society of Clinical Oncology guidelines as the main data sources (https://www.nccn.org, http://www.csco.org.cn), we collected records for the tumor types that fit the current definition of "rare tumors," and investigated the availability and efficacy of various treatment modalities. With respect to targeted therapy, of more than 100 rare tumor subtypes, only 16 tumor types were involved in targeted therapy studies, but the disease control rate and objective response rate of rare tumors with targetable mutations are better than those treated with standard treatment. With respect to immunotherapy, of more than 100 rare tumor subtypes, the research on immunotherapy involved less than 17 tumor types. Some curative effect has been preliminarily observed, but only skin squamous cell carcinoma has been approved by the FDA as an indication for Libtayo (PD-1, cemiplimab-rwlc). These results suggest that even in the context of scarcity of clinical trials and guidelines for diagnosis and treatment, there are still some rare tumors included in these studies, which has yielded promising preliminary results for targeted therapy and immunotherapy.

Immunotherapy is revolutionary cancer treatment. Programmed cell death protein-1 and programmed cell death ligand-1 (PD-L1) checkpoint inhibitors can benefit a variety of malignant tumors patients, which has been shown in many studies (4–6). PD-L1 overexpression (7, 8), mismatch repair deficiency (dMMR) (9–11), microsatellite instability-high status (MSI-H) (10–12), or high tumor mutational burden (TMB-H) (13–15) are the main predictive molecular biomarkers in these studies. Human leukocyte antigen class I (HLA-I) is a prognostic biomarker of great concern, representing the impact of host germline genetics on immune checkpoint inhibitors (ICIs) therapies response. CD8 + T cells have been shown to be the main factor in the antitumor activity of ICIs, and the peptide presentation process on the cell surface depends on HLA-I (16, 17). More diverse tumor antigens presented to T cells can benefit from heterozygous HLA-I genotypes (18). Some studies support that patients with HLA-I heterozygosity, had longer overall survival (OS) in pan-cancers (17), while others show that it wasn't the case in non-small-cell lung cancer (NSCLC) (19).

Within rare tumors, some reports have shown that immunotherapy has demonstrated the efficacy in some subtypes, including biliary tumors, neuroendocrine tumors (NETs), and carcinoma of unknown primary (CUP), among others (20–23). The same predictive molecular biomarkers that are used for common cancers (described above) were used in these studies (20, 22, 23), and whether HLA-I heterozygosity improves OS is still unknown.

The purpose of this study was to analyze the prevalence of the immunotherapy-related indicators described above within rare tumors in China, so as to provide more insight into the treatment options for these patients.

METHODS

Patient Recruitment

According to the definition and update of rare tumors published/established by the China National Cancer Center (3), we collected and retrospectively analyzed data on immunotherapy-related indicators from a total of 852 rare tumors patients in the Geneplus database, including 136 reports of PD-L1 expression, 821 reports of TMB, 705 of MSI and 355 of HLA-I heterozygosity.

The patients were enrolled from multiple medical canters and hospitals in China from September 2015 to February 2020. After signed written informed consent, all patients were tested by next generation sequencing (NGS) in Geneplus-Beijing Institute. Meanwhile, all patients were stratified into different clinicopathological groups according to the OncoTrees. During data analysis, two subtype tumors namely biliary tumors (including gallbladder cancer and extrahepatic cholangiocarcinoma) and

Abbreviations: CSF, cerebrospinal fluid; CUP, carcinoma of unknown primary; dMMR, mismatch repair-deficient; FDA, Food and Drug Administration; FFPE, formalin-fixed paraffin-embedded; HLA-I, human leukocyte antigen class I; ICIs, immune checkpoint inhibitors; IHC, immunohistochemistry; InDels, Small insertions and deletions; MSI, microsatellite instability; NETs, neuroendocrine tumors; NGS, next generation sequencing; NSCLC, non-small-cell lung cancer; OS, overall survival; PCR, polymerase chain reaction; PD-L1, programmed cell death ligand-1; SNV, single nucleotide variants; TMB, tumor mutational burden.

NETs drew our attentions due to the high prevalence of TMB. (**Supplementary Table 1**)

PD-L1 Expression

PD-L1 expression was assessed in formalin fixed paraffin embedded (FFPE) tumor tissues using the PD-L1 IHC 22C3 pharmDx assay (Dako, Carpinteria, CA, USA) in 94 patients; using the SP263 pharmDx assay (Ventana Automated Systems, Inc., Tucson, AZ, USA) in 21 patients; and using an unknown method in 21 patients (The PD-L1 test results of these patients were obtained from the previous medical records, and the detection method was not described).

The 22C3 pharmDx assay were performed according to the manufacturers' instructions. The sections were stained with the anti-PD-L1 22C3 mouse monoclonal primary antibody, and then the EnVision FLEX visualization system (Agilent, Santa Clara, CA, USA) was performed on an Autostainer Link 48 system (Dako). The negative control reagents and cell line were also tested simultaneously as control (24).

For SP263 pharm Dx assay, OptiView DAB IHC Detection kit (Ventana Medical Systems, Basel, Switzerland) was used to stain the sections with SP263 anti-PD-L1 rabbit monoclonal primary antibody, and the analysis was performed on Ventana Bench-Mark XT automated staining platform (Ventana Automated Systems).

The results of PD-L1 immunohistochemistry (IHC) were interpreted by pathologists. The expression of PD-L1 in both tumor cells and immune cells was evaluated. The criterion of PD-L1 positive staining in tumor cells was that the complete or partial circumferential linear membrane staining can be distinguished from background and diffuse cytoplasmic staining at any intensity (25). After recording the proportion of positive cells on the whole section, the PD-L1 positive rate of tumor cells was scored relative to the whole tumor area (26). PD-L1 expression in tumor infiltrating lymphocytes was defined as any staining intensity in cell membrane or cytoplasm. The threshold of PD-L1 positive was 1%.

Next-Generation Sequencing

All tissue samples included in this study were reexamined pathologically to confirm the histological classification and to ensure that at least 20% of the tumor cells were present for adequate detection. Genomic profiling was performed by Gene +Seq 2000 instrument or Illumina Nextseq CN 500 in the Geneplus-Beijing laboratory, which was accredited by American College of Pathologists (27, 28). Briefly, QIAamp DNA FFPE Tissue kit (Qiagen, Valencia, CA) was used to extract genomic tumor DNA from serial sections of FFPE tumor tissues. ctDNA was isolated from 4 to 5mL of plasma using the QIAamp Circulating Nucleic Acid Kit (Qiagen, Valencia, CA). DNA from leukocytes was extracted using the DNeasy Blood Kit (Qiagen, Valencia, CA). Sequencing libraries were prepared from ctDNA using KAPA DNA Library Preparation Kits (Kapa Biosystems, Wilmington, MA, USA), and genomic DNA sequencing libraries were prepared with Illumina TruSeq DNA Library Preparation Kits (Illumina, San Diego, CA). Libraries were hybridized to custom-designed biotinylated oligonucleotide probes (Roche NimbleGen, Madison, WI, USA) targeting 1,021 genes (~1.4 Mbp genomic regions of 1,021 cancer-related genes) (**Supplementary Table 2**) and HLA-I locus (A, B, and C). Prepared libraries were sequenced on using the Illumina Nextseq CN 500 (Illumina, San Diego, CA) or Gene+Seq 2000 (Geneplus-Beijing, China). Target capture sequencing required a minimal mean effective depth of coverage of 100× in leukocytes, 300× in tumor tissue and 1,000× in cell-free DNA samples.

Sequencing data were analyzed using default parameters. After removing adaptor sequences and low-quality reads, Burrows-Wheeler Aligner (BWA; version 0.7.12-r1039) was used to aligned the clean reads to the reference human genome (hg19). GATK (version 3.4-46-gbc02625) was performed for realignment and recalibration. MuTect (version 1.1.4) and NChot were used for single nucleotide variants (SNV) calling (29). GATK and CONTRA (v2.0.8) were performed to identify small inserts and deletions (InDels), and somatic copy number alternations, respectively. Finally, Integrative Genomics Viewer was used to manually verified all of the final candidate variants.

Biomarker Analysis

TMB Analysis

Somatic nonsynonymous SNV and InDels mutations in coding regions, with allele frequency ≥ 0.03 in tumor tissue sample or ≥ 0.005 in ctDNA sample respective, were included in TMB calculation. TMB was defined as the number of above mutations per megabase of genome. Based on 2000 samples from Geneplus database, the threshold of TMB-H was identified as the top quartile and determined to be ≥ 9 mutations per megabase (30, 31).

MSI Status

MSIsensor (v0.2) was used to inferred the MSI statuses, which reported the percentage of somatic unstable microsatellites in predefined microsatellite regions in our panel based on chi-squared test (32). All parameters used the default settings. According to the MSIsensor scores of tumor samples and matched normal samples, the MSI-H threshold was established by MSI polymerase chain reaction (PCR) and MMR IHC cross validation. And the threshold of MSI-H was 8.

HLA-I Typing

HLA-I typing was done using the OptiType v1.0 to obtain the four-digit HLA type at each locus of a patient (33). OptiType performs HLA typing using a combinatorial optimization approach. Reads were mapped to a reference panel consisting of HLA Class I allele sequences centered around their most polymorphic, and functionally most important region, exons 2 and 3 (34). HLA I-homozygous was defined as homozygosity for at least one HLA-I locus (A, B, or C), and HLA I- heterozygous as heterozygosity for all of the three HLA-I locus.

RESULTS

Clinicopathological Characteristics of Patients

Eight hundred and fifty-two patients (852) with rare tumors were included in this study. **Table 1** summarized the

TABLE 1 | Clinicopathological characteristics of patients.

Characteristic	Pts. (N=852) (%)
Age, years	
median	54
range	1–91
Gender	
female	395(46.4%)
male	457(53.6%)
Specimen.	
tumor tissue	671(78.8%)
ctDNA	160(18.8%)
pleural effusion	10(1.2%)
peritoneal effusion	10(1.2%)
CSF	1(0.1%)
System	
1.head and neck	33(3.9%)
2.digestive	98(11.5%)
3.respiratory	78(9.2%)
4.reproductive	31(3.6%)
5.urinary	6(0.7%)
6.multiple system	25(2.9%)
7.skin	16(1.9%)
8.soft tissue	180(21.1%)
9.bone	6(0.7%)
10.endocrine	2(0.2%)
11.neural	260(30.5%)
12.CUP	117(13.7%)

clinicopathological characteristics of all patients. The median age was 54, and male patients accounted for 53.6% (457/852). Among these patients, 671, 160, 10, 10, and 1 patients respectively used tumor tissue, ctDNA, pleural effusion, peritoneal effusion, as well as cerebrospinal fluid (CSF) samples for genetic analysis. These 852 cases included 91 tumor subtypes in rare tumor types, with neural, soft tissue, CUP, digestive, and respiratory systems as the top 5 tumors systems including 264, 180, 113, 98, and 78 patients, respectively.

Predictive Factors

Within the 136 patients who underwent PD-L1 immunohistochemistry, 65 patients had PD-L1 positive tumors (47.8%). CUP, respiratory, multiple system, digestive and soft tissue systems were the top 5 systems with 76.5% (13/17), 65.4% (17/26), 44.4% (4/9), 40.0% (8/20), and 39.4% (13/33) positivity rates, respectively.

Somatic mutations were detected in most patients (98.9%, 843/852). The most common mutant genes were TP53 (40.8%), TERT (17.2%), and CNKN2A (13.4%) (Top 20 mutant genes were summarized in **Figure 1**). Except NF2, KIT and TERT were the most common mutant genes in multiple system, soft tissue system and neural system, respectively, TP53 was the most common mutant gene in the other nine systems (Top 5 mutant genes in 12 systems were summarized in **Figure 2**).

TMB-H was identified in 127 patients among 821 patients (15.5%). Prevalence of TMB-H varied widely across tumor systems, ranging from 0% in patients with bone system disease to 50.0% in patients in urinary or endocrine system disease. Urinary, endocrine, respiratory, skin and CUP systems were the top 5 systems with 50.0% (3/6), 50.0% (1/2), 27.8% (20/72), 26.7% (4/15), and 21.2% (24/113) TMB-H rate, respectively. Considering the tumor subtypes, NETs and biliary tumors were both higher, reaching 50% (9/18) and 25.4% (15/59) respectively.

MSI-H was identified in 7.4% patients (52/705). Bone, neural, respiratory, reproductive and head and neck systems were the top 5 systems with 25.0% (1/4), 15.6% (39/250), 5.0% (3/60), 5.0% (1/20), and 4.8% (1/21) positivity rates, respectively.

It should be noted that the rates of PD-L1 positivity, TMB-H, and MSI-H in CUP were relatively high, with 76.5% (13/17), 21.1% (24/113), and 4.5% (4/89), respectively. While the proportion of both TMB-H and MSI-H in soft tissue sarcomas

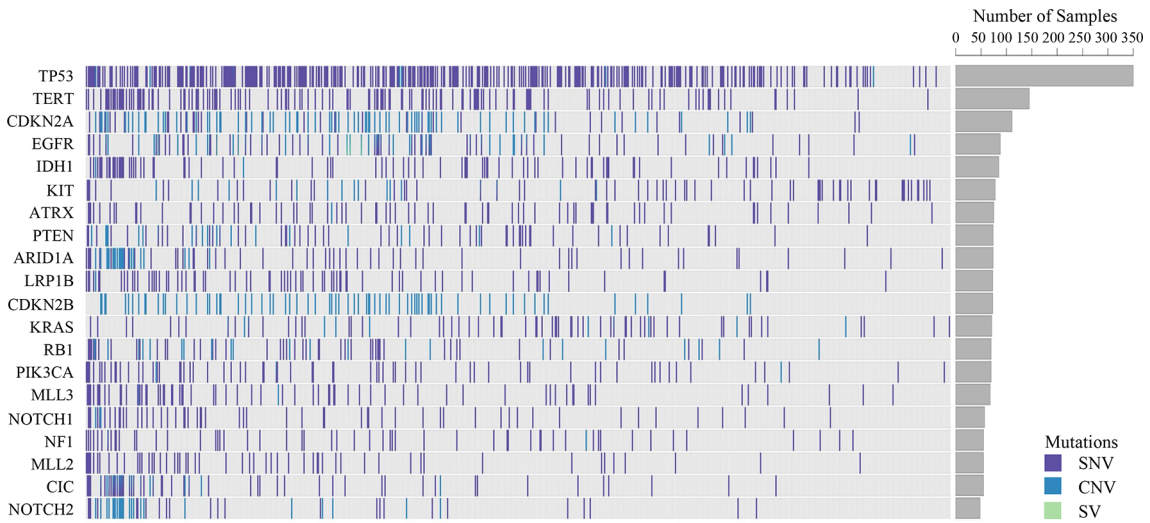

FIGURE 1 | Top 20 mutant genes of all samples.

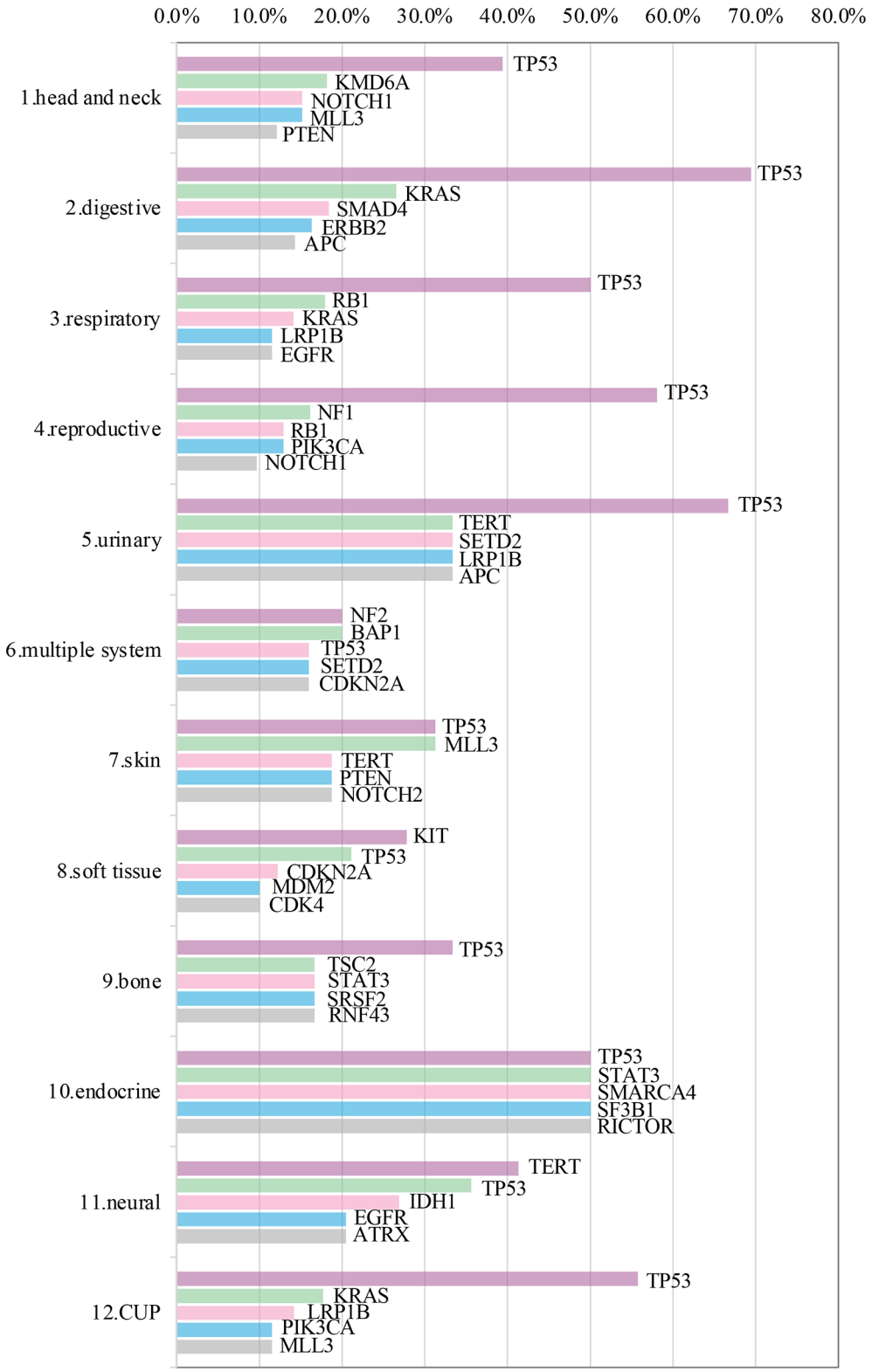

FIGURE 2 | Top 5 mutant genes in 12 systems.

was very low, with 4.1% (7/171) and 2.1% (3/143) respectively. (Prevalence of immunotherapy related indicators in rare tumor samples are summarized in **Table 2** and **Figure 3**).

Among the above patients, 135 patients were tested for both TMB and PD-L1, while 685 patients were tested for both TMB and MSI. The consistency ratio of TMB results and PD-L1 results was 54.8% (78/135), while that of TMB and MSI was 87.3% (598/685) (**Table 3**). We summarized the consistency data of five systems with larger sample size, including soft tissue, respiratory, digestive, CUP, and neural system. The consistency data of most systems were consistent with the overall consistency data, but there were some special cases in some systems, including the consistency ratio of TMB and PD-L1 in digestive system was as high as 70.0% (14/20), and that of TMB and MSI in respiratory system was as low as 69.5% (41/59) (**Figure 4**).

Prognostic Factors

A total of 78.9% (280/355) patients were identified as HLA class I-heterozygous. The top 5 systems were urinary, multiple

TABLE 3 | Consistency analysis of tumors mutational burden (TMB) and human leukocyte antigen class I (HLA-I) with programmed cell death ligand-1 (PD-L1) and microsatellite instability (MSI).

Testing method	TMB (tissue)		TMB (ctDNA)		HLA-I	
	High	Low	High	Low	Het	Hom
PD-L1 (+)	8	50	1	6	40	12
PD-L1 (–)	4	60	1	5	48	14
MSI-H	37	14	0	0		
MSS	59	533	14	28		

TABLE 2 | Prevalence of immunotherapy related indicators in rare tumor samples.

Systems	PD-L1 test	PD-L1(+)	%	22C3 test	22C3 (+)	%	SP263 test	SP263 (+)	%	TMB test	TMB-H	%	MSI test	MSI-H	%	HLA-I	HLA-I Het	%
Total	136	65	47.8	94	38	40.4	21	18	85.7	821	127	15.5	705	52	7.4	355	280	78.9
1.head and neck	8	3	37.5	5	1	20.0	1	1	100.0	31	6	19.4	21	1	4.8	17	15	88.2
2.digestive	20	8	40.0	13	3	23.1	6	5	83.3	96	19	19.8	78	0	0.0	68	52	76.5
biliary	11	5	45.5	7	2	28.6	3	3	100.0	59	15	25.4	51	0	0.0	40	29	72.5
3.respiratory	26	17	65.4	13	9	69.2	5	5	100.0	72	20	27.8	60	3	5.0	33	28	84.8
neuroendocrine	6	2	33.3	2	1	50.0	1	1	100.0	18	9	50.0	17	1	5.9	6	5	83.3
4.reproductive	3	1	33.3	2	1	50.0				30	2	6.7	20	1	5.0	9	7	77.8
5.urinary										6	3	50.0	6	0	0.0	2	2	100.0
6.multiple system	9	4	44.4	7	3	42.9	1	0	0.0	23	2	8.7	20	0	0.0	18	16	88.9
7.skin	6	1	16.7	4	0	0.0	2	1	50.0	15	4	26.7	13	0	0.0	13	10	76.9
8.soft tissue	33	13	39.4	24	7	29.2	4	4	100.0	171	7	4.1	143	3	2.1	80	63	78.8
9.bone										5	0	0.0	4	1	25.0	4	3	75.0
10.endocrine										2	1	50.0	1	0	0.0			
11.neural	14	5	35.7	12	4	33.3				257	39	15.2	250	39	15.6	47	36	76.6
12.CUP	17	13	76.5	14	10	71.4	2	2	100.0	113	24	21.2	89	4	4.5	64	48	75.0

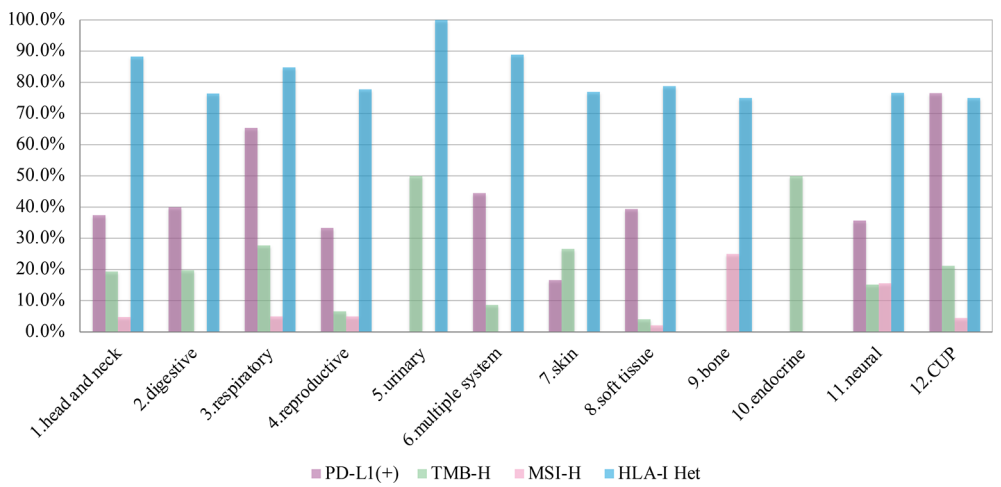

FIGURE 3 | The prevalence of programmed cell death ligand-1 (PD-L1) positive, tumors mutational burden (TMB)-H, microsatellite instability (MSI)-H, and human leukocyte antigen class I (HLA)-I Het in 12 systems.

A. Soft tissue system

	TMB		
	High	Low	Total
PD-L1(+)	0(0%)	12(100%)	12
PD-L1(-)	0(0%)	19(100%)	19
Total	0(0%)	31(100%)	31
Consistency ratio	61.3%		

B. Soft tissue system

	TMB		
	High	Low	Total
MSI-H	2(67%)	1(33%)	3
MSS	3(2%)	135(98%)	138
Total	5(4%)	136(96%)	141
Consistency ratio	97.2%		

C. Soft tissue system

	HLA-I		
	Het	Hom	Total
PD-L1(+)	6(55%)	5(45%)	11
PD-L1(-)	12(71%)	5(29%)	17
Total	18(64%)	10(36%)	28
Consistency ratio	39.3%		

D. Respiratory system

	TMB		
	High	Low	Total
PD-L1(+)	4(27%)	11(73%)	15
PD-L1(-)	1(14%)	6(86%)	7
Total	5(23%)	17(77%)	22
Consistency ratio	45.5%		

E. Respiratory system

	TMB		
	High	Low	Total
MSI-H	2(67%)	1(33%)	3
MSS	17(30%)	39(70%)	56
Total	19(32%)	40(68%)	59
Consistency ratio	69.5%		

F. Respiratory system

	HLA-I		
	Het	Hom	Total
PD-L1(+)	10(83%)	2(17%)	12
PD-L1(-)	6(100%)	0	6
Total	16(89%)	2(11%)	18
Consistency ratio	55.6%		

G. Digestive system

	TMB		
	High	Low	Total
PD-L1(+)	2(25%)	6(75%)	8
PD-L1(-)	0(0%)	12(100%)	12
Total	2(10%)	18(90%)	20
Consistency ratio	70.0%		

H. Digestive system

	TMB		
	High	Low	Total
MSI-H	0	0	0
MSS	15(19%)	63(81%)	78
Total	15(19%)	63(81%)	78
Consistency ratio	80.8%		

I. Digestive system

	HLA-I		
	Het	Hom	Total
PD-L1(+)	7(88%)	1(13%)	8
PD-L1(-)	8(67%)	4(33%)	12
Total	15(75%)	5(25%)	20
Consistency ratio	55.0%		

J. CUP

	TMB		
	High	Low	Total
PD-L1(+)	1(8%)	11(92%)	12
PD-L1(-)	1(25%)	3(75%)	4
Total	2(13%)	14(88%)	16
Consistency ratio	25.0%		

K. CUP

	TMB		
	High	Low	Total
MSI-H	3(75%)	1(25%)	4
MSS	15(19%)	66(81%)	81
Total	18(21%)	67(79%)	85
Consistency ratio	81.2%		

L. CUP

	HLA-I		
	Het	Hom	Total
PD-L1(+)	9(90%)	1(10%)	10
PD-L1(-)	2(50%)	2(50%)	4
Total	11(79%)	3(21%)	14
Consistency ratio	78.6%		

M. Neural system

	TMB		
	High	Low	Total
PD-L1(+)	0(0%)	6(100%)	6
PD-L1(-)	2(22%)	7(78%)	9
Total	2(13%)	13(87%)	15
Consistency ratio	46.7%		

N. Neural system

	TMB		
	High	Low	Total
MSI-H	29(74%)	10(26%)	39
MSS	12(6%)	202(94%)	214
Total	41(16%)	212(84%)	253
Consistency ratio	91.3%		

O. Neural system

	HLA-I		
	Het	Hom	Total
PD-L1(+)	2(67%)	1(33%)	3
PD-L1(-)	7(78%)	2(22%)	9
Total	9(75%)	3(25%)	12
Consistency ratio	33.3%		

FIGURE 4 | Consistency analysis of tumors mutational burden (TMB) and human leukocyte antigen class I (HLA-I) with programmed cell death ligand-1 (PD-L1) and microsatellite instability (MSI) in main systems. **(A–C)** soft tissue systems, **(D–F)** respiratory system, **(G-I)** digestive system, **(J–L)** CUP, **(M–O)** neural system.

system, head and neck, respiratory and soft tissue system with 100% (2/2), 88.9% (16/18), 88.2% (15/17), 84.8% (28/33), and 78.8% (63/80) heterozygous rate, respectively (**Figure 3**). Among them, 114 patients were tested for PD-L1, and the consistency ratio of HLA-I results and PD-L1 results was 47.4% (54/114) (**Table 3**). The consistency of the five systems with larger sample size were also summarized, and the consistency ratio of HLA-I and PD-L1 in CUP was as high as 78.6% (11/14) (**Figure 4**).

DISCUSSION

The purpose of this study is to explore potential novel indications for the treatment of rare tumors in China. Results show that the

clinical benefit-related indicators for immunotherapy are frequently present in rare tumors, though their prevalence varied widely across tumor systems and subtypes.

PD-L1 is the first internationally recognized therapeutic indicator in immunotherapy. PD-L1 positivity is required in some indications approved for immunotherapy, including in NSCLC, gastric cancer, esophageal cancer, cervical cancer, head and neck tumor and triple negative breast cancer. We compared the prevalence of PD-L1 positivity in this study (47.8%) to those of several common cancers with approved indications of immunotherapy (**Figure 5**) (35–37). We found that the overall prevalence of PD-L1 positive in this study was higher than that of the above approved common tumors, except NSCLC (54.2% ~66%) and head and neck tumor (64.9%). This suggests that rare tumors have a greater chance to benefit from immunotherapy than most common tumors. In addition to advanced tumors, studies are also underway to assess the predictive value of PD-L1 expression for early-stage tumors. In a neoadjuvant study of NSCLC, major pathologic response was found to be positively correlated with PD-L1 expression. In patients who have never given anti-tumor therapy, if pathological remission can be proved to be related to PD-L1 expression, other interference factors that lead to the heterogeneity of tumor PD-L1 detection are excluded (38). The predictive value of PD-L1 in early-stage rare tumors is another interesting area to explore.

TMB is another promising immunotherapeutic biomarker. Many studies have found that high TMB in immunotherapy is highly correlated with clinical benefit. For example, TMB-H in tissue (defined as >200 mutations in exome) was associated with durable clinical benefit and longer progression-free survival in NSCLC patients treated with pembrolizumab as monotherapy. Similarly, in patients with melanoma given ipilimumab, higher TMB in tissue (evaluated by whole-exome sequencing and measured as a continuous variable) was also associated with improved outcomes (39, 40). Additionally, in NSCLC patients treated with nivolumab combined with ipilimumab, at least 10 mutations per megabase of tissue TMB were associated with improved clinical outcomes (41, 42). It was also observed that in NSCLC patients treated with durvalumab plus tremelimumab or atezolizumab, TMB with ≥16 mutations per megabase in ctDNA based on blood samples was associated with improved clinical outcomes (43, 44). Data of some small retrospective studies also showed that issue TMB was associated with improved outcomes in ICIs for multiple tumor types (45, 46), other studies including the prospective KEYNOTE-158 study suggested that, across multiple tumor types patients with ICIs therapy, increased levels of tissue TMB were associated with higher response rates (20, 47).

However, some studies have shown that TMB cannot predict the efficacy of immunotherapy. Several studies, including KEYNOTE-021 and KEYNOTE-189, have shown that TMB cannot predict the clinical outcomes of corresponding first-line immunotherapy for NSCLC (48, 49). The overall prevalence of TMB-H in this study was 15.5%, similar to that reported in the KEYNOTE-158 study. Also, in our study, NETs and biliary tumors had much higher TMB-H rates than that in the KEYNOTE-158 study (43.8% vs 29.3%, 25.5% vs 4.0%, respectively) (20, 50). Given the high prevalence of TMB-H status in rare tumors, the effect of TMB on immunotherapy response in rare tumors deserves further exploration.

MSI status, along with PD-L1 and TMB, is another possibly independent, predictive indication for ICIs. MSI-H has been confirmed in many studies to predict the response of various solid tumors to ICIs and has been approved by FDA as the first indication biomarker for pan-cancer immunotherapy (9, 51). MSI is most common in colon and endometrial cancer (highly associated with Lynch syndrome), where it can be as high as 15% and 28% respectively, but relatively low in other cancers (52, 53). According to several large-scale studies, the overall incidence of MSI-H in all cancers is about 3% (36, 51, 54). In these studies, in addition to colon and endometrial cancer, the incidence of MSI-H in gastric adenocarcinoma (3.4%~9%) and small intestinal malignancies (4.6%~8%) is also relatively high, while it is low in NSCLC (<1%) and melanoma (nearly 0). In our analysis, the prevalence of MSI-H in rare tumors in China was 7.4%, which was higher than that reported across all cancers. Additionally,

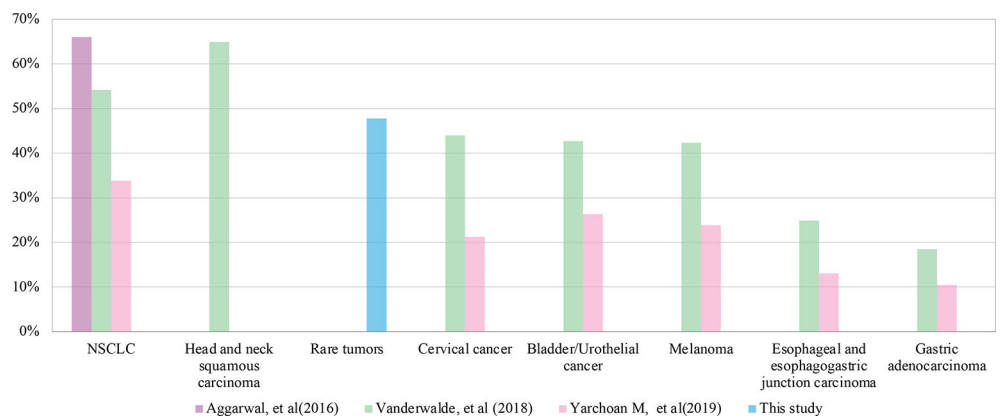

FIGURE 5 | Comparison of programmed cell death ligand-1 (PD-L1) positive rates between rare tumors and common tumors in different studies.

prevalence of MSI-H in head and neck, CUP and soft tissue systems tumors in this study was still higher than that reported in previous studies abroad (4.8% vs. 0.5%, 4.5% vs. 1.9%, 2.1% vs. 0.2%, respectively) (54).

This study also included HLA-I heterozygosity as a prognostic indicator of immunotherapy and was the first study on HLA-I heterozygosity in rare tumors. Previous studies have shown that in ICIs treatment patients across multiple cancer types (including NSCLC and melanoma), heterozygous HLA-I genotyps improved OS compared with patients who were homozygous for at least one HLA locus (17). Our data show a heterozygous rate of HLA-I of 78.9% in rare tumors, which was similar to that previously reported in NSCLC (77.5%~78.4%) (19).

In our analysis of the relationship between the indicators, the concordance between TMB and PD-L1 was only 54.8%, indicating they are independent in predicting the benefit of immunotherapy, which is the same as that of common tumors (55). The same situation was found in HLA-I and PD-L1, with a consistency of 47.4%. However, TMB and MSI showed a high positive correlation (87.3%), which was similar to that of colorectal cancers (36). The consistency data of most systems were consistent with the overall consistency data, but some systems shown particularity, which reminds us that further research can be put into these tumors.

Within the subgroups of rare tumors, we noted that the positivity rates of PD-L1, TMB-H and MSI-H in CUP were relatively high, indicating that immunotherapy is a worthwhile treatment option. The proportion of both TMB-H and MSI-H in soft tissue sarcomas is very low, suggesting that patients with such tumors are less likely to benefit from immunotherapy.

Due to the small number of cases in each rare tumor subtype, it is difficult to compare the details of each tumor subtype in this study. So we classified tumor subtypes into various tumor systems, and then compared the indicators. In addition, since the patients of some rare tumor systems were limited, especially in the urinary, bone and endocrine systems, the prevalence of the four indicators analyzed in this study may be divergent from the actual situation. However, this study captures the overall situation of immunotherapy-related indicators of rare tumors and supports that a considerable proportion of patients with rare tumors can benefit from immunotherapy.

Based on the previous study (CITE) and this study, we designed the PLATFORM study. PLATFORM is an open, non-randomized, multicohort, single arm, single center phase II clinical study in advanced rare solid tumors that have been treated with or without standard treatment. The main purpose of the PLATFORM study is to evaluate the safety and efficacy of targeted drugs approved in China and to evaluate/test targeted therapy for specific tumor driver genes in patients with advanced rare solid tumor patients who have corresponding targets, as well as to evaluate the safety and efficacy of ICIs (PD-1 antibodies) in patients with advanced rare solid tumors who have no druggable target mutations. Patients with advanced rare solid tumors who failed or did not have standard treatment will be included in the study. Based on the results of gene detection, the subjects carrying the targets "EGFR mutation, ALK gene fusion, ROS-1 gene fusion, MET gene amplification or mutation, BRAF mutation, BRCA1/2 mutation, HER-2 positive, KIT mutation and CDKN2A mutation" will be divided into 13 arms according to the types of gene variation, and will be divided into 9 targeted treatment study groups and given the corresponding targeted drug/agent (Almonertinib, Dacomitinib, Alectinib, Crizotinib, Vemurafenib, Niraparib, Pyrotinib, Imatinib, Palbociclib). Subjects without the above targets will be enrolled in the immunotherapy group and treated with PD-1 inhibitor monotherapy. During the treatment, the usage and dosage of the above drugs, the principle of dose adjustment and matters needing attention will all be referred to the drug labels and instructions. All AE/SAE of the above drugs in advanced rare solid tumors will be collected for safety analysis. After the patients are enrolled in the corresponding targeted treatment group, they will be treated according to the standard dosage/manufacturer's recommended dosage until the disease progresses or intolerable adverse reactions occur. The PLATFORM study is the first platform study for rare tumors in the world. We look forward to increasing opportunities for Chinese patients with rare tumors to benefit from targeted therapy and immunotherapy through this world leading research method and innovative structure/design. (NCT04423185)

The most important purpose of this study is to raise awareness of the necessity of rare tumor research among Chinese clinical workers, government officials and drug investigators around the world. Even though there is no consensus and effective treatment guidelines in China, we think that promoting the development of new drugs and treatment strategies of rare tumors will be fruitful. In view of the high prevalence of immunotherapy related indicators in the rare tumors population and limited treatment options of these patients, adequate efforts should be made for rare tumors in the near future.

CONCLUSIONS

This study included 852 tumor samples from patients whose tumors met the definition of rare tumor in China. We analyzed the prevalence of immunotherapy predictors and prognostic indicators, including PD-L1, TMB, MSI, and HLA-I, and their consistency. The results showed that a considerable proportion of rare tumor patients are positive for the above indicators, and especially that nearly half of patients were PD-L1 positive, suggesting that they could benefit from immunotherapy. Comprehensive genomic profiling may offer novel therapeutic modalities for patients with rare tumors to solve the dilemma of limited treatment options. All of the above facilitates the development of new drug investigations and treatment improvement for rare tumors in the future.

DATA AVAILABILITY STATEMENT

The datasets presented in this study can be found in online repositories. The names of the repository/repositories

and accession number(s) can be found in the article/ **Supplementary Material**.

AUTHOR CONTRIBUTIONS

NL designed the study. ZZ directed the data analysis and gave important suggestion on the revision. XY helped design the study but was not involved in the data analysis and revision. SW performed the study and analyzed the data. SW, YF, NJ, SX, QL, RC, and NL composed the manuscript. All authors contributed to the article and approved the submitted version.

ACKNOWLEDGMENTS

We thank the patients for voluntarily providing valuable medical and genetic data for scientific analysis.

SUPPLEMENTARY MATERIAL

The Supplementary Material for this article can be found online at: https://www.frontiersin.org/articles/10.3389/fimmu.2021.631483/full#supplementary-material

Supplementary Table 1 | Patients' clinicopathological subgroups and immunotherapy related indicators data.

Supplementary Table 2 | 1021 genes list.

REFERENCES

1. Gatta G, van der Zwan JM, Casali PG, Siesling S, Dei Tos AP, Kunkler I, et al. Rare cancers are not so rare: the rare cancer burden in Europe. *Eur J Cancer* (2011) 47(17):2493–511. doi: 10.1016/j.ejca.2011.08.008
2. Greenlee RT, Goodman MT, Lynch CF, Platz CE, Havener LA, Howe HL. The occurrence of rare cancers in U.S. adults, 1995-2004. *Public Health Rep* (2010) 125(1):28–43. doi: 10.1177/003335491012500106
3. Wang S, Chen R, Tang Y, Yu Y, Fang Y, Huang H, et al. Comprehensive Genomic Profiling of Rare Tumors: Routes to Targeted Therapies. *Front Oncol* (2020) 10:536. doi: 10.3389/fonc.2020.00536
4. Darvin P, Toor SM, Sasidharan Nair V, Elkord E. Immune checkpoint inhibitors: recent progress and potential biomarkers. *Exp Mol Med* (2018) 50 (12):1–11. doi: 10.1038/s12276-018-0191-1
5. Ribas A, Wolchok JD. Cancer immunotherapy using checkpoint blockade. *Science* (2018) 359(6382):1350–5. doi: 10.1126/science.aar4060
6. Akinleye A, Rasool Z. Immune checkpoint inhibitors of PD-L1 as cancer therapeutics. *J Hematol Oncol* (2019) 12(1):92. doi: 10.1186/s13045-019-0779-5
7. Patel SP, Kurzrock R. PD-L1 Expression as a Predictive Biomarker in Cancer Immunotherapy. *Mol Cancer Ther* (2015) 14(4):847–56. doi: 10.1158/1535-7163.MCT-14-0983
8. Mok TSK, Wu YL, Kudaba I, Kowalski DM, Cho BC, Turna HZ, et al. Pembrolizumab versus chemotherapy for previously untreated, PD-L1-expressing, locally advanced or metastatic non-small-cell lung cancer (KEYNOTE-042): a randomised, open-label, controlled, phase 3 trial. *Lancet* (2019) 393(10183):1819–30. doi: 10.1016/S0140-6736(18)32409-7
9. Le DT, Uram JN, Wang H, Bartlett BR, Kemberling H, Eyring AD, et al. PD-1 Blockade in Tumors with Mismatch-Repair Deficiency. *N Engl J Med* (2015) 372(26):2509–20. doi: 10.1056/NEJMoa1500596
10. Overman MJ, McDermott R, Leach JL, Lonardi S, Lenz HJ, Morse MA, et al. Nivolumab in patients with metastatic DNA mismatch repair-deficient or microsatellite instability-high colorectal cancer (CheckMate 142): an open-label, multicentre, phase 2 study. *Lancet Oncol* (2017) 18(9):1182–91. doi: 10.1016/S1470-2045(17)30422-9
11. Le DT, Kim TW, Van Cutsem E, Geva R, Jager D, Hara H, et al. Phase II Open-Label Study of Pembrolizumab in Treatment-Refractory, Microsatellite Instability-High/Mismatch Repair-Deficient Metastatic Colorectal Cancer: KEYNOTE-164. *J Clin Oncol* (2020) 38(1):11–9. doi: 10.1200/JCO.19.02107
12. Marcus L, Lemery SJ, Keegan P, Pazdur R. FDA Approval Summary: Pembrolizumab for the Treatment of Microsatellite Instability-High Solid Tumors. *Clin Cancer Res* (2019) 25(13):3753–8. doi: 10.1158/1078-0432.CCR-18-4070
13. Samstein RM, Lee CH, Shoushtari AN, Hellmann MD, Shen R, Janjigian YY, et al. Tumor mutational load predicts survival after immunotherapy across multiple cancer types. *Nat Genet* (2019) 51(2):202–6. doi: 10.1038/s41588-018-0312-8
14. Reck M, Schenker M, Lee KH, Provencio M, Nishio M, Lesniewski-Kmak K, et al. Nivolumab plus ipilimumab versus chemotherapy as first-line treatment in advanced non-small-cell lung cancer with high tumour mutational burden: patient-reported outcomes results from the randomised, open-label, phase III CheckMate 227 trial. *Eur J Cancer* (2019) 116:137–47. doi: 10.1016/j.ejca.2019.05.008
15. Jiang T, Shi J, Dong Z, Hou L, Zhao C, Li X, et al. Genomic landscape and its correlations with tumor mutational burden, PD-L1 expression, and immune cells infiltration in Chinese lung squamous cell carcinoma. *J Hematol Oncol* (2019) 12(1):75. doi: 10.1186/s13045-019-0762-1
16. Gubin MM, Zhang X, Schuster H, Caron E, Ward JP, Noguchi T, et al. Checkpoint blockade cancer immunotherapy targets tumour-specific mutant antigens. *Nature* (2014) 515(7528):577–81. doi: 10.1038/nature13988
17. Chowell D, Morris LGT, Grigg CM, Weber JK, Samstein RM, Makarov V, et al. Patient HLA class I genotype influences cancer response to checkpoint blockade immunotherapy. *Science* (2018) 359(6375):582–7. doi: 10.1126/science.aao4572
18. Chowell D, Krishna C, Pierini F, Makarov V, Rizvi NA, Kuo F, et al. Evolutionary divergence of HLA class I genotype impacts efficacy of cancer immunotherapy. *Nat Med* (2019) 25(11):1715–20. doi: 10.1038/s41591-019-0639-4
19. Negrao MV, Lam VK, Reuben A, Rubin ML, Landry LL, Roarty EB, et al. PD-L1 Expression, Tumor Mutational Burden, and Cancer Gene Mutations Are Stronger Predictors of Benefit from Immune Checkpoint Blockade than HLA Class I Genotype in Non-Small Cell Lung Cancer. *J Thorac Oncol* (2019) 14 (6):1021–31. doi: 10.1016/j.jtho.2019.02.008
20. Marabelle A, Fakih M, Lopez J, Shah M, Shapira-Frommer R, Nakagawa K, et al. Association of tumour mutational burden with outcomes in patients with advanced solid tumours treated with pembrolizumab: prospective biomarker analysis of the multicohort, open-label, phase 2 KEYNOTE-158 study. *Lancet Oncol* (2020) 21(10):1353–65. doi: 10.1016/S1470-2045(20)30445-9
21. Naing A, Meric-Bernstam F, Stephen B, Karp DD, Hajjar J, Rodon Ahnert J, et al. Phase 2 study of pembrolizumab in patients with advanced rare cancers. *J Immunother Cancer* (2020) 8(1):e000347. doi: 10.1136/jitc-2019-000347
22. D'Angelo SP, Russell J, Lebbe C, Chmielowski B, Gambichler T, Grob JJ, et al. Efficacy and Safety of First-line Avelumab Treatment in Patients With Stage IV Metastatic Merkel Cell Carcinoma: A Preplanned Interim Analysis of a Clinical Trial. *JAMA Oncol* (2018) 4(9):e180077. doi: 10.1001/jamaoncol.2018.0077
23. Mehnert JM, Panda A, Zhong H, Hirshfield K, Damare S, Lane K, et al. Immune activation and response to pembrolizumab in POLE-mutant endometrial cancer. *J Clin Invest* (2016) 126(6):2334–40. doi: 10.1172/JCI84940
24. Kim H, Kwon HJ, Park SY, Park E, Chung JH. PD-L1 immunohistochemical assays for assessment of therapeutic strategies involving immune checkpoint inhibitors in non-small cell lung cancer: a comparative study. *Oncotarget* (2017) 8(58):98524–32. doi: 10.18632/oncotarget.21567

25. Phillips T, Simmons P, Inzunza HD, Cogswell J, Novotny J Jr, Taylor C, et al. Development of an automated PD-L1 immunohistochemistry (IHC) assay for non-small cell lung cancer. *Appl Immunohistochem Mol Morphol* (2015) 23 (8):541–9. doi: 10.1097/PAI.0000000000000256
26. Roach C, Zhang N, Corigliano E, Jansson M, Toland G, Ponto G, et al. Development of a Companion Diagnostic PD-L1 Immunohistochemistry Assay for Pembrolizumab Therapy in Non-Small-cell Lung Cancer. *Appl Immunohistochem Mol Morphol* (2016) 24(6):392–7. doi: 10.1097/PAI.0000000000000408
27. Sun S, Liu Y, Eisfeld AK, Zhen F, Jin S, Gao W, et al. Identification of Germline Mismatch Repair Gene Mutations in Lung Cancer Patients With Paired Tumor-Normal Next Generation Sequencing: A Retrospective Study. *Front Oncol* (2019) 9:550. doi: 10.3389/fonc.2019.00550
28. Zhuo M, Guan Y, Yang X, Hong L, Wang Y, Li Z, et al. The Prognostic and Therapeutic Role of Genomic Subtyping by Sequencing Tumor or Cell-Free DNA in Pulmonary Large-Cell Neuroendocrine Carcinoma. *Clin Cancer Res* (2020) 26(4):892–901. doi: 10.1158/1078-0432.CCR-19-0556
29. Yang X, Chu Y, Zhang R, Han Y, Zhang L, Fu Y, et al. Technical Validation of a Next-Generation Sequencing Assay for Detecting Clinically Relevant Levels of Breast Cancer-Related Single-Nucleotide Variants and Copy Number Variants Using Simulated Cell-Free DNA. *J Mol Diagn* (2017) 19(4):525–36. doi: 10.1016/j.jmoldx.2017.04.007
30. Jia Q, Wu W, Wang Y, Alexander PB, Sun C, Gong Z, et al. Local mutational diversity drives intratumoral immune heterogeneity in non-small cell lung cancer. *Nat Commun* (2018) 9(1):5361. doi: 10.1038/s41467-018-07767-w
31. Wang Y, Zhao C, Chang L, Jia R, Liu R, Zhang Y, et al. Circulating tumor DNA analyses predict progressive disease and indicate trastuzumab-resistant mechanism in advanced gastric cancer. *EBioMedicine* (2019) 43:261–9. doi: 10.1016/j.ebiom.2019.04.003
32. Niu B, Ye K, Zhang Q, Lu C, Xie M, McLellan MD, et al. MSIsensor: microsatellite instability detection using paired tumor-normal sequence data. *Bioinformatics* (2014) 30(7):1015–6. doi: 10.1093/bioinformatics/btt755
33. Szolek A, Schubert B, Mohr C, Sturm M, Feldhahn M, Kohlbacher O. OptiType: precision HLA typing from next-generation sequencing data. *Bioinformatics* (2014) 30(23):3310–6. doi: 10.1093/bioinformatics/btu548
34. Szolek A. HLA Typing from Short-Read Sequencing Data with OptiType. *Methods Mol Biol* (2018) 1802:215–23. doi: 10.1007/978-1-4939-8546-3_15
35. Aggarwal C, Abreu DR, Felip E, Carcereny E, Gottfried M, Wehler T, et al. Prevalence of PD-L1 expression in patients with non-small cell lung cancer screened for enrollment in KEYNOTE-001, -010, and -024 , in ESMO. *Ann Oncol* (2016) 27(S6):VI363. doi: 10.1093/annonc/mdw378.14
36. Vanderwalde A, Spetzler D, Xiao N, Gatalica Z, Marshall J. Microsatellite instability status determined by next-generation sequencing and compared with PD-L1 and tumor mutational burden in 11,348 patients. *Cancer Med* (2018) 7(3):746–56. doi: 10.1002/cam4.1372
37. Yarchoan M, Albacker LA, Hopkins AC, Montesion M, Murugesan K, Vithayathil TT, et al. PD-L1 expression and tumor mutational burden are independent biomarkers in most cancers. *JCI Insight* (2019) 4(6):e126908. doi: 10.1172/jci.insight.126908
38. Gao S, Li N, Gao S, Xue Q, Ying J, Wang S, et al. Neoadjuvant PD-1 inhibitor (Sintilimab) in NSCLC. *J Thorac Oncol* (2020) 15(5):816–26. doi: 10.1016/j.jtho.2020.01.017
39. Van Allen EM, Miao D, Schilling B, Shukla SA, Blank C, Zimmer L, et al. Genomic correlates of response to CTLA-4 blockade in metastatic melanoma. *Science* (2015) 350(6257):207–11. doi: 10.1126/science.aad0095
40. Rizvi NA, Hellmann MD, Snyder A, Kvistborg P, Makarov V, Havel JJ, et al. Cancer immunology. Mutational landscape determines sensitivity to PD-1 blockade in non-small cell lung cancer. *Science* (2015) 348(6230):124–8. doi: 10.1126/science.aaa1348
41. Hellmann MD, Ciuleanu TE, Pluzanski A, Lee JS, Otterson GA, Audigier-Valette C, et al. Nivolumab plus Ipilimumab in Lung Cancer with a High Tumor Mutational Burden. *N Engl J Med* (2018) 378(22):2093–104. doi: 10.1056/NEJMoa1801946
42. Ready N, Hellmann MD, Awad MM, Otterson GA, Gutierrez M, Gainor JF, et al. First-Line Nivolumab Plus Ipilimumab in Advanced Non-Small-Cell Lung Cancer (CheckMate 568): Outcomes by Programmed Death Ligand 1 and Tumor Mutational Burden as Biomarkers. *J Clin Oncol* (2019) 37 (12):992–1000. doi: 10.1200/JCO.18.01042
43. Rizvi NA, Cho BC, Reinmuth N, Lee KH, Ahn M-J, Luft A, et al. Durvalumab with or without tremelimumab vs platinum-based chemotherapy as first-line treatment for metastatic non-small cell lung cancer: MYSTIC, in ESMO. *Ann Oncol* (2018) 29(S10):X40–1. doi: 10.1093/annonc/mdy511.005
44. Velcheti V, Kim ES, Mekhail T, Dakhil C, Stella PJ, Shen X, et al. Socinski, Prospective clinical evaluation of blood-based tumor mutational burden (bTMB) as a predictive biomarker for atezolizumab (atezo) in 1L non-small cell lung cancer (NSCLC): Interim B-F1RST results., in ASCO. *J Clin Oncol* (2018) 36(15):S12001. doi: 10.1200/JCO.2018.36.15_suppl.12001
45. Cristescu R, Mogg R, Ayers M, Albright A, Murphy E, Yearley J, et al. Pan-tumor genomic biomarkers for PD-1 checkpoint blockade-based immunotherapy. *Science* (2018) 362(6411):eaar3593. doi: 10.1126/science.aar3593
46. Goodman AM, Kato S, Bazhenova L, Patel SP, Frampton GM, Miller V, et al. Tumor Mutational Burden as an Independent Predictor of Response to Immunotherapy in Diverse Cancers. *Mol Cancer Ther* (2017) 16(11):2598–608. doi: 10.1158/1535-7163.MCT-17-0386
47. Yarchoan M, Hopkins A, Jaffee EM. Tumor Mutational Burden and Response Rate to PD-1 Inhibition. *N Engl J Med* (2017) 377(25):2500–1. doi: 10.1056/NEJMc1713444
48. Langer C, Gadgeel S, Borghaei H, Patnaik A, Powell S, Gentzler R, et al. OA04.05 KEYNOTE-021: TMB and Outcomes for Carboplatin and Pemetrexed With or Without Pembrolizumab for Nonsquamous NSCLC, in WCLC. *J Thorac Oncol* (2019) 14(10):S216. doi: 10.1016/j.jtho.2019.08.426
49. Garassino M, Rodriguez-Abreu D, Gadgeel S, Esteban E, Felip E, Speranza G, et al. OA04.06 Evaluation of TMB in KEYNOTE-189: Pembrolizumab Plus Chemotherapy vs Placebo Plus Chemotherapy for Nonsquamous NSCLC. *J Thorac Oncol* (2019) 14(10):S216–7. doi: 10.1016/j.jtho.2019.08.427
50. Shao C, Li G, Huang L, Pruitt S, Castellanos E, Frampton G, et al. Prevalence of High Tumor Mutational Burden and Association With Survival in Patients With Less Common Solid Tumors. *JAMA Netw Open* (2020) 3(10):e2025109. doi: 10.1001/jamanetworkopen.2020.25109
51. Le DT, Durham JN, Smith KN, Wang H, Bartlett BR, Aulakh LK, et al. Mismatch repair deficiency predicts response of solid tumors to PD-1 blockade. *Science* (2017) 357(6349):409–13. doi: 10.1126/science.aan6733
52. Gupta R, Sinha S, Paul RN. The impact of microsatellite stability status in colorectal cancer. *Curr Probl Cancer* (2018) 42(6):548–59. doi: 10.1016/j.currproblcancer.2018.06.010
53. Cancer Genome Atlas Research N, Kandoth C, Schultz N, Cherniack AD, Akbani R, Liu Y, et al. Integrated genomic characterization of endometrial carcinoma. *Nature* (2013) 497(7447):67–73. doi: 10.1038/nature12113
54. Trabucco SE, Gowen K, Maund SL, Sanford E, Fabrizio DA, Hall MJ, et al. A Novel Next-Generation Sequencing Approach to Detecting Microsatellite Instability and Pan-Tumor Characterization of 1000 Microsatellite Instability-High Cases in 67,000 Patient Samples. *J Mol Diagn* (2019) 21 (6):1053–66. doi: 10.1016/j.jmoldx.2019.06.011
55. Rizvi H, Sanchez-Vega F, La K, Chatila W, Jonsson P, Halpenny D, et al. Molecular Determinants of Response to Anti-Programmed Cell Death (PD)-1 and Anti-Programmed Death-Ligand 1 (PD-L1) Blockade in Patients With Non-Small-Cell Lung Cancer Profiled With Targeted Next-Generation Sequencing. *J Clin Oncol* (2018) 36(7):633–41. doi: 10.1200/JCO.2017.75.3384

Conflict of Interest: The authors declare that the research was conducted in the absence of any commercial or financial relationships that could be construed as a potential conflict of interest.

frontiers in Immunology

ORIGINAL RESEARCH
published: 24 March 2021
doi: 10.3389/fimmu.2021.647209

PNOC Expressed by B Cells in Cholangiocarcinoma Was Survival Related and LAIR2 Could Be a T Cell Exhaustion Biomarker in Tumor Microenvironment: Characterization of Immune Microenvironment Combining Single-Cell and Bulk Sequencing Technology

Zheng Chen[1†], Mincheng Yu[1†], Jiuliang Yan[1†], Lei Guo[1†], Bo Zhang[1†], Shuang Liu[2†], Jin Lei[1], Wentao Zhang[1], Binghai Zhou[3], Jie Gao[1], Zhangfu Yang[1], Xiaoqiang Li[4], Jian Zhou[1], Jia Fan[1], Qinghai Ye[1], Hui Li[1*], Yongfeng Xu[1*] and Yongsheng Xiao[1*]*

[1] Liver Cancer Institute, Zhongshan Hospital, Fudan University and Key Laboratory of Carcinogenesis and Cancer Invasion, Ministry of Education, Shanghai, China, [2] Neurosurgery Department of Zhongshan Hospital, Fudan University, Shanghai, China, [3] Department of Hepatobiliary and Pancreatic Surgery, The Second Affiliated Hospital of Nanchang University, Nanchang, China, [4] Department of Thoracic Surgery, Peking University Shenzhen Hospital, Shenzhen, China

Background: Cholangiocarcinoma was a highly malignant liver cancer with poor prognosis, and immune infiltration status was considered an important factor in response to immunotherapy. In this investigation, we tried to locate immune infiltration related genes of cholangiocarcinoma through combination of bulk-sequencing and single-cell sequencing technology.

Methods: Single sample gene set enrichment analysis was used to annotate immune infiltration status in datasets of TCGA CHOL, GSE32225, and GSE26566. Differentially expressed genes between high- and low-infiltrated groups in TCGA dataset were yielded and further compressed in other two datasets through backward stepwise regression in R environment. Single-cell sequencing data of GSE138709 was loaded by Seurat software and was used to examined the expression of infiltration-related gene set. Pathway changes in malignant cell populations were analyzed through scTPA web tool.

Results: There were 43 genes differentially expressed between high- and low-immune infiltrated patients, and after further compression, PNOC and LAIR2 were significantly correlated with high immune infiltration status in cholangiocarcinoma. Through analysis of single-cell sequencing data, PNOC was mainly expressed by infiltrated B cells in tumor microenvironment, while LAIR2 was expressed by Treg cells and partial GZMB+ CD8 T cells, which were survival related and increased in tumor tissues. High B cell infiltration

OPEN ACCESS

Edited by:
Wei Wei,
Institute for Systems Biology (ISB), United States

Reviewed by:
Chutamas Thepmalee, University of Phayao, Thailand
David Linnaeus Gibbs, Institute for Systems Biology (ISB), United States

***Correspondence:**
Qinghai Ye
ye.qinghai@zs-hospital.sh.cn
Hui Li
li.hui1@zs-hospital.sh.cn
Yongfeng Xu
xu.yongfeng@zs-hospital.sh.cn
Yongsheng Xiao
xiao.yongsheng@zs-hospital.sh.cn

[†]These authors have contributed equally to this work and share first authorship

Specialty section:
This article was submitted to Cancer Immunity and Immunotherapy, a section of the journal Frontiers in Immunology

Received: *29 December 2020*
Accepted: *03 March 2021*
Published: *24 March 2021*

Citation:
Chen Z, Yu M, Yan J, Guo L, Zhang B, Liu S, Lei J, Zhang W, Zhou B, Gao J, Yang Z, Li X, Zhou J, Fan J, Ye Q, Li H, Xu Y and Xiao Y (2021) PNOC Expressed by B Cells in Cholangiocarcinoma Was Survival Related and LAIR2 Could Be a T Cell Exhaustion Biomarker in Tumor Microenvironment: Characterization of Immune Microenvironment Combining Single-Cell and Bulk Sequencing Technology. Front. Immunol. 12:647209. doi: 10.3389/fimmu.2021.647209

levels were related to better overall survival. Also, malignant cell populations demonstrated functionally different roles in tumor progression.

Conclusion: PNOC and LAIR2 were biomarkers for immune infiltration evaluation in cholangiocarcinoma. PNOC, expressed by B cells, could predict better survival of patients, while LAIR2 was a potential marker for exhaustive T cell populations, correlating with worse survival of patients.

Keywords: cholangiocarcinoma, immune infiltration, biomarker, single-cell sequencing technology, immunotherapy

INTRODUCTION

Cholangiocarcinoma (CCA) has long been deemed as a malignancy with poor prognosis in liver cancer. Patients conflicted by cholangiocarcinoma often are found in late stages, who were not candidates for surgery and seldom benefit from chemotherapy or comprehensive treatment (1, 2). Though blockade of programmed cell death receptor 1/programmed cell death receptor ligand 1 (PD1/PDL1) axis with mono-antibody, Pembrolizumab and Nivolumab, has shed light on partial patients, who showed high PDL1 expression in tumors, the overall treating efficacy in advanced CCA patients still needs further observation (3–6). Understanding tumor immune microenvironment (TIME) and infiltration status of CCA could better guide the clinical appliance of immunotherapy (7–9).

With the development of single-cell sequencing (scRNA-seq), investigators could further examine gene expression in individual cells and try to locate functional difference between different clinical phenotypes, especially in immune cells that have infiltrated the tumor (10–12). Characterization of CCA immune microenvironment is limited, so in this study to characterize immune cell components in TIME, we combined bulk sequencing data with scRNA-seq data, which could provide a better understanding of functional cell clusters related to disease severity. We found B cell infiltration levels in CCA TIME were related to patients' overall survival (OS), and propronociceptin (PNOC), which was highly expressed by B cell populations in CCA, could be an independent indicator for better prognosis. Also, in CCA, leukocyte associated immunoglobulin like receptor 2 (LAIR2) was highly expressed by regulatory T cells (Tregs) and part of CD8+/GZMB+ T cells, which could be an indicator of exhaustive immune status in CCA patients. In addition, CCA cell sub-populations demonstrated heterogeneous metabolic and signal transduction activities, in which some CCA cells showed highly activated PD1/PDL1 axis signals, justifying the application of anti-PD1 combining therapy in CCA patients.

METHODS

Datasets for Analysis and Derivation of Gene List

In this investigation, dataset of cholangiocarcinoma (CHOL) in database (n = 36) of the Cancer Genome Atlas (TCGA) (https://www.cancer.gov/about-nci/organization/ccg/research/structural-genomics/tcga) was used to analyze the differentially expressed genes between high- and low-immune infiltration groups (13). After searching Gene Expression Omnibus (GEO) database, data series with patient count over 100 were located, and the datasets with largest patient counts (GSE32225, n = 149; GSE26566, n = 104) were chosen for further immune infiltration classification (14, 15). Single cell sequencing data of five intrahepatic cholangiocarcinoma patients was procured from dataset of GSE138709 (16). The clinical information for patients' cohorts were publicly accessible, which does not require additional endorsement from the local ethic committee. The immune meta gene list for 28 immune cell types were downloaded from TISBID database (http://cis.hku.hk/TISIDB/index.php) (17). Workflow of this Investigation was provided in **Figure 1**.

Calculation of Immune Infiltration Scores in Bulk Sequencing Samples and Analysis of Differentially Expressed Genes Between Groups

In our analysis, single sample gene set enrichment analysis (ssGSEA) for immune infiltration annotation was performed to calculate respective immune infiltration scores of 28 immune cell types, which includes cell types of activated CD4 T cell, activated CD8 T cell, activated dendritic cell, CD56 bright natural killer (NK) cell, central memory CD4 T cell, central memory CD8 T cell, NK cell, NK T cell, type 1 T helper cell, type 17 T helper cell, CD56 dim NK cell, immature dendritic cell, macrophage, myeloid derived suppressive cell (MDSC), neutrophil, plasmacytoid dendritic cell, regulatory T cell (Treg), type 2 T helper cell, activated B cell, eosinophil, gamma delta T cell, immature B cell, mast cell, memory B cell, monocyte and T follicular helper cell (18). Differentially expressed genes between groups were analyzed using edgeR package, contrasting high- with low-immune infiltrated patients (19, 20).

Gene Set Enrichment Analysis

Gene set enrichment analysis (GSEA) was used to demonstrate the altered pathways between patient groups in this study, using software of GSEA v4.1.0 (Broad Institute, Inc., Massachusetts Institute of Technology, and Regents of the University of California) (21). The annotation of changed pathways in this investigation was performed with hallmarks gene set (version: 7.2).

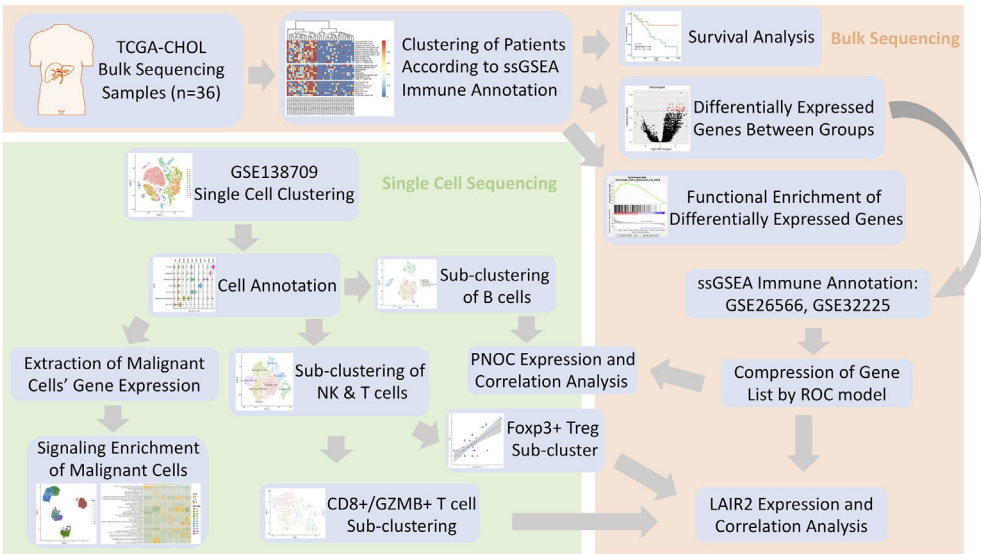

FIGURE 1 | Flowchart of Investigation.

Gene Ontology and Pathway Enrichment

DAVID database was used for gene ontology (GO) analysis, which included biological process, cellular compartment, and molecular function (https://david.ncifcrf.gov/summary.jsp) (22). The protein domains of differentially expressed genes between groups were also analyzed and downloaded from the database for demonstration. REACTOME database was also linked for annotation of significantly changed pathways between groups (www.reactome.org) (23).

Single Cell Data Processing

For single cell sequencing analysis, raw data for GSE138709 were downloaded from portal website, and package of Seurat was used to process data in R (version: 4.0.3) with R studio (version: 1.3.1903) (24–26). The raw data GSE138709 were loaded with Seurat, and cells were filtered with the criteria of >20% mitochondria related genes or more than 6,000 genes expressed. A total of 32,627 cells were included for further analysis, and variable features of each sample were analyzed after normalization. Then we used Seurat function of FindIntegrateionAnchors to merged sample files with common anchors among variables (dims=1:20, k.filter=30) (26). Merged data of cells were clustered into 15 cell populations using function of FindClusters (resolution = 0.3). Respective reduction of cell clustering, including UMAP, TSNE, and PCA, were performed. For cell population annotation, we used the signatures chosen in the original publication (16). For NK and T cell cluster, signatures of CD7, FGFBP2, KLRF1, CD2, CD3D, and CD3E were chosen for annotation. For malignancy and cholangiocyte, signatures of EPCAM, KRT19, KRT7, FXYD2, TM4SF4, and ANXA4 were chosen. For monocytes, CD14 and CD11C were chosen for annotation. For B cell cluster, CD79A, MS4A1 were chosen. For endothelial cells, signatures of ENG and VWF were chosen for annotation. For hepatocytes, APOC3, FABP1, and APOA1 were chosen for annotation. And for fibroblasts, ACTA2 and COL1A2 were chosen for demonstration.

Analysis of Pathway Changes in Malignant Cholangiocarcinoma Cells

To compute and analyze pathway scores in malignant cholangiocarcinoma cells, we used scTPA, which is a web tool for single-cell analysis of activated pathways (http://sctpa.bio-data.cn:8080/index.html) (27, 28). The malignant cell expression matrix was extracted by sample origins in malignancy and cholangiocyte cluster, and then expression matrix was uploaded online. Analyzed results were downloaded for further analysis and demonstration.

Correlation Between Specific Genes and Immune Infiltration Scores

TIMER 2.0 web tool (http://timer.cistrome.org) was used for correlation of gene expression with immune cell infiltration scores, which included scores calculated by CIBERSORT and MCP-counter methods (29–31). Scores of TCGA CHOL sequencing data calculated by other infiltration estimating methods were also downloaded from website for analysis.

Correlation Between Specific Gene Markers

Database GEPIA (http://gepia.cancer-pku.cn) was used for correlation analysis between PNOC, LAIR2, and a series of immune regulators in bulk sequencing data of CHOL and hepatocellular carcinoma (LIHC) in TCGA database (32).

Survival Analysis of Genes in Outside Database

Survival analysis of specific genes was performed in outside database, KMplotter, which is an integrated portal for tumor survival analysis, combining genomics data of microarray with clinical information (33).

Statistics

Survival analysis in this investigation was performed with R packages survival and survminer in R environment, which were used to find the best cutoff values for survival comparison between groups (34). Package of pheatmap was used to construct heat maps (35). Dot plots for correlation analysis and bar plots for GO analysis were generated by packages ggplot2, using spearman correlation test, and GOplot respectively (36, 37). A generalized linear model (GLM) in R was used for prediction of immune infiltration status, using differentially expressed genes, and then stepwise algorithm (backward) was used to choose the appropriate model by an information criterion (AIC) extracted from formerly fitted model ($AIC = -2*\log L + k* edf$; L: likelihood; edf: the equivalent degrees of freedom). Receiver operating characteristics (ROC) were examined using package plotROC. P value under 0.05 was considered significant.

RESULTS

Cholangiocarcinoma Patients in TCGA Dataset Were Clustered Into High- and Low-Immune Infiltrated Groups With Different Prognosis

Using immune gene list for 28 immune infiltrating cell populations, we generated scores for each immune cell type. After clustering cholangiocarcinoma patients according to the calculated scores, we found there was a clearly different immune status between groups (**Figure 2A**). We also used gene lists for immune stimulators, inhibitors, MHC molecules, chemokine, and chemokine receptors to calculate the corresponding scores, and in high-immune infiltration patients, expression levels for those genes were much higher (**Figure 2B**). Patients with high immune infiltration showed better prognosis (**Figure 2C**).

Differentially Expressed Genes Between High- and Low-Infiltrated Patients Were Mainly About Immune Functions, and Inflammatory Signals Were Highly Enriched in High-Immune Infiltrated Patients

Differentially expressed genes between high- and low-infiltrated groups were analyzed, and only a set of 43 genes were up-regulated in high-infiltrated patients (**Figures 2D, E**) Pathway enrichment showed the up-regulated gene set was mainly about inflammatory signals, immune stimulation, and PD1 axis (**Figures 3A, B**). Gene ontology enrichment for 43 gene set showed those genes were involved in the process of adaptive immune responses and T cell signaling (**Figures 3C, D**). The protein functional enrichment showed most of the 43 genes were immunoglobulins (**Figures 3E, F**). Among those genes that were significantly survival-related, all could indicate better overall survival with higher expression (**Figures 3G–L**). Further gene set enrichment analysis between groups showed hallmarks of complement signaling, IL2/STAT5 signaling, IL6/JAK/STAT3 signaling, inflammatory response signaling, interferon gamma signaling, and TNFA signaling *via* NFKB were highly enriched (**Figures 3M–R**).

Several Genes Were Associated With Immune Infiltration Status by Stepwise Regression Model

We further calculated immune infiltration scores for datasets of GSE26566 and GSE32225, and after clustering patients into high- and low-infiltration groups, we used backward stepwise regression model to compress the 43 gene set in prediction of immune infiltration status in the two datasets respectively (**Table 1**). In both models (GSE26566: infiltration score = 6.846 – 0.053*SH2D1A – 0.061*PNOC – 0.021*LAIR2; GSE32225: infiltration score = −1.690 + 0.014*SH2D1A – 0.007*LAIR2 – 0.010*ICOS + 0.019*HEMGN + 0.012*GTSF1L), LAIR2 were related to high-immune infiltration status (**Supplementary Figure 4**).

Further Demonstration of CCA Tumor Microenvironment Showed PNOC Was Mainly Expressed by B Cell, Which Was Also an Indicator for Better Prognosis

In addition to bulk sequencing analysis, we analyzed the immune microenvironment of intrahepatic cholangiocarcinoma with single cell sequencing dataset GSE138709. We further clustered cell populations into 15 clusters, and using genes CD7, CD3D, KRT19, FXYD2, CD14, CD1C, CD79A, VWF, APOC3, and ACTA2, we classified 15 cell clusters into 7 cell populations, which were fibroblasts, NK and T cells, malignancy and cholangiocytes, endothelial cells, monocytes, hepatocytes, and B cells (**Figures 4A–C**). Proportions of cells in different tissue types showed most cells in malignancy and cholangiocyte cluster were from tumor samples, while most cells in NK&T cell cluster were form adjacent samples. Also, a high portion of fibroblasts were also seen in tumor samples (**Figures 4D–F**).

We found PNOC was highly expressed in tumors, though the difference between normal and tumor tissues was not significant (**Figure 5A**). We further examined genes' expression, selected by stepwise regression models, in single cell populations, and PNOC was mainly expressed by B cell cluster. After sub-clustering, activated B cells, plasma cells, and naive B cells all showed expression of PNOC (**Figures 5B–D**). We further examined the correlations between PNOC and scores for B cell infiltration in TCGA CHOL samples, calculated by ssGSEA and MCPcounter methods, and results showed PNOC was

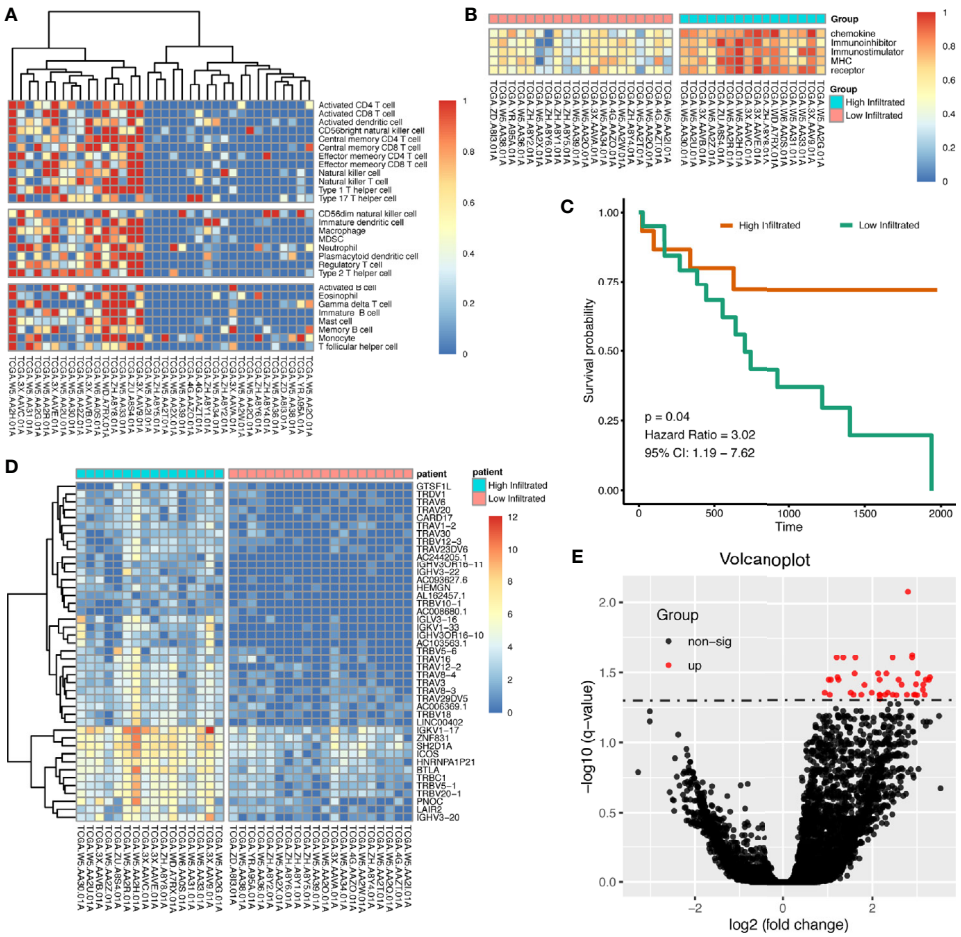

FIGURE 2 | Patients with cholangiocarcinoma were divided into differentially immune infiltrated groups with different prognosis. **(A)** Clustering of CCA patients according to immune infiltration status calculated by ssGSEA method. **(B)** Whole scores of chemokine, chemokine receptor, immune stimulator, immune inhibitor, and MHC expression levels between groups. **(C)** Survival difference between high- and low-immune infiltrated cholangiocarcinoma patients. **(D, E)** Differentially expressed genes between high- and low-immune infiltrated patients.

highly correlated with B cells (**Figures 5E–H**). Also, we found high B cell infiltration scores in cholangiocarcinoma were related to better prognosis, though survival benefits of high immature B cell and memory B cell scores were not significant due to small sample size (**Figures 5I–L**). We further used database GEPIA to examine B cell markers' correlation with PNOC, and results showed PNOC was highly correlated with CD19, CD79A, CD27, and FCRL5 in bulk sequencing data of CHOL (Coefficients >0.95) (**Figures 5M–P**).

LAIR2 Was Up-regulated in CCA Samples, Which Was Mainly Expressed by Regulatory T Cells and a Subset of CD8+/GZMB+ T Cells

We further divided NK and T cells populations into sub-clusters, and LAIR2 was found to be expressed by Foxp3+ regulatory T cell and CD8+/GZMB+ T cell clusters (**Figures 6A, B**). In TCGA CHOL samples, LAIR2 expression was increased in tumor samples (**Figure 6C**). After further clustering of CD8+/GZMB+ T cells into five sub-clusters, we found four of them showed expression of LAIR2, in which sub-cluster 2 demonstrated higher expression (**Figures 6D, E**). In addition, in comparison to immune stimulators (CD28, CD40), immune inhibitors (TGFB1, CD96, TIGIT, and LAG3) were highly expressed by all those sub-clusters, especially clusters 1 and 3 (**Figure 6F**). We further correlated LAIR2 expression with Treg scores and CD8+ T cell scores in TCGA CHOL samples, calculated by CIBERSORT and ssGSEA methods, and results showed LAIR2 was correlated to those cell populations (**Figures 6G–J**). We correlated LAIR2 with Treg cell markers (CD4, FOXP3, CD25, and CD39) and CD8+ T cell markers (CD8A, GZMB, TIM3, and PD1) in CHOL dataset, which all demonstrated high coefficients. Though the correlation between PD1 and LAIR2 was obvious, the corresponding

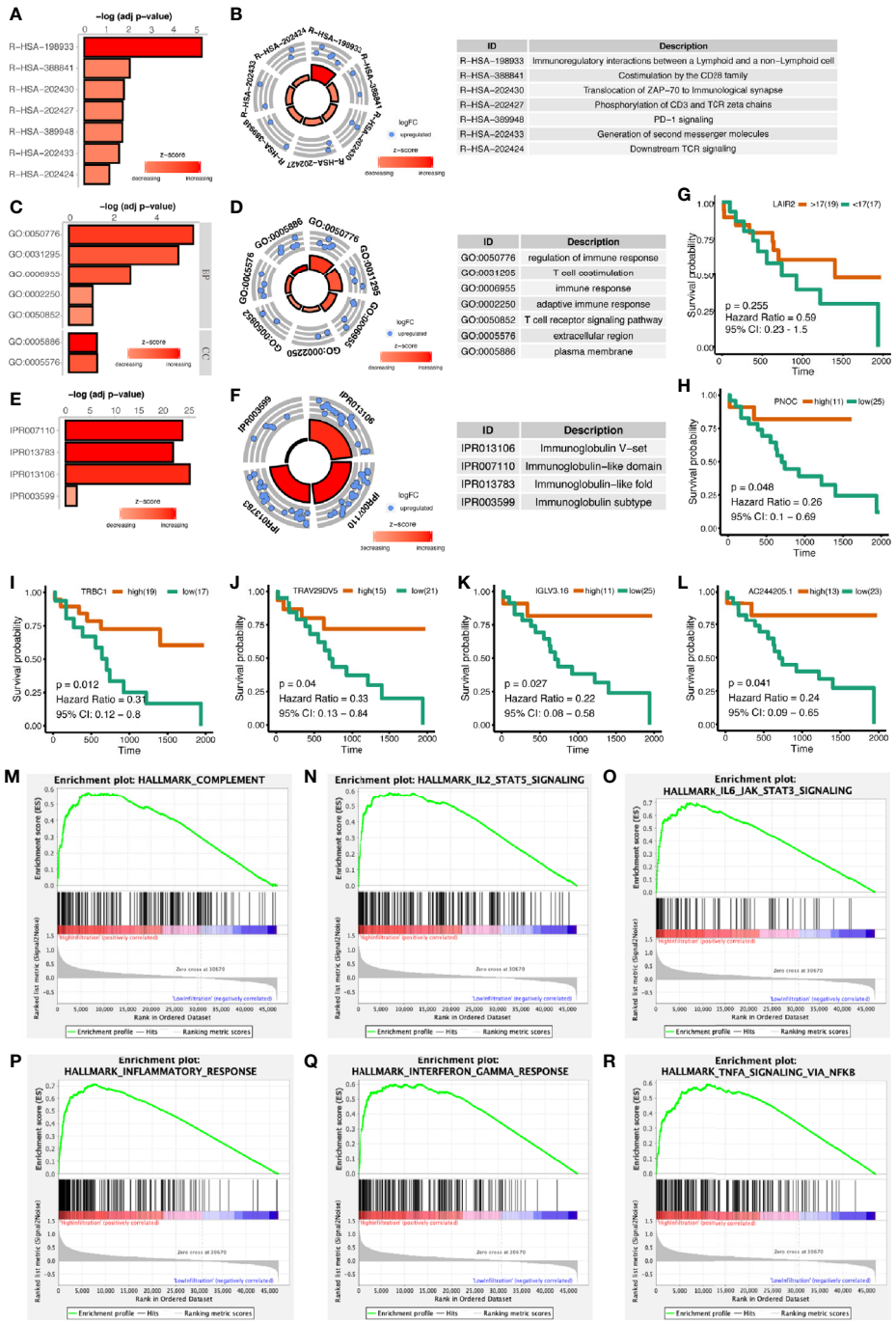

FIGURE 3 | Functional Enrichment of Differentially Expressed Genes Between High- and Low-Immune Infiltration Groups. **(A, B)** Pathway enrichment of differentially expressed genes in REACTOME database. **(C, D)** Gene ontology enrichment of differentially expressed genes. **(E, F)** Protein function enrichment of differentially expressed genes. **(G–L)** Among differentially expressed genes, PNOC, TRBC1, TRAV29DV5, IGLV3.16, and AC244205.1 were significantly correlated with CCA patients' overall survival, while LAIR2 did not achieve significance. **(M–R)** Signatures of complement pathway, IL2-STAT5 pathway, IL6-Jak-STAT3 pathway, inflammatory response pathway, interferon-gamma response pathway, and TNF *via* NFKB pathway were highly enriched in high-immune infiltrated patients.

coefficient did not achieve significance (**Figures 6O–R**). Considering immune regulation was performed through cooperation of immune regulators, we additionally analyzed the correlation between LAIR2, PNOC, and commonly acknowledged immune regulators, and results showed both LAIR2 and PNOC were significantly highly correlated with a bunch of immune inhibitors and stimulators in TCGA CHOL sequencing samples (**Figure 7**).

TABLE 1 | Stepwise Regression Model for Compression of Immune Infiltration Related Genes.

Datasets		Estimate	Std. Error	z value	Pr(>|z|)
GSE26566	(Intercept)	6.84600446	1.44844569	4.72644885	2.28E-06
	SH2D1A	−0.0527032	0.01226927	−4.2955398	1.74E-05
	PNOC	−0.0612851	0.04286357	−1.4297708	0.15278282
	LAIR2	−0.0205321	0.00803995	−2.5537545	0.01065684
GSE32225	(Intercept)	−1.6900303	1.95226226	−0.8656779	0.38666682
	SH2D1A	0.01434228	0.01042714	1.37547498	0.16898424
	LAIR2	−0.0074253	0.00197153	−3.7662633	0.00016571
	ICOS	−0.0098082	0.00372504	−2.6330564	0.00846203
	HEMGN	0.0187238	0.00680099	2.75309954	0.00590339
	GTSF1L	0.0122422	0.00485591	2.52109161	0.01169914

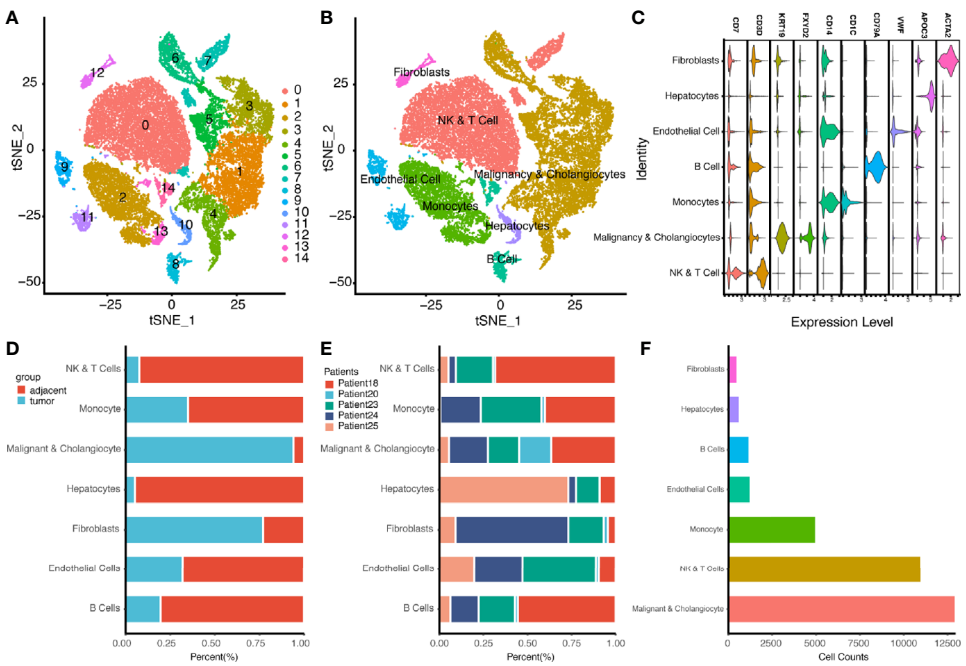

FIGURE 4 | Single Cell Atlas of CCA Patients According to Dataset GSE138709. **(A, B)** Cell clusters for GSE138709 of five CCA patients. **(C)** Cell markers for clusters' annotation. **(D)** Portions of adjacent and tumor tissues in different cell clusters. **(E)** Patient portions in different cell clusters. **(F)** Numbers for cell clusters in dataset after filtration.

CCA Cells Demonstrated Heterogeneous Pathway Changes in Single Cell Level, Which Indicated Functional Variance and Malignant Potentials of Different Cancer Cell Clusters

We further extracted malignancy expression matrix from chonlangiocytes' expression and calculated REACTOME pathway scores for each cell. After clustering of malignant cells according to calculated scores, cells were clustered into 11 populations (**Supplementary Figures 2A, B**). Of notice, clusters 11, 2, 7, 8, and 9 demonstrated highly malignant traits with high expression of signatures in cell mitotic cycle, IL1 signaling, PD1 signaling, and PI3K signaling (**Supplementary Figure 2C**).

DISCUSSION

In our analysis, we used bulk sequencing data of cholangiocarcinoma patients in TCGA database to calculate the immune infiltration scores of different immune cell populations, and then we compared expression difference between groups, locating immune infiltration highly associated genes; we found PNOC was mainly expressed by infiltrated B cells, which was survival related, while LAIR2 was mainly expressed by Tregs and partial CD8+/GZMB+ T cells, indicating exhaustive immune status of T cells.

Prepronociceptin (PNOC) was formerly reported to be a pre-protein for a series of products, which act as pain regulators in signal transduction (38). Recent study showed PNOC is involved in long-term opioid response, alcoholic states, and inflammation

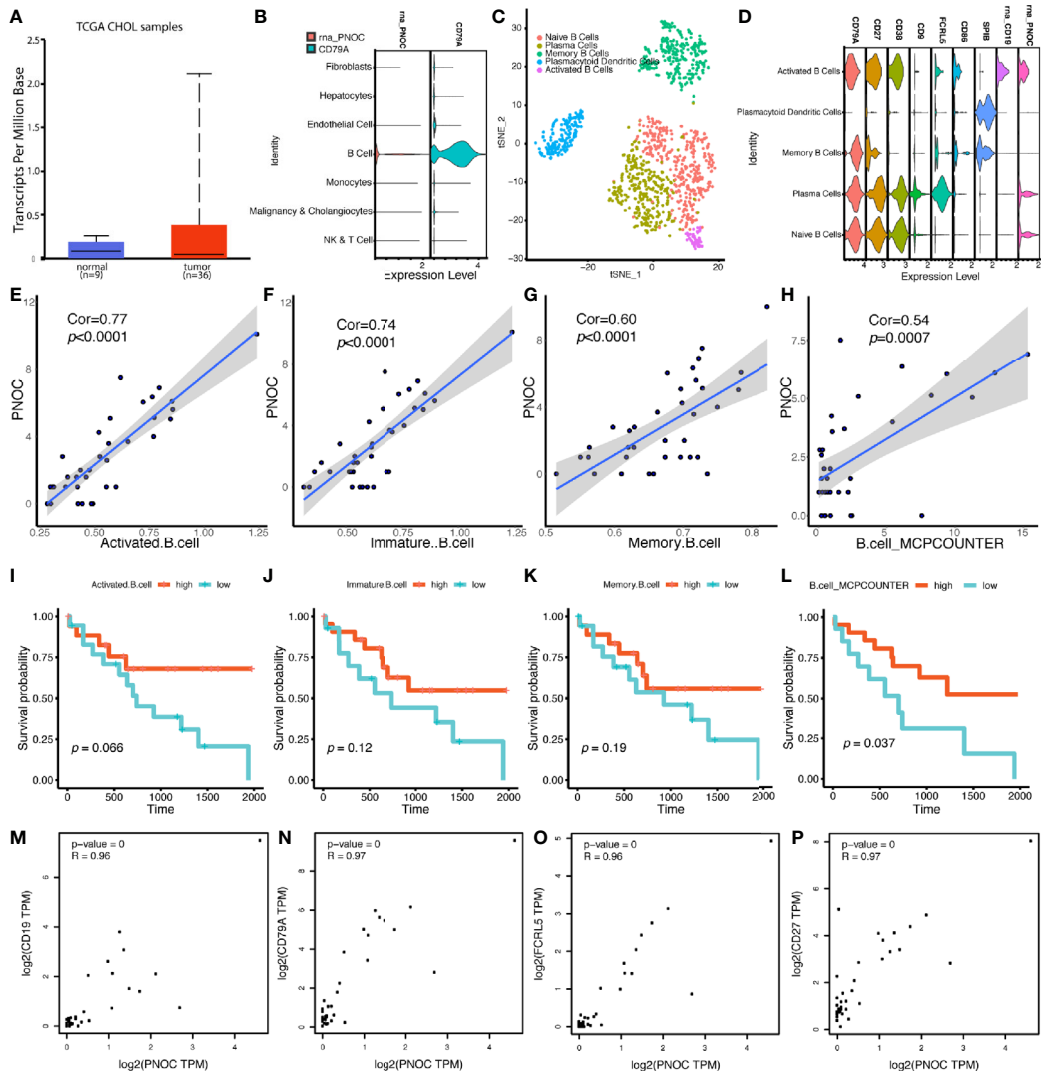

FIGURE 5 | PNOC Was Highly Expressed by B Cell Populations in CCA, and B Cell Infiltration Levels in CCA Indicated Better Overall Survival. **(A)** PNOC was highly expressed in CCA tumors in TCGA database, though significant difference was not achieved. **(B)** PNOC was mainly expressed by B cells in single cell levels. **(C)** Further cluster of B cell populations. **(D)** Markers for sub B cell populations. **(E–H)** Correlation between PNOC expression and scores for activated CD8+ T cell, immature B cell, memory B cell, and whole B cell calculated by ssGSEA and MCPcounter methods. **(I–L)** B cell infiltration levels for activated CD8+ T cell, immature B cell, memory B cell, and whole B cell calculated by ssGSEA and MCPcounter methods were correlated with CCA patients' overall survival. **(M–P)** Correlation between CD19, CD79A, FCRL5, CD27, and PNOC in CHOL bulk sequencing samples from GEPIA database.

process (39–44). In cancer investigations, PNOC was related to high inflammatory status and oxidative stress in C6 glioma cells, which also was highly up-regulated in pediatric brainstem ganglioglioma tissues and epithelial ovarian cancer, and in analysis of high-risk gastrointestinal stromal tumor, PNOC was reported as a prognostic biomarker (45–48). In a study of mRNA and microRNA network in colorectal cancer, PNOC and its targeting microRNAs were also prognostic markers for evaluation of patients (49). In our analysis, PNOC was up-regulated in cholangiocarcinoma samples, though the difference didn't achieve significance. Low expression of PNOC may explain why only one model of GEO datasets included PNOC for prediction of high-immune infiltration; further analysis showed, PNOC was highly expressed by B cell populations in TIME. Expression of PNOC and infiltrating levels of B cell populations in CHOL were both survival-related, and in our analysis, differentially expressed immune genes between high- and low-immune infiltration groups were mainly immunoglobulins, indicating B cell infiltration was crucial in humoral anti-tumor responses. We also examined the prognostic values of PNOC in hepatocellular carcinoma, and we found patients with high PNOC expression also had better overall survival, indicating PNOC could be an independent biomarker for patients' evaluation (**Supplementary Figure 3B**).

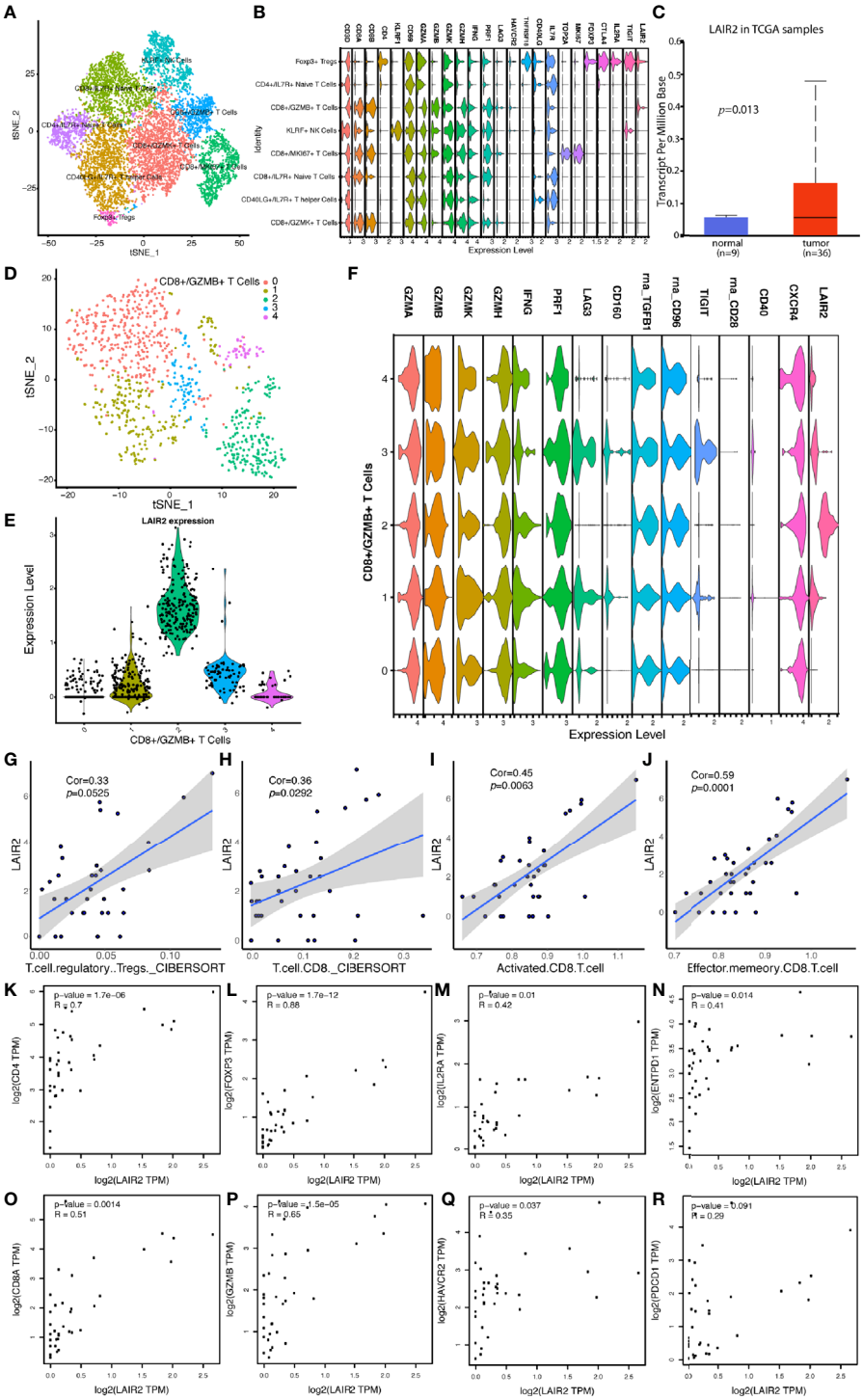

FIGURE 6 | LAIR2 Was Highly Expressed by Regulatory T Cells and CD8+/GZMB+ T Cell Subset. **(A)** TSNE reduction for demonstration of NK and T cell atlas. **(B)** Markers for sub T and NK cell populations. **(C)** LAIR2 expression levels between CCA tumor and normal tissues in TCGA database. **(D)** Further cluster of CD8 +/GZMB+ T cells. **(E)** LAIR2 expression in further clustered CD8+/GZMB+ T cell sub-populations. **(F)** Functional markers' expression levels between further clustered CD8+/GZMB+ T cell sub-populations. **(G–J)** Correlation between LAIR2 expression and scores for regulatory T cell and CD8+ T cell calculated by CIBERSORT or ssGSEA method. **(K–N)** Correlation between LAIR2 and Treg markers [CD4, FOXP3, IL2RA (CD25), and ENTPD1 (CD39)] in CHOL bulk sequencing data from GEPIA database. **(O–R)** Correlation between CD8A, GZMB, HAVCR2 (TIM3), PDCD1 (PD1), and LAIR2 in CHOL bulk sequencing data.

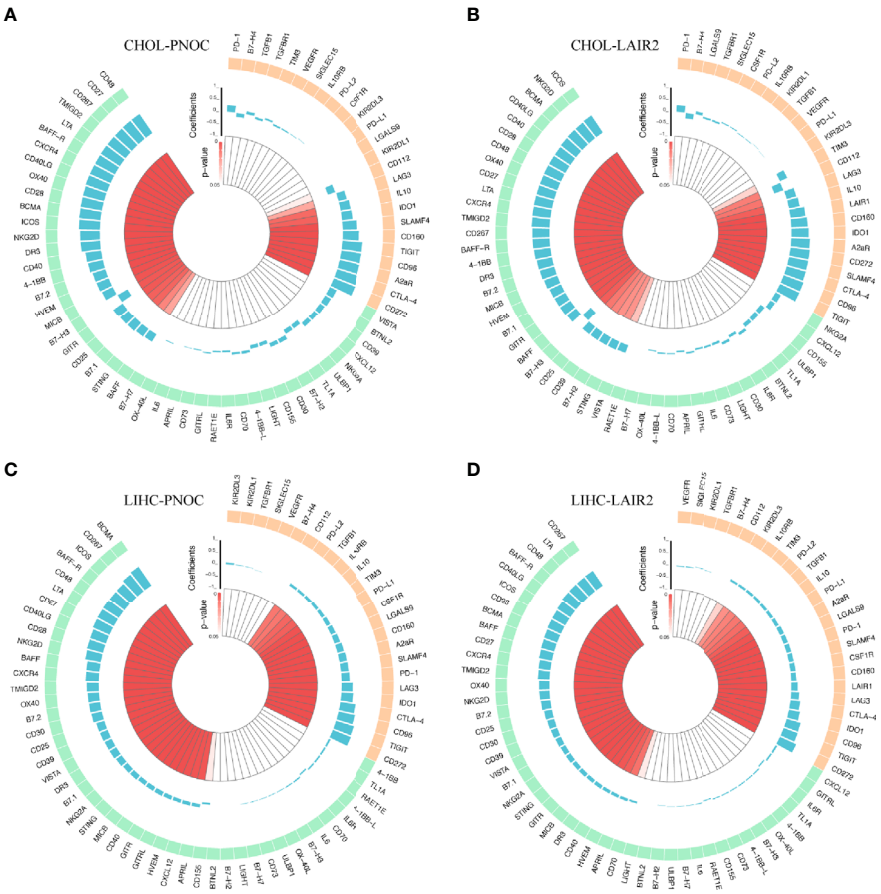

FIGURE 7 | Correlation Between LAIR2, PNOC, and Acknowledged Immune Checkpoints in TCGA CHOL and LIHC Datasets. **(A)** Correlation between expression of PNOC and immune regulators in CHOL dataset. **(B)** Correlation between expression of LAIR2 and immune regulators in CHOL dataset. **(C)** Correlation between expression of PNOC and immune regulators in LIHC dataset. **(D)** Correlation between expression of LAIR2 and immune regulators in LIHC dataset. (Immune inhibitors were marked with light orange, while immune stimulators were marked with light green. P values over 0.05 were not significant and were marked with white color.)

High PNOC expression could predict highly infiltrated TIME. The specific roles of PNOC, expressed by B cells in TIME regulation, still need further experiments to illustrate.

Leukocyte associated immunoglobulin like receptor 2 (LAIR2) was previously reported as a close member to leukocyte associated immunoglobulin like receptor 1 (LAIR1), which is deemed as an immune inhibitor expressed by immune cells (50–52). According to publications, expression of LAIR1 was detected in various immune cell populations, and it has immune receptor tyrosine-based inhibition motif (ITIM), recruiting SHP-1, SHP-2, and Src kinase after phosphorylation (53, 54). Collagen in tumor matrix and damaged tissues is a common ligand for LAIR1 in broad spectrum, inhibiting immune cell functions after ligation, while LAIR2 was found to be a soluble protein with similar extracellular domain, which could block LAIR1 binding by competing ligands (55–58). Former studies also showed in autoimmune diseases, expression of LAIR2 was increased, and genetic single nucleotide polymorphism of LAIR2 was related to susceptibility of autoimmune diseases (59–62). The knowledge of LAIR2 in TIME regulation is limited, however, LAIR2 could interfere platelet activation and adhesion, and secreted LAIR2 could inhibit classical and lectin pathways of complement system in killing pathogens (58, 63). Overexpression of LAIR2 in lung cancer could increase immune infiltration levels and rescue exhaustive CD8+ T cells' function (58). In our analysis, the mRNA expression of LAIR2 in Tregs and partial CD8+/GZMB+ T cells, in comparison to LAIR1, which was widely expressed by various cell populations, could be an indicator of exhaustive immune status. Former studies showed LAIR1 was expressed by macrophages, dendritic cells, as well as other CD14+ cells in inflammation, and scientists hypothesized LAIR1 could be both a threshold receptor and negative feedback receptor (64, 65). In our analysis, LAIR1 was not related to immune infiltration status in CHOL, and we believed mRNA expression of LAIR2 may be increased to offset LAIR1's function in feedback loop, highlighting the role of baseline LAIR2 expression. Though LAIR2 in bulk sequencing data of CHOL was not survival-related, high LAIR2 expression in LIHC could indicate worse prognosis

(**Supplementary Figure 3A**). We further examined coefficients for correlations between LAIR2 and other acknowledged immune regulators, such as CD28, LAG3, CD40, CXCR4, and TIGIT, in CHOL and LIHC datasets respectively, most of which achieved significance with high coefficients.

In addition, we analyzed the pathway changes in intrahepatic cholangiocarcinoma cell populations, finding functionally heterogeneous cancer cell clusters. Those malignant cells were clustered into 11 populations, in which several clusters showed high self-replication potentials, while others showed activated PI3K signal cascade through FGFR interaction. Also, cluster 2 and cluster 11 cells showed immune evasion potentials by increasing human lymphocyte associated antigens, and in cluster 7, expression of PDL1 (CD274) was increased. These functionally different cell populations in tumor justify the need of combining immune therapy in cholangiocarcinoma, and PNOC and LAIR2 could be clinical biomarkers for patient evaluation before immune therapy, predicting patients' survival and tumor immune infiltration accordingly.

There are some limitations of our study. First, though we combined bulk sequencing and single cell sequencing data to characterize TIME of CHOL, protein expression were not examined, and further experiments should be conducted for confirmation. Second, immune regulating roles of PNOC, expressed by B cells, and LAIR2, expressed by Tregs and partial CD8+/GZMB+ T cells, in TIME are still in mist, which shall be further investigated.

CONCLUSION

High B cell infiltration level could indicate better prognosis in CCA. PNOC was mainly expressed by B cells in TIME and could be an independent indicator for better prognosis. LAIR2 was mainly expressed by Treg and partial CD8+/GZMB T cells, which could be an indicator for exhaustive T cell populations in TME. Both PNOC and LAIR2 were correlated with high immune infiltration levels in CCA patients.

DATA AVAILABILITY STATEMENT

Publicly available datasets were analyzed in this study. This data can be found here: CHOL and LIHC in TCGA database: https://www.cancer.gov/about-nci/organization/ccg/research/structural-genomics/tcga: GSE32225: https://www.ncbi.nlm.nih.gov/geo/query/acc.cgi?acc=GSE32225, GSE26566: https://www.ncbi.nlm.nih.gov/geo/query/acc.cgi?acc=GSE26566, GSE138709: https://www.ncbi.nlm.nih.gov/geo/query/acc.cgi?acc=GSE138709.

ETHICS STATEMENT

Ethical review and approval was not required for the study on human participants in accordance with the local legislation and institutional requirements. Written informed consent for participation was not required for this study in accordance with the national legislation and the institutional requirements.

AUTHOR CONTRIBUTIONS

ZC, MY, JY, LG, BZ, and SL contributed to designing and analyzing process of the investigation, drafting the manuscript afterwards. JL, WZ, BHZ, JG, ZY, and XL helped to collect data and perform analysis correspondingly. JZ, JF, QY, HL, YFX, and YSX reviewed the whole manuscript, adapting the manuscript for final submission. All authors contributed to the article and approved the submitted version.

FUNDING

This research was funded by National Nature Science Foundation of China (81871924, 81572844, 81572301, 81802893, 81502487, 81972829), Natural Science Foundation of Guangdong Province of China (Grant Nos. 2017A030310641, 2018A030313762), and Foundation of Shanghai Municipal Commission of Health and Family Planning (20174Y0072).

SUPPLEMENTARY MATERIAL

The Supplementary Material for this article can be found online at: https://www.frontiersin.org/articles/10.3389/fimmu.2021.647209/full#supplementary-material

Supplementary Table 1 | Immune Infiltration Classification of Patients in Datasets of GSE26566 and GSE32225.

Supplementary Table 2 | Coefficients for LAIR2 and PNOC in Association With Treg, CD8+ T cells and B cells in Bulk Sequencing Data of CCA in TCGA Database Calculated by TIMER 2.0.

Supplementary Table 3 | Clinical information for CHOL bulk sequencing samples in TCGA database.

Supplementary Figure 1 | Expression of Immune Inhibitors and Stimulators in High- and Low-Immune Infiltration Patients.

Supplementary Figure 2 | Heterogeneous Pathway Changes in Intrahepatic Cholangiocarcinoma Cells Demonstrated Different Functional Status of Sub-cell Populations. **(A)** Heatmap for pathway scores of different cholangiocarcinoma cell sub-populations. **(B)** UMAP reduction for demonstration of cholangiocarcinoma cell sub-populations. **(C)** Heatmap for genes' expression in PD1 signaling, Cell Cycle Mitotic signaling, IL-1 signaling, and PI3K-FGFR signaling between groups.

Supplementary Figure 3 | Both of PNOC and LAIR2 Were Related to Overall Survival of HCC Patients. **(A)** High expression of LAIR2 indicated worse survival in HCC patients. **(B)** High expression of PNOC indicated better survival in HCC patients.

Supplementary Figure 4 | ROC Plots for Immune Infiltration Models' Evaluation. **(A)** ROC curves for regression model of immune infiltration score and each infiltration-related gene in dataset of GSE26566. **(B)** ROC curves for regression model of immune infiltration score and each infiltration-related gene in dataset of GSE32225 (AUC, area under curve).

REFERENCES

1. Jain A, Kwong LN, Javle M. Genomic Profiling of Biliary Tract Cancers and Implications for Clinical Practice. *Curr Treat options Oncol* (2016) 17(11):58. doi: 10.1007/s11864-016-0432-2
2. Chun YS, Javle M. Systemic and Adjuvant Therapies for Intrahepatic Cholangiocarcinoma. *Cancer control J Moffitt Cancer Center* (2017) 24 (3):1073274817729241. doi: 10.1177/1073274817729241
3. Sabbatino F, Villani V, Yearley JH, Deshpande V, Cai L, Konstantinidis IT, et al. PD-L1 and HLA Class I Antigen Expression and Clinical Course of the Disease in Intrahepatic Cholangiocarcinoma. *Clin Cancer Res* (2016) 22 (2):470–8. doi: 10.1158/1078-0432.CCR-15-0715
4. Kriegsmann M, Roessler S, Kriegsmann K, Renner M, Longuespee R, Albrecht T, et al. Programmed cell death ligand 1 (PD-L1, CD274) in cholangiocarcinoma - correlation with clinicopathological data and comparison of antibodies. *BMC Cancer* (2019) 19(1):72. doi: 10.1186/s12885-018-5254-0
5. Rimassa L, Personeni N, Aghemo A, Lleo A. The immune milieu of cholangiocarcinoma: From molecular pathogenesis to precision medicine. *J Autoimmun* (2019) 100:17–26. doi: 10.1016/j.jaut.2019.03.007
6. Saeed A, Park R, Al-Jumayli M, Al-Rajabi R, Sun W. Biologics, Immunotherapy, and Future Directions in the Treatment of Advanced Cholangiocarcinoma. *Clin colorectal Cancer* (2019) 18(2):81–90. doi: 10.1016/j.clcc.2019.02.005
7. Fontugne J, Augustin J, Pujals A, Compagnon P, Rousseau B, Luciani A, et al. PD-L1 expression in perihilar and intrahepatic cholangiocarcinoma. *Oncotarget* (2017) 8(15):24644–51. doi: 10.18632/oncotarget.15602
8. Ghidini M, Cascione L, Carotenuto P, Lampis A, Trevisani F, Previdi MC, et al. Characterisation of the immune-related transcriptome in resected biliary tract cancers. *Eur J Cancer (Oxford Engl 1990)* (2017) 86:158–65. doi: 10.1016/j.ejca.2017.09.005
9. Mou H, Yu L, Liao Q, Hou X, Wu Y, Cui Q, et al. Successful response to the combination of immunotherapy and chemotherapy in cholangiocarcinoma with high tumour mutational burden and PD-L1 expression: a case report. *BMC Cancer* (2018) 18(1):1105. doi: 10.1186/s12885-018-5021-2
10. Ren X, Zhang Z. Understanding tumor-infiltrating lymphocytes by single cell RNA sequencing. *Adv Immunol* (2019) 144:217–45. doi: 10.1016/bs.ai.2019.08.004
11. Bao X, Shi R, Zhao T, Wang Y, Anastasov N, Rosemann M, et al. Integrated analysis of single-cell RNA-seq and bulk RNA-seq unravels tumour heterogeneity plus M2-like tumour-associated macrophage infiltration and aggressiveness in TNBC. *Cancer Immunol Immunother* (2020) 70(1):189–202.. doi: 10.1007/s00262-020-02669-7
12. Lee HW, Chung W, Lee HO, Jeong DE, Jo A, Lim JE, et al. Single-cell RNA sequencing reveals the tumor microenvironment and facilitates strategic choices to circumvent treatment failure in a chemorefractory bladder cancer patient. *Genome Med* (2020) 12(1):47. doi: 10.1186/s13073-020-00741-6
13. Tomczak K, Czerwinska P, Wiznerowicz M. The Cancer Genome Atlas (TCGA): an immeasurable source of knowledge. *Contemp Oncol (Poznan Poland)* (2015) 19(1a):A68–77. doi: 10.5114/wo.2014.47136
14. Andersen JB, Spee B, Blechacz BR, Avital I, Komuta M, Barbour A, et al. Genomic and genetic characterization of cholangiocarcinoma identifies therapeutic targets for tyrosine kinase inhibitors. *Gastroenterology* (2012) 142(4):1021–31.e15. doi: 10.1053/j.gastro.2011.12.005
15. Sia D, Hoshida Y, Villanueva A, Roayaie S, Ferrer J, Tabak B, et al. Integrative molecular analysis of intrahepatic cholangiocarcinoma reveals 2 classes that have different outcomes. *Gastroenterology* (2013) 144(4):829–40. doi: 10.1053/j.gastro.2013.01.001
16. Zhang M, Yang H, Wan L, Wang Z, Wang H, Ge C, et al. Single cell transcriptomic architecture and intercellular crosstalk of human intrahepatic cholangiocarcinoma. *J hepatology* (2020) 73(5):1118–30. doi: 10.1016/j.jhep.2020.05.039
17. Ru B, Wong CN, Tong Y, Zhong JY, Zhong SSW, Wu WC, et al. TISIDB: an integrated repository portal for tumor-immune system interactions. *Bioinf (Oxford England)* (2019) 35(20):4200–2. doi: 10.1093/bioinformatics/btz210
18. Foroutan M, Bhuva DD, Lyu R, Horan K, Cursons J, Davis MJ. Single sample scoring of molecular phenotypes. *BMC Bioinf* (2018) 19(1):404. doi: 10.1186/s12859-018-2435-4
19. Robinson MD, McCarthy DJ, Smyth GK. edgeR: a Bioconductor package for differential expression analysis of digital gene expression data. *Bioinf (Oxford England)* (2010) 26:139–40. doi: 10.1093/bioinformatics/btp616
20. McCarthy DJ, Chen Y, Smyth GK. Differential expression analysis of multifactor RNA-Seq experiments with respect to biological variation. *Nucleic Acids Res* (2012) 40:4288–97. doi: 10.1093/nar/gks042
21. Subramanian A, Tamayo P, Mootha VK, Mukherjee S, Ebert BL, Gillette MA, et al. Gene set enrichment analysis: a knowledge-based approach for interpreting genome-wide expression profiles. *Proc Natl Acad Sci U S A* (2005) 102(43):15545–50. doi: 10.1073/pnas.0506580102
22. Huang da W, Sherman BT, Lempicki RA. Systematic and integrative analysis of large gene lists using DAVID bioinformatics resources. *Nat Protoc* (2009) 4 (1):44–57. doi: 10.1038/nprot.2008.211
23. Fabregat A, Jupe S, Matthews L, Sidiropoulos K, Gillespie M, Garapati P, et al. The Reactome Pathway Knowledgebase. *Nucleic Acids Res* (2018) 46:D649–D55. doi: 10.1093/nar/gkx1132
24. R Core Team. *R: A language and environment for statistical computing* Vienna, Austria: R Foundation for Statistical Computing (2019). Available at: https://www.R-project.org/.
25. RStudio Team. *.RStudio: Integrated Development for R.* Boston, MA: RStudio, Inc. (2015). Available at: http://www.rstudio.com/.
26. Stuart T, Butler A, Hoffman P, Hafemeister C, Papalexi E, Mauck WM, 3rd, et al. Comprehensive Integration of Single-Cell Data. *Cell* (2019) 177(7):1888–902.e21. doi: 10.1016/j.cell.2019.05.031
27. Zhang Y, Ma Y, Huang Y, Zhang Y, Jiang Q, Zhou M, et al. Benchmarking algorithms for pathway activity transformation of single-cell RNA-seq data. *Comput Struct Biotechnol J* (2020) 18:2953–61. doi: 10.1016/j.csbj.2020.10.007
28. Zhang Y, Zhang Y, Hu J, Zhang J, Guo F, Zhou M, et al. scTPA: a web tool for single-cell transcriptome analysis of pathway activation signatures. *Bioinf (Oxford England)* (2020) 36(14):4217–9. doi: 10.1093/bioinformatics/btaa532
29. Newman AM, Liu CL, Green MR, Gentles AJ, Feng W, Xu Y, et al. Robust enumeration of cell subsets from tissue expression profiles. *Nat Methods* (2015) 12(5):453–7. doi: 10.1038/nmeth.3337
30. Becht E, Giraldo NA, Lacroix L, Buttard B, Elarouci N, Petitprez F, et al. Estimating the population abundance of tissue-infiltrating immune and stromal cell populations using gene expression. *Genome Biol* (2016) 17 (1):218. doi: 10.1186/s13059-016-1113-y
31. Li T, Fan J, Wang B, Traugh N, Chen Q, Liu JS, et al. TIMER: A Web Server for Comprehensive Analysis of Tumor-Infiltrating Immune Cells. *Cancer Res* (2017) 77(21):e108–e10. doi: 10.1158/0008-5472.CAN-17-0307
32. Tang Z, Li C, Kang B, Gao G, Li C, Zhang Z. GEPIA: a web server for cancer and normal gene expression profiling and interactive analyses. *Nucleic Acids Res* (2017) 45(W1):W98–102. doi: 10.1093/nar/gkx247
33. Nagy Á, Lánczky A, Menyhárt O, Győrffy B. Validation of miRNA prognostic power in hepatocellular carcinoma using expression data of independent datasets. *Sci Rep* (2018) 8(1):9227. doi: 10.1038/s41598-018-27521-y
34. Alboukadel K, Marcin K, Przemyslaw B. *survminer: Drawing Survival Curves using 'ggplot2'*. R package version 0.4.8. (2020). https://CRAN.R-project.org/package=survminer.
35. Kolde R. *pheatmap: Pretty Heatmaps.* R package version 1.0.12. (2019). https://CRAN.R-project.org/package=pheatmap.
36. Wickham H. *ggplot2: Elegant Graphics for Data Analysis*. Springer-Verlag New York (2016).
37. Walter W, Sánchez-Cabo F, Ricote M. GOplot: an R package for visually combining expression data with functional analysis. *Bioinf (Oxford England)* (2015) 31(17):2912–4. doi: 10.1093/bioinformatics/btv300
38. Rodriguez-Romaguera J, Ung RL, Nomura H, Otis JM, Basiri ML, Namboodiri VMK, et al. Prepronociceptin-Expressing Neurons in the Extended Amygdala Encode and Promote Rapid Arousal Responses to Motivationally Salient Stimuli. *Cell Rep* (2020) 33(6):108362. doi: 10.1016/j.celrep.2020.108362
39. Kuzmin A, Bazov I, Sheedy D, Garrick T, Harper C, Bakalkin G. Expression of pronociceptin and its receptor is downregulated in the brain of human alcoholics. *Brain Res* (2009) 1305 Suppl(Suppl):S80–5. doi: 10.1016/j.brainres.2009.05.067
40. Zhang L, Stuber F, Stamer UM. Inflammatory mediators influence the expression of nociceptin and its receptor in human whole blood cultures. *PLoS One* (2013) 8(9):e74138. doi: 10.1371/journal.pone.0074138

41. Peppin JF, Raffa RB. Delta opioid agonists: a concise update on potential therapeutic applications. *J Clin Pharm Ther* (2015) 40(2):155–66. doi: 10.1111/jcpt.12244
42. Carboni L, Romoli B, Romualdi P, Zoli M. Repeated nicotine exposure modulates prodynorphin and pronociceptin levels in the reward pathway. *Drug Alcohol Depend* (2016) 166:150–8. doi: 10.1016/j.drugalcdep.2016.07.002
43. Guzeldemir-Akcakanat E, Sunnetci-Akkoyunlu D, Orucguney B, Cine N, Kan B, Yılmaz EB, et al. Gene-Expression Profiles in Generalized Aggressive Periodontitis: A Gene Network-Based Microarray Analysis. *J periodontology* (2016) 87(1):58–65. doi: 10.1902/jop.2015.150175
44. Randesi M, van den Brink W, Levran O, Blanken P, Butelman ER, Yuferov V, et al. Variants of opioid system genes are associated with non-dependent opioid use and heroin dependence. *Drug Alcohol Depend* (2016) 168:164–9. doi: 10.1016/j.drugalcdep.2016.08.634
45. Chan MH, Kleinschmidt-Demasters BK, Donson AM, Birks DK, Foreman NK, Rush SZ. Pediatric brainstem gangliogliomas show overexpression of neuropeptide prepronociceptin (PNOC) by microarray and immunohistochemistry. *Pediatr Blood Cancer* (2012) 59(7):1173–9. doi: 10.1002/pbc.24232
46. Jin S, Zhu W, Li J. Identification of key genes related to high-risk gastrointestinal stromal tumors using bioinformatics analysis. *J Cancer Res Ther* (2018) 14(Supplement):S243–s7. doi: 10.4103/0973-1482.207068
47. Zhang Y, Luan D, Liu Y, Li H, Dong J, Zhang X, et al. Helicid Reverses Lipopolysaccharide-Induced Inflammation and Promotes GDNF Levels in C6 Glioma Cells through Modulation of Prepronociceptin. *Chem Biodiversity* (2020) 17(7):e2000063. doi: 10.1002/cbdv.202000063
48. Mamoor S. Prepronociceptin is differentially expressed in epithelial ovarian cancer. (2020). doi: 10.31219/osf.io/m382t
49. Jiang D, Xie X, Lu Z, Liu L, Qu Y, Wu S, et al. Establishment of a Colorectal Cancer-Related MicroRNA-mRNA Regulatory Network by Microarray and Bioinformatics. *Front Genet* (2020) 11:560186. doi: 10.3389/fgene.2020.560186
50. Lebbink RJ, de Ruiter T, Adelmeijer J, Brenkman AB, van Helvoort JM, Koch M, et al. Collagens are functional, high affinity ligands for the inhibitory immune receptor LAIR-1. *J Exp Med* (2006) 203(6):1419–25. doi: 10.1084/jem.20052554
51. Meyaard L. The inhibitory collagen receptor LAIR-1 (CD305). *J Leukocyte Biol* (2008) 83(4):799–803. doi: 10.1189/jlb.0907609
52. Zarrin AA, Monteiro RC. Editorial: The Role of Inhibitory Receptors in Inflammation and Cancer. *Front Immunol* (2020) 11:633686. doi: 10.3389/fimmu.2020.633686
53. Meyaard L, Hurenkamp J, Clevers H, Lanier LL, Phillips JH. Leukocyte-associated Ig-like receptor-1 functions as an inhibitory receptor on cytotoxic T cells. *J Immunol (Baltimore Md 1950)* (1999) 162(10):5800–4.
54. Meyaard L. LAIR and collagens in immune regulation. *Immunol Lett* (2010) 128(1):26–8. doi: 10.1016/j.imlet.2009.09.014
55. Lebbink RJ, van den Berg MC, de Ruiter T, Raynal N, van Roon JA, Lenting PJ, et al. The soluble leukocyte-associated Ig-like receptor (LAIR)-2 antagonizes the collagen/LAIR-1 inhibitory immune interaction. *J Immunol (Baltimore Md 1950)* (2008) 180(3):1662–9. doi: 10.4049/jimmunol.180.3.1662
56. Lebbink RJ, Raynal N, de Ruiter T, Bihan DG, Farndale RW, Meyaard L. Identification of multiple potent binding sites for human leukocyte associated Ig-like receptor LAIR on collagens II and III. *Matrix Biol J Int Soc Matrix Biol* (2009) 28(4):202–10. doi: 10.1016/j.matbio.2009.03.005
57. Lenting PJ, Westerlaken GH, Denis CV, Akkerman JW, Meyaard L. Efficient inhibition of collagen-induced platelet activation and adhesion by LAIR-2, a soluble Ig-like receptor family member. *PLoS One* (2010) 5(8):e12174. doi: 10.1371/journal.pone.0012174
58. Peng DH, Rodriguez BL, Diao L, Chen L, Wang J, Byers LA, et al. Collagen promotes anti-PD-1/PD-L1 resistance in cancer through LAIR1-dependent CD8(+) T cell exhaustion. *Nat Commun* (2020) 11(1):4520. doi: 10.1038/s41467-020-18298-8
59. Olde Nordkamp MJ, van Roon JA, Douwes M, de Ruiter T, Urbanus RT, Meyaard L. Enhanced secretion of leukocyte-associated immunoglobulin-like receptor 2 (LAIR-2) and soluble LAIR-1 in rheumatoid arthritis: LAIR-2 is a more efficient antagonist of the LAIR-1-collagen inhibitory interaction than is soluble LAIR-1. *Arthritis Rheum* (2011) 63(12):3749–57. doi: 10.1002/art.30612
60. Simone R, Pesce G, Antola P, Merlo DF, Bagnasco M, Saverino D. Serum LAIR-2 is increased in autoimmune thyroid diseases. *PLoS One* (2013) 8(5):e63282. doi: 10.1371/journal.pone.0063282
61. Camargo CM, Augusto DG, Petzl-Erler ML. Differential gene expression levels might explain association of LAIR2 polymorphisms with pemphigus. *Hum Genet* (2016) 135(2):233–44. doi: 10.1007/s00439-015-1626-6
62. Farias TDJ, Augusto DG, de Almeida RC, Malheiros D, Petzl-Erler ML. Screening the full leucocyte receptor complex genomic region revealed associations with pemphigus that might be explained by gene regulation. *Immunology* (2019) 156(1):86–93. doi: 10.1111/imm.13003
63. Olde Nordkamp MJ, Boross P, Yildiz C, Jansen JH, Leusen JH, Wouters D, et al. Inhibition of the classical and lectin pathway of the complement system by recombinant LAIR-2. *J Innate Immun* (2014) 6(3):284–92. doi: 10.1159/000354976
64. Carvalheiro T, Garcia S, Pascoal Ramos MI, Giovannone B, Radstake T, Marut W, et al. Leukocyte Associated Immunoglobulin Like Receptor 1 Regulation and Function on Monocytes and Dendritic Cells During Inflammation. *Front Immunol* (2020) 11:1793. doi: 10.3389/fimmu.2020.01793
65. Rumpret M, Drylewicz J, Ackermans LJE, Borghans JAM, Medzhitov R, Meyaard L. Functional categories of immune inhibitory receptors. *Nat Rev Immunol* (2020) 20(12):771–80. doi: 10.1038/s41577-020-0352-z

Conflict of Interest: The authors declare that the research was conducted in the absence of any commercial or financial relationships that could be construed as a potential conflict of interest.

frontiers in Oncology

REVIEW
published: 26 May 2021
doi: 10.3389/fonc.2021.696716

Immunotherapy in the Treatment of Urothelial Bladder Cancer: Insights From Single-Cell Analysis

Jingyu Zang[1†], *Kaiyan Ye*[1†], *Yang Fei*[1], *Ruiyun Zhang*[2], *Haige Chen*[2*] *and Guanglei Zhuang*[1*]

[1] State Key Laboratory of Oncogenes and Related Genes, Shanghai Cancer Institute, Ren Ji Hospital, School of Medicine, Shanghai Jiao Tong University, Shanghai, China, [2] Department of Urology, Ren Ji Hospital, School of Medicine, Shanghai Jiao Tong University, Shanghai, China

Urothelial bladder cancer (UBC) is a global challenge of public health with limited therapeutic options. Although the emergence of cancer immunotherapy, most notably immune checkpoint inhibitors, represents a major breakthrough in the past decade, many patients still suffer from unsatisfactory clinical outcome. A thorough understanding of the fundamental cellular and molecular mechanisms responsible for antitumor immunity may lead to optimized treatment guidelines and new immunotherapeutic strategies. With technological developments and protocol refinements, single-cell approaches have become powerful tools that provide unprecedented insights into the kaleidoscopic tumor microenvironment and intricate cell-cell communications. In this review, we summarize recent applications of single-cell analysis in characterizing the UBC multicellular ecosystem, and discuss how to leverage the high-resolution information for more effective immune-based therapies.

Keywords: urothelial bladder cancer, immunotherapy, immune checkpoints, single-cell analysis, tumor microenvironment

OPEN ACCESS

Edited by:
Qihui Shi,
Fudan University, China

Reviewed by:
Yin Tang,
Institute for Systems Biology (ISB), United States
Zhuo Wang,
Fudan University, China

***Correspondence:**
Guanglei Zhuang
zhuangguanglei@gmail.com
Haige Chen
rjbladder@163.com

[†]These authors have contributed equally to this work

Specialty section:
This article was submitted to Cancer Immunity and Immunotherapy, a section of the journal Frontiers in Oncology

Received: *17 April 2021*
Accepted: *11 May 2021*
Published: *26 May 2021*

Citation:
Zang J, Ye K, Fei Y, Zhang R, Chen H and Zhuang G (2021) Immunotherapy in the Treatment of Urothelial Bladder Cancer: Insights From Single-Cell Analysis. Front. Oncol. 11:696716. doi: 10.3389/fonc.2021.696716

INTRODUCTION

Urothelial bladder cancer (UBC) accounts for more than half a million new diagnoses and 212,536 deaths annually (1). Approximately 75% of primary UBC cases are non-muscle invasive bladder cancer (NMIBC), which is typically treated with transurethral resection (TURBT) followed by intravesical instillation of chemotherapeutics or Bacillus Calmette-Guérin (BCG) (2–4). Muscle invasive bladder cancer (MIBC) is the minor yet more lethal disease modality, for which optimizing medical care and reducing morbidity after radical cystectomy are major goals (4–6). Clinical management of UBC patients is undergoing rapid changes as tumor immunotherapies, molecular targeted agents, and antibody-drug conjugates have increasingly become viable options (7, 8). In particular, immune checkpoint inhibitors (ICIs) harness patients' own immune system to counteract malignant cells and represent a major breakthrough in recent years. Since 2016, up to five different ICIs targeting programmed cell death protein 1 (PD-1), i.e., pembrolizumab and nivolumab, or programmed cell death ligand 1 (PD-L1), i.e., atezolizumab, avelumab and durvalumab, are approved by FDA for the treatment of late-stage urothelial carcinoma. However, only about 20% of UBC patients show an effective response to anti-PD-1/PD-L1 monotherapy,

which often fails to translate into long-term survival benefit compared with standard chemotherapy (9–14).

Extensive studies have been focused on dissecting the cellular and molecular mechanisms underlying the immune response of UBC, in order to identify clinical biomarkers to predict ICI treatment efficacy, and to design novel single or combination trials of more effective regimens (15–17). Accumulative evidence suggests that tumor cells and the associated nontumor constituents in UBC microenvironment interact to modulate cancer immunogenicity and immunotherapeutic outcomes (18–20). Therefore, a comprehensive characterization of diverse cell types and states in the context of UBC oncogenesis and treatment is of paramount importance. Conventional methodologies often yield incomplete and mixed signals attributable to both malignant and nonmalignant cells, precluding precise evaluation on the biological determinants of ICI effects (21, 22). The emerging single-cell technologies, along with blossoming bioinformatic tools, promise to provide a high-resolution tumor immune landscape and exert a prominent impact on the field of UBC immunotherapy. By analyzing the genomic (23), transcriptomic (24–27), and proteomic (28, 29) features at a high-throughput manner, single-cell approaches generate new insights into complex systems like UBC. The rich information allows to infer heterogeneous cellular compositions, study dynamic cell state transitions, and construct cell-cell communication networks, which collectively may transform our understanding of responsiveness and resistance to PD-1/PD-L1 inhibitors, and fuel rational development of new immune-modulating therapies and combinations.

In this review, we update the current progress of cancer immunotherapy in UBC, summarize the applications of cutting-edge single-cell analysis in decoding the tumor multicellular ecosystem, and discuss future prospects for using these high-dimensional multi-faceted data to guide more effective immune checkpoint therapies.

THE ADVANCES AND CHALLENGES OF IMMUNOTHERAPY FOR UBC

Conventional Therapies for UBC

UBC can be divided into NMIBC and MIBC according to the depth of tumor invasion. The two disease entities have unique pathological characteristics and distinct standard treatment guidelines (7). NMIBCs refer to neoplasms staged as Ta, T1, or CIS (carcinoma *in situ*), and are usually managed with TURBT followed by a single dose of intravesical chemotherapy to kill free-floating tumor cells. After the initial TURBT, patients with intermediate or high likelihood of recurrence will receive adjuvant intravesical BCG as maintenance therapy to reduce the risk of progression (30, 31). For patients who have intolerable adverse effects or fail BCG therapy owing to persistent or worsening disease, the most effective treatment is radical cystectomy (32). UBC lesions invading the muscular layer or perivesical tissues (T2-T4) are categorized as MIBC. Neoadjuvant platinum-based chemotherapy (NAC) plus radical cystectomy is the standard of care for localized MIBC. However, only 20% of patients are eligible to receive NAC (33), and almost half of them still have residual disease after NAC, leading to poor prognosis (34). Moreover, approximately 4% of newly diagnosed UBCs present distal metastasis (4), for which the mainstay of treatment has long been systemic cytotoxic chemotherapy. It is noteworthy that bladder preservation is associated with better quality of life and therefore under active investigations as an attractive alternative in the management of both NMIBC and MIBC. While the survival improvement achieved with conventional therapies has reached a plateau and there are few advances in UBC treatment over the past decades, the paradigm is being considerably shifted with the development and application of immune checkpoint therapeutics (**Figure 1**).

Immune Checkpoint Inhibitors for UBC

Second-Line Therapy

Second-line ICIs are suitable for UBC patients with advanced disease who have previously received platinum-based chemotherapy and subsequently progressed or metastasized. In the KEYNOTE-045 phase III trial (11), patients receiving pembrolizumab experienced improved overall survival (OS) compared to second-line physician's choice of chemotherapy (10.3 *vs* 7.4 months; HR, 0.73 [95% CI, 0.59-0.91]; $P = .002$). Based on these results, pembrolizumab was approved as a second-line treatment for those whose disease progressed during or after platinum-based chemotherapy. In addition, avelumab (JAVELIN Solid Tumor) (12) and nivolumab (CheckMate 275) (13) also gained accelerated FDA approval as second-line agents, both of which demonstrated clinical benefit in the advanced or metastatic setting.

Unfortunately, a major setback emerged as some ICIs originally granted accelerated approval on the basis of phase II trials did not achieve clinical confirmation in subsequent phase III studies. For example, despite promising phase II data (IMvigor210) (14), atezolizumab did not improve OS in a phase III randomized trial (IMvigor211) compared with second-line chemotherapy (11.1 *vs* 10.6 months; HR, 0.87 [95% CI, 0.63-1.21]; $P = .41$) (35). Likewise, according to the phase III study (DANUBE), durvalumab failed to prolong OS (14.4 *vs* 12.1 months; HR, 0.89 [95% CI, 0.71-1.11]; $P = .30$) (36). As a result, these two drugs have been officially withdrawn from the second-line treatment of bladder cancer (7).

First-Line Therapy

Pembrolizumab and atezolizumab were given accelerated approval for the first-line treatment of cisplatin-ineligible advanced or metastatic UBC, following KEYNOTE-052 (37) and IMvigor210 (14) phase II trials. Nevertheless, treatment with pembrolizumab and atezolizumab only yielded an objective response rate (ORR) of 24% and 23%, respectively. Both studies assessed the ICI efficacy in relation to PD-L1 expression status and found that PD-L1 score alone was not sufficient to precisely predict the treatment responsiveness. Other potential predictive biomarkers, such as tumor

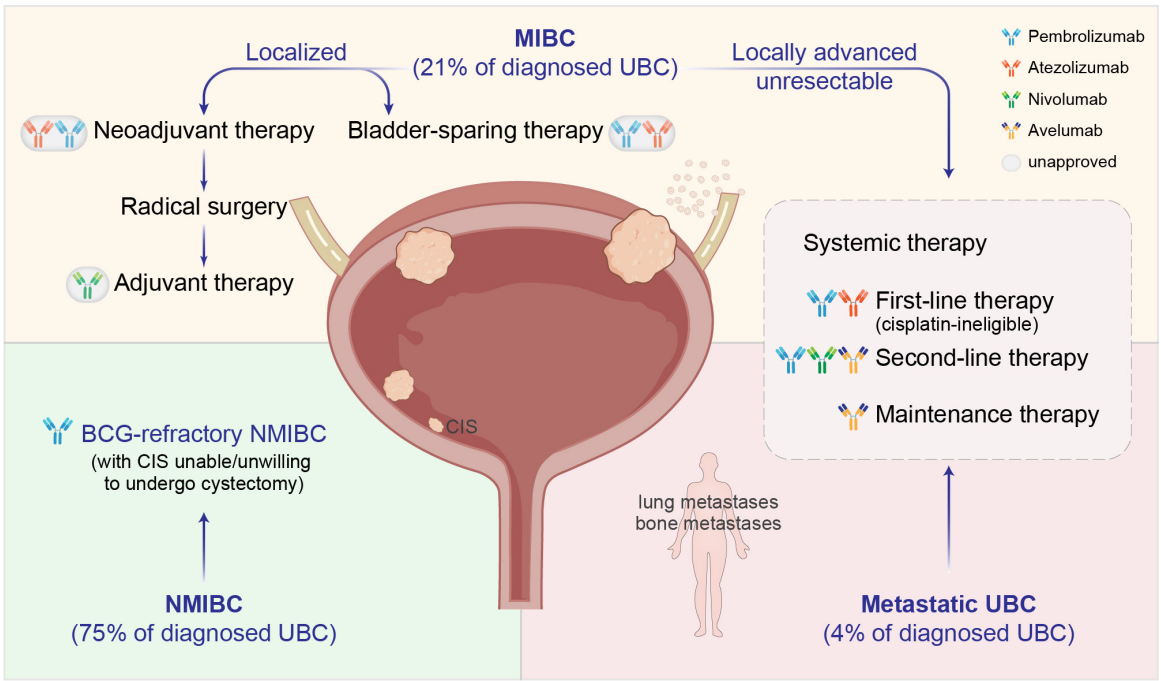

FIGURE 1 | Clinical management of UBC with immune checkpoint inhibitors (ICIs). Dark-colored antibodies: currently approved ICIs; circled light-colored antibodies: in clinical trials. BCG, Bacillus Calmette-Guérin; CIS, carcinoma *in situ*.

mutational burden (TMB) and relevant gene expression profiling (GEP), are being investigated without consensus guidelines in practice.

In contrast, three recent trials with cisplatin-eligible patients consistently showed that first-line ICI monotherapy was not superior to chemotherapy in unresectable locally advanced or metastatic UBC. All these large randomized phase III trials, i.e., IMvigor130, KEYNOTE-361, and DANUBE, observed similar performance of three ICI drugs and platinum-containing chemotherapy in the front-line setting (36, 38–40). Even though the chemoimmunotherapy combo showed some efficacy signals, this result, as it currently stands, appears not to be practice-changing. The next step is to further explore the combination of different ICIs, as well as immunotherapy plus other targeted drugs, in multiple ongoing phase III trials including CheckMate 901, NILE, LEAP-011 and EV-302 (41–44).

Maintenance Therapy

Javelin Bladder 100 was the first phase III trial to establish the role of maintenance immunotherapy immediately following first-line chemotherapy in advanced or metastatic urothelial carcinoma (45). For patients who did not have disease progression with standard chemotherapy (4-6 cycles of gemcitabine plus cisplatin or carboplatin), the addition of maintenance avelumab to best supportive care significantly prolonged overall survival (21.4 *vs* 14.3 months; HR, 0.69 [95% CI, 0.56-0.86]; $P = .001$). The evident improvement of patient outcomes has led to the FDA approval of avelumab as maintenance therapy in this disease setting (46). However, although no new safety signals were identified, there was a higher incidence of adverse events in the avelumab group than in the control group and 11.9% of the patients receiving maintenance avelumab discontinued the therapy because of side effects.

Adjuvant Therapy

The role of adjuvant immunotherapy in MIBC patients after cystectomy remains to be elucidated by prospective clinical studies. One phase III trial (IMvigor010) did not meet its primary endpoint of improved disease-free survival in the atezolizumab group over observation (19.4 *vs* 16.6 months; HR, 0.89 [95% CI, 0.74-1.08]; $P = .24$) (47). On the other hand, first results from the phase III CheckMate 274 trial supported use of nivolumab in MIBC after radical surgery (48). Additional high-quality evidence is required to formulate treatment guidelines recommending adjuvant ICIs for MIBC patients with high-risk pathologic features.

Neoadjuvant Therapy

Clinical trials of perioperative immunotherapy are ongoing in patients with advanced urothelial carcinoma. In PURE-01 phase II study, 42% of patients treated with pembrolizumab achieved pathologic complete response (pCR) and up to 54% downstaged to pT1 or lower disease (49). The ABACUS phase II study reported a pCR rate of 31% and the majority of patients

underwent surgery successfully after neoadjuvant atezolizumab therapy (50). Encouraged by these results, a series of phase III trials assessing ICIs as monotherapy or in combination have been initiated (51). Although neoadjuvant ICIs demonstrate promising antitumor activity, they also pose new challenges in clinical decision-making (52). First, the evaluation criteria of neoadjuvant therapy efficacy are not unified at present. Second, when the patients meet the standard of surgical treatment, and whether curative surgery should be averted or delayed if pCR is achieved are all issues to be considered (4). Third, not all patients benefit from neoadjuvant ICI treatment and selective biomarkers are urgently needed. Finally, during the treatment, immune cells may infiltrate into tumor tissues, causing lesion enlargement and pseudoprogressive imaging findings. Therefore, distinguishing between real progression and so-called "tumor flare" is of necessity (53).

Bladder-Sparing Therapy

As a reasonable alternative to radical cystectomy, trimodal therapy (TMT) combines maximal TURBT with concomitant radiosensitizing chemotherapy and external-beam radiotherapy to devise bladder-sparing strategies in well-selected patients. Given that ICIs may further augment the immune response triggered by radiotherapy-induced tumor cell death (5), several studies are evaluating the potential synergy between chemoradiation and immunotherapy, including KEYNOTE-992 and SWOG S1806, two phase III randomized trials investigating ICIs in bladder-sparing treatment of MIBC (4, 54, 55). Of particular note, the incorporation of clinical biomarkers is a major consideration to carefully gauge which patients are optimal candidates for organ-preserving opportunities and if salvage cystectomy is needed during the course of less aggressive treatment.

BCG-Refractory NMIBC

For patients having BCG-refractory NMIBC with CIS who are unable or unwilling to undergo cystectomy, pembrolizumab was recently approved on the basis of results from KEYNOTE-057 phase II study (56, 57). The complete response (CR) rate was 40.6%, and nearly half of responding patients experienced a CR lasting at least 12 months. During the course of pembrolizumab treatment, no patient's disease progressed to muscle-invasive or metastatic bladder cancer. Additional trials evaluating the use of immunotherapy in NMIBC including the phase III KEYNOTE-676 are underway (58).

Mechanism of Action for PD-1/PD-L1 Checkpoint Blockade

To fulfill a robust and durable clinical benefit of tumor immunotherapy, immense efforts have been taken to comprehensively understand the mechanism of action for PD-1/PD-L1 checkpoint blockade (20). Under physiological conditions, to avoid damaging autologous cells during prolonged immune response, the activation of T lymphocytes is strictly counterbalanced by inhibitory signals, such as immune checkpoint pathways, resulting in hyporesponsive adaptation while limiting detrimental immunopathology. As a particularly important regulatory axis, PD-L1 binds to the PD-1 receptor and functions as the brake of immune cells by suppressing lymphocyte proliferation and cytokine secretion (59, 60). In the process of neoplastic initiation and development, accumulating somatic aberrations give rise to tumor-specific neoantigens, which can be recognized by host defense system as nonself (60, 61). To elicit effective immune responses, a serial of stepwise events, termed the 'cancer-immunity cycle' (**Figure 2**), must proceed and expand iteratively (62). In brief, the release of neoantigens (step 1) and their presentation by dendritic cells (step 2), is followed by effector T cell priming and activation (step 3), trafficking to (step 4) and infiltrating the tumor bed (step 5), consequently resulting in recognition (step 6) and killing of target cells (step 7) to deliver additional tumor-associated antigens (step 1 again). This cyclic process leads to an accumulation of immune-stimulatory factors that amplify and broaden T cell responses. However, the generation of immunity to cancer is not always optimal, and can be halted by immune regulatory feedback mechanisms. For example, tumor cells often abnormally express PD-L1 to engage PD-1 and resist immune attack. Currently approved ICIs in UBC target the PD-1/PD-L1 interaction and reinvigorate the cytotoxic capacity of T lymphocytes against malignant cells (63). Nonetheless, other modes of immunosuppression may exist to impair the intact cancer-immunity cycle and tumor responsiveness to ICI treatment (20, 64–66). At present, immunohistochemistry staining, lymphocyte cell surface protein labeling, and bulk-level high-throughput sequencing, are commonly used to analyze the relevant immune characteristics. However, these approaches yield incomplete or mixed signals from the multicellular microenvironment, which largely ignore biological complexity and intratumoral heterogeneity. With recent advances in single-cell technologies, comprehensive profiling of tumor immune components and their functional properties would facilitate the characterization of diverse cell types and states, shed light on the inherent immune biology related to bladder cancer, and provide unique and nuanced insights into primary or acquired resistance to anticancer immunotherapies (67).

APPLYING SINGLE-CELL TECHNOLOGIES TO UBC

Samples for Consideration

Generally, FFPE (formalin-fixed and paraffin-embedded) or snap-frozen clinical samples, though readily available, can only be used for single-nucleus sequencing (68). The method may work well for DNA but not RNA detection, because the profiling of nuclear RNA ignores its cytoplasmic counterpart and cannot represent the whole picture of cellular transcriptome (69). Therefore, single-cell workflows based on viable cell suspension remain the preferred approach, despite technical challenges associated with immediate collection and processing of fresh

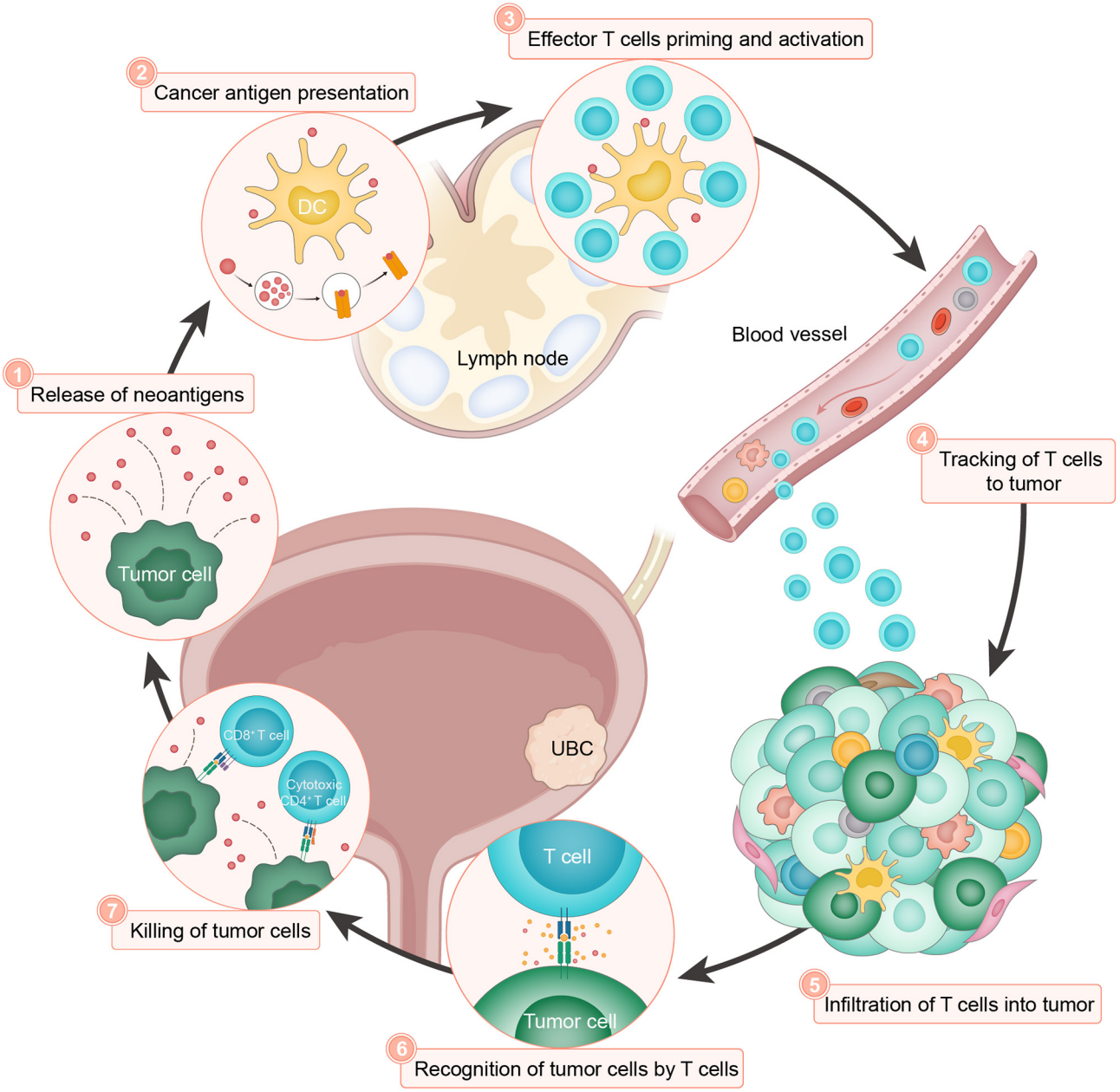

FIGURE 2 | The cancer-immunity cycle in UBC. The cancer-immunity cycle is based on the illustration by Chen and Mellman (62). The cancer-immunity cycle can be divided into seven major steps, starting with the release of neoantigens from the cancer cells (step 1) and ending with the killing of cancer cells (step 7). DC, dendritic cell.

tissues (68). In addition, longitudinal observation of cell types and states during a treatment course is of vast importance but requires repeated tumor biopsies, which is usually unfeasible due to ethical issues. To circumvent this limitation, murine bladder cancer induced by continuous exposure to carcinogenic chemicals serves as an alternative system. Genetically engineered mouse model (GEMM) or patient-derived xenograft (PDX) in immunodeficient animals can also be exploited (18, 70, 71). Of note, co-engraftment of human hematopoietic stem cells partly recapitulates the human tumor immune microenvironment and may be helpful to enable interactions between PDX and immune cells, allowing for experimental evaluation of immunotherapy (71). Moreover, patient-derived organoid (PDO) provides an ex vivo platform for studying tumor evolution and drug response (72, 73). Of special note, the urine from UBC patients, compared to peripheral blood, is a faithful and rich source of tumor-derived materials including DNA, protein, and exfoliated cells (74–77). Thus, single-cell analysis of urinary lymphocytes can be potentially employed as a noninvasive strategy to monitor

tumor immune microenvironment at the cellular level. Indeed, there is evidence that the number of urinary lymphocytes is significantly increased following intravesical BCG instillation in patients with NMIBC (78). In MIBC, urine-derived and tumor-infiltrating lymphocytes closely resemble each other in immune checkpoint landscape and T cell receptor repertoire (75). Therefore, urinary exfoliated immune cells represent a dynamic liquid biopsy for UBC that may be subjected to single-cell interrogation.

Single-Cell Analysis of UBC

Single-Cell RNA Sequencing

To date, single-cell RNA sequencing (scRNA-seq) is the most mature single-cell genomic approach and has a wide spectrum of novel analytic tools to facilitate data interpretation (79–83). The major application of scRNA-seq is to systematically characterize heterogeneous cell types and molecular states in both healthy tissues and malignant conditions. For instance, a recent study created a single-cell transcriptomic map of human and mouse bladders, unveiling both conservative and heterogeneous aspects of bladder evolution (24). A subsequent study generated a single-cell atlas of primary bladder carcinoma and uncovered the protumor function of inflammatory cancer-associated fibroblasts (25). Sfakianos et al. identified lineage plasticity of human and mouse bladder cancer at single-cell resolution, which may contribute to innate tumor heterogeneity (26). In addition, comparative scRNA-seq analysis between pre- and post-tipifarnib MIBC PDX revealed an increased population of dormant drug-refractory tumor cells and simultaneous remodeling of tumor-supporting microenvironment (27).

Single-Cell T Cell Receptor Sequencing

T cells play a vital role in adaptive immunity and represent the major target of antitumor immunotherapy (84). T cell receptor (TCR) locates on the surface of T cells and recognizes antigenic peptides presented by major histocompatibility complex (MHC) molecules. Genetic recombination creates a diverse TCR repertoire during ontogeny or disease. The majority of TCRs are comprised of α and β chains (85), which can be reconstructed by single-cell T cell receptor sequencing (scTCR-seq) to elucidate T cell clones involved in immune response (86). Furthermore, the combined analysis of scRNA-seq and paired scTCR-seq may link the cellular phenotypes with specific clonotypes of T lymphocytes. Using this approach, Oh et al. demonstrated that $CD4^+$ T cells in bladder cancer exhibit multiple distinct tumor-specific states of regulatory T cells and cytotoxic $CD4^+$ T cells, which were clonally expanded (87, 88). In contrast, the states and repertoires of $CD8^+$ T cells, which were traditionally recognized as the main killers in immuno-oncology (89), were indistinguishable in bladder tumors compared with non-malignant tissues.

Single-Cell DNA Sequencing

According to the genomic coverage, single-cell DNA sequencing (scDNA-seq) mainly includes whole-genome scDNA-seq, whole-exome scDNA-seq, and panel scDNA-seq detecting a few genes of interest. Whole-genome or whole-exome scDNA-seq covers large genomic regions but is limited by sequencing depth, while panel scDNA-seq focuses on a narrow list of target genes but can achieve higher throughput and sequencing depth (90). Despite in its infancy, scDNA-seq has been applied to identify driver mutations and investigate cancer evolution. A notable example was that Yang et al. demonstrated the co-mutation of *ARID1A*, *GPRC5A*, and *MLL2* were the major self-renewal driver of human bladder cancer stem cells. Through phylogenetic analysis, the study also suggested the biclonal origin of bladder cancer stem cells from both bladder cancer non-stem cells and bladder epithelial stem cells (23).

CyTOF Mass Cytometry

Cytometry by time of flight (CyTOF) adopts the single-cell format of flow cytometry technique for multiparameter detection of protein expression using the precision of mass spectrometry (91). By employing a pre-selected panel of metal-labeled antibodies, dozens of surface or intracellular markers can be quantified at the same time to infer the potential identity and functionality of target cells. In a study to evaluate NMIBC response to BCG treatment, CyTOF was employed to observe a decreasing trend of T cell subsets in peripheral blood and corresponding tissue recruitment of immune cells in treated tumors (28), thus supporting the rationale of combining immunotherapy to overcome BCG resistance in NMIBC patients. Likewise, Megan et al., *via* CyTOF and RNA-seq analyses, uncovered higher $CD8^+$ T cell populations in murine bladder cancer upon DDR2 depletion and anti-PD-1 treatment, implying that DDR2 inhibition might fuel tumor response to ICIs (29).

Emerging Single-Cell Technologies

As an evolving field, numerous novel single-cell technologies are in rapid development to extract additional layers of biological information. For example, surface protein levels can also be measured in single cells by oligonucleotide-barcoded antibodies, as illustrated by various methods including CITE-seq and REAP-seq (92, 93). Another relevant knowledge tier is the cellular epigenetic state, and recently described scATAC-seq and scDNase-seq, among others, enable high-throughput examination of chromatin accessibility at single-cell resolution (94). One key attribute of tumor ecosystem is the spatial distribution of cellular niches which directly determines physical cell-cell interactions and intercellular signaling communications (95). Specialized tools integrating spatially resolved transcriptomics and advanced imaging infrastructure characterize gene expression profiles within a broader tissue context. Additionally, single-cell metabolomics is being added to the toolbox for metabolic deconvolution but currently is too premature to allow large-scale applications (96). We envision that future studies in UBC leveraging these rising single-cell technologies hold a great deal of promise to enrich our understanding of disease biology and accelerate the discovery of new therapeutic strategies.

POTENTIAL INSIGHTS FROM SINGLE-CELL ANALYSIS

Tumor Multicellular Ecosystem

It is increasingly evident that various cell populations residing at neoplastic lesions and the interplay of these cellular compartments strongly affect cancer progression and response to immunotherapeutics. Recently, single-cell studies have provided in-depth insights into the composition and architecture of tumor multicellular ecosystem in UBC. By profiling the transcriptome of 52,721 single cells from bladder urothelial carcinoma or peritumor mucosa samples, Chen et al. discovered seven annotated cell types including epithelial cells, endothelial cells, fibroblasts, B cells, myeloid cells, T cells, and mast cells (25). Despite the presence of adaptive lymphocytes, cancer cells exhibited intrinsic ability to evade immune surveillance by expressing lower levels of MHC-II molecules than normal epithelial cells. In addition to diverse clusters of myeloid cells, two distinct fibroblast subtypes were identified in UBC: inflammatory fibroblasts and myofibroblasts with the former expressing various cytokines and displaying pro-proliferative effects. It is especially noteworthy that a number of important observations in other cancers are recapitulated in UBC. First, unrelated human malignancies surprisingly harbour analogous cell types (97). Second, tumor cells consistently show a patient-specific expression pattern, whereas immune and stromal infiltrates are more homogenous across different subjects (98–101). Third, both innate and adaptive immunity are involved in cancer pathogenesis (102, 103). Fourth, individual cellular components crosstalk with each other and form intricate interaction networks (104). Collectively, the single-cell transcriptomic atlas reveals cellular and molecular complexity of the UBC ecosystem, and highlights ongoing intratumoral immune suppression as a potential therapeutically actionable abnormality.

T Cell Subsets and States in Cancer

The T cell infiltrates in human cancer largely determine natural disease behavior and also the probability of immunotherapeutic response. It has long been known that intratumoral T lymphocytes span across a spectrum of subsets and states, with the simplest distinction of $CD4^+$ and $CD8^+$ T cell populations (84). While the evidence for a predominant function of $CD8^+$ T cells in tumor control is compelling, the role of $CD4^+$ T cells used to be conceptualized as indirect by either supporting $CD8^+$ T cell-mediated tumor killing *via* a helper phenotype or restricting such processes *via* a regulatory phenotype (105). Oh et al. applied scRNA-seq and paired scTCR-seq to characterize the immune milieu of 7 MIBC patients (87). Reminiscent of heterogeneous T cell infiltrates defined in previous studies (106–108), a diverse range of T cell subtypes also existed in UBC, including both $CD4^+$ and $CD8^+$ T cells that could be further clustered into different functional subgroups. However, in contrast to the canonical view, two cytotoxic $CD4^+$ T cell populations were unexpectedly identified in bladder cancer that correlated with a significantly increased likelihood of clinical response to PD-L1 inhibition (87). Importantly, cytotoxic $CD4^+$ T Cells were clonally expanded in tumor lesions and possessed lytic capacity against autologous tumor cells in an MHC class II-dependent fashion. Although there are a number of caveats about this elegant work, e.g., mixed analysis of both treatment-naive and chemotherapy or immunotherapy-treated samples, the findings have substantial implications by pinpointing the underappreciated potential of cytotoxic $CD4^+$ T cells in UBC. Considering that ICIs ultimately rely on the activity of a pre-existing or newly induced tissue-resident T cell pool to achieve tumor elimination, the identification of cytotoxic $CD4^+$ T cells therefore redefines our thinking regarding UBC immunotherapies and further raises several crucial questions, such as whether these cells are associated with an ongoing tumor-specific immune response and how the current checkpoint inhibitors would impact them.

Tumor Cell Heterogeneity and Plasticity

As aforementioned, single-cell analyses highlight the divergent nature of cancer cells underlying the prevalent heterogeneity between and within individual tumors. This observation is perhaps not surprising given that each malignant cell is featured by a unique evolutionary trajectory and inherent biological stochasticity (109–111). Despite the diversity, specific transcriptional states may still be shared across a subpopulation of neoplastic cells or cancer patients. In the case of UBC, a string of studies on bulk gene expression profiles have identified distinct molecular subtypes in MIBC, including luminal-papillary, luminal, basal-squamous, luminal-infiltrated, and neuronal (16). Such a classification again attests to the differential transcriptome-wide programs operating in separate tumor cells and can be useful to stratify patients for prognosis or treatment. Remarkably, several reports suggest that responses to chemotherapy and immunotherapy are enriched in certain MIBC subtypes (112). Recent scRNA-seq of human and murine bladder cancers, however, revealed a hidden layer of complexity by demonstrating marked cell-autonomous heterogeneity and multidirectional plasticity of the urothelial lineage (26). Therefore, although the initial predominant molecular subtypes may substantially dictate UBC progression kinetics and therapeutic response, they also undergo dynamic changes during tumor growth or clinical treatment, e.g., chemotherapy (113) and immunotherapy. In turn, this subtype transition will presumably engender functional consequences, which should be discreetly considered in the use of immune-modulating agents.

OUTSTANDING QUESTIONS AND FUTURE PROSPECTS

Novel applications of single-cell technologies in characterizing UBC are currently limited in comparison to the rapid progress that has been seen in other human malignancies (114–117). As a result, our understanding of bladder cancer cell hierarchy and

tumor microenvironment is not complete, and more studies will be required to better delineate the abundance, localization, and functional orientation of each cellular component. For instance, the innate immune landscape like myeloid cell populations in UBC remains to be fully elucidated by single-cell analysis. Likewise, the makeup of antigen presenting cells as a crucial factor for efficient immune activation has been insufficiently described. Ideally, all the information should be decoded in a spatiotemporal context (19). As a relevant example, tertiary lymphoid structures (TLS) in human cancer, which are highly organized cellular aggregates resembling lymph nodes, have recently emerged as key sites for the generation of antitumor immunity with a prominent impact on disease outcome and immunotherapeutic response (118–121). We anticipate that single-cell analysis will soon become essential to resolve TLS composition, location, density and degree of maturation during UBC tumorigenesis and treatment.

The success of cancer immunotherapy has prompted intensified interest in defining the specific effector immune cells and fundamental mechanisms responsible for anti-tumor immunity. In addition, certain oncogenic pathways and transcriptional programs in malignant cells are associated with intrinsic sensitivity or resistance to immunotherapeutics (122, 123). These cumulative findings hold enormous promise to facilitate biomarker identification that can predict or monitor which patients would benefit from immunotherapy. The treatment stratification and surveillance are of paramount importance for UBC as ICI therapy is being aggressively advanced into the neoadjuvant and bladder-sparing settings, where inappropriate regimens could be potentially detrimental. Unfortunately, individual parameters have been proved unreliable and such a model has to take different elements that affect tumor-host interactions into account (17, 124). Thus, taking advantage of cutting-edge approaches such as single-cell sequencing and mass cytometry, which enable

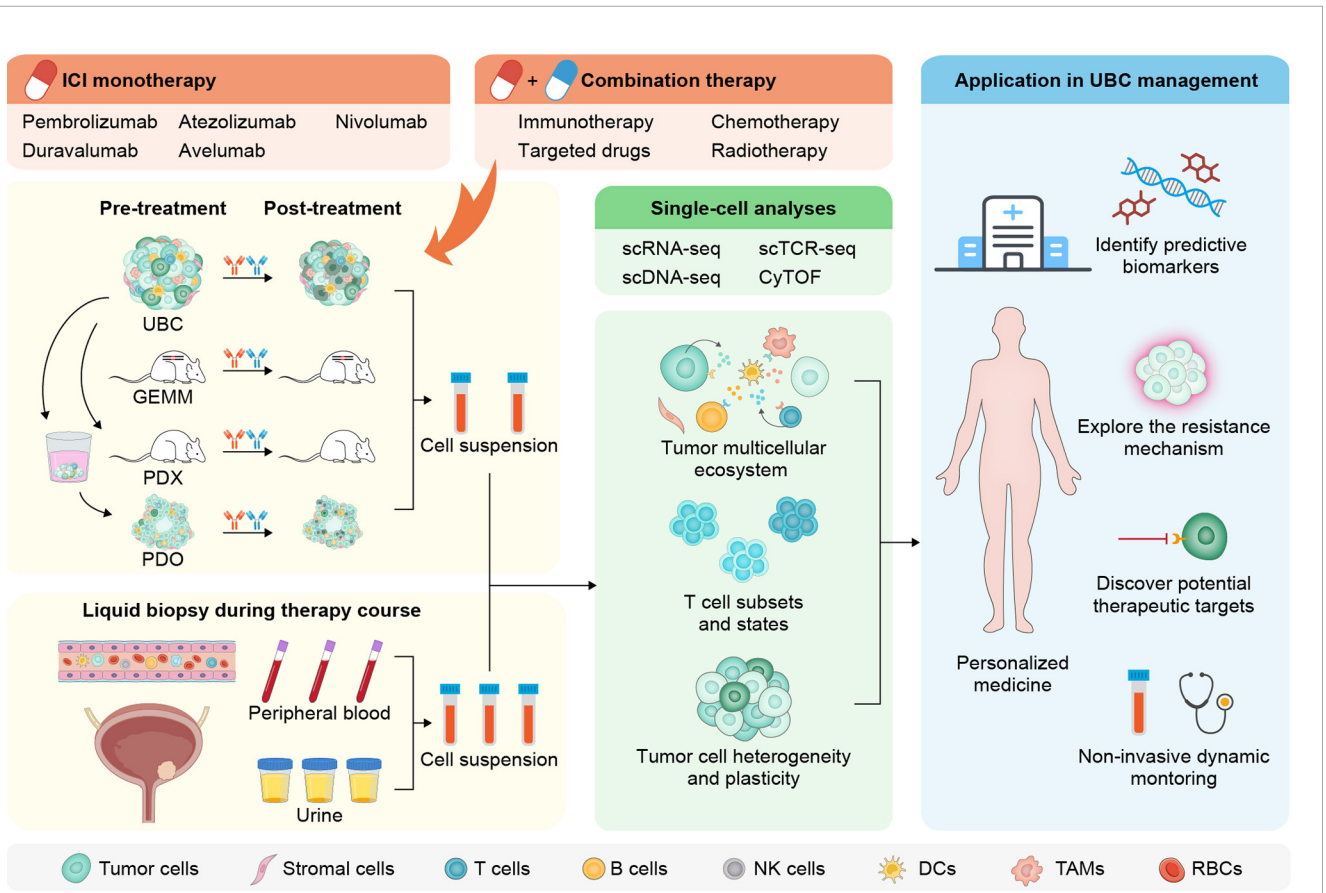

FIGURE 3 | Workflow and applications for single-cell analysis in the immunotherapy of UBC. After sampling before and after ICI monotherapy or combination therapy from UBC patients or alternative experimental models, single-cell suspensions with myriad cell types and states are preprocessed for downstream analysis. The longitudinal and noninvasive single-cell profiling on liquid biopsies from peripheral circulation or urine may aid dynamic monitoring of UBC patients (left panel). A variety of single-cell technologies enable comprehensive assessment of tumor, immune, and stromal cells to yield high-dimensional information (middle panel). Findings from the single-cell approaches promise to allow a detailed dissection of the mechanisms underlying immunotherapeutic response and resistance, and facilitate designing rational single or combination immune-based therapies (right panel). GEMM, genetically engineered mouse model; PDX, patient-derived xenograft; PDO, patient-derived organoid; scRNA-seq, single-cell RNA sequencing; scTCR-seq, single-cell T cell receptor sequencing; scDNA-seq, single-cell DNA sequencing; CyTOF, cytometry by time of flight; NK, natural killer; TAMs, tumor-associated macrophages; RBCs, red blood cells.

high-dimensional molecular analyses during the whole course of ICI treatment, will be valuable to simultaneously probe a wide range of immune subsets and regulators, and systemically nominate biomarker candidates for further detailed investigations.

Beyond anti-PD-1/PD-L1 monotherapy, a breadth of basic research and clinical trials are ongoing to explore the strategy of combined therapy in UBC treatment, such as different ICI pairs (e.g., nivolumab and ipilimumab), immunotherapy and targeted small molecules (e.g., erdafitinib) or antibody-drug conjugates (e.g., enfortumab vedotin and sacituzumab govitecan) (125–127). At the moment, many drug-development pipelines evaluate the efficacy of combo agents on the basis of a simple try-and-see approach. There are continued concerns about whether adverse effects will be additive and whether the antitumor response will be improved. We argue that data-driven design of synergistic drug combinations may most likely make a breakthrough for maximizing patient benefit from these transformative therapies, based on a comprehensive understanding of the bladder cancer ecosystem at the single-cell level.

Ultimately, the multiparametric data derived from single-cell technologies ought to assist UBC patient care and inform treatment recommendations. Achieving the ambitious goal will need joint efforts to develop standard operating procedures for benchmarking and implementing single-cell workflows that meet ethical, regulatory, and temporal requirements. With all foreseeable challenges, this venture would be imperative to transform bladder cancer management and necessitate very close collaboration among physicians, basic researchers and translational scientists. Recently launched large-scale initiatives, including the Human Tumor Atlas Network (HTAN) and the Tumor Profiler (TuPro) study, are poised to accelerate the standardization of key protocols, best-practice guidelines, quality control solutions, metadata schemata, and analytic pipelines (128, 129). These projects may lead to refined diagnostics in precision oncology and pave the way for the translation of single-cell profiling into clinical decision-making.

CONCLUSIONS

The recent decade has witnessed unprecedented advances in the clinical management of urothelial carcinoma with the advent of various ICIs. The ever-expanding applicable range of ICI therapies in UBC highlights the significant potential of immune-targeted agents and advocates a more thorough interrogation of their mechanistic underpinnings. Despite remaining questions, a number of studies using high-resolution single-cell techniques begin to reveal the identity and state of multiple cell types, the variety and uniqueness of tumor-infiltrating T lymphocytes, as well as the heterogeneity and plasticity of bladder cancer cells. This wealth of information has allowed a better understanding of dysfunctional antitumor immunity in UBC and variable responses to immunotherapy across patients (**Figure 3**). However, single-cell methods are still nascent, and over the coming years, an emerging repertoire of multiplexed assays with spatial readout will further enhance their capabilities. In addition, single-cell approaches coupled with noninvasive blood- or urine-based liquid biopsies are instrumental to dynamically evaluate therapeutic efficacy and monitor disease relapse. With these innovative toolkits available, future work should focus on establishing a molecular taxonomy for each cell composition, defining the cellular geography within neoplastic lesions, unravelling passive or adaptive changes upon immune-modulating regimens, and deploying single-cell analysis in prospective trials and clinical practice. The renewed insights are likely to offer novel opportunities for developing companion biomarkers to assign UBC patients into the most effective treatment modalities, and designing rational single or combination immunotherapies with improved response rate and prolonged overall survival.

AUTHOR CONTRIBUTIONS

JZ and KY contributed equally to the literature search, figure visualization, and manuscript drafting. YF and RZ helped with data curation. HC and GZ conceptualized and supervised the project. All authors contributed to the article and approved the submitted version.

FUNDING

This work was supported by the National Natural Science Foundation of China (81672514, 81902562), Shanghai Natural Science Foundation (16ZR1420300, 18410720400, 19431907400), Ren Ji Hospital Research Funding Projects (RJZZ18-020, PYIII-17-017, PY2018-IIC-02), Shanghai Jiao Tong University School of Medicine Research Funding Projects (TM201708), and Foundation of Shanghai Hospital Development Center (SHDC12015125).

REFERENCES

1. Sung H, Ferlay J, Siegel RL, Laversanne M, Soerjomataram I, Jemal A, et al. Global Cancer Statistics 2020: GLOBOCAN Estimates of Incidence and Mortality Worldwide for 36 Cancers in 185 Countries. *CA Cancer J Clin* (2021) 71:209–49. doi: 10.3322/caac.21660
2. van Rhijn BW, Burger M, Lotan Y, Solsona E, Stief CG, Sylvester RJ, et al. Recurrence and Progression of Disease in non-Muscle-Invasive Bladder Cancer: From Epidemiology to Treatment Strategy. *Eur Urol* (2009) 56:430–42. doi: 10.1016/j.eururo.2009.06.028
3. Sylvester RJ, Oosterlinck W, Witjes JA. The Schedule and Duration of Intravesical Chemotherapy in Patients With non-Muscle-Invasive Bladder Cancer: A Systematic Review of the Published Results of Randomized Clinical Trials. *Eur Urol* (2008) 53:709–19. doi: 10.1016/j.eururo.2008.01.015
4. Lenis AT, Lec PM, Chamie K, Mshs MD. Bladder Cancer: A Review. *Jama* (2020) 324:1980–91. doi: 10.1001/jama.2020.17598
5. Sanli O, Dobruch J, Knowles MA, Burger M, Alemozaffar M, Nielsen ME, et al. Bladder Cancer. *Nat Rev Dis Primers* (2017) 3:17022. doi: 10.1038/nrdp.2017.22

6. Witjes JA, Bruins HM, Cathomas R, Compérat EM, Cowan NC, Gakis G, et al. European Association of Urology Guidelines on Muscle-invasive and Metastatic Bladder Cancer: Summary of the 2020 Guidelines. *Eur Urol* (2021) 79:82–104. doi: 10.1016/j.eururo.2020.03.055
7. National Comprehensive Cancer Network. *Bladder Cancer (Version 2.2020)* (2021). Available at: https://www.nccn.org/professionals/physician_gls/pdf/bladder.pdf (Accessed March 23, 2021).
8. Alifrangis C, McGovern U, Freeman A, Powles T, Linch M. Molecular and Histopathology Directed Therapy for Advanced Bladder Cancer. *Nat Rev Urol* (2019) 16:465–83. doi: 10.1038/s41585-019-0208-0
9. Hargadon KM, Johnson CE, Williams CJ. Immune Checkpoint Blockade Therapy for Cancer: An Overview of FDA-approved Immune Checkpoint Inhibitors. *Int Immunopharmacol* (2018) 62:29–39. doi: 10.1016/j.intimp.2018.06.001
10. Rosenberg JE, Hoffman-Censits J, Powles T, van der Heijden MS, Balar AV, Necchi A, et al. Atezolizumab in Patients With Locally Advanced and Metastatic Urothelial Carcinoma Who Have Progressed Following Treatment With Platinum-Based Chemotherapy: A Single-Arm, Multicentre, Phase 2 Trial. *Lancet* (2016) 387:1909–20. doi: 10.1016/s0140-6736(16)00561-4
11. Bellmunt J, de Wit R, Vaughn DJ, Fradet Y, Lee JL, Fong L, et al. Pembrolizumab as Second-Line Therapy for Advanced Urothelial Carcinoma. *N Engl J Med* (2017) 376:1015–26. doi: 10.1056/NEJMoa1613683
12. Patel MR, Ellerton J, Infante JR, Agrawal M, Gordon M, Aljumaily R, et al. Avelumab in Metastatic Urothelial Carcinoma After Platinum Failure (JAVELIN Solid Tumor): Pooled Results From Two Expansion Cohorts of an Open-Label, Phase 1 Trial. *Lancet Oncol* (2018) 19:51–64. doi: 10.1016/s1470-2045(17)30900-2
13. Sharma P, Retz M, Siefker-Radtke A, Baron A, Necchi A, Bedke J, et al. Nivolumab in Metastatic Urothelial Carcinoma After Platinum Therapy (CheckMate 275): A Multicentre, Single-Arm, Phase 2 Trial. *Lancet Oncol* (2017) 18:312–22. doi: 10.1016/s1470-2045(17)30065-7
14. Balar AV, Galsky MD, Rosenberg JE, Powles T, Petrylak DP, Bellmunt J, et al. Atezolizumab as First-Line Treatment in Cisplatin-Ineligible Patients With Locally Advanced and Metastatic Urothelial Carcinoma: A Single-Arm, Multicentre, Phase 2 Trial. *Lancet* (2017) 389:67–76. doi: 10.1016/s0140-6736(16)32455-2
15. Aggen DH, Drake CG. Biomarkers for Immunotherapy in Bladder Cancer: A Moving Target. *J Immunother Cancer* (2017) 5:94. doi: 10.1186/s40425-017-0299-1
16. Robertson AG, Kim J, Al-Ahmadie H, Bellmunt J, Guo G, Cherniack AD, et al. Comprehensive Molecular Characterization of Muscle-Invasive Bladder Cancer. *Cell* (2017) 171:540–556.e525. doi: 10.1016/j.cell.2017.09.007
17. van Dijk N, Funt SA, Blank CU, Powles T, Rosenberg JE, van der Heijden MS. The Cancer Immunogram as a Framework for Personalized Immunotherapy in Urothelial Cancer. *Eur Urol* (2019) 75:435–44. doi: 10.1016/j.eururo.2018.09.022
18. Yofe I, Dahan R, Amit I. Single-Cell Genomic Approaches for Developing the Next Generation of Immunotherapies. *Nat Med* (2020) 26:171–7. doi: 10.1038/s41591-019-0736-4
19. Vitale I, Shema E, Loi S, Galluzzi L. Intratumoral Heterogeneity in Cancer Progression and Response to Immunotherapy. *Nat Med* (2021) 27:212–24. doi: 10.1038/s41591-021-01233-9
20. Schneider AK, Chevalier MF, Derré L. The Multifaceted Immune Regulation of Bladder Cancer. *Nat Rev Urol* (2019) 16:613–30. doi: 10.1038/s41585-019-0226-y
21. Sweis RF, Spranger S, Bao R, Paner GP, Stadler WM, Steinberg G, et al. Molecular Drivers of the Non-T-cell-Inflamed Tumor Microenvironment in Urothelial Bladder Cancer. *Cancer Immunol Res* (2016) 4:563–8. doi: 10.1158/2326-6066.Cir-15-0274
22. Riaz N, Havel JJ, Makarov V, Desrichard A, Urba WJ, Sims JS, et al. Tumor and Microenvironment Evolution During Immunotherapy with Nivolumab. *Cell* (2017) 171:934–949.e916. doi: 10.1016/j.cell.2017.09.028
23. Yang Z, Li C, Fan Z, Liu H, Zhang X, Cai Z, et al. Single-Cell Sequencing Reveals Variants in ARID1A, GPRC5A and MLL2 Driving Self-renewal of Human Bladder Cancer Stem Cells. *Eur Urol* (2017) 71:8–12. doi: 10.1016/j.eururo.2016.06.025
24. Yu Z, Liao J, Chen Y, Zou C, Zhang H, Cheng J, et al. Single-Cell Transcriptomic Map of the Human and Mouse Bladders. *J Am Soc Nephrol* (2019) 30:2159–76. doi: 10.1681/asn.2019040335
25. Chen Z, Zhou L, Liu L, Hou Y, Xiong M, Yang Y, et al. Single-Cell RNA Sequencing Highlights the Role of Inflammatory Cancer-Associated Fibroblasts in Bladder Urothelial Carcinoma. *Nat Commun* (2020) 11:5077. doi: 10.1038/s41467-020-18916-5
26. Sfakianos JP, Daza J, Hu Y, Anastos H, Bryant G, Bareja R, et al. Epithelial Plasticity can Generate Multi-Lineage Phenotypes in Human and Murine Bladder Cancers. *Nat Commun* (2020) 11:2540. doi: 10.1038/s41467-020-16162-3
27. Lee HW, Chung W, Lee HO, Jeong DE, Jo A, Lim JE, et al. Single-Cell RNA Sequencing Reveals the Tumor Microenvironment and Facilitates Strategic Choices to Circumvent Treatment Failure in a Chemorefractory Bladder Cancer Patient. *Genome Med* (2020) 12:47. doi: 10.1186/s13073-020-00741-6
28. Lim CJ, Nguyen PHD, Wasser M, Kumar P, Lee YH, Nasir NJM, et al. Immunological Hallmarks for Clinical Response to BCG in Bladder Cancer. *Front Immunol* (2020) 11:615091. doi: 10.3389/fimmu.2020.615091
29. Tu MM, Lee FYF, Jones RT, Kimball AK, Saravia E, Graziano RF, et al. Targeting DDR2 Enhances Tumor Response to anti-PD-1 Immunotherapy. *Sci Adv* (2019) 5:eaav2437. doi: 10.1126/sciadv.aav2437
30. Lamm DL, Blumenstein BA, Crissman JD, Montie JE, Gottesman JE, Lowe BA, et al. Maintenance Bacillus Calmette-Guerin Immunotherapy for Recurrent TA, T1 and Carcinoma in Situ Transitional Cell Carcinoma of the Bladder: A Randomized Southwest Oncology Group Study. *J Urol* (2000) 163:1124–9. doi: 10.1016/S0022-5347(05)67707-5
31. Sylvester RJ, van der MA, Lamm DL. Intravesical Bacillus Calmette-Guerin Reduces the Risk of Progression in Patients With Superficial Bladder Cancer: A Meta-Analysis of the Published Results of Randomized Clinical Trials. *J Urol* (2002) 168:1964–70. doi: 10.1097/01.ju.0000034450.80198.1c
32. Yates DR, Brausi MA, Catto JW, Dalbagni G, Rouprêt M, Shariat SF, et al. Treatment Options Available for Bacillus Calmette-Guérin Failure in non-Muscle-Invasive Bladder Cancer. *Eur Urol* (2012) 62:1088–96. doi: 10.1016/j.eururo.2012.08.055
33. Galsky MD, Hahn NM, Rosenberg J, Sonpavde G, Hutson T, Oh WK, et al. Treatment of Patients With Metastatic Urothelial Cancer "Unfit" for Cisplatin-based Chemotherapy. *J Clin Oncol* (2011) 29:2432–8. doi: 10.1200/jco.2011.34.8433
34. Bhindi B, Frank I, Mason RJ, Tarrell RF, Thapa P, Cheville JC, et al. Oncologic Outcomes for Patients With Residual Cancer at Cystectomy Following Neoadjuvant Chemotherapy: A Pathologic Stage-matched Analysis. *Eur Urol* (2017) 72:660–4. doi: 10.1016/j.eururo.2017.05.016
35. Powles T, Durán I, van der Heijden MS, Loriot Y, Vogelzang NJ, De Giorgi U, et al. Atezolizumab Versus Chemotherapy in Patients With Platinum-Treated Locally Advanced or Metastatic Urothelial Carcinoma (Imvigor211): A Multicentre, Open-Label, Phase 3 Randomised Controlled Trial. *Lancet* (2018) 391:748–57. doi: 10.1016/s0140-6736(17)33297-x
36. Powles T, van der Heijden MS, Castellano D, Galsky MD, Loriot Y, Petrylak DP, et al. Durvalumab Alone and Durvalumab Plus Tremelimumab Versus Chemotherapy in Previously Untreated Patients With Unresectable, Locally Advanced or Metastatic Urothelial Carcinoma (DANUBE): A Randomised, Open-Label, Multicentre, Phase 3 Trial. *Lancet Oncol* (2020) 21:1574–88. doi: 10.1016/s1470-2045(20)30541-6
37. Balar AV, Castellano D, O'Donnell PH, Grivas P, Vuky J, Powles T, et al. First-Line Pembrolizumab in Cisplatin-Ineligible Patients With Locally Advanced and Unresectable or Metastatic Urothelial Cancer (KEYNOTE-052): A Multicentre, Single-Arm, Phase 2 Study. *Lancet Oncol* (2017) 18:1483–92. doi: 10.1016/s1470-2045(17)30616-2
38. Galsky MD, Arija JÁA, Bamias A, Davis ID, De Santis M, Kikuchi E, et al. Atezolizumab with or without Chemotherapy in Metastatic Urothelial Cancer (Imvigor130): A Multicentre, Randomised, Placebo-Controlled Phase 3 Trial. *Lancet* (2020) 395:1547–57. doi: 10.1016/s0140-6736(20)30230-0
39. Alva A, Csőszi T, Ozguroglu M, Matsubara N, Geczi L, Cheng SYS, et al. Lba23 Pembrolizumab (P) Combined With Chemotherapy (C) vs C Alone as First-Line (1L) Therapy for Advanced Urothelial Carcinoma (UC): KEYNOTE-361. *Ann Oncol* (2020) 31:S1155. doi: 10.1016/j.annonc.2020.08.2252

40. Szabados B, Prendergast A, Jackson-Spence F, Choy J, Powles T. Immune Checkpoint Inhibitors in Front-line Therapy for Urothelial Cancer. *Eur Urol Oncol* (2021). doi: 10.1016/j.euo.2021.02.010
41. Galsky MD, Powles T, Li S, Hennicken D, Sonpavde G. A Phase 3, Open-Label, Randomized Study of Nivolumab Plus Ipilimumab or Standard of Care (SoC) vs SoC Alone in Patients (Pts) With Previously Untreated Unresectable or Metastatic Urothelial Carcinoma (Muc; CheckMate 901). *J Clin Oncol* (2018) 36:TPS4588–TPS4588. doi: 10.1200/JCO.2018.36.15_suppl.TPS4588
42. Herchenhorn D, Freire V, Oliveira T, Tarouquella J. Sequential Therapies for Advanced Urothelial Cancer: Hope Meets New Challenges. *Crit Rev Oncol Hematol* (2021) 160:103248. doi: 10.1016/j.critrevonc.2021.103248
43. Mollica V, Rizzo A, Montironi R, Cheng L, Giunchi F, Schiavina R, et al. Current Strategies and Novel Therapeutic Approaches for Metastatic Urothelial Carcinoma. *Cancers (Basel)* (2020) 12:1449–92. doi: 10.3390/cancers12061449
44. Dietrich B, Srinivas S. Urothelial Carcinoma: The Evolving Landscape of Immunotherapy for Patients with Advanced Disease. *Res Rep Urol* (2018) 10:7–16. doi: 10.2147/rru.S125635
45. Powles T, Park SH, Voog E, Caserta C, Valderrama BP, Gurney H, et al. Avelumab Maintenance Therapy for Advanced or Metastatic Urothelial Carcinoma. *N Engl J Med* (2020) 383:1218–30. doi: 10.1056/NEJMoa2002788
46. Food and Drug Administration. *FDA Approves Avelumab for Urothelial Carcinoma Maintenance Treatment* (2020). Available at: https://www.fda.gov/drugs/drug-approvals-and-databases/fda-approves-avelumab-urothelial-carcinoma-maintenance-treatment (Accessed April, 15, 2021).
47. Bellmunt J, Hussain M, Gschwend JE, Albers P, Oudard S, Castellano D, et al. Adjuvant Atezolizumab Versus Observation in Muscle-Invasive Urothelial Carcinoma (Imvigor010): A Multicentre, Open-Label, Randomised, Phase 3 Trial. *Lancet Oncol* (2021) 22:525–37. doi: 10.1016/s1470-2045(21)00004-8
48. Bajorin DF, Witjes JA, Gschwend J, Schenker M, Valderrama BP, Tomita Y, et al. First Results From the Phase 3 CheckMate 274 Trial of Adjuvant Nivolumab vs Placebo in Patients who Underwent Radical Surgery for High-Risk Muscle-Invasive Urothelial Carcinoma (MIUC). *J Clin Oncol* (2021) 39:391–1. doi: 10.1200/JCO.2021.39.6_suppl.391
49. Necchi A, Anichini A, Raggi D, Briganti A, Massa S, Lucianò R, et al. Pembrolizumab as Neoadjuvant Therapy Before Radical Cystectomy in Patients With Muscle-Invasive Urothelial Bladder Carcinoma (Pure-01): An Open-Label, Single-Arm, Phase II Study. *J Clin Oncol* (2018) 36:3353–60. doi: 10.1200/jco.18.01148
50. Powles T, Kockx M, Rodriguez-Vida A, Duran I, Crabb SJ, Van Der Heijden MS, et al. Clinical Efficacy and Biomarker Analysis of Neoadjuvant Atezolizumab in Operable Urothelial Carcinoma in the ABACUS Trial. *Nat Med* (2019) 25:1706–14. doi: 10.1038/s41591-019-0628-7
51. Rouanne M, Bajorin DF, Hannan R, Galsky MD, Williams SB, Necchi A, et al. Rationale and Outcomes for Neoadjuvant Immunotherapy in Urothelial Carcinoma of the Bladder. *Eur Urol Oncol* (2020) 3:728–38. doi: 10.1016/j.euo.2020.06.009
52. Benitez JC, Remon J, Besse B. Current Panorama and Challenges for Neoadjuvant Cancer Immunotherapy. *Clin Cancer Res* (2020) 26:5068–77. doi: 10.1158/1078-0432.Ccr-19-3255
53. Seymour L, Bogaerts J, Perrone A, Ford R, Schwartz LH, Mandrekar S, et al. iRECIST: Guidelines for Response Criteria for Use in Trials Testing Immunotherapeutics. *Lancet Oncol* (2017) 18:e143–52. doi: 10.1016/s1470-2045(17)30074-8
54. Broughman JR, Vuong W, Mian OY. Current Landscape and Future Directions on Bladder Sparing Approaches to Muscle-Invasive Bladder Cancer. *Curr Treat Options Oncol* (2020) 22:3. doi: 10.1007/s11864-020-00800-5
55. Osterman CK, Milowsky MI. New and Emerging Therapies in the Management of Bladder Cancer. *F1000Res* (2020) 9:1146–60. doi: 10.12688/f1000research.26841.1
56. Food and Drug Administration. *FDA Approves Pembrolizumab for BCG-unresponsive, High-Risk non-Muscle Invasive Bladder Cancer* (2020). Available at: https://www.fda.gov/drugs/resources-information-approved-drugs/fda-approves-pembrolizumab-bcg-unresponsive-high-risk-non-muscle-invasive-bladder-cancer (Accessed March 15, 2021).
57. Balar AV, Kulkarni GS, Uchio EM, Boormans J, Mourey L, Krieger LEM, et al. Keynote 057: Phase II Trial of Pembrolizumab (Pembro) for Patients (Pts) With High-Risk (HR) Nonmuscle Invasive Bladder Cancer (NMIBC) Unresponsive to Bacillus Calmette-Guérin (BCG). *J Clin Oncol* (2019) 37:350–0. doi: 10.1200/JCO.2019.37.7_suppl.350
58. Kamat AM, Shore ND, Hahn NM, Alanee S, Nishiyama H, Shariat S, et al. Keynote-676: Phase 3 Study of Bacillus Calmette-Guerin (BCG) with or without Pembrolizumab (Pembro) for High-Risk (HR) non–Muscle Invasive Bladder Cancer (NMIBC) That is Persistent or Recurrent Following BCG Induction. *J Clin Oncol* (2019) 37:TPS502–2. doi: 10.1200/JCO.2019.37.7_suppl.TPS502
59. Pardoll DM. The Blockade of Immune Checkpoints in Cancer Immunotherapy. *Nat Rev Cancer* (2012) 12:252–64. doi: 10.1038/nrc3239
60. Zhang Y, Zhang Z. The History and Advances in Cancer Immunotherapy: Understanding the Characteristics of Tumor-Infiltrating Immune Cells and Their Therapeutic Implications. *Cell Mol Immunol* (2020) 17:807–21. doi: 10.1038/s41423-020-0488-6
61. Stratton MR, Campbell PJ, Futreal PA. The Cancer Genome. *Nature* (2009) 458:719–24. doi: 10.1038/nature07943
62. Chen DS, Mellman I. Oncology Meets Immunology: The Cancer-Immunity Cycle. *Immunity* (2013) 39:1–10. doi: 10.1016/j.immuni.2013.07.012
63. Topalian SL, Drake CG, Pardoll DM. Immune Checkpoint Blockade: A Common Denominator Approach to Cancer Therapy. *Cancer Cell* (2015) 27:450–61. doi: 10.1016/j.ccell.2015.03.001
64. Khong HT, Restifo NP. Natural Selection of Tumor Variants in the Generation of "Tumor Escape" Phenotypes. *Nat Immunol* (2002) 3:999–1005. doi: 10.1038/ni1102-999
65. Blank C, Gajewski TF, Mackensen A. Interaction of PD-L1 on Tumor Cells With PD-1 on Tumor-Specific T Cells as a Mechanism of Immune Evasion: Implications for Tumor Immunotherapy. *Cancer Immunol Immunother* (2005) 54:307–14. doi: 10.1007/s00262-004-0593-x
66. Rabinovich GA, Gabrilovich D, Sotomayor EM. Immunosuppressive Strategies That are Mediated by Tumor Cells. *Annu Rev Immunol* (2007) 25:267–96. doi: 10.1146/annurev.immunol.25.022106.141609
67. Guruprasad P, Lee YG, Kim KH, Ruella M. The Current Landscape of Single-Cell Transcriptomics for Cancer Immunotherapy. *J Exp Med* (2021) 218:e20201574. doi: 10.1084/jem.20201574
68. Lim B, Lin Y, Navin N. Advancing Cancer Research and Medicine With Single-Cell Genomics. *Cancer Cell* (2020) 37:456–70. doi: 10.1016/j.ccell.2020.03.008
69. Habib N, Avraham-Davidi I, Basu A, Burks T, Shekhar K, Hofree M, et al. Massively Parallel Single-Nucleus RNA-seq with Dronc-Seq. *Nat Methods* (2017) 14:955–8. doi: 10.1038/nmeth.4407
70. Wang L, Smith BA, Balanis NG, Tsai BL, Nguyen K, Cheng MW, et al. A Genetically Defined Disease Model Reveals That Urothelial Cells can Initiate Divergent Bladder Cancer Phenotypes. *Proc Natl Acad Sci USA* (2020) 117:563–72. doi: 10.1073/pnas.1915770117
71. Byrne AT, Alférez DG, Amant F, Annibali D, Arribas J, Biankin AV, et al. Interrogating Open Issues in Cancer Precision Medicine with Patient-Derived Xenografts. *Nat Rev Cancer* (2017) 17:254–68. doi: 10.1038/nrc.2016.140
72. Lee SH, Hu W, Matulay JT, Silva MV, Owczarek TB, Kim K, et al. Tumor Evolution and Drug Response in Patient-Derived Organoid Models of Bladder Cancer. *Cell* (2018) 173:515–528.e517. doi: 10.1016/j.cell.2018.03.017
73. Mullenders J, de Jongh E, Brousali A, Roosen M, Blom JPA, Begthel H, et al. Mouse and Human Urothelial Cancer Organoids: A Tool for Bladder Cancer Research. *Proc Natl Acad Sci USA* (2019) 116:4567–74. doi: 10.1073/pnas.1803595116
74. Wang Z, Chen J, Yang L, Cao M, Yu Y, Zhang R, et al. Single-Cell Sequencing-Enabled Hexokinase 2 Assay for Noninvasive Bladder Cancer Diagnosis and Screening by Detecting Rare Malignant Cells in Urine. *Anal Chem* (2020) 92:16284–92. doi: 10.1021/acs.analchem.0c04282
75. Wong YNS, Joshi K, Khetrapal P, Ismail M, Reading JL, Sunderland MW, et al. Urine-Derived Lymphocytes as a non-Invasive Measure of the Bladder Tumor Immune Microenvironment. *J Exp Med* (2018) 215:2748–59. doi: 10.1084/jem.20181003
76. Chen A, Fu G, Xu Z, Sun Y, Chen X, Cheng KS, et al. Detection of Urothelial Bladder Carcinoma Via Microfluidic Immunoassay and Single-Cell Dna

Copy-Number Alteration Analysis of Captured Urinary-Exfoliated Tumor Cells. *Cancer Res* (2018) 78:4073–85. doi: 10.1158/0008-5472.Can-17-2615
77. Lodewijk I, Dueñas M, Rubio C, Munera-Maravilla E, Segovia C, Bernardini A, et al. Liquid Biopsy Biomarkers in Bladder Cancer: A Current Need for Patient Diagnosis and Monitoring. *Int J Mol Sci* (2018) 19:2514–47. doi: 10.3390/ijms19092514
78. Pieraerts C, Martin V, Jichlinski P, Nardelli-Haefliger D, Derre L. Detection of Functional Antigen-Specific T Cells From Urine of non-Muscle Invasive Bladder Cancer Patients. *Oncoimmunology* (2012) 1:694–8. doi: 10.4161/onci.20526
79. Tang F, Barbacioru C, Wang Y, Nordman E, Lee C, Xu N, et al. mRNA-Seq Whole-Transcriptome Analysis of a Single Cell. *Nat Methods* (2009) 6:377–82. doi: 10.1038/nmeth.1315
80. Ramsköld D, Luo S, Wang YC, Li R, Deng Q, Faridani OR, et al. Full-Length mRNA-Seq From Single-Cell Levels of RNA and Individual Circulating Tumor Cells. *Nat Biotechnol* (2012) 30:777–82. doi: 10.1038/nbt.2282
81. Picelli S, Faridani OR, Björklund AK, Winberg G, Sagasser S, Sandberg R. Full-Length RNA-seq From Single Cells Using Smart-Seq2. *Nat Protoc* (2014) 9:171–81. doi: 10.1038/nprot.2014.006
82. Hashimshony T, Senderovich N, Avital G, Klochendler A, de Leeuw Y, Anavy L, et al. Cel-Seq2: Sensitive Highly-Multiplexed Single-Cell RNA-Seq. *Genome Biol* (2016) 17:77. doi: 10.1186/s13059-016-0938-8
83. Zheng GX, Terry JM, Belgrader P, Ryvkin P, Bent ZW, Wilson R, et al. Massively Parallel Digital Transcriptional Profiling of Single Cells. *Nat Commun* (2017) 8:14049. doi: 10.1038/ncomms14049
84. Wu J, Abraham SN. The Roles of T Cells in Bladder Pathologies. *Trends Immunol* (2021) 42:248–60. doi: 10.1016/j.it.2021.01.003
85. Davis MM. T Cell Receptor Gene Diversity and Selection. *Annu Rev Biochem* (1990) 59:475–96. doi: 10.1146/annurev.bi.59.070190.002355
86. Gohil SH, Iorgulescu JB, Braun DA, Keskin DB, Livak KJ. Applying High-Dimensional Single-Cell Technologies to the Analysis of Cancer Immunotherapy. *Nat Rev Clin Oncol* (2021) 18:244–56. doi: 10.1038/s41571-020-00449-x
87. Oh DY, Kwek SS, Raju SS, Li T, McCarthy E, Chow E, et al. Intratumoral CD4(+) T Cells Mediate Anti-Tumor Cytotoxicity in Human Bladder Cancer. *Cell* (2020) 181:1612–1625.e1613. doi: 10.1016/j.cell.2020.05.017
88. Sacher AG, St Paul M, Paige CJ, Ohashi PS. Cytotoxic CD4(+) T Cells in Bladder Cancer-a New License to Kill. *Cancer Cell* (2020) 38:28–30. doi: 10.1016/j.ccell.2020.06.013
89. van der Leun AM, Thommen DS, Schumacher TN. Cd8(+) T Cell States in Human Cancer: Insights from Single-Cell Analysis. *Nat Rev Cancer* (2020) 20:218–32. doi: 10.1038/s41568-019-0235-4
90. Gawad C, Koh W, Quake SR. Single-Cell Genome Sequencing: Current State of the Science. *Nat Rev Genet* (2016) 17:175–88. doi: 10.1038/nrg.2015.16
91. Angelo M, Bendall SC, Finck R, Hale MB, Hitzman C, Borowsky AD, et al. Multiplexed Ion Beam Imaging of Human Breast Tumors. *Nat Med* (2014) 20:436–42. doi: 10.1038/nm.3488
92. Stoeckius M, Hafemeister C, Stephenson W, Houck-Loomis B, Chattopadhyay PK, Swerdlow H, et al. Simultaneous Epitope and Transcriptome Measurement in Single Cells. *Nat Methods* (2017) 14:865–8. doi: 10.1038/nmeth.4380
93. Peterson VM, Zhang KX, Kumar N, Wong J, Li L, Wilson DC, et al. Multiplexed Quantification of Proteins and Transcripts in Single Cells. *Nat Biotechnol* (2017) 35:936–9. doi: 10.1038/nbt.3973
94. Minnoye L, Marinov GK, Krausgruber T, Pan L, Marand AP, Secchia S, et al. Chromatin Accessibility Profiling Methods. *Nat Rev Methods Primers* (2021) 1:10. doi: 10.1038/s43586-020-00008-9
95. Larsson L, Frisén J, Lundeberg J. Spatially Resolved Transcriptomics Adds a New Dimension to Genomics. *Nat Methods* (2021) 18:15–8. doi: 10.1038/s41592-020-01038-7
96. Artyomov MN, Van den Bossche J. Immunometabolism in the Single-Cell Era. *Cell Metab* (2020) 32:710–25. doi: 10.1016/j.cmet.2020.09.013
97. Ren X, Zhang L, Zhang Y, Li Z, Siemers N, Zhang Z. Insights Gained from Single-Cell Analysis of Immune Cells in the Tumor Microenvironment. *Annu Rev Immunol* (2021) 39:583–609. doi: 10.1146/annurev-immunol-110519-071134
98. Tirosh I, Izar B, Prakadan SM, Wadsworth MH,2, Treacy D, Trombetta JJ, et al. Dissecting the Multicellular Ecosystem of Metastatic Melanoma by Single-Cell RNA-Seq. *Science* (2016) 352:189–96. doi: 10.1126/science.aad0501
99. Puram SV, Tirosh I, Parikh AS, Patel AP, Yizhak K, Gillespie S, et al. Single-Cell Transcriptomic Analysis of Primary and Metastatic Tumor Ecosystems in Head and Neck Cancer. *Cell* (2017) 171:1611–1624.e1624. doi: 10.1016/j.cell.2017.10.044
100. Izar B, Tirosh I, Stover EH, Wakiro I, Cuoco MS, Alter I, et al. A Single-Cell Landscape of High-Grade Serous Ovarian Cancer. *Nat Med* (2020) 26:1271–9. doi: 10.1038/s41591-020-0926-0
101. Filbin MG, Tirosh I, Hovestadt V, Shaw ML, Escalante LE, Mathewson ND, et al. Developmental and Oncogenic Programs in H3K27M Gliomas Dissected by Single-Cell RNA-Seq. *Science* (2018) 360:331–5. doi: 10.1126/science.aao4750
102. Cheng S, Li Z, Gao R, Xing B, Gao Y, Yang Y, et al. A Pan-Cancer Single-Cell Transcriptional Atlas of Tumor Infiltrating Myeloid Cells. *Cell* (2021) 184:792–809.e723. doi: 10.1016/j.cell.2021.01.010
103. Lavin Y, Kobayashi S, Leader A, Amir ED, Elefant N, Bigenwald C, et al. Innate Immune Landscape in Early Lung Adenocarcinoma by Paired Single-Cell Analyses. *Cell* (2017) 169:750–765.e717. doi: 10.1016/j.cell.2017.04.014
104. Zhang M, Yang H, Wan L, Wang Z, Wang H, Ge C, et al. Single-Cell Transcriptomic Architecture and Intercellular Crosstalk of Human Intrahepatic Cholangiocarcinoma. *J Hepatol* (2020) 73:1118–30. doi: 10.1016/j.jhep.2020.05.039
105. Antony PA, Piccirillo CA, Akpinarli A, Finkelstein SE, Speiss PJ, Surman DR, et al. Cd8+ T Cell Immunity Against a Tumor/Self-Antigen is Augmented by CD4+ T Helper Cells and Hindered by Naturally Occurring T Regulatory Cells. *J Immunol* (2005) 174:2591–601. doi: 10.4049/jimmunol.174.5.2591
106. Peng J, Sun BF, Chen CY, Zhou JY, Chen YS, Chen H, et al. Single-Cell RNA-seq Highlights Intra-Tumoral Heterogeneity and Malignant Progression in Pancreatic Ductal Adenocarcinoma. *Cell Res* (2019) 29:725–38. doi: 10.1038/s41422-019-0195-y
107. Chiou SH, Tseng D, Reuben A, Mallajosyula V, Molina IS, Conley S, et al. Global Analysis of Shared T cell Specificities in Human non-Small Cell Lung Cancer Enables HLA Inference and Antigen Discovery. *Immunity* (2021) 54:586–602.e588. doi: 10.1016/j.immuni.2021.02.014
108. Braun DA, Street K, Burke KP, Cookmeyer DL, Denize T, Pedersen CB, et al. Progressive Immune Dysfunction with Advancing Disease Stage in Renal Cell Carcinoma. *Cancer Cell* (2021) 39:632–48. doi: 10.1016/j.ccell.2021.02.013
109. Burrell RA, McGranahan N, Bartek J, Swanton C. The Causes and Consequences of Genetic Heterogeneity in Cancer Evolution. *Nature* (2013) 501:338–45. doi: 10.1038/nature12625
110. Rosenthal R, Cadieux EL, Salgado R, Bakir MA, Moore DA, Hiley CT, et al. Neoantigen-Directed Immune Escape in Lung Cancer Evolution. *Nature* (2019) 567:479–85. doi: 10.1038/s41586-019-1032-7
111. George JT, Levine H. Implications of Tumor-Immune Coevolution on Cancer Evasion and Optimized Immunotherapy. *Trends Cancer* (2021) 7:373–83. doi: 10.1016/j.trecan.2020.12.005
112. Kamoun A, de Reyniès A, Allory Y, Sjödahl G, Robertson AG, Seiler R, et al. A Consensus Molecular Classification of Muscle-invasive Bladder Cancer. *Eur Urol* (2020) 77:420–33. doi: 10.1016/j.eururo.2019.09.006
113. Choi W, Porten S, Kim S, Willis D, Plimack ER, Hoffman-Censits J, et al. Identification of Distinct Basal and Luminal Subtypes of Muscle-Invasive Bladder Cancer with Different Sensitivities to Frontline Chemotherapy. *Cancer Cell* (2014) 25:152–65. doi: 10.1016/j.ccr.2014.01.009
114. Salcedo A, Tarabichi M, Espiritu SMG, Deshwar AG, David M, Wilson NM, et al. A Community Effort to Create Standards for Evaluating Tumor Subclonal Reconstruction. *Nat Biotechnol* (2020) 38:97–107. doi: 10.1038/s41587-019-0364-z
115. Skinnider MA, Squair JW, Kathe C, Anderson MA, Gautier M, Matson KJE, et al. Cell Type Prioritization in Single-Cell Data. *Nat Biotechnol* (2021) 39:30–4. doi: 10.1038/s41587-020-0605-1
116. Gao R, Bai S, Henderson YC, Lin Y, Schalck A, Yan Y, et al. Delineating Copy Number and Clonal Substructure in Human Tumors from Single-Cell Transcriptomes. *Nat Biotechnol* (2021) 39:599–608. doi: 10.1038/s41587-020-00795-2
117. Narayan A, Berger B, Cho H. Assessing Single-Cell Transcriptomic Variability Through Density-Preserving Data Visualization. *Nat Biotechnol* (2021). doi: 10.1038/s41587-020-00801-7

118. Sautès-Fridman C, Petitprez F, Calderaro J, Fridman WH. Tertiary Lymphoid Structures in the Era of Cancer Immunotherapy. *Nat Rev Cancer* (2019) 19:307–25. doi: 10.1038/s41568-019-0144-6
119. Meylan M, Petitprez F, Lacroix L, Di Tommaso L, Roncalli M, Bougoüin A, et al. Early Hepatic Lesions Display Immature Tertiary Lymphoid Structures and Show Elevated Expression of Immune Inhibitory and Immuno suppressive Molecules. *Clin Cancer Res* (2020) 26:4381–9. doi: 10.1158/1078-0432.Ccr-19-2929
120. Cabrita R, Lauss M, Sanna A, Donia M, Skaarup Larsen M, Mitra S, et al. Tertiary Lymphoid Structures Improve Immunotherapy and Survival in Melanoma. *Nature* (2020) 577:561–5. doi: 10.1038/s41586-019-1914-8
121. Helmink BA, Reddy SM, Gao J, Zhang S, Basar R, Thakur R, et al. B Cells and Tertiary Lymphoid Structures Promote Immunotherapy Response. *Nature* (2020) 577:549–55. doi: 10.1038/s41586-019-1922-8
122. Spranger S, Gajewski TF. Impact of Oncogenic Pathways on Evasion of Antitumour Immune Responses. *Nat Rev Cancer* (2018) 18:139–47. doi: 10.1038/nrc.2017.117
123. Peng W, Chen JQ, Liu C, Malu S, Creasy C, Tetzlaff MT, et al. Loss of PTEN Promotes Resistance to T Cell–Mediated Immunotherapy. *Cancer Discov* (2016) 6:202. doi: 10.1158/2159-8290.CD-15-0283
124. Roviello G, Catalano M, Nobili S, Santi R, Mini E, Nesi G. Focus on Biochemical and Clinical Predictors of Response to Immune Checkpoint Inhibitors in Metastatic Urothelial Carcinoma: Where do we Stand? *Int J Mol Sci* (2020) 21:7935–48. doi: 10.3390/ijms21217935
125. Rodriguez-Vida A, Perez-Gracia JL, Bellmunt J. Immunotherapy Combinations and Sequences in Urothelial Cancer: Facts and Hopes. *Clin Cancer Res* (2018) 24:6115–24. doi: 10.1158/1078-0432.Ccr-17-3108
126. van Dijk N, Gil-Jimenez A, Silina K, Hendricksen K, Smit LA, de Feijter JM, et al. Preoperative Ipilimumab Plus Nivolumab in Locoregionally Advanced Urothelial Cancer: The NABUCCO Trial. *Nat Med* (2020) 26:1839–44. doi: 10.1038/s41591-020-1085-z
127. Tran L, Xiao JF, Agarwal N, Duex JE, Theodorescu D. Advances in Bladder Cancer Biology and Therapy. *Nat Rev Cancer* (2021) 21:104–21. doi: 10.1038/s41568-020-00313-1
128. Rozenblatt-Rosen O, Regev A, Oberdoerffer P, Nawy T, Hupalowska A, Rood JE, et al. The Human Tumor Atlas Network: Charting Tumor Transitions Across Space and Time at Single-Cell Resolution. *Cell* (2020) 181:236–49. doi: 10.1016/j.cell.2020.03.053
129. Irmisch A, Bonilla X, Chevrier S, Lehmann KV, Singer F, Toussaint NC, et al. The Tumor Profiler Study: Integrated, Multi-Omic, Functional Tumor Profiling for Clinical Decision Support. *Cancer Cell* (2021) 39:288–93. doi: 10.1016/j.ccell.2021.01.004

Conflict of Interest: The authors declare that the research was conducted in the absence of any commercial or financial relationships that could be construed as a potential conflict of interest.

frontiers in Immunology

REVIEW
published: 07 June 2021
doi: 10.3389/fimmu.2021.689091

Single-Cell TCR and Transcriptome Analysis: An Indispensable Tool for Studying T-Cell Biology and Cancer Immunotherapy

Anna Pasetto[1]* *and Yong-Chen Lu*[2,3]*

[1] Department of Laboratory Medicine, Division of Clinical Microbiology, ANA FUTURA, Karolinska Institutet, Stockholm, Sweden, [2] Department of Pathology, University of Arkansas for Medical Sciences, Little Rock, AR, United States, [3] Winthrop P. Rockefeller Cancer Institute, University of Arkansas for Medical Sciences, Little Rock, AR, United States

T cells have been known to be the driving force for immune response and cancer immunotherapy. Recent advances on single-cell sequencing techniques have empowered scientists to discover new biology at the single-cell level. Here, we review the single-cell techniques used for T-cell studies, including T-cell receptor (TCR) and transcriptome analysis. In addition, we summarize the approaches used for the identification of T-cell neoantigens, an important aspect for T-cell mediated cancer immunotherapy. More importantly, we discuss the applications of single-cell techniques for T-cell studies, including T-cell development and differentiation, as well as the role of T cells in autoimmunity, infectious disease and cancer immunotherapy. Taken together, this powerful tool not only can validate previous observation by conventional approaches, but also can pave the way for new discovery, such as previous unidentified T-cell subpopulations that potentially responsible for clinical outcomes in patients with autoimmunity or cancer.

Keywords: single cell, cancer immune, tumor microenviroment (TME), TCR - T cell receptor, immunotherapy

OPEN ACCESS

Edited by:
Qihui Shi,
Fudan University, China

Reviewed by:
Meiyi Li,
Fudan University, China
Jing Ge,
Institut Pasteur of Shanghai (CAS), China

***Correspondence:**
Anna Pasetto
anna.pasetto@ki.se
Yong-Chen Lu
YLu@uams.edu

Specialty section:
This article was submitted to Cancer Immunity and Immunotherapy, a section of the journal Frontiers in Immunology

Received: *31 March 2021*
Accepted: *10 May 2021*
Published: *07 June 2021*

Citation:
Pasetto A and Lu Y (2021) Single-Cell TCR and Transcriptome Analysis: An Indispensable Tool for Studying T-Cell Biology and Cancer Immunotherapy. Front. Immunol. 12:689091. doi: 10.3389/fimmu.2021.689091

INTRODUCTION

T-Cell Receptor

A T-cell receptor (TCR) is a heterodimer consisting of two chains, TCRα and TCRβ chains, that allow the recognition of peptides in the contest of major histocompatibility complex (MHC) molecules. Each of the two chains is made of a variable region and a constant region that are spliced together during the T cell development that happens in the thymus. In TCRβ chain, there are two constant region gene segments, Cβ1 and Cβ2, with some shared sequences. In TCRα chain, there is only one constant region gene segment, Cα. The variable region of the β chain consists of three gene segments called variable (V), diversity (D) and junctional (J), but the α chain only consists of the V and J segments. In human, 42 V segments, 2 D and 12 J are identified in β chain locus; and 43 V and 58 J for the α locus. Within each V segment, there are three hypervariable regions, or complementarity-determining regions (CDR1, CDR2 and CDR3). While CDR1 and CDR2 are encoded by the V segment, the CDR3 regions results from the juxtaposition of the V, (D) and J

regions during somatic recombination. The joining of the V(D)J regions is imprecise, and nucleotides can be lost or added (e.g. the P and N nucleotides) during the process, resulting in a unique and unpredictable amino acid sequence for each CDR3 (1). It is clear that the structure of the TCR allows for great variability, which is further increased by the heterodimeric pairing of the α and β chains. It is estimated that the total number of possible combination could be greater than 10^{18} (2). The great variability of TCRs is essential to enable their unique ability to recognize antigenic targets, either pathogens or tumor cells. Lastly, the process of antigen recognition is also complicated. It relies on multiple interactions. The TCR needs to contact the MHC molecule on the cell surface, mostly by specific interactions with CDR1 and CDR2. The TCR also interacts with the peptide presented by the MHC molecule, mostly by specific interaction with the CDR3.

In the field of cancer immunotherapy, the identification not only of cancer antigens, but also of the antigen-specific TCRs, is a major research topic. Despite the evidence of tumor-specific T cells in cancer patients both among the tumor infiltrating lymphocytes (3–5) and in the peripheral blood (6–9), the presence of these cells is often not sufficient to induce cancer regressions even after checkpoint immunotherapy (10, 11). The reasons for these mixed clinical results are still not fully elucidated and cannot be addressed with a simple explanation. Nevertheless, it is commonly hypothesized that such antigen-specific T cells display an exhaustion phenotype that cannot easily be reverted (12), especially in the contest of an immunosuppressive tumor microenvironment (13). Adoptive cell therapy can potentially overcome these limitation by both increasing the number of cancer-specific T cells *ex vivo* before reinfusion and also by engineering these T cells with more powerful TCRs (14). The genetic transfer of TCRs requires the identification and isolation of powerful and specific TCRs. As described earlier, TCRs are heterodimers and only the match between the correct TCRα and β chain would enable a specific antigen recognition. TCR pairing is therefore one of the major challenges in the process of TCR identification.

Several approaches have been proposed to overcome the challenge of TCR pairing. Once a population of reactive T cells is identified, next-generation sequencing of bulk TCR clonotypes can provide a list of dominant TCRα and β clones that could be then paired accordingly to their frequency (15, 16). This approach gives the best results when the population of interest is fairly oligoclonal (most dominant TCRβ clonotype ≥ ~20%), but it is possible that the most dominant clonotypes need to be paired with each other using a matrix before the correct match is found. Another method that has been utilized to match TCRα and TCRβ chains from a bulk T-cell population is the Pairseq from Adaptive Biotechnologies (17). This approach is also based on next generation sequencing of both TCRα and TCRβ chains from a T cell subset, but the pairing of the chains is assigned with a statistical algorithm. The last approach is TCR sequencing at the single-cell level. This represents the best approach because it allows to quickly identify the correct TCRα and β pairs from each single cell present in a T-cell population of interest. Several different technical approaches have been utilized for single-cell TCR sequencing. In the following sessions, we will describe these robust and successful methods.

SINGLE-CELL TCR AND TRANSCRIPTOME SEQUENCING

Step One: The Isolation of Single T Cells

The first step in each single-cell sequencing technology is the isolation of single cells (**Figure 1A**). The conventional technique developed to isolate single T cells to obtain clonal T cell lines is called limiting dilution. This approach is relatively simple. However, due to the statistical distribution of cells per well, it is not very efficient. Typically, only one third of the wells contain a single cell when starting with a concentration of 0.5 cells per aliquot (18). Micromanipulation is another technique developed mainly to isolate embryos or stem cells, but it could be applied to T cells, particularly since the potential of generating human induced pluripotent stem cells to differentiate into anti-tumor T cells has been explore (19). A microscope-guided capillary pipette is used to pick single cells from a suspension culture (20). Laser-capture microdissection is similarly used to isolate individual cells or cell compartment from solid-tissue samples, such as biopsies, paraffin-embedded or cryo-fixed tissues (21–23). The main limitation with these approaches is that they are low-throughput and time-consuming.

To overcome such limitation, several approaches have been developed. One approach that has been commonly used is fluorescence-activated cell sorting (FACS), where the T cells are isolated based on the staining of pMHC multimers (8) or surface markers, such as PD-1 (15) or CD137 (16). This methodology allows to choose a specific population of interest but has the requirement of a high number of cells as starting materials. Microfluidic isolation of cells has the advantage of low sample consumption. When performed in closed systems, it also reduces the risk of contamination (24). The commercial platform Fluidigm C1 is an example of automated system for single cell capture coupled with cell-lysis, RNA extraction and cDNA synthesis. A more recent commercial system, the Chromium Controller from 10X Genomics, has recently gained popularity. The system is based on microdroplets, where cells are captured in aqueous droplets dispersed in oil phase. This system enables the isolation of tens of thousands of single cells simultaneously with high throughput and high capture efficiency (25). Notably, in the majority of experiments, no special modifications are needed for isolating single cells from T cells, compared to other cell types. However, because of the relatively smaller size of T cells, the microfluidics technique needs to be adjusted accordingly. For example, T cells can only be captured by the smallest, 5-10 μm integrated fluidic circuits (IFCs) using a Fluidigm C1 system.

Step Two: TCR and Gene Amplification

The next step after single T-cell capture involves in the reverse transcription and amplification of TCR and/or genes of interest.

In the following section, we describe the most common strategies for single-cell analysis (**Figure 1B**).

Multiplex PCR

The very first methodology developed to sequence TCRα and TCRβ chains was based on multiplex PCR followed by Sanger sequencing of the different amplicons (26). Although useful for the isolation of specific TCR clones, this methodology did not have the adequate throughput capacity to give an estimation of the TCR diversity in an T cell population. Only after the technical break-thought of multiple parallel sequencing (also called "next-generation sequencing" or NGS), it became possible to obtain a comprehensive knowledge of the TCR arrangement including V–J segments and the complete CDR3 sequence. A simple but effective approach to amplify the TCRs consists in a multiplex PCR where a pool of forward primers complementary to the different V segments of the TCRs and either a pool of reverse primers complementary to the different J segments or two reverse primers complementary to the C regions. The J segment primers are mainly utilized when TCR sequences are amplified from genomic DNA due to the intronic sequences. It's possible to amplify TCR sequences from cDNA using the same pool of primers (27). However, only cDNA, but not genomic DNA, can be amplified using reverse primers complementary to the constant regions (28). Subsequently, additional genes associated with specific T cell functions (*e.g.* cytokines) can be

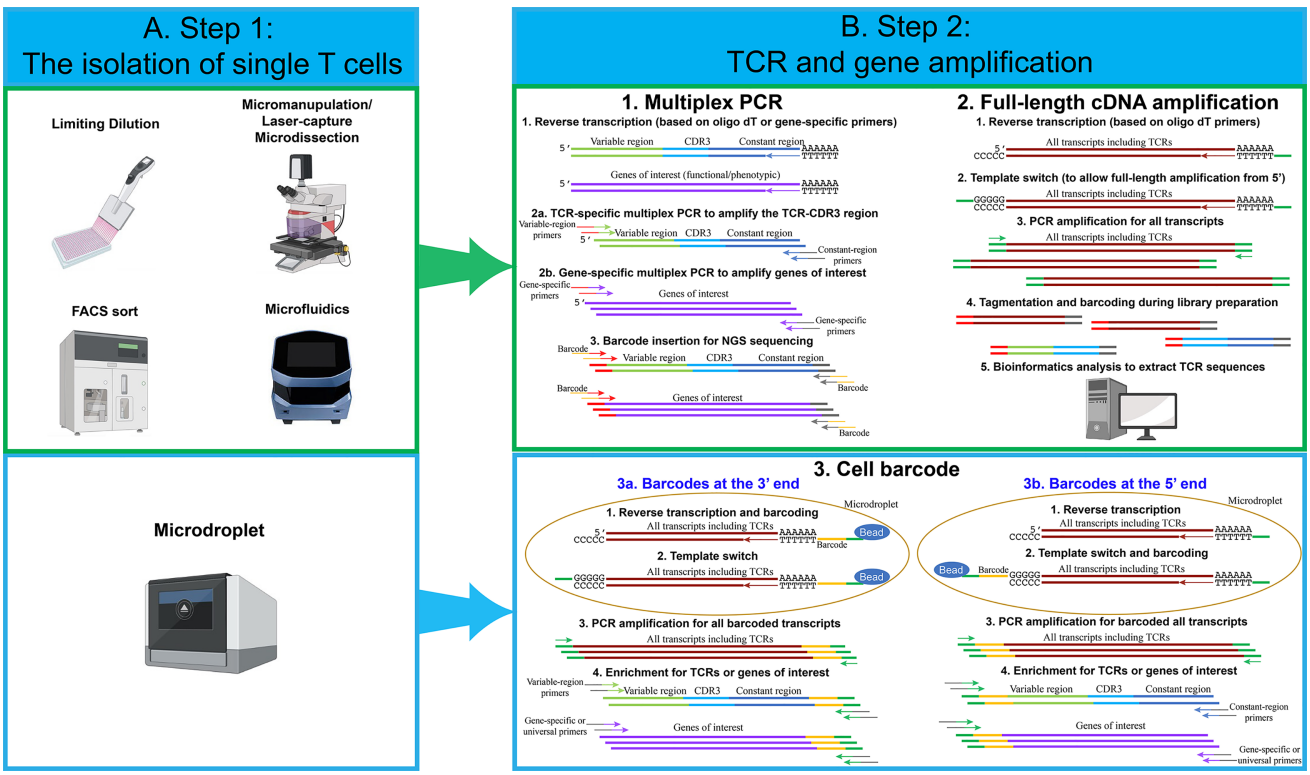

FIGURE 1 | An overview of single-cell isolation techniques, followed by TCR and gene amplification strategies. **(A)** Several techniques have been used to isolate single cells. The most frequently used techniques are FACS sort and microdroplet techniques. For limiting dilution, micromanipulation, FACS sort and microfluidics techniques, multiplex PCR and full-length cDNA amplification approach can be used to perform single-cell TCR and transcriptome sequencing. For the microdroplet technique, cell barcode approach is used to perform single-cell TCR and transcriptome sequencing. **(B)** For the multiplex PCR approach, individual single cells are lysed in individual PCR tubes or wells. Reverse transcription is performed using oligo dT or gene-specific primers. Two PCR reactions are performed in individual wells using TCR or gene-specific primers. Notably, for each PCR reaction, approximately 70 variable-region forward primers are required to amplify the majority of TCRs. Two constant-region reverse primers are required, including one primer for constant-region Cα and one primer for constant-region Cβ1 and Cβ2. Lastly, barcodes for individual wells are added by an additional PCR reaction. Single-cell PCR products from individual wells are pooled and sequenced. For the full-length cDNA amplification approach, individual single cells are lysed in individual PCR tubes or wells, and reverse transcription is performed using oligo dT. All transcripts, including TCRs and genes of interests, are amplified by PCR reactions. Full-length cDNA products are cut into small fragments by tagmentation. Barcodes for individual wells are added by an additional PCR reaction. Single-cell PCR products from individual wells are pooled and sequenced. Bioinformatic analysis is used to extract TCR sequences and calculate the expression levels for genes of interests. For the cell barcode approach, single cells are lysed in individual microdroplets, and the cell barcodes for individual single cells are added either at the 3' or at the 5' end of the transcripts. For 3' barcoding, barcodes are added at the reverse transcription step. After reverse transcription and template switch, all single-cell transcripts are pooled and amplified. Similar to the multiplex PCR approach, a pool of about 70 variable-region forward primers are required to amplify TCRs and genes of interest. Lastly, PCR products are sequenced and analyzed. For 5' barcoding, barcodes are added at the template switch step. After barcoding, all of the single-cell transcripts are pooled and amplified. Unlike 3' barcoding, only two constant-region reverse primers are required for each PCR reaction. Lastly, PCR products are sequenced and analyzed. Notably, for both 5' and 3' barcoding, tagmentation and PCR amplification by universal primers can be utilized, in order to analyze all transcripts and obtain whole-transcriptome data.

also amplified in the same reaction. The introduction of short nucleotides, or barcodes, during the PCR reaction, makes it possible to pool the different amplicons and perform high-throughput sequencing by NGS (29). More recently, the technological developments have resulted in mainly two methods commonly used to perform the amplification of the single cell transcriptome that can be divided into full-length cDNA amplification and cell barcode approach.

Full-Length cDNA Amplification

This approach generates a sequencing library separately for each single-cell transcriptome. While it is more expensive than targeting specific genes, it has the benefit of broader data collection (*e.g.* on isoforms, etc.). The full-length approach has also been used to identify TCR sequences for several applications, including TCR repertoire analysis and pairing of TCRα and β chains. This approach is often used when the single cells are captured in individual wells, for example, after FACS sort or when captured by a microfluidic device. After cell lysis, the mRNA molecules are reverse transcribed using oligo dT primers at the 3′end. A universal sequence is added at the 5′end by a template-switch strategy. The template switch strategy is usually employed when there is a variation about the exact sequence of a gene, such as TCR variable region, or when we intend to amplify all transcripts. The strategy employed is based on the particular behavior of the reverse transcriptase that adds a stretch of non-template dCTPs at the 3′ end of the cDNA. This stretch of dCTPs can bind to a specifically designed oligo that contains a complementary stretch of poly-G followed by a universal sequence (30).

Once the universal sequence is introduced at the 5′end of each transcript, the full-length transcript (from the 5' to the 3' end) can be amplified. The amplification step is followed by a "tagmentation" step, usually using a transposase that can insert Tag sequences that are then used to insert barcodes. The libraries prepared with this method are not enriched for the TCR sequences. Therefore, to extract each TCR sequence, it is necessary to use a bioinformatic tool. For TCRs, the traditional reference-based assembly, where the sequences obtained are compared to a reference genome, is combined with *de novo* assembly for the CDR3 region that has to be reconstructed based only from the actual sequences. Several tools have been developed to perform this type of analysis. An example is TraCeR, a computational method that allows to reconstruct the variable sequence of TCRα and TCRβ chains through use of a "combinatorial recombinome" library of all possible TCR sequences, this method was initially used in combination with the FluidigmC1 System (31, 32). Another computational method is "single-cell TCRseq" (33) that employs several consecutive steps to first identify and count RNA reads mapping to specific TCR V and C regions, then perform multiple alignments to create consensus V and C gene sequences. Finally, gaps in the sequence are filled similarly to *de novo* transcript assembly. A similar multistep approach is also used by TRAPeS (TCR Reconstruction Algorithm for Paired-End Single-cell) (34). In this software, the V and J segments are first identified for each chain. Subsequently, a set of putative CDR3 reads are identified as potential match to the one from the previously identified V and J segments. Lastly, an algorithm is used to reconstruct the CDR3 region from the putative CDR3 reads. We also utilized a similar approach to assemble TCR sequences (35). The TCR sequence reads were first aligned to V segments, and then TCR reads with identical CDR3 region sequences were merged to assemble the full-length TCR sequences. Lastly, VDJ Puzzle is a useful tool that allows to reconstruct the TCR sequence from single cell transcriptome data (36). This method was first described to link the TCR sequence from antigen-specific cells based on their gene expression profile.

Cell Barcode

The cell-barcode strategy adds cell barcodes, about 10-20 bp random nucleotide sequences, to individual single cells. This makes it possible to pool all transcripts coming from thousands of cells, increasing the throughput and decreasing the cost dramatically (17, 37). This approach is usually employed after each cell has been captured into a microdroplet and lysed. In addition to cell barcodes, molecular barcodes are often added at the same time. Molecular barcodes, also known as unique molecular identifiers (UMIs), are about 10 bp random nucleotide sequences, which allow us to identify each individual molecules/transcripts. The advantage of UMI technique is that the UMI counting will not be altered even after imbalanced PCR amplification.

For the cell barcodes at the 3' end, all mRNA transcripts present in the cells are reverse transcribed using oligo dT primers containing both the cell barcodes and molecular barcodes. Next, the template switch strategy is used to add a universal sequence at the 5' end. This enables the PCR amplification of all transcripts. Lastly, a set of variable-region forward primers and gene-specific forward primers are utilized to enrich TCRs and other genes of interest. An additional PCR reaction is required to add necessary DNA sequences for next-generation sequencing.

For the cell barcodes at the 5' end, all mRNA transcripts are reverse transcribed using oligo dT primers, but the cell barcodes and molecular barcodes are added at the 5' end during the template switch step. Next, all transcripts are pooled and amplified by PCR. TCR and other genes of interest can be amplified by constant-region reverse primers and gene-specific reverse primers. Lastly, an additional PCR reaction is used to add necessary DNA sequences for next-generation sequencing. Notably, the whole-transcriptome analysis can be achieved by both 5' and 3' end barcoding. After the PCR amplification and an additional tagmentation step for all transcripts, transcripts at the 5' end or 3' end can be processed and sequenced. Because cell barcodes and molecular barcodes are required to be retained in the entire process, only the gene sequences near the 5' or 3' end, approximately 200-500 bp, can be sequenced. As the results, the information of full-length transcripts, including isoforms, is lost using this strategy.

The strengths and weaknesses of different strategies are summarized in **Tables 1** and **2**. In recent years, the single-cell field has been in favor of the microdroplets with cell barcode approach, because a higher number of cells can be obtained, compared to other approaches. Although the microdroplet approach is less sensitive to detect low abundant genes, this

TABLE 1 | Comparison between multiplex PCR approach and full-length cDNA amplification approach.

Multiplex PCR	Full-length cDNA amplification
More sensitive for individual genes or TCRs	Less sensitive
Lower cost	Higher cost for deeper sequencing
A set of ~70 primers for TCR variable region is required*	Only a set of universal primers is required*
Impossible to obtain whole-transcriptome data	Available whole-transcriptome data
Impossible to obtain full-length TCR sequences	Available full-length TCR sequences

**Another set of primers is required for nested PCR amplification.*

TABLE 2 | Comparison between cell barcodes at the 5' end and 3' end.

Barcodes at the 3' end	Barcodes at the 5' end
More efficient to add barcodes	Less efficient to add barcodes
A set of ~70 primers for TCR variable region is required*	Only 2 primers for TCR constant region are required*
Suitable for all types of cells	Only suitable for TCR and BCR studies
More kits and applications available due to popularity	Less kits and applications available

**Another set of primers is required for nested PCR amplification.*

concern is outweighed by the high cell numbers and robust bioinformatic tools. In addition, microdroplets with barcodes at 5' end can use a minimum number of primers for TCR amplification, compared to barcodes at 3' end. As a result, 5' barcoding is more suitable for T-cell studies that require TCR sequence information, such as clonality analysis.

SPATIAL TRANSCRIPTOMICS

Single-cell samples are often prepared by enzymatic or mechanical dissociation. As a result, spatial information is lost during the sample preparation. However,the interactions between T cells and the adjacent cells in the tumor microenvironment may influence the transcriptome of individual T cells. Stahl PL et al. have developed a new technique to provide two-dimensional, spatial information, which can complement single-cell transcriptome data analysis (38). In this technique, mRNA transcripts from a tissue section are captured on an array by oligo dT-based probes, which contain spatial barcodes and UMIs (**Figure 2**). Similar to the single-cell transcriptome analysis with barcodes at 3' end, transcripts containing barcodes at 3' are amplified and sequenced. This technique has improved significantly in recent years, and it can now reach near the single-cell resolution, at approximately

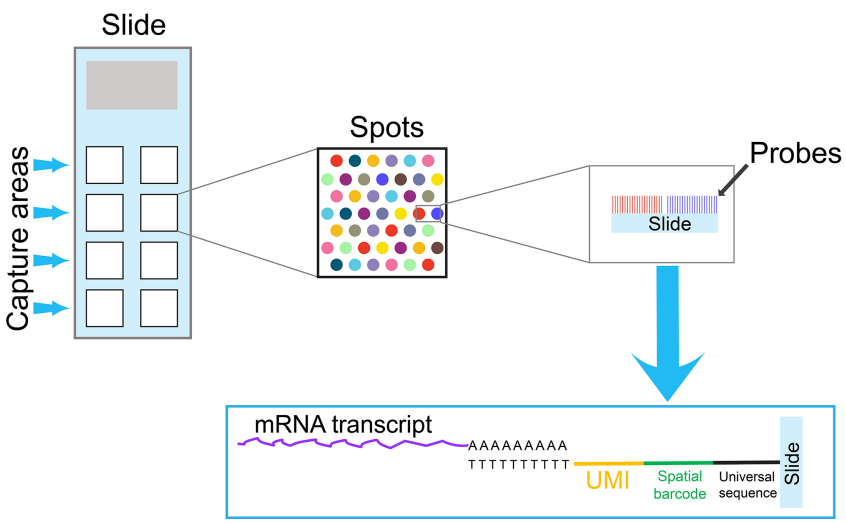

FIGURE 2 | An overview of a spatial transcriptomics technique. A specialized slide contains several capture areas. Each capture area contains thousands of spots, and each spot is coated by oligo dT-based probes. To obtain spatial information, mRNA transcripts from a tissue section are captured by these oligo dT-based probes on spots. Because probes on each spot contain a unique spatial barcode and UMIs, the spatial information can be preserved in the subsequent PCR reactions. Similar to the single-cell cell barcode approach with 3' barcoding, transcripts containing spatial barcodes at the 3' end are amplified by PCR reactions and sequenced. The data obtained from spatial transcriptomics can combine with single-cell transcriptome data to obtain comprehensive information for cell-cell interactions in the tissue microenvironment.

1-10 cell resolution per spot, depending on the tissue type. In addition, spatial information can combine with traditional immunofluorescence staining to detect both mRNA and protein expression at the same time.

Since the initial publication, scientists have used this spatial transcriptomics technique on a variety of tissue specimens. We have identified two publications related to T-cell studies. Thrane K et al. utilized this technique to study melanoma lymph node biopsies, and they were able to visualize the transcriptional landscape within the tissue (39). The lymphoid area in close proximity to the tumor region showed a specific expression pattern, which might reflect the unique feature in tumor microenvironment. Notably, an IFN-γ gene signature, likely from activated T cells, was identified within the transition area between melanoma and lymphoid areas. In another study, Ji AL et al. combined the techniques of spatial transcriptomics, single-cell transcriptome and multiplexed ion beam imaging to study the architecture of cutaneous squamous cell carcinoma (40). In addition to a tumor-specific keratinocyte population that they identified, they also observed regulatory T cells co-localized with $CD8^+$ T cells in the compartmentalized tumor stroma. Taken together, spatial transcriptomics may have significant potential in the future study.

T-CELL NEOANTIGEN IDENTIFICATION

Cancer is caused by a series of genetic alterations that occur in normal cells and are responsible for their transformation in malignant cells. These alterations confer an advantage to the affected cells, such as increased proliferation and inhibition of apoptosis. However, these can also result in the production of mutant proteins that are immunogenic and can be targeted by the immune-system. When such mutated proteins become targets for the immune-system, they can be called neoantigens. Because neoantigens are not expressed by normal cells, they represent attractive targets for cancer therapy. In the vast majority of cases the identified neoantigens arise by single amino-acid substitutions. The mutated peptides can be processed and presented by MHC molecules, and then the peptide/MHC complexes can be recognized by T cells. The presence of neoantigen-reactive T cells have been identified across different cancer histology, like lung cancer (41, 42) bladder cancer (43), head and neck cancer (44, 45), ovarian cancer (46–49) pancreatic cancer (50, 51) and gastrointestinal epithelial malignancies (35, 52–54). Interestingly, the T cells identified in these studies recognized unique somatic mutations, with few exceptions where the T cells recognized hot spot mutations on oncogenes, like KRAS (55, 56) and p53 (9, 47, 48, 54). Additional studies are needed in order to evaluate systematically the immune-response against hot spot mutations in these highly valuable targets.

Single cell sequencing is a powerful tool for T cell biology discovery and can be employed to dissect specific functional and phenotypical signatures. T cells have the ability to recognize specific antigens in the contest of MHC molecules, and this ability can be harnessed to develop anticancer therapies, therapies against autoimmune diseases and antiviral therapies. The "holy grail" of T cell immunology would be to predict the antigen-specificity of a T cell simply by studying its TCR sequence and structure. Although this antigen-prediction is not available yet, several technologies have been developed to identify an epitope recognized by a given T cell and rapidly isolate its TCR. In the following sections we will describe some of the most successful approaches used to identify T cell antigens and their specific TCRs.

pMHC Multimers

One of the most common approaches used for this purpose is based on the capacity of T cells to bind pMHC multimers. If the multimers are labelled with fluorescent probes, the T cells can be identified and isolated by flow cytometry (57). This strategy can only be applied when the target epitope is known and also suitable to be presented on pMHC multimers. Typically class I epitopes give more specific binding than class II. Despite these limitations this approach has been effective to discover important cancer antigens that could be used for immunotherapy (58, 59). A more recent version of this strategy employs pMHC multimers labelled with DNA barcodes [TetTCR-Seq (60)] which has the advantage of high-throughput and the possibility to integrate single-cell transcriptomics, T cell phenotype and TCR sequence isolation. To address specific binding and recognition of class II restricted epitope, Graham DB et al. developed a high-throughput approach for screening of DNA-encoded pMHC class II libraries to provide functional recognition by TCRs identified from single cell sequencing (61). Additionally, DNA-barcodes were linked to magnetic nanoparticles, as described by Peng et al. (62), to identify $CD8^+$ neoantigen-specific T cells from tumor and blood samples of melanoma patients. This last study highlights how both the antigen-binding specificity and the sensitivity in detecting rare T-cell populations is important to identify reactive T cells from clinical samples.

Screening of Antigenic Libraries

In the previous section, we described examples of technologies that enabled to isolate specific TCRs for known antigens. This type of approach is very useful when the specific antigen and its MHC-binding epitope is known, for example when targeting viral antigens or shared cancer antigens (both mutated and normal proteins). A different situation is represented by T cells and TCRs that have been isolated based on some particular characteristic (*e.g.* the expression of a specific marker or their high frequency in a particular T cell subset), but their specificity is unknown. There are several strategies that can be used to identify the cognate peptide for orphan TCRs (63). Most approaches are based on empirical testing where the T cell activation status is evaluated after co-culture with the candidate antigens (15, 16, 64). An interesting variation of these approaches consists in the screening of pMHC libraries, where the TCRs are isolated based on their affinity to the different pMHC, but without knowing the antigenic specificity (63).

SINGLE-CELL STUDIES ON T-CELL BIOLOGY AND CANCER IMMUNOTHERAPY

Single-cell transcriptome analysis has been used to study the biology of T cells in several areas, including T-cell development, differentiation, and responses during infection and autoimmunity. The role of T cells in tumor microenvironment and cancer immunotherapy is also a topic for intensive studies (**Figure 3**). Single-cell TCR analysis can also provide important information for these studies, such as TCR pairing and clonality. Furthermore, it has been demonstrated that combining TCR and gene expression information can provide deeper understanding for T cell-mediated immune responses (29). Because many high-quality manuscripts using single-cell techniques have been published in recent years, we would like to focus our discussion on some of outstanding publications utilizing single-cell transcriptome data alone or together with the TCR sequencing data. Notably, high-dimensional flow cytometry or mass cytometry (CyTOF) can investigate over a dozen of cell-surface markers at the single-cell level (65). For the scope of this article, we will not discuss findings generated by this technique.

T-CELL DEVELOPMENT AND DIFFERENTIATION

The thymus is the key organ for T cell development. Abnormalities of T-cell development, including positive and negative selections, can lead to autoimmune diseases (66, 67). Park JE et al. performed a comprehensive single-cell study on prenatal and postnatal thymus samples, including adult samples (68). Pseudo-time analysis showed that gene markers and trajectory for T cell development were consistent with previously knowledge in mice (69). However, the authors also identified a previous unknown subset, GNG4^{+} CD8αα^{+} T cells in the thymus. This subset of T cells could fully mature into a CD8A^{high}/CD8B^{low} phenotype, but T cells from the mouse counterpart could become triple negative (CD8A^{low} CD8B^{low} CD4^{low}) cells.

T cells can further differentiate in the peripheral tissue. Li N et al. utilized single-cell sequencing and other techniques to characterize CD4^{+} T cell compartment in the human fetal intestine (70). Additionally, through the single-cell trajectory analysis, the authors observed the generation of memory-like CD4^{+} T cells in the human fetal intestine. In another report, Galletti G et al. used single-cell analysis to study human CD8^{+} memory T cells from peripheral blood under physiological conditions, and identified two previously unrecognized subsets of stem-like CD8^{+} memory T cells (71). The PD-1^{-} TIGIT^{-} subset was committed to a functional lineage, whereas the PD-1^{+} TIGIT^{+} subset was committed to a dysfunctional, exhausted-like lineage. Lastly, using the transcriptome and TCR sequencing analysis, Patil V et al. identified the CD4^{+} cytotoxic T cell population within the T_{EMRA} (effector memory T cells expressing CD45RA) subset (72). In addition, they could identify four distinct subsets within the CD4^{+} cytotoxic T cell population, based on single-cell transcriptome analysis. These studies provide insights on the potentially durable immunity generated by T cells.

T-Cell Biology in Autoimmunity

T cells play an important role in autoimmunity. Corridoni D et al. utilized single-cell transcriptome analysis to study colonic CD8^{+} T cells in health and ulcerative colitis, an inflammatory bowel disease (73). They found that IL-26 was expressed in terminally differentiated, dysfunctional CD8^{+} T cells from ulcerative colitis. Human IL-26 could attenuate immune responses in a mouse model of acute colitis. Next, Strobl J et al. used single-cell technique to study tissue-resident memory T cells in skin, and they identified RUNX3 and LGALS3 as new markers for this type of T cells (74). They also identified a large number of host-derived tissue-resident memory T cells in skin lesions from patients developing graft-versus-host disease, suggesting the potential contribution of these cells to this disease. Lastly, Seumois G et al. studied the roles of CD4^{+} T helper cells and regulatory T cells in patients with asthma, and

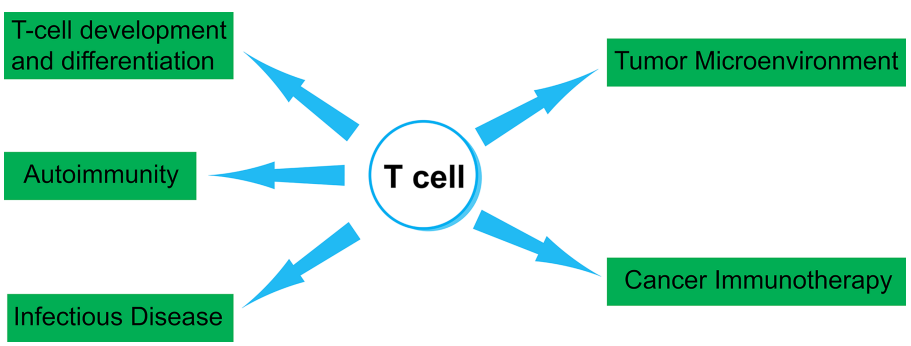

FIGURE 3 | Several aspects of T-cell biology that can be studied by single-cell techniques. In this review article, we summarize studies that utilized single-cell TCR and transcriptome analysis. Those studies include fields in T-cell development and differentiation, autoimmunity, infectious disease, tumor microenvironment and cancer immunotherapy.

they identified $CD4^+$ T cell subsets that might contribute to the pathogenesis of allergy and asthma (75).

The Role of T Cells in Infectious Diseases

Single-cell analysis has become a powerful tool to analyze T-cell responses during the infection. For example, Kazer SW et al. studied peripheral blood mononuclear cells from four individuals with acute HIV infection, and they discovered gene response modules that were different between cell subsets and were changed during the course of the infection (76). More importantly, during COVID-19 pandemic, several studies utilized single-cell analysis to study T cells from COVID-19 patients (77–82). In one of the studies, abundant exhausted T cells with skewed TCR repertoire were found in the immune landscape of severe COVID-19 patients (79). In another study, single-cell sequencing was performed on immune cells isolated from cerebrospinal fluid (CSF) in COVID-19 patients with neurological sequelae (82). Those CSF T cells showed a reduced interferon response compared to viral encephalitis.

T-Cell Biology in Tumor Microenvironment

Single-cell technique has been used insensitively to study T-cell biology in tumor microenvironment. T-cell transcriptome profiles in the majority of cancer types have been published (32, 83–91). Li H et al. studied intra-tumoral T cells isolated from 25 melanoma patients (92). They discovered a significant portion of the $CD8^+$ T cells were in a gradient of "transitional" states, between a healthy/cytotoxic T-cell state and a dysfunctional T-cell state. In addition, T cells in the dysfunctional state still had proliferative capacity and formed large T-cell clones. In another study, Ghorani E et al. utilized single-cell analysis and high-dimensional flow cytometry analysis to analyze non-small cell lung cancer specimens (93). They found the correlation between T-cell differentiation status and tumor mutational burden. The authors proposed that the characterization of intratumoral T cells might help to predict the outcome of immunotherapy. Lastly, Oh DY et al. studied T cells isolated from bladder cancer and identified several subsets of $CD4^+$ T cells containing gene signatures for cytotoxic T cells.

T Cells and Cancer Immunotherapy

Investigators have utilized single-cell techniques to study intratumoral T cells prior and after checkpoint immunotherapy for melanoma (94, 95). One of the important findings was the identification of a $CD8^+$ T cell subset that expressed TCF7, a key transcription factor for "memory-like", proliferation-competent, exhausted T cells (96–98). In addition, the presence of $TCF7^+CD8^+$ T cells could predict clinical response to checkpoint immunotherapy. Next, Luoma AM et al. utilized single-cell analysis to study T cell populations in colitis, a common and severe side effect of checkpoint immunotherapy (99). They observed a substantial fraction of colitis-associated $CD8^+$ T cells that were likely originated from tissue-resident populations, identified by single-cell TCR clonality analysis. Similarly, studies were carried out to perform single-cell TCR/transcriptome analysis on peripheral blood T cells after checkpoint immunotherapy (91, 100). This approach was able to identify genes associated with clinical responses as a result (100).

Chimeric antigen receptor (CAR) T cell therapy has shown dramatical clinical responses against B-cell malignancies. The majority of the CAR designs utilized two different co-stimulatory domains derived from CD28 and 4-1BB molecules. Boroughs AC et al. attempted to use single-cell transcriptome analysis to identify gene signatures associated with different CAR designs (101). The authors identify a transcriptional signature shared between CAR designs, as well as a unique, distinct signature associated with 4-1BB co-stimulatory domain, compared to CD28 co-stimulatory domain. In another study, Sheih A et al. took advantage of highly-diverse, endogenous TCR sequences and utilized these sequences as natural barcodes (102). They were able to track CAR T cells after therapy and perform single-cell analysis by following these barcodes. Taken together, the results obtained by single-cell analysis provides more insights on how to improve the cell products for CAR T-cell therapy.

CAVEATS ON EXPERIMENTAL DESIGN AND DATA INTERPRETATION

Single-cell TCR and transcriptome analysis is a very powerful tool, but it can be very costly as well. We hope those outstanding publications described above can help readers to design single-cell experiments and acquire data that cannot be obtained by other approaches. One of the common errors is to utilized a single-cell sequencing approach even when the proposed research goals can be simply accomplished by "bulk" RNA-seq analysis, which not only costs less, but also can acquire higher quality of data, especially for low abundance transcripts.

Although the data quality of single-cell transcriptome has improved significantly in recent years, the single-cell data still suffer from the sensitivity issue for low abundance transcripts, also known as technical dropouts. Several computational algorithms have been developed to specifically address this issue for single-cell transcriptome analysis (103–105). However, the performance of these algorithms is still far from perfect, and the results may differ between algorithms (106). Therefore, researchers are still needed to beware of potential artifact and bias involved in the data analysis and interpretation. We still highly recommend researchers to validate the observations by another independent approach, such as flow cytometry or targeted sequencing.

Another important caveat is that the observations tend to be simplified, leading to binary thinking. The commonly used clustering technique in single cells analysis is based on the assumption that cells are defined into discrete populations, which might not reflect the true biology. Van der Leun et al. have proposed that T cells in the tumor microenvironment are in a gradient of cell states rather than discrete populations (107). Therefore, we should be cautious about data interpretation using the clustering technique.

FUTURE PERSPECTIVE: HIGHLY PERSONALIZED, T CELL-BASED CANCER IMMUNOTHERAPY

Studies utilizing adoptive cell transfer of tumor-infiltrating lymphocytes (TIL) have shown that this approach can result in durable and complete regressions of advanced cancer diseases, in particular metastatic melanoma. Very frequently, reactivities against neoantigens were present among the infused TIL (108–110). Despite the evidence of clinical responses, the adoptive transfer of neoantigen-reactive TIL has several limitations. The transferred cells are highly differentiated and can have a limited proliferative ability, leading to lack of persistence *in vivo* after adoptive cell transfer (111, 112). Additionally, because it is impossible to control the skewing of the T cell repertoire during expansion, the neoantigen-specific TIL could lead to low abundance in the infusion product. For the same reason, it is also very difficult to control the number and the quality of the neoantigen that are targeted. To overcome some of these limitations, the genetic transfer of neoantigen-specific TCRs has been proposed (113–115). With this approach, it will be possible to introduce highly specific TCRs into less differentiated cells, and to combine TCRs with several specificities, affinities and HLA restrictions in one infusion product, potentially increasing the possibility of clinical response (14). This approach has nevertheless its own challenges, which are mainly related to finding a reliable source of neoantigen-reactive T cells from where to isolate the TCRs, as well as rapidly and efficiently transferring the TCRs to new recipient cells for treatment.

In targeting unique somatic mutations by adoptive T-cell therapy, it is equally important to consider other aspects that may reduce the efficacy of the therapy. Tumor heterogeneity is a major obstacle not only because the targeted neoantigen may not be expressed on every cell, but also because the MHC elements may not be expressed uniformly or even lost (116, 117). Another factor to consider is that the T cell functionality may not be always optimal even in the presence of the neoantigen-specific TCR. Several reports have highlighted the dysfunctionality of exhausted T cells in cancer patients (118, 119). Therefore, a desirable therapeutic approach would target several neoantigens, possibly restricted to different HLA elements and would be carried out by the most effective T cells. Different strategies have been proposed to overcome some of the most important issues, such as the selection of T cell subsets with a stem-like phenotype to improve persistence and antitumor activity (120) or the genetic modification of T cells to secrete IL-12 in order to promote HLA expression and cross-presentation by surrounding cells in the tumor microenvironment (121).

In summary, the single-cell TCR and transcriptome analysis has enabled T-cell biologists to ask critical questions and obtain interesting findings. This newly available research tool may help us to improve the current immunotherapy and develop new treatments for cancer and other diseases. We look forward to more exciting discoveries in the coming years.

AUTHOR CONTRIBUTIONS

AP and YL contribute equally in writing and discussion. All authors contributed to the article and approved the submitted version.

FUNDING

AP was supported by the Sjöberg Foundation, Region Stockholm Centrum För Innovativ Medicin (CIMED), Svenska Läkaresällskapet, Cancerfonden, Ruth och Richard Julins Stiftelse. YL was supported by funding from the Winthrop P. Rockefeller Cancer Institute.

REFERENCES

1. Turner SJ, Doherty PC, McCluskey J, Rossjohn J. Structural Determinants of T-Cell Receptor Bias in Immunity. *Nat Rev Immunol* (2006) 6(12):883–94. doi: 10.1038/nri1977
2. Arstila TP, Casrouge A, Baron V, Even J, Kanellopoulos J, Kourilsky P. A Direct Estimate of the Human Alphabeta T Cell Receptor Diversity. *Science* (1999) 286(5441):958–61. doi: 10.1126/science.286.5441.958
3. Rosenberg SA, Yang JC, Sherry RM, Kammula US, Hughes MS, Phan GQ, et al. Durable Complete Responses in Heavily Pretreated Patients With Metastatic Melanoma Using T-Cell Transfer Immunotherapy. *Clin Cancer Res* (2011) 17(13):4550–7. doi: 10.1158/1078-0432.CCR-11-0116
4. Stevanovic S, Pasetto A, Helman SR, Gartner JJ, Prickett TD, Howie B, et al. Landscape of Immunogenic Tumor Antigens in Successful Immunotherapy of Virally Induced Epithelial Cancer. *Science* (2017) 356(6334):200–5. doi: 10.1126/science.aak9510
5. Tran E, Turcotte S, Gros A, Robbins PF, Lu YC, Dudley ME, et al. Cancer Immunotherapy Based on Mutation-Specific CD4+ T Cells in a Patient With Epithelial Cancer. *Science* (2014) 344(6184):641–5. doi: 10.1126/science.1251102
6. Gros A, Parkhurst MR, Tran E, Pasetto A, Robbins PF, Ilyas S, et al. Prospective Identification of Neoantigen-Specific Lymphocytes in the Peripheral Blood of Melanoma Patients. *Nat Med* (2016) 22(4):433–8. doi: 10.1038/nm.4051
7. Cafri G, Yossef R, Pasetto A, Deniger DC, Lu YC, Parkhurst M, et al. Memory T Cells Targeting Oncogenic Mutations Detected in Peripheral Blood of Epithelial Cancer Patients. *Nat Commun* (2019) 10(1):449. doi: 10.1038/s41467-019-08304-z
8. Cohen CJ, Gartner JJ, Horovitz-Fried M, Shamalov K, Trebska-McGowan K, Bliskovsky VV, et al. Isolation of Neoantigen-Specific T Cells From Tumor and Peripheral Lymphocytes. *J Clin Invest* (2015) 125(10):3981–91. doi: 10.1172/JCI82416
9. Malekzadeh P, Yossef R, Cafri G, Paria BC, Lowery FJ, Jafferji M, et al. Antigen Experienced T Cells From Peripheral Blood Recognize P53 Neoantigens. *Clin Cancer Res* (2020) 26(6):1267–76. doi: 10.1158/1078-0432.CCR-19-1874
10. Topalian SL, Hodi FS, Brahmer JR, Gettinger SN, Smith DC, McDermott DF, et al. Safety, Activity, and Immune Correlates of Anti-PD-1 Antibody in Cancer. *N Engl J Med* (2012) 366(26):2443–54. doi: 10.1056/NEJMoa1200690
11. Le DT, Uram JN, Wang H, Bartlett BR, Kemberling H, Eyring AD, et al. PD-1 Blockade in Tumors With Mismatch-Repair Deficiency. *N Engl J Med* (2015) 372(26):2509–20. doi: 10.1056/NEJMoa1500596
12. Gattinoni L, Klebanoff CA, Restifo NP. Paths to Stemness: Building the Ultimate Antitumour T Cell. *Nat Rev Cancer* (2012) 12(10):671–84. doi: 10.1038/nrc3322

13. Kerkar SP, Restifo NP. Cellular Constituents of Immune Escape Within the Tumor Microenvironment. *Cancer Res* (2012) 72(13):3125–30. doi: 10.1158/0008-5472.CAN-11-4094
14. Klebanoff CA, Rosenberg SA, Restifo NP. Prospects for Gene-Engineered T Cell Immunotherapy for Solid Cancers. *Nat Med* (2016) 22(1):26–36. doi: 10.1038/nm.4015
15. Pasetto A, Gros A, Robbins PF, Deniger DC, Prickett TD, Matus-Nicodemos R, et al. Tumor- and Neoantigen-Reactive T-Cell Receptors can be Identified Based on Their Frequency in Fresh Tumor. *Cancer Immunol Res* (2016) 4 (9):734–43. doi: 10.1158/2326-6066.CIR-16-0001
16. Parkhurst M, Gros A, Pasetto A, Prickett T, Crystal JS, Robbins P, et al. Isolation of T-Cell Receptors Specifically Reactive With Mutated Tumor-Associated Antigens From Tumor-Infiltrating Lymphocytes Based on CD137 Expression. *Clin Cancer Res* (2017) 23(10):2491–505. doi: 10.1158/1078-0432.CCR-16-2680
17. Howie B, Sherwood AM, Berkebile AD, Berka J, Emerson RO, Williamson DW, et al. High-Throughput Pairing of T Cell Receptor Alpha and Beta Sequences. *Sci Transl Med* (2015) 7(301):301ra131. doi: 10.1126/scitranslmed.aac5624
18. Hwang B, Lee JH, Bang D. Single-Cell RNA Sequencing Technologies and Bioinformatics Pipelines. *Exp Mol Med* (2018) 50(8):96. doi: 10.1038/s12276-018-0071-8
19. Good ML, Vizcardo R, Maeda T, Tamaoki N, Malekzadeh P, Kawamoto H, et al. Using Human Induced Pluripotent Stem Cells for the Generation of Tumor Antigen-Specific T Cells. *J Vis Exp* (2019) 152. doi: 10.3791/59997
20. Guo F, Li L, Li J, Wu X, Hu B, Zhu P, et al. Single-Cell Multi-Omics Sequencing of Mouse Early Embryos and Embryonic Stem Cells. *Cell Res* (2017) 27(8):967–88. doi: 10.1038/cr.2017.82
21. Nichterwitz S, Chen G, Aguila Benitez J, Yilmaz M, Storvall H, Cao M, et al. Laser Capture Microscopy Coupled With Smart-Seq2 for Precise Spatial Transcriptomic Profiling. *Nat Commun* (2016) 7:12139. doi: 10.1038/ncomms12139
22. Foley JW, Zhu C, Jolivet P, Zhu SX, Lu P, Meaney MJ, et al. Gene Expression Profiling of Single Cells From Archival Tissue With Laser-Capture Microdissection and Smart-3SEQ. *Genome Res* (2019) 29(11):1816–25. doi: 10.1101/gr.234807.118
23. Schutze K, Lahr G. Identification of Expressed Genes by Laser-Mediated Manipulation of Single Cells. *Nat Biotechnol* (1998) 16(8):737–42. doi: 10.1038/nbt0898-737
24. Whitesides GM. The Origins and the Future of Microfluidics. *Nature* (2006) 442(7101):368–73. doi: 10.1038/nature05058
25. Clambey ET, Davenport B, Kappler JW, Marrack P, Homann D. Molecules in Medicine Mini Review: The Alphabeta T Cell Receptor. *J Mol Med (Berl)* (2014) 92(7):735–41. doi: 10.1007/s00109-014-1145-2
26. Kim SM, Bhonsle L, Besgen P, Nickel J, Backes A, Held K, et al. Analysis of the Paired TCR Alpha- and Beta-Chains of Single Human T Cells. *PloS One* (2012) 7(5):e37338. doi: 10.1371/journal.pone.0037338
27. Dziubianau M, Hecht J, Kuchenbecker L, Sattler A, Stervbo U, Rodelsperger C, et al. TCR Repertoire Analysis by Next Generation Sequencing Allows Complex Differential Diagnosis of T Cell-Related Pathology. *Am J Transplant* (2013) 13(11):2842–54. doi: 10.1111/ajt.12431
28. Tumeh PC, Harview CL, Yearley JH, Shintaku IP, Taylor EJ, Robert L, et al. PD-1 Blockade Induces Responses by Inhibiting Adaptive Immune Resistance. *Nature* (2014) 515(7528):568–71. doi: 10.1038/nature13954
29. Han A, Glanville J, Hansmann L, Davis MM. Linking T-Cell Receptor Sequence to Functional Phenotype at the Single-Cell Level. *Nat Biotechnol* (2014) 32(7):684–92. doi: 10.1038/nbt.2938
30. Zhu YY, Machleder EM, Chenchik A, Li R, Siebert PD. Reverse Transcriptase Template Switching: a SMART Approach for Full-Length Cdna Library Construction. *Biotechniques* (2001) 30(4):892–7. doi: 10.2144/01304pf02
31. Stubbington MJT, Lonnberg T, Proserpio V, Clare S, Speak AO, Dougan G, et al. T Cell Fate and Clonality Inference From Single-Cell Transcriptomes. *Nat Methods* (2016) 13(4):329–32. doi: 10.1038/nmeth.3800
32. Zheng C, Zheng L, Yoo JK, Guo H, Zhang Y, Guo X, et al. Landscape of Infiltrating T Cells in Liver Cancer Revealed by Single-Cell Sequencing. *Cell* (2017) 169(7):1342–1356 e16. doi: 10.1016/j.cell.2017.05.035
33. Redmond D, Poran A, Elemento O. Single-Cell Tcrseq: Paired Recovery of Entire T-Cell Alpha and Beta Chain Transcripts in T-Cell Receptors From Single-Cell Rnaseq. *Genome Med* (2016) 8(1):80. doi: 10.1186/s13073-016-0335-7
34. Afik S, Yates KB, Bi K, Darko S, Godec J, Gerdemann U, et al. Targeted Reconstruction of T Cell Receptor Sequence From Single Cell RNA-Seq Links CDR3 Length to T Cell Differentiation State. *Nucleic Acids Res* (2017) 45(16):e148. doi: 10.1093/nar/gkx615
35. Lu YC, Zheng Z, Robbins PF, Tran E, Prickett TD, Gartner JJ, et al. An Efficient Single-Cell RNA-Seq Approach to Identify Neoantigen-Specific T Cell Receptors. *Mol Ther* (2018) 26(2):379–89. doi: 10.1016/j.ymthe.2017.10.018
36. Eltahla AA, Rizzetto S, Pirozyan MR, Betz-Stablein BD, Venturi V, Kedzierska K, et al. Linking the T Cell Receptor to the Single Cell Transcriptome in Antigen-Specific Human T Cells. *Immunol Cell Biol* (2016) 94(6):604–11. doi: 10.1038/icb.2016.16
37. Ziegenhain C, Vieth B, Parekh S, Reinius B, Guillaumet-Adkins A, Smets M, et al. Comparative Analysis of Single-Cell RNA Sequencing Methods. *Mol Cell* (2017) 65(4):631–643 e4. doi: 10.1016/j.molcel.2017.01.023
38. Stahl PL, Salmen F, Vickovic S, Lundmark A, Navarro JF, Magnusson J, et al. Visualization and Analysis of Gene Expression in Tissue Sections by Spatial Transcriptomics. *Science* (2016) 353(6294):78–82. doi: 10.1126/science.aaf2403
39. Thrane K, Eriksson H, Maaskola J, Hansson J, Lundeberg J. Spatially Resolved Transcriptomics Enables Dissection of Genetic Heterogeneity in Stage III Cutaneous Malignant Melanoma. *Cancer Res* (2018) 78(20):5970–9. doi: 10.1158/0008-5472.CAN-18-0747
40. Ji AL, Rubin AJ, Thrane K, Jiang S, Reynolds DL, Meyers RM, et al. Multimodal Analysis of Composition and Spatial Architecture in Human Squamous Cell Carcinoma. *Cell* (2020) 182(2):497–514.e22. doi: 10.1016/j.cell.2020.05.039
41. Ye L, Creaney J, Redwood A, Robinson B. The Current Lung Cancer Neoantigen Landscape and Implications for Therapy. *J Thorac Oncol* (2021). doi: 10.1016/j.jtho.2021.01.1624
42. Lam H, McNeil LK, Starobinets H, DeVault VL, Cohen RB, Twardowski P, et al. An Empirical Antigen Selection Method Identifies Neoantigens That Either Elicit Broad Antitumor T-Cell Responses or Drive Tumor Growth. *Cancer Discovery* (2021) 11(3):696–713. doi: 10.1158/2159-8290.CD-20-0377
43. Wang C, Ding Y, Liu Y, Zhang Q, Xu S, Xia L, et al. Identification of Mutated Peptides in Bladder Cancer From Exomic Sequencing Data Reveals Negative Correlation Between Mutation-Specific Immunoreactivity and Inflammation. *Front Immunol* (2020) 11:576603. doi: 10.3389/fimmu.2020.576603
44. Wijetunga NA, Yu Y, Morris LG, Lee N, Riaz N. The Head and Neck Cancer Genome in the Era of Immunotherapy. *Oral Oncol* (2021) 112:105040. doi: 10.1016/j.oraloncology.2020.105040
45. Jiang AM, Ren MD, Liu N, Gao H, Wang JJ, Zheng XQ, et al. Tumor Mutation Burden, Immune Cell Infiltration, and Construction of Immune-Related Genes Prognostic Model in Head and Neck Cancer. *Int J Med Sci* (2021) 18(1):226–38. doi: 10.7150/ijms.51064
46. Lu X, Ji C, Jiang L, Zhu Y, Zhou Y, Meng J, et al. Tumour Microenvironment-Based Molecular Profiling Reveals Ideal Candidates for High-Grade Serous Ovarian Cancer Immunotherapy. *Cell Prolif* (2021) p:e12979. doi: 10.1111/cpr.12979
47. Malekzadeh P, Pasetto A, Robbins PF, Parkhurst MR, Paria BC, Jia L, et al. Neoantigen Screening Identifies Broad TP53 Mutant Immunogenicity in Patients With Epithelial Cancers. *J Clin Invest* (2019) 129(3):1109–14. doi: 10.1172/JCI123791
48. Deniger DC, Pasetto A, Robbins PF, Gartner JJ, Prickett TD, Paria BC, et al. T-Cell Responses to TP53 "Hotspot" Mutations and Unique Neoantigens Expressed by Human Ovarian Cancers. *Clin Cancer Res* (2018) 24(22):5562–73. doi: 10.1158/1078-0432.CCR-18-0573
49. Liu S, Matsuzaki J, Wei L, Tsuji T, Battaglia S, Hu Q, et al. Efficient Identification of Neoantigen-Specific T-Cell Responses in Advanced Human Ovarian Cancer. *J Immunother Cancer* (2019) 7(1):156. doi: 10.1186/s40425-019-0629-6
50. Burrack AL, Spartz EJ, Raynor JF, Wang I, Olson M, Stromnes IM. Combination PD-1 and PD-L1 Blockade Promotes Durable Neoantigen-

Specific T Cell-Mediated Immunity in Pancreatic Ductal Adenocarcinoma. *Cell Rep* (2019) 28(8):2140–2155 e6. doi: 10.1016/j.celrep.2019.07.059
51. Grant RC, Denroche R, Jang GH, Nowak KM, Zhang A, Borgida A, et al. Clinical and Genomic Characterisation of Mismatch Repair Deficient Pancreatic Adenocarcinoma. *Gut* (2020). doi: 10.1136/gutjnl-2020-320730
52. Parkhurst MR, Robbins PF, Tran E, Prickett TD, Gartner JJ, Jia L, et al. Unique Neoantigens Arise From Somatic Mutations in Patients With Gastrointestinal Cancers. *Cancer Discovery* (2019) 9(8):1022–35. doi: 10.1158/2159-8290.CD-18-1494
53. Gros A, Tran E, Parkhurst MR, Ilyas S, Pasetto A, Groh EM, et al. Recognition of Human Gastrointestinal Cancer Neoantigens by Circulating PD-1+ Lymphocytes. *J Clin Invest* (2019) 129(11):4992–5004. doi: 10.1172/JCI127967
54. Lo W, Parkhurst M, Robbins PF, Tran E, Lu YC, Jia L, et al. Immunologic Recognition of a Shared P53 Mutated Neoantigen in a Patient With Metastatic Colorectal Cancer. *Cancer Immunol Res* (2019) 7(4):534–43. doi: 10.1158/2326-6066.CIR-18-0686
55. Tran E, Robbins PF, Lu YC, Prickett TD, Gartner JJ, Jia L, et al. T-Cell Transfer Therapy Targeting Mutant KRAS in Cancer. *N Engl J Med* (2016) 375(23):2255–62. doi: 10.1056/NEJMoa1609279
56. Yossef R, Tran E, Deniger DC, Gros A, Pasetto A, Parkhurst MR, et al. Enhanced Detection of Neoantigen-Reactive T Cells Targeting Unique and Shared Oncogenes for Personalized Cancer Immunotherapy. *JCI Insight* (2018) 3(19):e122467. doi: 10.1172/jci.insight.122467
57. Klenerman P, Cerundolo V, Dunbar PR. Tracking T Cells With Tetramers: New Tales From New Tools. *Nat Rev Immunol* (2002) 2(4):263–72. doi: 10.1038/nri777
58. Boon T, van der Bruggen P. Human Tumor Antigens Recognized by T Lymphocytes. *J Exp Med* (1996) 183(3):725–9. doi: 10.1084/jem.183.3.725
59. Matsushita H, Vesely MD, Koboldt DC, Rickert CG, Uppaluri R, Magrini VJ, et al. Cancer Exome Analysis Reveals a T-Cell-Dependent Mechanism of Cancer Immunoediting. *Nature* (2012) 482(7385):400–4. doi: 10.1038/nature10755
60. Zhang SQ, Ma KY, Schonnesen AA, Zhang M, He C, Sun E, et al. High-Throughput Determination of the Antigen Specificities of T Cell Receptors in Single Cells. *Nat Biotechnol* (2018) 36:1156–9. doi: 10.1101/457069
61. Graham DB, Luo C, O'Connell DJ, Lefkovith A, Brown EM, Yassour M, et al. Antigen Discovery and Specification of Immunodominance Hierarchies for MHCII-Restricted Epitopes. *Nat Med* (2018) 24(11):1762–72. doi: 10.1038/s41591-018-0203-7
62. Peng S, Zaretsky JM, Ng AHC, Chour W, Bethune MT, Choi J, et al. Sensitive Detection and Analysis of Neoantigen-Specific T Cell Populations From Tumors and Blood. *Cell Rep* (2019) 28(10):2728–38.e7. doi: 10.1016/j.celrep.2019.07.106
63. Gee MH, Han A, Lofgren SM, Beausang JF, Mendoza JL, Birnbaum ME, et al. Antigen Identification for Orphan T Cell Receptors Expressed on Tumor-Infiltrating Lymphocytes. *Cell* (2018) 172(3):549–63.e16. doi: 10.1016/j.cell.2017.11.043
64. Kreiter S, Vormehr M, van de Roemer N, Diken M, Lower M, Diekmann J, et al. Mutant MHC Class II Epitopes Drive Therapeutic Immune Responses to Cancer. *Nature* (2015) 520(7549):692–6. doi: 10.1038/nature14426
65. Winkler F, Bengsch B. Use of Mass Cytometry to Profile Human T Cell Exhaustion. *Front Immunol* (2019) 10:3039. doi: 10.3389/fimmu.2019.03039
66. Starr TK, Jameson SC, Hogquist KA. Positive and Negative Selection of T Cells. *Annu Rev Immunol* (2003) 21:139–76. doi: 10.1146/annurev.immunol.21.120601.141107
67. Stritesky GL, Jameson SC, Hogquist KA. Selection of Self-Reactive T Cells in the Thymus. *Annu Rev Immunol* (2012) 30:95–114. doi: 10.1146/annurev-immunol-020711-075035
68. Park JE, Botting RA, Dominguez Conde C, Popescu DM, Lavaert M, Kunz DJ, et al. A Cell Atlas of Human Thymic Development Defines T Cell Repertoire Formation. *Science* (2020) 367(6480):eaay3224. doi: 10.1101/2020.01.28.911115
69. Kernfeld EM, Genga RMJ, Neherin K, Magaletta ME, Xu P, Maehr R. A Single-Cell Transcriptomic Atlas of Thymus Organogenesis Resolves Cell Types and Developmental Maturation. *Immunity* (2018) 48(6):1258–1270 e6. doi: 10.1016/j.immuni.2018.04.015
70. Li N, van Unen V, Abdelaal T, Guo N, Kasatskaya SA, Ladell K, et al. Memory CD4(+) T Cells are Generated in the Human Fetal Intestine. *Nat Immunol* (2019) 20(3):301–12. doi: 10.1038/s41590-018-0294-9
71. Galletti G, De Simone G, Mazza EMC, Puccio S, Mezzanotte C, Bi TM, et al. Two Subsets of Stem-Like CD8(+) Memory T Cell Progenitors With Distinct Fate Commitments in Humans. *Nat Immunol* (2020) 21(12):1552–62. doi: 10.1038/s41590-020-0791-5
72. Patil VS, Madrigal A, Schmiedel BJ, Clarke J, O'Rourke P, de Silva AD, et al. Precursors of Human CD4(+) Cytotoxic T Lymphocytes Identified by Single-Cell Transcriptome Analysis. *Sci Immunol* (2018) 3(19):eaan8664. doi: 10.1126/sciimmunol.aan8664
73. Corridoni D, Antanaviciute A, Gupta T, Fawkner-Corbett D, Aulicino A, Jagielowicz M, et al. Single-Cell Atlas of Colonic CD8(+) T Cells in Ulcerative Colitis. *Nat Med* (2020) 26(9):1480–90. doi: 10.1038/s41591-020-1003-4
74. Strobl J, Pandey RV, Krausgruber T, Bayer N, Kleissl L, Reininger B, et al. Long-Term Skin-Resident Memory T Cells Proliferate in Situ and are Involved in Human Graft-Versus-Host Disease. *Sci Transl Med* (2020) 12 (570):eabb7028. doi: 10.1126/scitranslmed.abb7028
75. Seumois G, Ramirez-Suastegui C, Schmiedel BJ, Liang S, Peters B, Sette A, et al. Single-Cell Transcriptomic Analysis of Allergen-Specific T Cells in Allergy and Asthma. *Sci Immunol* (2020) 5(48):eaba6087. doi: 10.1126/sciimmunol.aba6087
76. Kazer SW, Aicher TP, Muema DM, Carroll SL, Ordovas-Montanes J, Miao VN, et al. Integrated Single-Cell Analysis of Multicellular Immune Dynamics During Hyperacute HIV-1 Infection. *Nat Med* (2020) 26 (4):511–8. doi: 10.1101/654814
77. Meckiff BJ, Ramirez-Suastegui C, Fajardo V, Chee SJ, Kusnadi A, Simon H, et al. Imbalance of Regulatory and Cytotoxic SARS-Cov-2-Reactive CD4(+) T Cells in COVID-19. *Cell* (2020) 183(5):1340–53.e16. doi: 10.1016/j.cell.2020.10.001
78. Wilk AJ, Rustagi A, Zhao NQ, Roque J, Martinez-Colon GJ, McKechnie JL, et al. A Single-Cell Atlas of the Peripheral Immune Response in Patients With Severe COVID-19. *Nat Med* (2020) 26(7):1070–6. doi: 10.1038/s41591-020-0944-y
79. Zhang JY, Wang XM, Xing X, Xu Z, Zhang C, Song JW, et al. Single-Cell Landscape of Immunological Responses in Patients With COVID-19. *Nat Immunol* (2020) 21(9):1107–18. doi: 10.1038/s41590-020-0762-x
80. Kalfaoglu B, Almeida-Santos J, Tye CA, Satou Y, Ono M. T-Cell Hyperactivation and Paralysis in Severe COVID-19 Infection Revealed by Single-Cell Analysis. *Front Immunol* (2020) 11:589380. doi: 10.3389/fimmu.2020.589380
81. Liao M, Liu Y, Yuan J, Wen Y, Xu G, Zhao J, et al. Single-Cell Landscape of Bronchoalveolar Immune Cells in Patients With COVID-19. *Nat Med* (2020) 26(6):842–4. doi: 10.1038/s41591-020-0901-9
82. Heming M, Li X, Rauber S, Mausberg AK, Borsch AL, Hartlehnert M, et al. Neurological Manifestations of COVID-19 Feature T Cell Exhaustion and Dedifferentiated Monocytes in Cerebrospinal Fluid. *Immunity* (2021) 54 (1):164–75.e6. doi: 10.1016/j.immuni.2020.12.011
83. Lambrechts D, Wauters E, Boeckx B, Aibar S, Nittner D, Burton O, et al. Phenotype Molding of Stromal Cells in the Lung Tumor Microenvironment. *Nat Med* (2018) 24(8):1277–89. doi: 10.1038/s41591-018-0096-5
84. Tirosh I, Izar B, Prakadan SM, Wadsworth MH2nd, Treacy D, Trombetta JJ, et al. Dissecting the Multicellular Ecosystem of Metastatic Melanoma by Single-Cell RNA-Seq. *Science* (2016) 352(6282):189–96. doi: 10.1126/science.aad0501
85. Guo X, Zhang Y, Zheng L, Zheng C, Song J, Zhang Q, et al. Global Characterization of T Cells in Non-Small-Cell Lung Cancer by Single-Cell Sequencing. *Nat Med* (2018) 24(7):978–85. doi: 10.1038/s41591-018-0045-3
86. Azizi E, Carr AJ, Plitas G, Cornish AE, Konopacki C, Prabhakaran S, et al. Single-Cell Map of Diverse Immune Phenotypes in the Breast Tumor Microenvironment. *Cell* (2018) 174(5):1293–308.e36. doi: 10.1016/j.cell.2018.05.060
87. Savas P, Virassamy B, Ye C, Salim A, Mintoff CP, Caramia F, et al. Single-Cell Profiling of Breast Cancer T Cells Reveals a Tissue-Resident Memory Subset Associated With Improved Prognosis. *Nat Med* (2018) 24(7):986–93. doi: 10.1038/s41591-018-0078-7

88. Wagner J, Rapsomaniki MA, Chevrier S, Anzeneder T, Langwieder C, Dykgers A, et al. A Single-Cell Atlas of the Tumor and Immune Ecosystem of Human Breast Cancer. *Cell* (2019) 177(5):1330–45.e18. doi: 10.1016/j.cell.2019.03.005
89. Qian J, Olbrecht S, Boeckx B, Vos H, Laoui D, Etlioglu E, et al. A Pan-Cancer Blueprint of the Heterogeneous Tumor Microenvironment Revealed by Single-Cell Profiling. *Cell Res* (2020) 30(9):745–62. doi: 10.1038/s41422-020-0355-0
90. Sun Y, Wu L, Zhong Y, Zhou K, Hou Y, Wang Z, et al. Single-Cell Landscape of the Ecosystem in Early-Relapse Hepatocellular Carcinoma. *Cell* (2020) 84 (2):404–21. doi: 10.1016/j.cell.2020.11.041
91. Wu TD, Madireddi S, de Almeida PE, Banchereau R, Chen YJ, Chitre AS, et al. Peripheral T Cell Expansion Predicts Tumour Infiltration and Clinical Response. *Nature* (2020) 579(7798):274–8. doi: 10.1038/s41586-020-2056-8
92. Li H, van der Leun AM, Yofe I, Lubling Y, Gelbard-Solodkin D, van Akkooi ACJ, et al. Dysfunctional CD8 T Cells Form a Proliferative, Dynamically Regulated Compartment Within Human Melanoma. *Cell* (2019) 176 (4):775–789 e18. doi: 10.1016/j.cell.2018.11.043
93. Ghorani E, Reading JL, Henry JY, de Massy MR, Rosenthal R, Turati V, et al. The T Cell Differentiation Landscape is Shaped by Tumour Mutations in Lung Cancer. *Nat Cancer* (2020) 1(5):546–61. doi: 10.1038/s43018-020-0066-y
94. Jerby-Arnon L, Shah P, Cuoco MS, Rodman C, Su MJ, Melms JC, et al. A Cancer Cell Program Promotes T Cell Exclusion and Resistance to Checkpoint Blockade. *Cell* (2018) 175(4):984–97.e24. doi: 10.1016/j.cell.2018.09.006
95. Sade-Feldman M, Yizhak K, Bjorgaard SL, Ray JP, de Boer CG, Jenkins RW, et al. Defining T Cell States Associated With Response to Checkpoint Immunotherapy in Melanoma. *Cell* (2018) 175(4):998–1013.e20. doi: 10.1016/j.cell.2018.10.038
96. Wu T, Ji Y, Moseman EA, Xu HC, Manglani M, Kirby M, et al. The TCF1-Bcl6 Axis Counteracts Type I Interferon to Repress Exhaustion and Maintain T Cell Stemness. *Sci Immunol* (2016) 1(6):eaai8593. doi: 10.1126/sciimmunol.aai8593
97. Im SJ, Hashimoto M, Gerner MY, Lee J, Kissick HT, Burger MC, et al. Defining CD8+ T Cells That Provide the Proliferative Burst After PD-1 Therapy. *Nature* (2016) 537(7620):417–21. doi: 10.1038/nature19330
98. Henning AN, Roychoudhuri R, Restifo NP. Epigenetic Control of CD8(+) T Cell Differentiation. *Nat Rev Immunol* (2018) 18(5):340–56. doi: 10.1038/nri.2017.146
99. Luoma AM, Suo S, Williams HL, Sharova T, Sullivan K, Manos M, et al. Molecular Pathways of Colon Inflammation Induced by Cancer Immunotherapy. *Cell* (2020) 182(3):655–71.e22. doi: 10.1016/j.cell.2020.06.001
100. Fairfax BP, Taylor CA, Watson RA, Nassiri I, Danielli S, Fang H, et al. Peripheral CD8(+) T Cell Characteristics Associated With Durable Responses to Immune Checkpoint Blockade in Patients With Metastatic Melanoma. *Nat Med* (2020) 26(2):193–9. doi: 10.1038/s41591-019-0734-6
101. Boroughs AC, Larson RC, Marjanovic ND, Gosik K, Castano AP, Porter CBM, et al. A Distinct Transcriptional Program in Human CAR T Cells Bearing the 4-1BB Signaling Domain Revealed by Scrna-Seq. *Mol Ther* (2020) 28(12):2577–92. doi: 10.1016/j.ymthe.2020.07.023
102. Sheih A, Voillet V, Hanafi LA, DeBerg HA, Yajima M, Hawkins R, et al. Clonal Kinetics and Single-Cell Transcriptional Profiling of CAR-T Cells in Patients Undergoing CD19 CAR-T Immunotherapy. *Nat Commun* (2020) 11(1):219. doi: 10.1038/s41467-019-13880-1
103. Huang M, Wang J, Torre E, Dueck H, Shaffer S, Bonasio R, et al. SAVER: Gene Expression Recovery for Single-Cell RNA Sequencing. *Nat Methods* (2018) 15(7):539–42. doi: 10.1038/s41592-018-0033-z
104. van Dijk D, Sharma R, Nainys J, Yim K, Kathail P, Carr AJ, et al. Recovering Gene Interactions From Single-Cell Data Using Data Diffusion. *Cell* (2018) 174(3):716–29.e27. doi: 10.1016/j.cell.2018.05.061
105. Stuart T, Butler A, Hoffman P, Hafemeister C, Papalexi E, Mauck WM3rd, et al. Comprehensive Integration of Single-Cell Data. *Cell* (2019) 177 (7):1888–902.e21. doi: 10.1016/j.cell.2019.05.031
106. Hou W, Ji Z, Ji H, Hicks SC. A Systematic Evaluation of Single-Cell RNA-Sequencing Imputation Methods. *Genome Biol* (2020) 21(1):218. doi: 10.1186/s13059-020-02132-x
107. van der Leun AM, Thommen DS, Schumacher TN. CD8(+) T Cell States in Human Cancer: Insights From Single-Cell Analysis. *Nat Rev Cancer* (2020) 20(4):218–32. doi: 10.1038/s41568-019-0235-4
108. Lu YC, Yao X, Crystal JS, Li YF, El-Gamil M, Gross C, et al. Efficient Identification of Mutated Cancer Antigens Recognized by T Cells Associated With Durable Tumor Regressions. *Clin Cancer Res* (2014) 20(13):3401–10. doi: 10.1158/1078-0432.CCR-14-0433
109. Robbins PF, Lu YC, El-Gamil M, Li YF, Gross C, Gartner J, et al. Mining Exomic Sequencing Data to Identify Mutated Antigens Recognized by Adoptively Transferred Tumor-Reactive T Cells. *Nat Med* (2013) 19 (6):747–52. doi: 10.1038/nm.3161
110. Prickett TD, Crystal JS, Cohen CJ, Pasetto A, Parkhurst MR, Gartner JJ, et al. Durable Complete Response From Metastatic Melanoma After Transfer of Autologous T Cells Recognizing 10 Mutated Tumor Antigens. *Cancer Immunol Res* (2016) 4(8):669–78. doi: 10.1158/2326-6066.CIR-15-0215
111. Klebanoff CA, Scott CD, Leonardi AJ, Yamamoto TN, Cruz AC, Ouyang C, et al. Memory T Cell-Driven Differentiation of Naive Cells Impairs Adoptive Immunotherapy. *J Clin Invest* (2016) 126(1):318–34. doi: 10.1172/JCI81217
112. Lu YC, Jia L, Zheng Z, Tran E, Robbins PF, Rosenberg SA. Single-Cell Transcriptome Analysis Reveals Gene Signatures Associated With T-Cell Persistence Following Adoptive Cell Therapy. *Cancer Immunol Res* (2019) 7 (11):1824–36. doi: 10.1158/2326-6066.CIR-19-0299
113. Lu YC, Robbins PF. Cancer Immunotherapy Targeting Neoantigens. *Semin Immunol* (2016) 28(1):22–7. doi: 10.1016/j.smim.2015.11.002
114. Tran E, Robbins PF, Rosenberg SA. 'Final Common Pathway' of Human Cancer Immunotherapy: Targeting Random Somatic Mutations. *Nat Immunol* (2017) 18(3):255–62. doi: 10.1038/ni.3682
115. Yamamoto TN, Kishton RJ, Restifo NP. Developing Neoantigen-Targeted T Cell-Based Treatments for Solid Tumors. *Nat Med* (2019) 25(10):1488–99. doi: 10.1038/s41591-019-0596-y
116. Anderson P, Aptsiauri N, Ruiz-Cabello F, Garrido F. HLA Class I Loss in Colorectal Cancer: Implications for Immune Escape and Immunotherapy. *Cell Mol Immunol* (2021) 18(3):556–65. doi: 10.1038/s41423-021-00634-7
117. Montes P, Bernal M, Campo LN, Gonzalez-Ramirez AR, Jimenez P, Garrido P, et al. Tumor Genetic Alterations and Features of the Immune Microenvironment Drive Myelodysplastic Syndrome Escape and Progression. *Cancer Immunol Immunother* (2019) 68(12):2015–27. doi: 10.1007/s00262-019-02420-x
118. Tao X, Wu X, Huang T, Mu D. Identification and Analysis of Dysfunctional Genes and Pathways in CD8(+) T Cells of Non-Small Cell Lung Cancer Based on RNA Sequencing. *Front Genet* (2020) 11:352. doi: 10.3389/fgene.2020.00352
119. Bauer CA. Immunosuppressive Betaig-H3 Links Tumour Stroma and Dysfunctional T Cells in Pancreatic Cancer. *Gut* (2019) 68(4):581. doi: 10.1136/gutjnl-2018-317735
120. Sabatino M, Hu J, Sommariva M, Gautam S, Fellowes V, Hocker JD, et al. Generation of Clinical-Grade CD19-Specific CAR-Modified CD8+ Memory Stem Cells for the Treatment of Human B-Cell Malignancies. *Blood* (2016) 128(4):519–28. doi: 10.1182/blood-2015-11-683847
121. Kerkar SP, Goldszmid RS, Muranski P, Chinnasamy D, Yu Z, Reger RN, et al. IL-12 Triggers a Programmatic Change in Dysfunctional Myeloid-Derived Cells Within Mouse Tumors. *J Clin Invest* (2011) 121(12):4746–57. doi: 10.1172/JCI58814

Conflict of Interest: The authors declare that the research was conducted in the absence of any commercial or financial relationships that could be construed as a potential conflict of interest.

frontiers in Immunology

REVIEW
published: 09 June 2021
doi: 10.3389/fimmu.2021.697412

Applications of Single-Cell Omics in Tumor Immunology

Junwei Liu[1], Saisi Qu[1], Tongtong Zhang[2], Yufei Gao[3], Hongyu Shi[4], Kaichen Song[1], Wei Chen[1,3] and Weiwei Yin[1,5]**

[1] Department of Cardiology of the Second Affiliated Hospital, Zhejiang University School of Medicine, Key Laboratory for Biomedical Engineering of the Ministry of Education, College of Biomedical Engineering and Instrument Science, Zhejiang University, Hangzhou, China, [2] Department of Hepatobiliary and Pancreatic Surgery, The Center for Integrated Oncology and Precision Medicine, Affiliated Hangzhou First People's Hospital, Zhejiang University School of Medicine, Hangzhou, China, [3] School of Mechanical Engineering, Zhejiang University, Hangzhou, China, [4] Department of Biological Testing, Zhejiang Puluoting Health Technology Co., Ltd., Hangzhou, China, [5] Department of Thoracic Surgery, Sir Run Run Shaw Hospital, Zhejiang University, Hangzhou, China

The tumor microenvironment (TME) is an ecosystem that contains various cell types, including cancer cells, immune cells, stromal cells, and many others. In the TME, cancer cells aggressively proliferate, evolve, transmigrate to the circulation system and other organs, and frequently communicate with adjacent immune cells to suppress local tumor immunity. It is essential to delineate this ecosystem's complex cellular compositions and their dynamic intercellular interactions to understand cancer biology and tumor immunology and to benefit tumor immunotherapy. But technically, this is extremely challenging due to the high complexities of the TME. The rapid developments of single-cell techniques provide us powerful means to systemically profile the multiple omics status of the TME at a single-cell resolution, shedding light on the pathogenic mechanisms of cancers and dysfunctions of tumor immunity in an unprecedently resolution. Furthermore, more advanced techniques have been developed to simultaneously characterize multi-omics and even spatial information at the single-cell level, helping us reveal the phenotypes and functionalities of disease-specific cell populations more comprehensively. Meanwhile, the connections between single-cell data and clinical characteristics are also intensively interrogated to achieve better clinical diagnosis and prognosis. In this review, we summarize recent progress in single-cell techniques, discuss their technical advantages, limitations, and applications, particularly in tumor biology and immunology, aiming to promote the research of cancer pathogenesis, clinically relevant cancer diagnosis, prognosis, and immunotherapy design with the help of single-cell techniques.

Keywords: single-cell omics, immunotherapy, cancer, TCR (T cell receptor), biomarkers

OPEN ACCESS

Edited by:
Qihui Shi,
Fudan University, China

Reviewed by:
Yao Lu,
Chinese Academy of Sciences (CAS), China
Yuliang Deng,
Shanghai Jiao Tong University, China

****Correspondence:***
Weiwei Yin
wwyin@zju.edu.cn
Wei Chen
jackweichen@zju.edu.cn

Specialty section:
This article was submitted to Cancer Immunity and Immunotherapy, a section of the journal Frontiers in Immunology

Received: *19 April 2021*
Accepted: *17 May 2021*
Published: *09 June 2021*

Citation:
Liu J, Qu S, Zhang T, Gao Y, Shi H, Song K, Chen W and Yin W (2021) Applications of Single-Cell Omics in Tumor Immunology. Front. Immunol. 12:697412. doi: 10.3389/fimmu.2021.697412

INTRODUCTION

The tumor microenvironment (TME) is a complex ecosystem that consists of many different cell types, including tumor cells, immune cells, and many others. All these cells are tightly inter-associated and interact with each other. The heterogeneous milieu of TME induces various progression patterns of different cancers and leads to distinct treatment responses across

different patients (1). Among that, the levels of T cell infiltration, the polarization of tumor-associated macrophages (TAM) can be varied, thereby affecting the prognosis of patients differently, the expression of PD-1 and PD-L1 in TME, the mutational landscapes, and the drug responses of malignant cells can also be distinct in different patients, relating to different efficacies of immune checkpoint blockade (ICB) therapies (2–4).

The previous genomic, transcriptomic, and proteomic cancer studies have helped develop multiple mutational- or molecular-target therapies and elevate treatment responses across different patients (5). However, the clinical benefits of these target-directed therapies are still limited. Only a small subset of patients is treatable, leading to emergent demand of using more precise methods to dissect characteristics of individual patients for developing better cancer treatments especially personalized tumor immunotherapy.

In this review, we introduce the state-of-art technological advances of single-cell omics and discuss corresponding computational methods for single-cell data analysis and their applications in cancer research. All of these further inspire and guide the design of and applications of single-cell techniques in basic and translational clinical cancer research.

THE DEVELOPMENT OF SINGLE-CELL TECHNOLOGIES

The development of methods in single-cell isolation, indexing, and sequencing allows in-depth profiling of the tumor milieu from different cellular scales with extremely high dimensions (6). Based on single omics, methods for integrated omics have also been developed for simultaneous detection of different omics, including genomic, transcriptomic, proteomic, and spatial information of single cells (7). Despite multiple challenges that remain to be addressed, these methods have been very powerful in uncovering the cellular basis of the heterogeneous tumor microenvironment and greatly expanded our understanding of cancers and tumor immunology in many aspects. In this session, we introduce the technical details of single-cell methods applied in understanding the tumor microenvironment (**Figure 1**).

Mass Cytometry and Imaging Mass Cytometry

Flow cytometry, as a widely used single-cell labeling and sorting technique, has facilitated the understanding of cellular composition and diversity in various tissues (8), but its spectral overlap between nearby channels limits the number of detected markers and unable to unveil many functionally important cell subsets (9). To overcome this problem, mass cytometry, also named cytometry by time of flight mass spectrometry (CyTOF), was developed with a more specific channel signal (10, 11). CyTOF uses rare element isotopes to replace the commonly used fluorochrome to conjugate monoclonal antibodies (mAbs) in flow cytometry. These isotopes usually do not exist in cells, and the purity of rare element isotopes and their accurate detection by mass spectrometry significantly increase the detectable dimension of a single cell to over 100 markers theoretically, and due to the technical limits of isotope labeling onto mAbs, the marker number on single cells to date can only reach 45 (10–12). Meanwhile, CyTOF has already demonstrated its power and accuracy over flow cytometry in cell profiling when applied to analyze fresh and frozen PBMC or tumor tissues at the single-cell level (13). Unfortunately, CyTOF cannot be used for cell sorting, and its throughput is 25~50 times lower than flow cytometry due to extra time expense for isotope quantification (8).

Beyond profiling the homogenously stained single cells isolated from tissue samples, imaging CyTOF was developed to profile the cells' spatial information in the target tissue (14). Similar to the multicolor immunofluorescence staining, imaging CyTOF can simultaneously detect over 30 types of rare element isotopes conjugated on antibodies to stain tissue sections. A high-resolution laser is used to ablate the target tissue section point by point, and the ionized elements were streamed into the ICP-MS for isotope measurement. Finally, a high-dimensional tissue imaging is reconstructed by integrating the subcellular spatial information of each point on the tissue sample (14).

Moreover, CyTOF can also be used in the quantification of epigenetic modification (e.g., phosphorylation, histone modification) (15), transcripts (16), and antigen-specific T cells (17) at the single-cell level by designated mAbs that target chromatin marks, ligation assay for RNA, and multiplexed peptide-major-histocompatibility-complex (pMHC)-tetramer staining for antigen-specific T cells, respectively, allowing an integrated inspection of cellular functionality in a multi-omics manner.

Single-Cell RNA Sequencing

Methods for profiling single-cell transcriptome have been developed and rapidly evolved to overcome limited markers detected on individual cells by CyTOF, improve the single-cell resolution of traditional bulk RNA sequencing (RNA-seq), and identify rare cell populations and their functional dynamics at the transcriptomic level (18). The first published single-cell RNA sequencing (scRNA-seq) method successfully detected 5,270 more genes in one blastomere compared to the microarray assay using hundreds of blastomeres, allowing the precise whole-transcriptome characterization at a single-cell level (19). And integrating the 'cell-specific barcodes' into the synthesized cDNA sequences (20, 21), the throughput of scRNA-seq improved from a few hundreds of cells to thousands of cells.

Multiple scRNA-seq or sc-nucleus RNA-seq protocols were developed to enhance the scale, the sensitivity, or the accuracy of single-cell transcriptome quantification (22). These methods can be categorized into plate-based or microfluidic-based platforms. For the plate-based platform, the representative method is Smart-seq, which is currently upgraded into a third-generation, Smart-seq3 (23). In Smart-seq3, a 5' unique molecular identifier (UMI) is integrated into the full-length cDNA for counting transcripts, achieving the precise quantification of transcript isoforms. Other plate-based platforms, such as cell expression by linear amplification and sequencing (CEL-seq2) and massively parallel single-cell RNA sequencing (MARS-seq2), integrate the Fluidigm C1 system or liquid-handling robot to

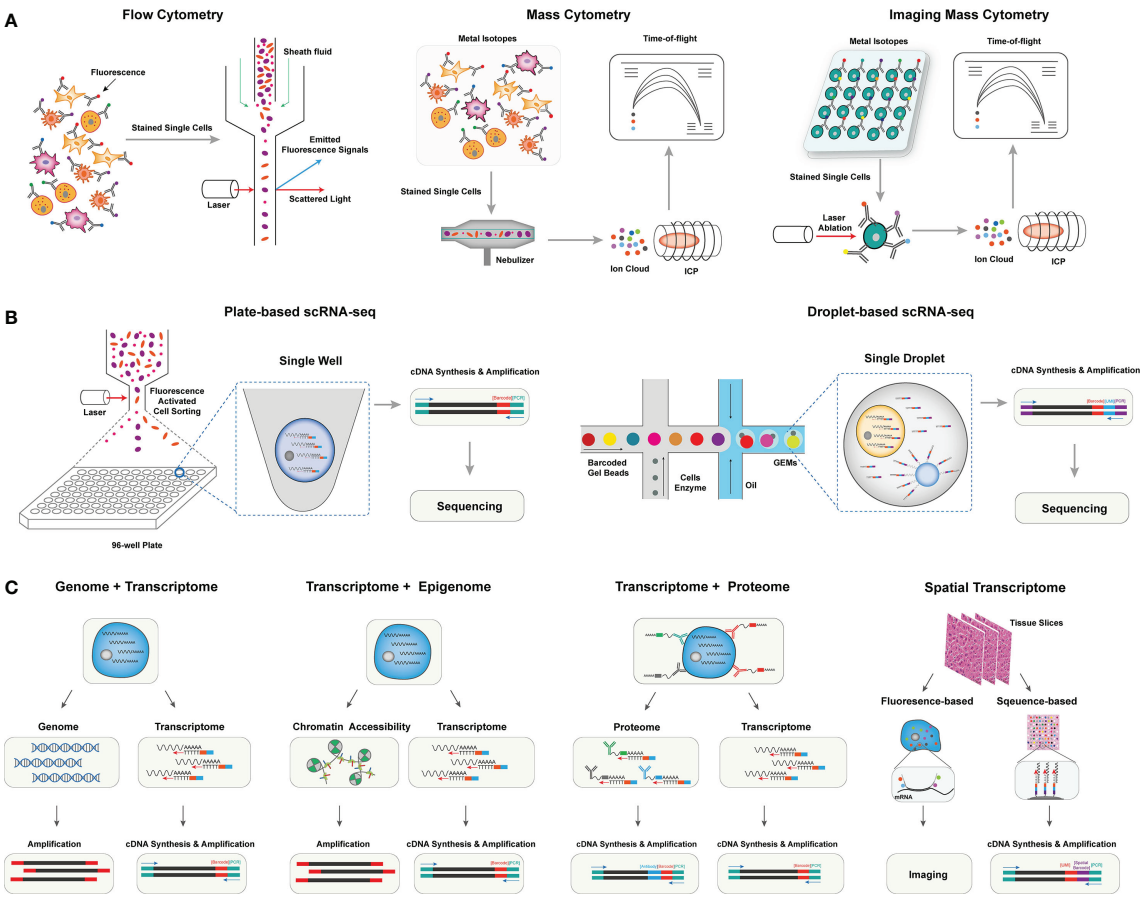

FIGURE 1 | The overview of single-cell omics techniques. **(A)** The overview of single-cell cytometry systems, including flow cytometry with fluorescence-labeled antibodies for single isolated cells (left), mass cytometry with metal isotope-conjugated antibodies isolated single cells (middle), and imaging mass cytometry with metal isotope-conjugated antibodies labeled on tissues (right). **(B)** The overview of two canonical scRNA-seq platforms, including plate-based scRNA-seq methods with sorted cells barcoded within each well (left), and droplet-based scRNA-seq method, single cells were barcoded within individual droplets (right). **(C)** The overview of single-cell multi-omics techniques, including library preparing for genomic, epigenomic, proteomic, and spatial indexing with transcriptomic of single cells simultaneously.

improve the data quality and reduce labor cost, respectively (24, 25). Applying a bead-based microfluidic system has dramatically pushed the field into a real high-throughput area for the microfluidic platform. In a single experiment, the microfluidic system can capture 3,000~10,000 droplets, each of which encapsulates a single-cell and a single-bead carrying specific DNA-barcoded primers (26–28). The transcripts in single droplets are then captured, reversely transcribed, and barcoded with cell barcodes and UMIs. These procedures well replace the single-well-based cell sorting and library construction steps in the plate-based platform and dramatically increase the detection number of single cells in each sample. Other strategies have also been used to profile the transcripts in single cells, such as the split-pool-based cell barcoding strategy (29–31) and the integration of beads with the microwell-based platform (32). Although there are still challenges in different aspects, such as cost, sequencing depth, and gene coverages, these scRNA-seq methods have enabled the profiling of single cells with more than thousands of genes per cell. The data dimension is significantly higher than the cytometry-based systems.

Single-Cell Multi-Omics Technologies

The interconnections and relations of genome, epigenome, transcriptome, and proteome determine the function of single cells, which requires a comprehensive understanding of the biology process across multi-omics simultaneously at the single-cell level (33). In the following session, we will focus on reviewing single-cell multi-omics technologies, that could simultaneously measure at least two of different omics including genomics, transcriptomics, epigenomics, proteomics, and spatial information at the single-cell level.

Yin et al. introduced the sci-L3-RNA/DNA co-assay to simultaneously measure the genomics and transcriptomics in single cells (34). In sci-L3-RNA-/DNA co-assay, single cellular DNA and mRNA were respectively barcoded by Tn5 transposon intersection and by poly-T primer, both of them carrying

barcoding sequences and UMIs. Both libraries were prepared with three-level split-pool indexing and linear amplification for downstream analysis. Another strategy is to physically separate the nucleus and cytosol of a single cell and construct the library for each component individually. Following this strategy, direct nuclear tagmentation and RNA sequencing (DNTR-seq) (35) separately obtained the whole-genome sequencing and full-length cDNA sequencing from single cells with ultra-high resolutions. Besides directly obtaining the whole genome of single cells, the cDNA sequences from mRNA could also be used to detect the mutation status of single cells (36, 37), especially for identifying tumor-specific mutations across different tumor cell populations.

Open chromatin regions are also important functional characteristics for revealing cellular genomic regulations. With the assay development for transposase-accessible chromatin using sequencing (ATAC-seq), exploring open chromatin in single cells becomes possible. ATAC-seq enables fast and precise epigenomic profiling by integrating the sequencing adaptors into the accessible chromatin by prokaryotic Tn5 enzyme (38). Combining ATAC-seq with single-cell isolation and barcoding techniques enables access to open chromatin in single cells (39). Moreover, as both the transposed chromatin fragments and the synthesized cDNA fragments of cellular transcripts can be adapted into the same cell barcoding ID, Cao et al. and Chen et al. successfully detected chromatin accessibility and transcriptome simultaneously at the single-cell level (40, 41). Simultaneous high-throughput ATAC and RNA expression with sequencing (SHARE-seq) is another method to evaluate the relationship between chromatin accessibility and gene expression in single cells and identify the priming role of chrome accessibility in transcriptomic regulation, which is helpful to infer cell differentiation (42). Meanwhile, multiple in silico algorithms, such as model-based analyses of transcriptome and regulome (MAESTRO) and Signac (43, 44), have been correspondingly developed to integrated analyze scRNA-seq and scATAC-seq data in single cells.

The protein expression can directly reflect the functionality and biological states of cells. As a result, flow cytometry and CyTOF have been broadly used in biological researches for protein expression quantification despite their limited dimensions compared to scRNA-seq. To overcome this limitation, Stoeckius et al. came up with the idea of using specifically designed DNA sequences to label and barcode the protein-specific mAbs (45). The detection number of antibody-labeled proteins is significantly increased to more than 200 (46), which is five times more than the detection number in CyTOF. CITE-seq uses a poly-A tail in the antibodies-conjugated oligonucleotides to achieve compatibility with the mRNA capturing system (45). And in the commercial platform (e.g., Feature Barcoding by 10X Genomics), the barcoding strategy is further improved so that the transcriptomic and proteomic libraries are barcoded with poly-A capture sequences and antibody-specific capture sequences separately (47). Besides, Zhang et al. used DNA-barcoded pMHC tetramers to specifically label and sequence antigen-specific T cells (48). A similar strategy was also used to remove experimental and amplification bias by staining oligo-labeled surface proteins ubiquitously expressed on cells from different samples (49).

The in-situ cellular spatial information is essential to accurately capture the biological functions of cells in their physiological context. It is particularly important to investigate the spatial information in the tumor microenvironment (TME), such as tissue-specific T cell infiltration, the spatial distribution, and interaction of cellular ligands and receptors, and the distribution of malignant cells, to improve our understanding of tumorigenesis and tumor-specific immune escape in TME (50). The spatial transcriptome methods can be mainly classified into fluorescence or sequencing-based methods, which have also been comprehensively reviewed by Asp et al. (51). Based on the technique of fluorescence in situ hybridization (FISH) (52), seqFISH+ enables visualization transcripts at local sites and can image more than 10,000 genes at subcellular resolution with upgraded optical resolution and barcoding strategy (53). Despite the high spatial resolution, the applications of fluorescence-based platforms are usually hampered by the intensive experiment procedures and the design of the transcript probe. In contrast, the application of cellular barcoding strategies in scRNA-seq enables in-situ barcoding of local cells in tissues. The most challenging for this strategy is to demultiplex the physical locations with the detected barcoding sequences. In Slide-seq and high-definition spatial transcriptomics (HDST) assays (54–56), arrayed barcoding beads are used to capture spatial whole-transcriptomes, and the resolution of the reconstructed spatial map depends on the designed bead arrays. In another microfluidic-based method (57), the tissue slide was separately barcoded by parallel microfluidic channels within different directions, and the different combinations of barcodes can recover the spatial information.

Innovative Computational Methods for Single-Cell Analysis

Accompanied by the increased capability of generating high-dimensional and high-throughput single-cell data in one experiment, interpreting the biological functions of cells and functional alterations in disease status becomes even more challenging (58). Hie et al. summarized the typical computational workflow for single-cell RNA-seq data analysis, including data preprocessing, batch correction, clustering, and functional annotation of single cells (59). Among that, the methods for inferring cell lineage trajectories under different stimuli are broadly applied to understand cellular dynamics and interactions. Besides, with the development of single-cell multi-omics techniques, integrating multi-omics single-cell data is also computationally challenging (7).

Saelens et al. comprehensively benchmarked the performance of 45 trajectory inference methods (60), highlighting that the preset trajectory topology of computational methods can affect the inference results and that the performance of different methods can vary with different datasets. The most limitation of these methods, including Monocle3 (61), partition-based

graph abstraction (PAGA) (62), and Slingshot (63), is that the cell trajectory estimation calculated by the cell-cell distance ignores the inherited cellular information. Instead, the innovative method RNA Velocity (64, 65) addresses this issue by quantifying the spliced and unspliced transcripts of single cells and connecting cells with similar transcripts splicing states. Another method, CytoTRACE, leverages the number of detected genes to reflect the developmental potential of single cells, providing a robust performance to delineate cellular trajectories (66). Furthermore, the DNA sequencing information, including T cell receptor sequencing, can also be used as cellular labels for inferring cellular dynamics and lineage tracing (67, 68).

The integrative analyses of single-cell multi-omics data consider the status of single cells from different scales of biological features and delineate cell types based on cell similarities in higher feature space, which are challenged by the different characteristics of single omic data and batch effects across multiple data samples. Ma et al. comprehensively summarized the data integration methods for analyzing single-cell multi-omics data (7). One strategy is to estimate the cellular distances within individual omics and then calculate the "weighted-nearest neighbor " distance for integrated analysis of multiple-omics data (46). Another one exploits a modified statistic framework to identify low-dimensional variations across data modalities for data integration (69). In other methods, multi-view machine learning (70), canonical correlation (71), and deep generative model (72) have also been used for multi-omic single-cell data integration.

APPLICATION OF SINGLE-CELL OMICS IN TUMOR IMMUNOLOGY

With the aid of single-cell methods, the heterogeneity of tumor cells and their interaction in the local microenvironment have been deeply and comprehensively interrogated. The single-cell data has been extensively used for identifying biomarkers for cancer diagnosis, prognosis prediction, and new treatable targets in designated clinical cohorts. The Human Tumor Atlas Network (HTAN) project (73) has put forward a framework of mapping tumor atlases in molecular, cellular, anatomical, and clinical fields, aiming to interrogate the single-cell data for clinical transitions thoroughly. In the following session, we mainly focus on applying different single-cell multi-omics techniques in establishing the cellular atlas of tumor ecosystem, T cell dynamics, and their interactions contributing to tumor diagnosis, treatment, and prognosis. The typical applications are correspondingly listed (**Figure 2** and **Table 1**).

Dissecting Tumor Microenvironments at the Single-Cell Level

Taking advantage of high throughput and high dimensional proteomic single-cell analysis, CyTOF has been used to dissect the immune composition of TME in different types of tumors. In the study of early lung adenocarcinoma (74), Lavin et al. profiled the immune atlas in paired tumor lesions, normal lung tissues, and peripheral blood. They revealed a tumor-specific depletion of $CD8^+$ T effector cells and the tumor-enriched macrophages with the expression of PPARγ potentially contributing to immune suppression in TME. This study provides potential immunotherapies for targeting macrophages in lung cancer. By comparing the immune atlas of clear cell renal cell carcinoma (ccRCC) and normal renal tissues (82), Chevrier et al. identified the polymorphic expressions of exhausted markers and CD38 on $PD\text{-}1^+$ exhausted T cells in tumors and a special subset of $CD38^+$ tumor-associated macrophages (TAM) highly associated with the immunosuppressed T cell subsets. Further integrating the tumor-infiltrating frequencies of immune cell subsets with clinical outcomes, they identified the abundance of several TAM subsets that can predict the progression-free survival of patients. Additionally, CyTOF and imaging CyTOF have also been combined with profiling the ecosystem of malignant cells and immune cells in breast cancer. Wagner et al. simultaneously compared the immune and malignant cell components of breast tumor, juxta-tumor, and mammoplasty tissue samples. The phenotypic abnormality of tumor cells and dynamics of immune cells suggests the tumor-immune combined

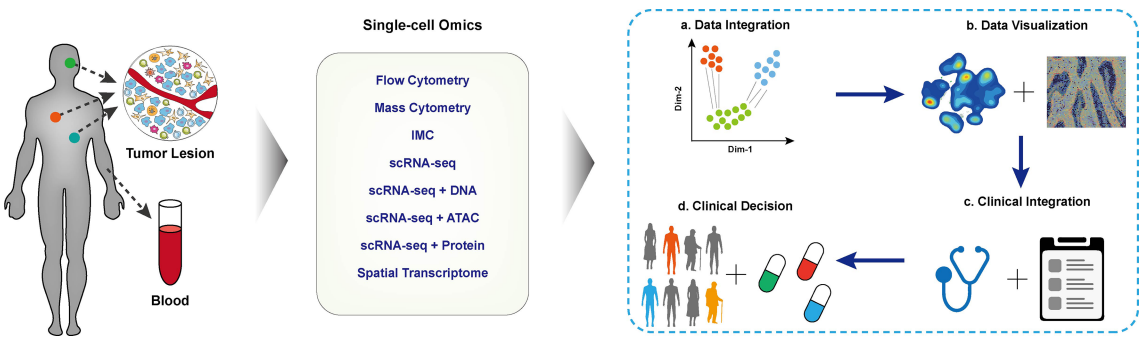

FIGURE 2 | Applications of single-cell techniques in clinical cancer research. The schematic diagram of cancer research with single-cell techniques, blood or tissue samples of the designated patient cohort was collected and performed single-cell profiling. The collected data were integrated for downstream analysis and visualization. With in-depth integration with clinical characteristics, biomarkers for clinical decisions, disease prognosis, and tumor immunotherapy.

TABLE 1 | Selected cancer research with Single-Cell omic technologies.

Cancer type	Single-cell methods	Highlights	Ref
Early lung adenocarcinoma	CyTOF, scRNA-seq	Comparing the paired immune signatures across tumor lesion, normal lung tissue, and blood, Lavin et al. Identified the tumor lesion-specific immune regulations, especially the modifications of innate immune cells	(74)
Breast cancer	Imaging mass cytometry	The high-dimensional pathology images of breast cancers characterized the disease-related spatial resolved cellular signatures.	(77)
Hepatocellular carcinoma	scRNA-seq	In-depth integration of single-cell data with bioinformatic methods, Zhang et al. identified the migration of immune cells, especially the LAMP3+ dendritic cells, potentially contributing to lymphocyte activation.	(87)
Myeloproliferative neoplasms	scRNA-seq + genotyping	Integrating the cellular mutation genotypes and transcriptomic data, Nam et al. revealed the upregulation of NF-κB and IRE1-XBP1 pathways in mutated cells. And the modifications of mutations in transcriptomic outputs.	(82)
Mixed-phenotype acute leukemias	scRNA-seq + protein, scATAC-seq	By comparing the transcriptomic and epigenetic blood development maps between healthy and MPAL patients, Granja et al. uncovered the patient-specific regulatory networks, such as the RUNX1 regulation of CD69 in tumor patients.	(47)
Primary pancreatic tumors	scRNA-seq, spatial transcriptomics	With intersection analyses of scRNA-seq data and spatial transcriptomic data, Moncada et al. revealed the interactions of different cells in tumor microenvironments, especially the colocalization of inflammatory fibroblasts and cancer cells.	(86)
Basal or squamous cell carcinoma	scRNA-seq + TCR	Comparisons between the tissue TCR repertoires before and after immunotherapies, Yost et al. uncovered the new entered T cell clonotypes rather than the exhausted T cell clonotypes that may respond to immunotherapy.	(105)
Hepatocellular carcinoma	scRNA-seq	By comparing the immune landscape between primary and early-relapse HCC patients, Sun et al. indicated the innate-like CD8 T cells might contribute to an early relapse of HCC.	(119)
Pancreatic ductal adenocarcinoma	snRNA-seq, spatial transcriptomics	Comparisons of the PDAC samples before and after chemoradiotherapy, Hwang et al. revealed the basal rather than the classical phenotype of malignant cells might benefit the therapy efficiency with single-cell and spatial transcriptomic inspections.	(121)

phenotypes of breast tumor patients independent of the clinical grade and subtypes, suggesting the local interactions could be more critical for prognosis treatment efficacy (83). Using imaging CyTOF, Jackson et al. established the highly multiplexed molecular spatial maps of breast tumor microenvironments with different clinical subtypes and grades. Interrogating the single-cell pathology features, they further proposed that the subgroups of patients by pathology features in the tumor microenvironment could better predict patients' overall survival and provide new strategies for clinical subtyping (75).

With higher dimension capability, scRNA-seq provides an opportunity to more broadly and systematically profile TME and its associated immune atlas with many more critical functional aspects (84). For example, with scRNA-seq, Azizi et al. identified the continuous cellular states of T cells and myeloid cells in breast cancers (85). They proposed that both TCR signals and environmental stimuli could module T cell functionality to combine TCR clonotypes with T cell phenotypes. scRNA-seq also enables more comprehensive lineage analyses to reflect the dynamic immune cell responses during tumorigenesis. With RNA Velocity analysis (64) and mitochondrial-based lineage tracing (86), Zhang et al. revealed that a subset of $LAMP3^{+}$ dendritic cells could migrate from tumors to hepatic lymph nodes to trigger systematic adaptive immune responses (76).

Integrating the genotyping and single-cell transcriptomic data of myeloproliferative neoplasm cells, Nam et al. comprehensively delineated the contributions of CALR mutation in the differentiation of hematopoietic stem and progenitor cells (HSPCs). They also revealed that the CALR mutation more affected the cellular gene expressions at a later differentiation stage and further identified the mutation-specific activation of the IRE1-XBP1 pathway in HSPCs as a potential therapeutic target (77). With single-cell sequencing the genomics and transcriptomics of acute myeloid leukemia (AML) malignant cells, van Galen et al. identified six subsets of malignant AML cells across developmental hierarchies. They revealed the determination role of genotype in the compositions of AML cells in patients and further determined that the differentiated AML cells could suppress the function of T cells. The genotype-specific phenotype of AML cells and the immunosuppressive functionality of differentiated AML cells could further guide the genotype-specific immunotherapies in AML (87). Single-cell triple omics sequencing (scTrio-seq), a platform that simultaneously profiles genomic, epigenomic, and transcriptomic on individual cells, is able to delineate the more complex insights of the coordinated regulations of copy number variations, DNA methylation, and gene expressions in malignant cells of hepatocellular carcinomas and colorectal cancer (88, 89). Moreover, comparing the epigenomic regulatory networks of bone marrow and peripheral blood mononuclear cells between healthy and mixed-phenotype acute leukemia (MPAL) patients, Granja et al. uncovered the common regulation factors and revealed RUNX1 as an oncogene to upregulate CD69 in MPAL (47). Integrating scRNA-seq and spatial transcriptomic data in pancreatic ductal adenocarcinoma, Moncada et al. intersected the region-specific gene expression with cell type-specific gene expression. They revealed that the stress-response cancer cells were colocalized with IL-6 releasing inflammatory fibroblasts, supporting the IL-6 induced stress-response mechanism in cancers (78). Thus, the integration of single-cell multi-omics allows a more comprehensive exploration of cancer evolution, local cellular interactions, and immune regulations in the tumor microenvironment, strengthening our understanding of cancer pathogenesis and immune suppression (90, 91).

Evolution of Cancer Cells in Tumorigenesis and Drug Resistance

In-depth single-cell characterization of cancer cells in the TME, and their dynamic regulations in tumorigenesis, metastasis, and drug responses can uncover the heterogeneity of cancer cells and their causality with clinical outcomes (90, 92). The scRNA-seq profiling of diverse cancer cells in oligodendroglioma patients revealed a subset of undifferentiated malignant cells with stem cell phenotypes and proliferating potentials, suggesting the primary roles of cancer stem cells (CSCs) in cancer evolution (93). Integrating the genetically engineered mouse models (GEMMs) and scRNA-seq, Marjanovic et al. mimicked and profiled the progression of human lung adenoma and adenocarcinoma. They identified a subset of $TIGIT^+$ cells with the high-plasticity cell state (HPCS) and annotated these cells as transitioning tumor cells that contributed to tumor progression and chemoresistance (94). Neftel et al. also characterized four malignant cell subsets of glioblastoma using scRNA-seq with specific molecular features, and that the cellular transitions demonstrated the plasticity of malignant cells across distinct malignant cell subsets with additional cell barcoding and lineage tracing (95). All of these findings highlighted the impact of high-resolution single-cell profiling in understanding tumorigenesis and the evolution of cancer cells.

Metastasis is the dominant cause of the deaths of cancer patients, and its process is stochastic and dynamic (96). scRNA-seq study in human metastatic lung adenocarcinoma (LUAD) revealed a subset of cancer cells with distinct differentiation trajectory and gene signature of aggressive cell movement, proliferation, and apoptosis. And the gene signature of this cancer cell subset is enriched in later and metastatic tumor tissues and associated with a worse prognosis (97). Meanwhile, the applications of scRNA-seq and Cas9-enabled high-resolution lineage tracing of the xenograft model of LUAD cell line delineated comprehensive disseminate routes of metastatic cancer cells. And combining the phenotypical inspection of scRNA-seq data, Quinn et al. uncovered the characteristics of cancer cells with different metastatic ability and quantified their specific transcriptomic regulation in modulating metastasis (98).

The drug resistance of cancer cells severely limits the efficacy of chemotherapy or molecularly targeted therapies, and the cellular states and responses during treatments can determine further disease progression (4). In breast cancer, the single-cell profiling of docetaxel-resistant MCF7 breast cancer cells revealed a subset of cells with a stem-like phenotype and identified LEF1 as the critical molecule regulator in drug resistance (99). In melanoma, an immune evasion-specific malignant cell program identified by scRNA-seq can predict the clinical responses of immune checkpoint inhibitors (ICIs). Targeting the signal activation of CDK4/6 in this program can repress the drug resistance program and enhance the ICI efficacy (100). Meanwhile, a multimodal method (Perturb-CITE-seq) was applied to characterize the mechanisms of resistance of ICIs. Integrating the simultaneously RNA and protein profiling with Cas9 genomic knockout screens, Frangieh et al. validated the known mechanisms of resistance to ICIs, and further revealed a novel CD58 related resistance mechanism. Specifically, they found that downregulating the expression of CD58 could induce the expression of PD-L1 on malignant cells and reduce the co-stimulatory signal of the CD58-CD2 axis on $CD8^+$ T cells (101). Overall, the comprehensive interrogating of the cellular responses and drug resistances in malignant cells could uncover the new treatable targets and guide the combined therapies for cancer treatments.

T Cell Responses and TCR Repertoire in Tumor Immunity

T cells are essential adaptive immune cells that mediate tumor immunity. The promising immune checkpoint blockade (ICB) therapies mainly target T cells and recover T cell immunity through disrupting PD-1/PD-L1 and CTLA-4/CD80 or CD86 interactions or specifically activating tumor-antigen-specific T cell clones (102, 103). Unfortunately, only a small part of patients has beneficial responses with recovered anti-tumor T cell responses. Improving the ICB efficacy requires a more comprehensive understanding of dynamical T cell responses in patients during tumorigenesis and ICB treatments (104).

Platforms that integrate scRNA-seq data and scTCR-seq in individual T cells, such as Smart-seq3 and 10X Genomics single-cell immune profiling, enable a more precise delineation of immune responses and lineage tracking of T cells in tumorigenesis or under immunotherapy treatments (105). Smart-seq3, a representative of full-length sequencing platform, could read full-length CDR3 sequences of TCR$\alpha\beta$ chains in single cells but with limited throughput (23). 10X single-cell immune profiling, a commercial droplet-based platform that integrates TCR enrichment procedures, enables more efficient immune profiling of T cells (68).

Every T cell owns a unique TCR, which provides a valuable lineage tracking marker to investigate the dynamics of T cells, including T cell clonal expansion, functional changes of a TCR clonotype, and T cell migration across different tissues. The T cell landscape with the information of paired TCR α and β chains in liver cancers comprehensively discloses the transition route of exhausted $CD8^+$ T cells in HCC and highlights that a subset of $CD8^+$ T cells with intermediate levels of PDCD1 and TIGIT can be the target cells for immunotherapies (106). In another work, Zhang et al. developed an analysis algorithm (STRATRAC) to quantify the T cell expansion, migration, and transition with paired TCR repertoires (107). With the T cell transition analysis of exhausted $CD8^+$ T cells in colorectal tumors, Zhang et al. revealed a tight association of these cells with effector memory $CD8^+$ T cells but independence of the development trajectory of effector memory and recently activated effector memory $CD8^+$ T cells, suggesting a TCR-dependent fate decision in tumorigenesis. These works strengthen our understanding of the dynamics of T cell exhaustion in tumorigenesis. Furthermore, in-depth profiling of T cell dynamics before and after anti-PD-1 therapy in basal or squamous cell carcinoma suggests the newly entered T cell clonotypes, rather than the exhausted T cell clonotypes, respond to anti-PD-1 immunotherapy (79).

T cells are the dominant targets of immunotherapies, and their responses after immunotherapy treatments are critical to evaluate the clinical efficacy (108). Thereby, the clonal expansions and the accordant changes of TCR repertoires in tumors, normal adjacent tissue, and peripheral blood can be used for predicting the clinical responses to immunotherapies (109). Meanwhile, multiple computational methods have been developed to connect the similarities of TCR sequences with T cell functionalities, which would expand the applications of TCR repertoires in cancer research (110–112). Besides, the comprehensive inspection of T cells in tumors also directs adoptive T cell transfer (ACT) in cancer therapies to identify tumor-responsive T cells (104).

The Molecular Biomarkers for Tumor Diagnosis and Prognosis

The heterogeneities of the tumor microenvironment and strikingly different clinical outcomes in tumor patients require comprehensive molecular profiling to guide the personalized therapies. Multiple initiatives have been founded to identify tumor-specific biomarkers to facilitate better clinical decisions using integrative single-cell omics data analyses (73, 113, 114).

Several groups focused on seeking potential disease or prognosis-related biomarkers using CyTOF. Comparing the peripheral immune atlas of 20 melanoma patients before and after anti-PD-1 immunotherapy, Krieg et al. found that the frequency of $CD14^+CD16^-HLA\text{-}DR^+$ monocytes in peripheral blood before treatment was highly correlated to the response of anti-PD-1 immunotherapy and thus could help to stratify patients before anti-PD-1 immunotherapy treatment (115). In a similar study of dissecting immune profiling in classical Hodgkin lymphoma (116), the peripheral TCR diversities in $CD4^+$ T cells at baseline and during PD-1 blockade therapy were related to the clinical responses. Meanwhile, comparing the development of B cells in B cell precursor acute lymphoblastic leukemia patients and healthy controls, Good et al. revealed that the abnormal expansions of specific B cell subsets during development could predict disease relapse at the time of diagnosis (117). Although implemented in a small patient cohort, all of these strongly suggest the predictive capability of cellular composition changes in prognosis prediction and disease monitoring. Besides, the spatial inspection by imaging CyTOF in molecular colocalization of metastatic melanoma highlighted the association between the prior expression of β2m in TME and clinical outcomes of immunotherapy (118). Profiling the subcellular molecular maps of 483 breast tumor samples using imaging CyTOF in the METABRIC cohort, Ali et al. uncovered the genomic regulation of local tumor ecosystems, including cellular compositions and cellular neighborhoods. They intensively examined their clinical predictive roles in the prognosis of breast cancer (119). All these studies demonstrate the power of the single-cell CyTOF system in finding potential molecular biomarkers for cancer prognosis and predicting treatment efficacy.

scRNA-seq data has also been used in seeking molecular and cellular basis of TME. The distinct transcriptional signatures of malignant cells with different genomic backgrounds help classify tumor subtypes and the design of targeted treatments in a higher resolution (120). Comparing the ecosystems of primary and early-relapse HCC tissues, Sun et al. indicated and validated the enrichment of innate-like $CD161^+CD8^+$ T cells with limited cytotoxic ability in relapsed HCC tissues and may have poor response to the subclonal neoantigens in early-relapsed tumor cells, providing new targets to restrain HCC relapse (80). With the single-cell inspection of tumor-infiltrating lymphocytes in breast cancers, Savas et al. revealed a gene signature of tissue-resident memory $CD8^+$ T cells rather than the CD8 alone could better predict the patient's survival, suggesting these cells are potential regulatory targets of immunotherapy in breast cancer (121). More recently, Hwang et al. delineated the molecular taxonomy changes of TME in pancreatic ductal adenocarcinoma patients treated with or without neoadjuvant chemotherapy and radiotherapy by using the integrated single-nucleus RNA sequencing and spatially resolved transcriptomics analyses (81). They found that the basal-like or classical-like reprogramming of malignant cells was associated with distinct immune infiltration in tumors and further affected the treatment outcomes and clinical decisions.

Despite the durable clinical responses of chimeric antigen receptor T cell (CAR-T) therapy in treating hematological malignancies, the response rate, adverse events, and neurotoxicity during CAR-T treatment can vary across patients (122, 123). Single-cell omics have been applied to uncover the molecular biomarkers of clinical responses and monitor CAR-T cells' functional changes for better clinical application (124, 125). Using scRNA-seq, Deng et al. intensively interrogated the transcriptomic phenotypes of CAR-T cells in infusion products (IPs) with their consequent clinical outcomes on large B cell lymphoma patients (124). They revealed that the enrichment of the memory phenotype of CAR-T cells within IPs lead to positive clinical responses but that the enrichment of exhaustion phenotype of CAR-T cells associated with disease progression. Moreover, they also identified a subset of monocyte-like cells in IPs significantly related to high-grade immune effector cell-associated neurotoxicity syndrome (ICANS). Furthermore, Sheih et al. comprehensively profiled the temporal changes of $CD8^+$ CAR-T cells within IPs, peripheral blood early after infusion and after the peak of CAR-T cell expansion (125). Using the paired scRNA-seq and scTCR-seq, they identified the $CD8^+$ CAR-T cells, within timely increased relative frequency (IRF) clonotypes, highly expressed the gene signatures of T cell cytotoxicity and proliferation, suggesting their effective roles in anti-tumor responses. These studies guide the further applications of single-cell omics to deeper understand the mechanistic insights of effective CAR-T therapy, which would shed light on optimizing CAR-T therapy and uncovering the molecular biomarkers for predicting clinical outcomes.

Furthermore, a new concept of a three-dimensional cell atlas during tumor evolutions has been introduced by Human Tumor Atlas Network (HTAN) project (73), indicating the molecular, spatial, and clinical inspections of human tumors, which would

help uncover the fundamental mechanisms of tumorigenesis and new biomarkers for cancer screening, tumor metastasis, cancer immunotherapy, and drug responses in the future.

PERSPECTIVES

In this review, we comprehensively summarize the development of multiple single-cell omics techniques and their applications in cancer biology and cancer immunology. These innovative methods have extensively enhanced our understanding of tumorigenesis, the mechanisms of tumor-induced immune escape, and the dynamic responses to different tumor treatments. Although significant progress has been made, multiple challenges still exist, which could limit current studies and need to be further solved. In the CyTOF system, the preset and limited number of designated markers hinders the identification of novel or rare cell populations. Additional rare elements to increase the detectable number of channels are required to further assist their applications in the clinical field. In the scRNA-seq system, as the number of detected genes, the transcript-length coverage, and the measurement throughput varied across different platforms and assays, it is challenging to integrate and compare single-cell data from different systems. Meanwhile, the limited transcript capture efficiency of scRNA-seq methods leads to a high dropout of scRNA-seq data, resulting in a higher noise level than bulk RNA-seq (126). The common usage of 3' end transcript capture in scRNA-seq methods involves many non-informative transcripts, making the specific examination of interested transcripts infeasible and wasting the sequencing cost (127). Thus, an optimized system that is able to economically and efficiently generate scRNA-seq data with high data quality and uniform data format is emergently desired to achieve robust analysis of larger sample cohorts. Meanwhile, a more prospective direction in the future is to profile single cells with integrated multi-omics to enable better and deeper profiling of the complicated tumor ecosystem. Moreover, new computational tools to improve the integrated data quality, facilitate the biological interpretation, and speed up the analysis procedures are valuable to be developed.

Single-cell data-driven clinical translation is important and promising in cancer diagnosis and treatment. Due to the expensive cost of single-cell methods, the enrolled patient cohort in current cancer research is very small, leading to inconsistent and non-repeatable biological findings. How to interrogate enormous single-cell features with clinical outcomes is computationally challenging and requires more external validations. Moreover, the tissue sites, sample status, isolation methods, and timepoint for sample resections can be varied across different clinical studies, leading to unstable and non-repeatable single-cell biomarkers found in the clinical field. Thus, a more feasible single-cell framework for performing large-scale clinical studies and the resources for sharing and exploiting the published single-cell data mainly in the cancer field, are urgently needed for better clinical translation in the future.

In summary, single-cell omics techniques will be indispensable for investigating both basic and clinical problems in tumor biology, tumor immunology, and tumor immunotherapy in the future, as they provide broader and deeper insights in large patient cohort to inspire more precise and personalized medicine in cancer treatments.

AUTHOR CONTRIBUTIONS

JL, WY, WC, and SQ wrote the manuscript. TZ helped with the preparation of the figure, and all authors provided thoughtful advice to revise the manuscript. All authors contributed to the article and approved the submitted version.

FUNDING

This project was supported by the National Natural Science Foundation of China 31600751 to WY and the Ministry of Science and Technology of China No.2017ZX10203205 to WC.

ACKNOWLEDGMENTS

We thank the contributions of all authors and the support fundings in this project.

REFERENCES

1. Labani-Motlagh A, Ashja-Mahdavi M, Loskog A. The Tumor Microenvironment: A Milieu Hindering and Obstructing Antitumor Immune Responses. *Front Immunol* (2020) 11:940. doi: 10.3389/fimmu.2020.00940
2. Binnewies M, Roberts EW, Kersten K, Chan V, Fearon DF, Merad M, et al. Understanding the Tumor Immune Microenvironment (Time) for Effective Therapy. *Nat Med* (2018) 24:541–50. doi: 10.1038/s41591-018-0014-x
3. Petitprez F, Meylan M, de Reynies A, Sautes-Fridman C, Fridman WH. The Tumor Microenvironment in the Response to Immune Checkpoint Blockade Therapies. *Front Immunol* (2020) 11:784. doi: 10.3389/fimmu.2020.00784
4. Holohan C, Van Schaeybroeck S, Longley DB, Johnston PG. Cancer Drug Resistance: An Evolving Paradigm. *Nat Rev Cancer* (2013) 13:714–26. doi: 10.1038/nrc3599
5. Chae YK, Pan AP, Davis AA, Patel SP, Carneiro BA, Kurzrock R, et al. Path Toward Precision Oncology: Review of Targeted Therapy Studies and Tools to Aid in Defining "Actionability" of a Molecular Lesion and Patient Management Support. *Mol Cancer Ther* (2017) 16:2645–55. doi: 10.1158/1535-7163.MCT-17-0597
6. Lim B, Lin Y, Navin N. Advancing Cancer Research and Medicine With Single-Cell Genomics. *Cancer Cell* (2020) 37:456–70. doi: 10.1016/j.ccell.2020.03.008
7. Ma A, McDermaid A, Xu J, Chang Y, Ma Q. Integrative Methods and Practical Challenges for Single-Cell Multi-Omics. *Trends Biotechnol* (2020) 38:1007–22. doi: 10.1016/j.tibtech.2020.02.013
8. Bendall SC, Nolan GP, Roederer M, Chattopadhyay PK. A Deep Profiler's Guide to Cytometry. *Trends Immunol* (2012) 33:323–32. doi: 10.1016/j.it.2012.02.010
9. Szaloki G, Goda K. Compensation in Multicolor Flow Cytometry. *Cytometry. Part A J Int Soc Analytical Cytology* (2015) 87:982–5. doi: 10.1002/cyto.a.22736

10. Bandura DR, Baranov VI, Ornatsky OI, Antonov A, Kinach R, Lou X, et al. Mass Cytometry: Technique for Real Time Single Cell Multitarget Immunoassay Based on Inductively Coupled Plasma Time-of-Flight Mass Spectrometry. *Analytical Chem* (2009) 81:6813–22. doi: 10.1021/ac901049w
11. Spitzer MH, Nolan GP. Mass Cytometry: Single Cells, Many Features. *Cell* (2016) 165:780–91. doi: 10.1016/j.cell.2016.04.019
12. Newell EW, Cheng Y. Mass Cytometry: Blessed With the Curse of Dimensionality. *Nat Immunol* (2016) 17:890–5. doi: 10.1038/ni.3485
13. Gadalla R, Noamani B, MacLeod BL, Dickson RJ, Guo M, Xu W, et al. Validation of Cytof Against Flow Cytometry for Immunological Studies and Monitoring of Human Cancer Clinical Trials. *Front Oncol* (2019) 9:415. doi: 10.3389/fonc.2019.00415
14. Giesen C, Wang HA, Schapiro D, Zivanovic N, Jacobs A, Hattendorf B, et al. Highly Multiplexed Imaging of Tumor Tissues With Subcellular Resolution by Mass Cytometry. *Nat Methods* (2014) 11:417–22. doi: 10.1038/nmeth.2869
15. Cheung P, Vallania F, Dvorak M, Chang SE, Schaffert S, Donato M, et al. Single-Cell Epigenetics–Chromatin Modification Atlas Unveiled by Mass Cytometry. *Clin Immunol* (2018) 196:40–8. doi: 10.1016/j.clim.2018.06.009
16. Frei AP, Bava FA, Zunder ER, Hsieh EW, Chen SY, Nolan GP, et al. Highly Multiplexed Simultaneous Detection of Rnas and Proteins in Single Cells. *Nat Methods* (2016) 13:269–75. doi: 10.1038/nmeth.3742
17. Leong ML, Newell EW. Multiplexed Peptide-Mhc Tetramer Staining With Mass Cytometry. *Methods Mol Biol* (2015) 1346:115–31. doi: 10.1007/978-1-4939-2987-0_9
18. Stark R, Grzelak M, Hadfield J. Rna Sequencing: The Teenage Years. *Nat Rev Genet* (2019) 20:631–56. doi: 10.1038/s41576-019-0150-2
19. Tang F, Barbacioru C, Wang Y, Nordman E, Lee C, Xu N, et al. Mrna-Seq Whole-Transcriptome Analysis of a Single Cell. *Nat Methods* (2009) 6:377–82. doi: 10.1038/nmeth.1315
20. Schmidt WM, Mueller MW. Capselect: A Highly Sensitive Method for 5' Cap-Dependent Enrichment of Full-Length Cdna in Pcr-Mediated Analysis of Mrnas. *Nucleic Acids Res* (1999) 27:e31. doi: 10.1093/nar/27.21.e31
21. Islam S, Kjallquist U, Moliner A, Zajac P, Fan JB, Lonnerberg P, et al. Characterization of the Single-Cell Transcriptional Landscape by Highly Multiplex Rna-Seq. *Genome Res* (2011) 21:1160–7. doi: 10.1101/gr.110882.110
22. Mereu E, Lafzi A, Moutinho C, Ziegenhain C, McCarthy DJ, Alvarez-Varela A, et al. Benchmarking Single-Cell Rna-Sequencing Protocols for Cell Atlas Projects. *Nat Biotechnol* (2020) 38:747–55. doi: 10.1038/s41587-020-0469-4
23. Hagemann-Jensen M, Ziegenhain C, Chen P, Ramskold D, Hendriks GJ, Larsson AJM, et al. Single-Cell Rna Counting at Allele and Isoform Resolution Using Smart-Seq3. *Nat Biotechnol* (2020) 38(6):708–14. doi: 10.1038/s41587-020-0497-0
24. Keren-Shaul H, Kenigsberg E, Jaitin DA, David E, Paul F, Tanay A, et al. Mars-Seq2.0: An Experimental and Analytical Pipeline for Indexed Sorting Combined With Single-Cell Rna Sequencing. *Nat Protoc* (2019) 14:1841–62. doi: 10.1038/s41596-019-0164-4
25. Hashimshony T, Senderovich N, Avital G, Klochendler A, de Leeuw Y, Anavy L, et al. Cel-Seq2: Sensitive Highly-Multiplexed Single-Cell Rna-Seq. *Genome Biol* (2016) 17:77. doi: 10.1186/s13059-016-0938-8
26. Macosko EZ, Basu A, Satija R, Nemesh J, Shekhar K, Goldman M, et al. Highly Parallel Genome-Wide Expression Profiling of Individual Cells Using Nanoliter Droplets. *Cell* (2015) 161:1202–14. doi: 10.1016/j.cell.2015.05.002
27. Klein AM, Mazutis L, Akartuna I, Tallapragada N, Veres A, Li V, et al. Droplet Barcoding for Single-Cell Transcriptomics Applied to Embryonic Stem Cells. *Cell* (2015) 161:1187–201. doi: 10.1016/j.cell.2015.04.044
28. Zheng GX, Terry JM, Belgrader P, Ryvkin P, Bent ZW, Wilson R, et al. Massively Parallel Digital Transcriptional Profiling of Single Cells. *Nat Commun* (2017) 8:14049. doi: 10.1038/ncomms14049
29. Cao J, Packer JS, Ramani V, Cusanovich DA, Huynh C, Daza R, et al. Comprehensive Single-Cell Transcriptional Profiling of a Multicellular Organism. *Science* (2017) 357:661–7. doi: 10.1126/science.aam8940
30. Kuchina A, Brettner LM, Paleologu L, Roco CM, Rosenberg AB, Carignano A, et al. Microbial Single-Cell Rna Sequencing by Split-Pool Barcoding. *Science* (2020) 371:6531. doi: 10.1101/869248
31. Rosenberg AB, Roco CM, Muscat RA, Kuchina A, Sample P, Yao Z, et al. Single-Cell Profiling of the Developing Mouse Brain and Spinal Cord With Split-Pool Barcoding. *Science* (2018) 360:176–82. doi: 10.1126/science.aam8999
32. Hughes TK, Wadsworth MH2nd, Gierahn TM, Do T, Weiss D, Andrade PR, et al. Second-Strand Synthesis-Based Massively Parallel Scrna-Seq Reveals Cellular States and Molecular Features of Human Inflammatory Skin Pathologies. *Immunity* (2020) 53:878–894 e877. doi: 10.1016/j.immuni.2020.09.015
33. Zhu C, Preissl S, Ren B. Single-Cell Multimodal Omics: The Power of Many. *Nat Methods* (2020) 17:11–4. doi: 10.1038/s41592-019-0691-5
34. Yin Y, Jiang Y, Lam KG, Berletch JB, Disteche CM, Noble WS, et al. High-Throughput Single-Cell Sequencing With Linear Amplification. *Mol Cell* (2019) 76:676–690 e610. doi: 10.1016/j.molcel.2019.08.002
35. Zachariadis V, Cheng H, Andrews N, Enge M. A Highly Scalable Method for Joint Whole-Genome Sequencing and Gene-Expression Profiling of Single Cells. *Mol Cell* (2020) 80:541–53.e545. doi: 10.1016/j.molcel.2020.09.025
36. Petti AA, Williams SR, Miller CA, Fiddes IT, Srivatsari SN, Chen DY, et al. A General Approach for Detecting Expressed Mutations in Aml Cells Using Single Cell Rna-Sequencing. *Nat Commun* (2019) 10(1):1–16. doi: 10.1038/s41467-019-11591-1
37. Vu TN, Nguyen HN, Calza S, Kalari KR, Wang L, Pawitan Y. Cell-Level Somatic Mutation Detection From Single-Cell Rna Sequencing. *Bioinformatics* (2019) 35:4679–87. doi: 10.1093/bioinformatics/btz288
38. Buenrostro JD, Giresi PG, Zaba LC, Chang HY, Greenleaf WJ. Transposition of Native Chromatin for Fast and Sensitive Epigenomic Profiling of Open Chromatin, DNA-Binding Proteins and Nucleosome Position. *Nat Methods* (2013) 10:1213–8. doi: 10.1038/nmeth.2688
39. Buenrostro JD, Wu B, Litzenburger UM, Ruff D, Gonzales ML, Snyder MP, et al. Single-Cell Chromatin Accessibility Reveals Principles of Regulatory Variation. *Nature* (2015) 523:486–90. doi: 10.1038/nature14590
40. Cao J, Cusanovich DA, Ramani V, Aghamirzaie D, Pliner HA, Hill AJ, et al. Joint Profiling of Chromatin Accessibility and Gene Expression in Thousands of Single Cells. *Science* (2018) 361:1380–5. doi: 10.1126/science.aau0730
41. Chen S, Lake BB, Zhang K. High-Throughput Sequencing of the Transcriptome and Chromatin Accessibility in the Same Cell. *Nat Biotechnol* (2019) 37:1452–7. doi: 10.1038/s41587-019-0290-0
42. Ma S, Zhang B, LaFave LM, Earl AS, Chiang Z, Hu Y, et al. Chromatin Potential Identified by Shared Single-Cell Profiling of Rna and Chromatin. *Cell* (2020) 183(4):1103–16. doi: 10.1101/2020.06.17.156943
43. Wang C, Sun D, Huang X, Wan C, Li Z, Han Y, et al. Integrative Analyses of Single-Cell Transcriptome and Regulome Using Maestro. *Genome Biol* (2020) 21:1–28. doi: 10.1186/s13059-020-02116-x
44. Stuart T, Srivastava A, Lareau C, Satija R. Multimodal Single-Cell Chromatin Analysis With Signac. *bioRxiv* (2020). doi: 10.1101/2020.11.09.373613
45. Stoeckius M, Hafemeister C, Stephenson W, Houck-Loomis B, Chattopadhyay PK, Swerdlow H, et al. Simultaneous Epitope and Transcriptome Measurement in Single Cells. *Nat Methods* (2017) 14:865–8. doi: 10.1038/nmeth.4380
46. Hao Y, Hao S, Andersen-Nissen E, Mauck WM, Zheng S, Butler A, et al. Integrated Analysis of Multimodal Single-Cell Data. *bioRxiv* (2020). doi: 10.1101/2020.10.12.335331
47. Granja JM, Klemm S, McGinnis LM, Kathiria AS, Mezger A, Corces MR, et al. Single-Cell Multiomic Analysis Identifies Regulatory Programs in Mixed-Phenotype Acute Leukemia. *Nat Biotechnol* (2019) 37:1458–65. doi: 10.1038/s41587-019-0332-7
48. Zhang SQ, Ma KY, Schonnesen AA, Zhang M, He C, Sun E, et al. High-Throughput Determination of the Antigen Specificities of T Cell Receptors in Single Cells. *Nat Biotechnol* (2018) 36(12):1156–9. doi: 10.1101/457069
49. Stoeckius M, Zheng S, Houck-Loomis B, Hao S, Yeung BZ, Mauck WM3rd, et al. Cell Hashing With Barcoded Antibodies Enables Multiplexing and Doublet Detection for Single Cell Genomics. *Genome Biol* (2018) 19:224. doi: 10.1186/s13059-018-1603-1
50. Crosetto N, Bienko M, van Oudenaarden A. Spatially Resolved Transcriptomics and Beyond. *Nat Rev Genet* (2015) 16:57–66. doi: 10.1038/nrg3832
51. Asp M, Bergenstrahle J, Lundeberg J. Spatially Resolved Transcriptomes-Next Generation Tools for Tissue Exploration. *Bioessays* (2020) 42:e1900221. doi: 10.1002/bies.201900221
52. Raj A, Van Den Bogaard P, Rifkin SA, Van Oudenaarden A, Tyagi S. Imaging Individual Mrna Molecules Using Multiple Singly Labeled Probes. *Nat Methods* (2008) 5:877–9. doi: 10.1038/nmeth.1253

53. Eng CL, Lawson M, Zhu Q, Dries R, Koulena N, Takei Y, et al. Transcriptome-Scale Super-Resolved Imaging in Tissues by Rna Seqfish. *Nature* (2019) 568:235–9. doi: 10.1038/s41586-019-1049-y
54. Rodriques SG, Stickels RR, Goeva A, Martin CA, Murray E, Vanderburg CR, et al. Slide-Seq: A Scalable Technology for Measuring Genome-Wide Expression at High Spatial Resolution. *Science* (2019) 363:1463–7. doi: 10.1126/science.aaw1219
55. Stickels RR, Murray E, Kumar P, Li JL, Marshall JL, Di Bella DJ, et al. Highly Sensitive Spatial Transcriptomics at Near-Cellular Resolution With Slide-Seqv2. *Nat Biotechnol* (2020) 39(3):313–9. doi: 10.1038/s41587-020-0739-1
56. Vickovic S, Eraslan G, Salmen F, Klughammer J, Stenbeck L, Schapiro D, et al. High-Definition Spatial Transcriptomics for in Situ Tissue Profiling. *Nat Methods* (2019) 16:987–90. doi: 10.1038/s41592-019-0548-y
57. Liu Y, Yang M, Deng Y, Su G, Enninful A, Guo CC, et al. High-Spatial-Resolution Multi-Omics Sequencing Via Deterministic Barcoding in Tissue. *Cell* (2020) 183:1665–81.e1618. doi: 10.1016/j.cell.2020.10.026
58. Stegle O, Teichmann SA, Marioni JC. Computational and Analytical Challenges in Single-Cell Transcriptomics. *Nat Rev Genet* (2015) 16:133–45. doi: 10.1038/nrg3833
59. Hie B, Peters J, Nyquist SK, Shalek AK, Berger B, Bryson BD. Computational Methods for Single-Cell Rna Sequencing. *Annu Rev Biomed Data Sci* (2020) 3:339–64. doi: 10.1146/annurev-biodatasci-012220-100601
60. Saelens W, Cannoodt R, Todorov H, Saeys Y. A Comparison of Single-Cell Trajectory Inference Methods. *Nat Biotechnol* (2019) 37:547–54. doi: 10.1038/s41587-019-0071-9
61. Cao J, Spielmann M, Qiu X, Huang X, Ibrahim DM, Hill AJ, et al. The Single-Cell Transcriptional Landscape of Mammalian Organogenesis. *Nature* (2019) 566:496–502. doi: 10.1038/s41586-019-0969-x
62. Wolf FA, Hamey FK, Plass M, Solana J, Dahlin JS, Gottgens B, et al. Paga: Graph Abstraction Reconciles Clustering With Trajectory Inference Through a Topology Preserving Map of Single Cells. *Genome Biol* (2019) 20(1):1–9. doi: 10.1186/s13059-019-1663-x
63. Street K, Risso D, Fletcher RB, Das D, Ngai J, Yosef N, et al. Slingshot: Cell Lineage and Pseudotime Inference for Single-Cell Transcriptomics. *BMC Genomics* (2018) 19(1):1–16. doi: 10.1186/s12864-018-4772-0
64. La Manno G, Soldatov R, Zeisel A, Braun E, Hochgerner H, Petukhov V, et al. Rna Velocity of Single Cells. *Nature* (2018) 560:494–8. doi: 10.1038/s41586-018-0414-6
65. Bergen V, Lange M, Peidli S, Wolf FA, Theis FJ. Generalizing Rna Velocity to Transient Cell States Through Dynamical Modeling. *Nature Biotechnol* (2020) 38:1408–14. doi: 10.1038/s41587-020-0591-3
66. Gulati GS, Sikandar SS, Wesche DJ, Manjunath A, Bharadwaj A, Berger MJ, et al. Single-Cell Transcriptional Diversity is a Hallmark of Developmental Potential. *Science* (2020) 367(6476):405–11. doi: 10.1126/science.aax0249
67. Wagner DE, Klein AM. Lineage Tracing Meets Single-Cell Omics: Opportunities and Challenges. *Nat Rev Genet* (2020) 21:410–27. doi: 10.1038/s41576-020-0223-2
68. De Simone M, Rossetti G, Pagani M. Single Cell T Cell Receptor Sequencing: Techniques and Future Challenges. *Front Immunol* (2018) 9:1638. doi: 10.3389/fimmu.2018.01638
69. Argelaguet R, Arnol D, Bredikhin D, Deloro Y, Velten B, Marioni JC, et al. Mofa+: A Statistical Framework for Comprehensive Integration of Multi-Modal Single-Cell Data. *Genome Biol* (2020) 21:111. doi: 10.1186/s13059-020-02015-1
70. Nguyen ND, Wang D. Multiview Learning for Understanding Functional Multiomics. *PloS Comput Biol* (2020) 16:e1007677. doi: 10.1371/journal.pcbi.1007677
71. Zhang F, Wei K, Slowikowski K, Fonseka CY, Rao DA, Kelly S, et al. Defining Inflammatory Cell States in Rheumatoid Arthritis Joint Synovial Tissues by Integrating Single-Cell Transcriptomics and Mass Cytometry. *Nat Immunol* (2019) 20:928–42. doi: 10.1038/s41590-019-0378-1
72. Gayoso A, Steier Z, Lopez R, Regier J, Nazor KL, Streets A, et al. Joint Probabilistic Modeling of Single-Cell Multi-Omic Data With Totalvi. *Nat Methods* (2021) 18:272–82. doi: 10.1038/s41592-020-01050-x
73. Rozenblatt-Rosen O, Regev A, Oberdoerffer P, Nawy T, Hupalowska A, Rood JE, et al. The Human Tumor Atlas Network: Charting Tumor Transitions Across Space and Time at Single-Cell Resolution. *Cell* (2020) 181:236–49. doi: 10.1016/j.cell.2020.03.053
74. Lavin Y, Kobayashi S, Leader A, Amir ED, Elefant N, Bigenwald C, et al. Innate Immune Landscape in Early Lung Adenocarcinoma by Paired Single-Cell Analyses. *Cell* (2017) 169:750–765 e717. doi: 10.1016/j.cell.2017.04.014
75. Jackson HW, Fischer JR, Zanotelli VRT, Ali HR, Mechera R, Soysal SD, et al. The Single-Cell Pathology Landscape of Breast Cancer. *Nature* (2020) 578:615–20. doi: 10.1038/s41586-019-1876-x
76. Zhang Q, He Y, Luo N, Patel SJ, Han Y, Gao R, et al. Landscape and Dynamics of Single Immune Cells in Hepatocellular Carcinoma. *Cell* (2019) 179:829–845 e820. doi: 10.1016/j.cell.2019.10.003
77. Nam AS, Kim KT, Chaligne R, Izzo F, Ang C, Taylor J, et al. Somatic Mutations and Cell Identity Linked by Genotyping of Transcriptomes. *Nature* (2019) 571:355–60. doi: 10.1038/s41586-019-1367-0
78. Moncada R, Barkley D, Wagner F, Chiodin M, Devlin JC, Baron M, et al. Integrating Microarray-Based Spatial Transcriptomics and Single-Cell Rna-Seq Reveals Tissue Architecture in Pancreatic Ductal Adenocarcinomas. *Nat Biotechnol* (2020) 38:333–42. doi: 10.1038/s41587-019-0392-8
79. Yost KE, Satpathy AT, Wells DK, Qi Y, Wang C, Kageyama R, et al. Clonal Replacement of Tumor-Specific T Cells Following Pd-1 Blockade. *Nat Med* (2019) 25:1251–9. doi: 10.1038/s41591-019-0522-3
80. Sun Y, Wu L, Zhong Y, Zhou K, Hou Y, Wang Z, et al. Single-Cell Landscape of the Ecosystem in Early-Relapse Hepatocellular Carcinoma. *Cell* (2020) 184(2):404-21.e16. doi: 10.1016/j.cell.2020.11.041
81. Hwang WL, Jagadeesh KA, Guo JA, Hoffman HI, Yadollahpour P, Mohan R, et al. Single-Nucleus and Spatial Transcriptomics of Archival Pancreatic Cancer Reveals Multi-Compartment Reprogramming After Neoadjuvant Treatment. *BioRxiv* (2020). doi: 10.1158/1538-7445.PANCA20-PR-007
82. Chevrier S, Levine JH, Zanotelli VRT, Silina K, Schulz D, Bacac M, et al. An Immune Atlas of Clear Cell Renal Cell Carcinoma. *Cell* (2017) 169:736–49.e718. doi: 10.1016/j.cell.2017.04.016
83. Wagner J, Rapsomaniki MA, Chevrier S, Anzeneder T, Langwieder C, Dykgers A, et al. Bodenmiller B. A Single-Cell Atlas of the Tumor and Immune Ecosystem of Human Breast Cancer. *Cell* (2019) 177:1330–1345 e1318. doi: 10.1016/j.cell.2019.03.005
84. Gohil SH, Iorgulescu JB, Braun DA, Keskin DB, Livak KJ. Applying High-Dimensional Single-Cell Technologies to the Analysis of Cancer Immunotherapy. *Nat Rev Clin Oncol* (2020) 18(4):244–56. doi: 10.1038/s41571-020-00449-x
85. Azizi E, Carr AJ, Plitas G, Cornish AE, Konopacki C, Prabhakaran S, et al. Single-Cell Map of Diverse Immune Phenotypes in the Breast Tumor Microenvironment. *Cell* (2018) 174:1293–308.e1236. doi: 10.1016/j.cell.2018.05.060
86. Ludwig LS, Lareau CA, Ulirsch JC, Christian E, Muus C, Li LH, et al. Lineage Tracing in Humans Enabled by Mitochondrial Mutations and Single-Cell Genomics. *Cell* (2019) 176:1325–39.e1322. doi: 10.1016/j.cell.2019.01.022
87. van Galen P, Hovestadt V, Wadsworth Ii MH, Hughes TK, Griffin GK, Battaglia S, et al. Single-Cell Rna-Seq Reveals Aml Hierarchies Relevant to Disease Progression and Immunity. *Cell* (2019) 176:1265–81.e1224. doi: 10.1016/j.cell.2019.01.031
88. Bian S, Hou Y, Zhou X, Li X, Yong J, Wang Y, et al. Single-Cell Multiomics Sequencing and Analyses of Human Colorectal Cancer. *Science* (2018) 362:1060–3. doi: 10.1126/science.aao3791
89. Hou Y, Guo H, Cao C, Li X, Hu B, Zhu P, et al. Single-Cell Triple Omics Sequencing Reveals Genetic, Epigenetic, and Transcriptomic Heterogeneity in Hepatocellular Carcinomas. *Cell Res* (2016) 26:304–19. doi: 10.1038/cr.2016.23
90. Nam AS, Chaligne R, Landau DA. Integrating Genetic and non-Genetic Determinants of Cancer Evolution by Single-Cell Multi-Omics. *Nat Rev Genet* (2021) 22:3–18. doi: 10.1038/s41576-020-0265-5
91. Stuart T, Satija R. Integrative Single-Cell Analysis. *Nat Rev Genet* (2019) 20:257–72. doi: 10.1038/s41576-019-0093-7
92. Castro LNG, Tirosh I, Suvà ML. Decoding Cancer Biology One Cell at a Time. *Cancer Discovery* (2021) 11:960–70. doi: 10.1158/2159-8290.CD-20-1376
93. Tirosh I, Venteicher AS, Hebert C, Escalante LE, Patel AP, Yizhak K, et al. Single-Cell Rna-Seq Supports a Developmental Hierarchy in Human Oligodendroglioma. *Nature* (2016) 539:309–13. doi: 10.1038/nature20123
94. Marjanovic ND, Hofree M, Chan JE, Canner D, Wu K, Trakala M, et al. Emergence of a High-Plasticity Cell State During Lung Cancer Evolution. *Cancer Cell* (2020) 38:229–246. e213. doi: 10.1016/j.ccell.2020.06.012

95. Neftel C, Laffy J, Filbin MG, Hara T, Shore ME, Rahme GJ, et al. An Integrative Model of Cellular States, Plasticity, and Genetics for Glioblastoma. *Cell* (2019) 178:835–49.e821. doi: 10.1016/j.cell.2019.06.024
96. Chaffer CL, Weinberg RA. A Perspective on Cancer Cell Metastasis. *Science* (2011) 331:1559–64. doi: 10.1126/science.1203543
97. Kim N, Kim HK, Lee K, Hong Y, Cho JH, Choi JW, et al. Single-Cell Rna Sequencing Demonstrates the Molecular and Cellular Reprogramming of Metastatic Lung Adenocarcinoma. *Nat Commun* (2020) 11:1–15. doi: 10.1038/s41467-020-16164-1
98. Quinn JJ, Jones MG, Okimoto RA, Nanjo S, Chan MM, Yosef N, et al. Single-Cell Lineages Reveal the Rates, Routes, and Drivers of Metastasis in Cancer Xenografts. *Science* (2021) 371(6532):eabc1944. doi: 10.1126/science.abc1944
99. Prieto-Vila M, Usuba W, Takahashi R-U, Shimomura I, Sasaki H, Ochiya T, et al. Single-Cell Analysis Reveals a Preexisting Drug-Resistant Subpopulation in the Luminal Breast Cancer Subtype. *Cancer Res* (2019) 79:4412–25. doi: 10.1158/0008-5472.CAN-19-0122
100. Jerby-Arnon L, Shah P, Cuoco MS, Rodman C, Su M-J, Melms JC, et al. A Cancer Cell Program Promotes T Cell Exclusion and Resistance to Checkpoint Blockade. *Cell* (2018) 175:984–97.e924. doi: 10.1016/j.cell.2018.09.006
101. Frangieh CJ, Melms JC, Thakore PI, Geiger-Schuller KR, Ho P, Luoma AM, et al. Multimodal Pooled Perturb-Cite-Seq Screens in Patient Models Define Mechanisms of Cancer Immune Evasion. *Nat Genet* (2021) 53:332–41. doi: 10.1038/s41588-021-00779-1
102. Wei SC, Duffy CR, Allison JP. Fundamental Mechanisms of Immune Checkpoint Blockade Therapy. *Cancer Discovery* (2018) 8:1069–86. doi: 10.1158/2159-8290.CD-18-0367
103. Manfredi F, Cianciotti BC, Potenza A, Tassi E, Noviello M, Biondi A, et al. Tcr Redirected T Cells for Cancer Treatment: Achievements, Hurdles, and Goals. *Front Immunol* (2020) 11:1689. doi: 10.3389/fimmu.2020.01689
104. Waldman AD, Fritz JM, Lenardo MJ. A Guide to Cancer Immunotherapy: From T Cell Basic Science to Clinical Practice. *Nat Rev Immunol* (2020) 20:651–68. doi: 10.1038/s41577-020-0306-5
105. Redmond D, Poran A, Elemento O. Single-Cell Tcrseq: Paired Recovery of Entire T-Cell Alpha and Beta Chain Transcripts in T-Cell Receptors From Single-Cell Rnaseq. *Genome Med* (2016) 8:80. doi: 10.1186/s13073-016-0335-7
106. Zheng C, Zheng L, Yoo JK, Guo H, Zhang Y, Guo X, et al. Landscape of Infiltrating T Cells in Liver Cancer Revealed by Single-Cell Sequencing. *Cell* (2017) 169:1342–56.e1316. doi: 10.1016/j.cell.2017.05.035
107. Zhang L, Yu X, Zheng L, Zhang Y, Li Y, Fang Q, et al. Lineage Tracking Reveals Dynamic Relationships of T Cells in Colorectal Cancer. *Nature* (2018) 564:268–72. doi: 10.1038/s41586-018-0694-x
108. Kidman J, Principe N, Watson M, Lassmann T, Holt RA, Nowak AK, et al. Characteristics of Tcr Repertoire Associated With Successful Immune Checkpoint Therapy Responses. *Front Immunol* (2020) 11:587014. doi: 10.3389/fimmu.2020.587014
109. Wu TD, Madireddi S, de Almeida PE, Banchereau R, Chen YJ, Chitre AS, et al. Peripheral T Cell Expansion Predicts Tumour Infiltration and Clinical Response. *Nature* (2020) 579:274–8. doi: 10.1038/s41586-020-2056-8
110. Depuydt MAC, Prange KHM, Slenders L, Ord T, Elbersen D, Boltjes A, et al. Microanatomy of the Human Atherosclerotic Plaque by Single-Cell Transcriptomics. *Circ Res* (2020) 127:1437–55. doi: 10.1161/CIRCRESAHA.120.316770
111. Huang H, Wang C, Rubelt F, Scriba TJ, Davis MM. Analyzing the Mycobacterium Tuberculosis Immune Response by T-Cell Receptor Clustering With Gliph2 and Genome-Wide Antigen Screening. *Nat Biotechnol* (2020) 38(10):1194–202. doi: 10.1038/s41587-020-0505-4
112. Dash P, Fiore-Gartland AJ, Hertz T, Wang GC, Sharma S, Souquette A, et al. Quantifiable Predictive Features Define Epitope-Specific T Cell Receptor Repertoires. *Nature* (2017) 547:89–93. doi: 10.1038/nature22383
113. Irmisch A, Bonilla X, Chevrier S, Lehmann KV, Singer F, Toussaint NC, et al. The Tumor Profiler Study: Integrated, Multi-Omic, Functional Tumor Profiling for Clinical Decision Support. *Cancer Cell* (2021) 39(3):288–93. doi: 10.1016/j.ccell.2021.01.004
114. Rajewsky N, Almouzni G, Gorski SA, Aerts S, Amit I, Bertero MG, et al. Lifetime and Improving European Healthcare Through Cell-Based Interceptive Medicine. *Nature* (2020) 587:377–86. doi: 10.1038/s41586-020-2715-9
115. Krieg C, Nowicka M, Guglietta S, Schindler S, Hartmann FJ, Weber LM, et al. High-Dimensional Single-Cell Analysis Predicts Response to Anti-Pd-1 Immunotherapy. *Nat Med* (2018) 24:144–53. doi: 10.1038/nm.4466
116. Cader FZ, Hu X, Goh WL, Wienand K, Ouyang J, Mandato E, et al. A Peripheral Immune Signature of Responsiveness to Pd-1 Blockade in Patients With Classical Hodgkin Lymphoma. *Nat Med* (2020) 26(9):1468–79. doi: 10.1038/s41591-020-1006-1
117. Good Z, Sarno J, Jager A, Samusik N, Aghaeepour N, Simonds EF, et al. Single-Cell Developmental Classification of B Cell Precursor Acute Lymphoblastic Leukemia at Diagnosis Reveals Predictors of Relapse. *Nat Med* (2018) 24:474–83. doi: 10.1038/nm.4505
118. Martinez-Morilla S, Villarroel-Espindola F, Wong PF, Toki MI, Aung TN, Pelekanou V, et al. Biomarker Discovery in Patients With Immunotherapy-Treated Melanoma With Imaging Mass Cytometry. *Clin Cancer Res* (2021) 27(7):1987–96. doi: 10.1158/1538-7445.AM2020-2001
119. Ali HR, Jackson HW, Zanotelli VRT, Danenberg E, Fischer JR, Bardwell H, et al. Imaging Mass Cytometry and Multiplatform Genomics Define the Phenogenomic Landscape of Breast Cancer. *Nat Cancer* (2020) 1:163–75. doi: 10.1038/s43018-020-0026-6
120. Gonzalez-Silva L, Quevedo L, Varela I. Tumor Functional Heterogeneity Unraveled by Scrna-Seq Technologies. *Trends Cancer* (2020) 6:13–9. doi: 10.1016/j.trecan.2019.11.010
121. Savas P, Virassamy B, Ye C, Salim A, Mintoff CP, Caramia F, et al. Single-Cell Profiling of Breast Cancer T Cells Reveals a Tissue-Resident Memory Subset Associated With Improved Prognosis. *Nat Med* (2018) 24:986–93. doi: 10.1038/s41591-018-0078-7
122. Ramakrishna S, Shah NN. Using Single-Cell Analysis to Predict Car T Cell Outcomes. *Nat Med* (2020) 26(12):1813–4. doi: 10.1038/s41591-020-01157-w
123. Neelapu SS, Locke FL, Bartlett NL, Lekakis LJ, Miklos DB, Jacobson CA, et al. Axicabtagene Ciloleucel Car T-Cell Therapy in Refractory Large B-Cell Lymphoma. *New Engl J Med* (2017) 377:2531–44. doi: 10.1056/NEJMoa1707447
124. Deng Q, Han G, Puebla-Osorio N, Ma MCJ, Strati P, Chasen B, et al. Characteristics of Anti-Cd19 Car T Cell Infusion Products Associated With Efficacy and Toxicity in Patients With Large B Cell Lymphomas. *Nat Med* (2020) 26:1878–87. doi: 10.1038/s41591-020-1061-7
125. Sheih A, Voillet V, Hanafi L-A, DeBerg HA, Yajima M, Hawkins R, et al. Clonal Kinetics and Single-Cell Transcriptional Profiling of Car-T Cells in Patients Undergoing Cd19 Car-T Immunotherapy. *Nat Commun* (2020) 11:1–13. doi: 10.1038/s41467-019-13880-1
126. Gong W, Kwak I-Y, Pota P, Koyano-Nakagawa N, Garry DJ. Drimpute: Imputing Dropout Events in Single Cell Rna Sequencing Data. *BMC Bioinf* (2018) 19:1–10. doi: 10.1186/s12859-018-2226-y
127. Kanev K, Roelli P, Wu M, Wurmser C, Delorenzi M, Pfaffl MW, et al. Tailoring the Resolution of Single-Cell Rna Sequencing for Primary Cytotoxic T Cells. *Nat Commun* (2021) 12:1–11. doi: 10.1038/s41467-020-20751-7

Conflict of Interest: HS and WY are both co-founders of, and WC is the scientific consultant of Zhejiang Puluoting Health Technology Co., Ltd (PLT). HS is the CEO of the PLT.

The remaining authors declare that the research was conducted in the absence of any commercial or financial relationships that could be construed as a potential conflict of interest.

frontiers in Immunology

ORIGINAL RESEARCH
published: 06 July 2021
doi: 10.3389/fimmu.2021.694801

Multi-Omics Analysis Showed the Clinical Value of Gene Signatures of C1QC$^+$ and SPP1$^+$ TAMs in Cervical Cancer

Xiong Li[1,2], *Qinghua Zhang*[2], *Gang Chen*[1] *and Danfeng Luo*[1]*

[1] Department of Obstetrics and Gynecology, Tongji Hospital, Tongji Medical College, Huazhong University of Science and Technology, Wuhan, China, [2] Department of Obstetrics and Gynecology, the Central Hospital of Wuhan, Tongji Medical College, Huazhong University of Science and Technology, Wuhan, China

OPEN ACCESS

Edited by:
Wei Wei,
Institute for Systems Biology (ISB), United States

Reviewed by:
Reem Saleh,
Peter MacCallum Cancer Centre, Australia
Xiaosheng Wang,
China Pharmaceutical University, China

***Correspondence:**
Danfeng Luo
daluo@tjh.tjmu.edu.cn

Specialty section:
This article was submitted to Cancer Immunity and Immunotherapy, a section of the journal Frontiers in Immunology

Received: *13 April 2021*
Accepted: *21 June 2021*
Published: *06 July 2021*

Citation:
Li X, Zhang Q, Chen G and Luo D (2021) Multi-Omics Analysis Showed the Clinical Value of Gene Signatures of C1QC$^+$ and SPP1$^+$ TAMs in Cervical Cancer. Front. Immunol. 12:694801. doi: 10.3389/fimmu.2021.694801

Purpose: To evaluate the value of C1QC$^+$ and SPP1$^+$ TAMs gene signatures in patients with cervical cancer.

Methods: We compare the C1QC$^+$ and SPP1$^+$ TAMs gene signatures with the M1/M2 gene signatures at single cell level and bulk RNA-seq level and evaluate which gene signature can clearly divide TAMs and patients with cervical cancer into distinct clinical subclusters better.

Results: At single-cell level, C1QC$^+$ and SPP1$^+$ TAMs gene signatures, but not M1 and M2 gene signatures, could clearly divided TAMs into two subclusters in a colon cancer data set and an advanced basal cell data set. For cervical cancer data from TCGA, patients with C1QC^{high} and SPP1^{low} TAMs gene signatures have the best prognosis, lowest proportion (34.21%) of locally advanced cervical cancer (LACC), and highest immune cell infiltration, whereas patients with C1QC^{low} and SPP1^{high} TAMs gene signatures have the worst prognosis, highest proportion (71.79%) of LACC and lowest immune cell infiltration. Patients with C1QC^{high} and SPP1^{low} TAMs gene signature have higher expression of most of the Immune checkpoint molecules (ICMs) than patients with C1QC^{low} and SPP1^{high} TAMs gene signatures. The GSEA results suggested that subgroups of patients divided by C1QC$^+$ and SPP1$^+$ TAMs gene signatures showed different anti- or pro-tumor state.

Conclusion: C1QC$^+$ and SPP1$^+$ TAMs gene signatures, but not M1/M2 gene signatures, can divide cervical patients into subgroups with different prognosis, tumor stage, different immune cell infiltration, and ICMs expression. Our findings may help to find suitable treatment strategy for cervical cancer patients with different TAMs gene signatures.

Keywords: cervical cancer, TAMs (tumor associated myeloid cells), C1QC, SPP1 gene, single cell, immunity

INTRODUCTION

Despite initiatives to improve the prevention of cervical cancer with screening and vaccination, cervical cancer is still one of the leading causes of death among women worldwide (1). Improvements in survival have mainly been through effective surgery, technical radiotherapy, and addition of bevacizumab to standard chemotherapy in recent years (2, 3). However, women with advanced or recurrent disease still face a dismal prognosis with potentially considerable morbidity and mortality. Immunotherapy might be a novel choice to improve the clinical outcomes of these patients. On the established clinical benefit of PD-1/PD-L1 inhibitors in cervical cancer, the Food and Drug Administration (FDA) has approved pembrolizumab for patients with recurrent or metastatic cervical cancer with disease progression during or after chemotherapy. However, treatment options are still limited, extensive researches and clinical trials are needed to be carried out to identify novel Immunotherapy signatures and options (4, 5).

The tumor microenvironment (TME) are governed by crosstalks within and across various cellular compartments, including immune, malignant, endothelial, and stromal cells (6). Tumor-associated macrophages (TAMs), which are considered as the main components of the tumor microenvironment, reportedly play key roles in the initiation and progression of cancers (7, 8). The TAMs are highly dynamic and heterogeneous within and across different cancers (6, 9). TAMs' heterogeneity makes them with various functions. Different subsets of TAMs may show distinct functions. However, the distinction of different subsets of TAMs varied in different studies. In lung cancer and breast cancer, TAMs reportedly showed a continuous spectrum of phenotypes (10–12). In some other cancers, TAMs were classified into "traditional" pro-inflammatory (M1-like) or anti-inflammatory (M2-like) TAMs (6, 13). However, Lei et al. (10) reported that TAMs in colon cancer exhibited a remarkable dichotomy and were defined as $C1QC^+$ TAMs and $SPP1^+$ TAMs. Besides, the $C1QC^+$ TAMs and $SPP1^+$ TAMs could not be explained by the expression analyses based on genes associated with M1 and M2 TAMs in the colon cancer. The tumor angiogenesis, cell migration, ECM receptor interaction, and tumor vasculature pathways were enriched in $SPP1^+$ TAMs, whereas the complement activation and antigen processing and presentation pathways were significantly enriched in $C1QC^+$ TAMs. In addition, the combination of $C1QC^+$ and $SPP1^+$ TAMs gene signatures could separate patients from TCGA COAD and READ into subgroups of distinct prognosis. Based on that, patients with $C1QC^{high}$ and $SPP1^{low}$ TAMs gene signatures had the best prognosis, whereas patients with $C1QC^{low}$ and $SPP1^{high}$ TAMs gene signatures had the worst prognosis.

In different stages of cervical cancer, the phenotype of macrophages is constantly changing, which affects the ability of proliferation, invasion, and metastasis of cancer cells in many ways (14, 15). The number of TAMs in cervical lesion matrix changes with the progress of cervical cancer. However, whether TAMs in cervical cancer show as the M1 and M2 phenotypes or $C1QC^+$ and $SPP1^+$ TAMs phenotypes remains unknown. It is best to use the single cell sequencing technology to distinct subsets of TAMs of cervical cancer; however, there is no single cell sequencing database in cervical cancer to be used so far. However, we can use bulk transcriptome data of cervical patients from TCGA to evaluate the gene signatures of known TAMs subsets.

In this study, we compared the $C1QC^+$ and $SPP1^+$ TAMs gene signatures, as well as classic M1 and M2 gene signatures, using transcriptome data of TCGA cervical cancer patients. We aim to find the relationship between different TAMs gene signatures and clinical features and the mechanisms behind, which may provide suggestion to treatment of cervical cancer in clinic.

MATERIALS AND METHODS

Sources for Single Cell Data, Bulk RNA-Seq Data, and Immune Cell Infiltration Estimation of TCGA Samples

Processed single-cell data of colon cancer was obtained from Gene Expression Omnibus (GEO) (GSE146771) (10). While processed single-cell data of advanced basal cell carcinoma was obtained from GEO (GSE123814) (16).

Bulk RNA-seq gene expression data and clinical data of cervical cancer were downloaded from UCSC Xena (https://xenabrowser.net/datapages/). The bulk RNA-seq gene expressions were log2(TPM+1) transformed. Immune cell infiltration estimation of TCGA samples were downloaded from TIMER2.0 (http://timer.cistrome.org/), which included immune signatures of TCGA samples calculated using TIMER, CIBERSORT, and xCell (17). Tumor mutational burden (TMB) data of TCGA samples were obtained from Vésteinn et al.'s study (18).

Define $C1QC^+$ TAMs, $SPP1^+$ TAMs, and M1/M2 Gene Signatures

$C1QC^+$ TAMs and $SPP1^+$ TAMs gene signatures defined in Zhang et al.'s study were used in our paper (10). $C1QC^+$ TAMs gene signature include the following genes: C1QA, C1QB, ITM2B, C1QC, HLA-DMB, MS4A6A, CTSC, TBXAS1, TMEM176B, SYNGR2, ARHGDIB, TMEM176A, UCP2, CAPZB, MAF, TREM2, and MSR1, whereas $SPP1^+$ TAMs gene signature includes the following genes: SPP1, PCSK5, SLC11A1, VCAN, SLC25A37, FLNA, UPP1, BCL6, AQP9, TIMP1, VEGFA, ADM, MARCO, FN1, and IL1RN.

The M1/M2 gene signatures were obtained from Azizi et al.'s research (10, 11). Genes associated with "classically activated" (M1) macrophages include CCL5, CCR7, CD40, CD86, CXCL9, CXCL10, CXCL11, IDO1, IL1A, IL1B, IL6, IRF1, IRF5, and KYNU, while CCL4, CCL13, CCL18, CCL20, CCL22, CD276, CLEC7A, CTSA, CTSB, CTSC, CTSD, FN1, IL4R, IRF4, LYVE1, MMP9, MMP14, MMP19, MSR1, TGFB1, TGFB2, TGFB3, TNFSF8, TNFSF12, VEGFA, VEGFB, and VEGFC were used to define the signature of "alternatively activated" (M2) macrophages (10).

Single-Cell Data Analysis

Processed single-cell RNA-seq data were obtained as described above. The annotation information of cell types were included in the metadata as described by the original articles (10, 16). The Seurat v3 (version 3.2.2) R package was used to analyze the processed scRNA-seq data (19). The function AddModuleScore in Seurat was used to calculate C1QC$^+$ TAMs, SPP1$^+$ TAMs, and M1/M2 gene signatures using their gene sets, respectively.

TCGA Bulk RNA-Seq Data Analysis

For the bulk RNA-seq data of TCGA cervical cancer samples, the mean expression of genes in the given signatures (C1QC$^+$ TAMs, SPP1$^+$ TAMs, and M1/M2 gene signatures) were used as the signature scores. Also, the mean expression of given signatures was grouped into high and low expression groups by the 55th and 45th quantile values (10). Immune cell infiltration estimation of TCGA samples was visualized as heatmaps using the R package ComplexHeatmap (20). Immunotherapy responses were predicted by TIDE (Tumor Immune Dysfunction and Exclusion) as described in a previous study (21).

Gene Set Enrichment Analysis

Different gene expression between patients with C1QC^{high} and SPP1^{low} TAMs gene signatures and patients with C1QC^{low} and SPP1^{high} TAMs gene signatures were calculated with LIMMA (version 3.46.0) package. Sorted (by log fold change) different expression gene list was used to perform the gene set enrichment analysis (GSEA) by using clusterProfiler (version 3.18.0) package (22).

Statistical Analysis

Either Pearson's chi-square test or Fisher's exact test was used to assess the different clinicopathological factors according to the different C1QC$^+$ TAMs, SPP1$^+$ TAMs gene signatures groups. Wilcoxon signed-rank test was used to compare gene and gene signatures between different group of patients. Kaplan-Meier survival curves among different groups were plotted using R function ggsurvplot. Cox proportional hazards model implemented in the R package survival was used to find the predict factors of prognostic. All statistical analyses were performed using R (v4.0.3). All figures were plotted by using R. P values <0.05 were considered as statistically significant difference.

RESULTS

C1QC$^+$ TAMs and SPP1$^+$ TAMs Gene Signatures Can Divide TAMs Into Two Different Subsets in Colon Cancer and Advanced Basal Cell Carcinoma

In Lei's paper (10), they found that TAMs showed a remarkable dichotomy and could be marked as C1QC$^+$ TAMs and SPP1$^+$ TAMs. Also, the C1QC$^+$ TAMs and SPP1$^+$ TAMs were different from "classically activated" M1 and "alternatively activated" M2 macrophages. We used single-cell data from Lei's paper and found that C1QC$^+$ TAMs gene signature and SPP1$^+$ TAMs gene signatures have high expressions in two different TAMs subsets, respectively (**Figure 1**), whereas M1 and M2 gene signatures did not have high expressions in different subsets of TAMs (**Figure 1**). To validate if C1QC$^+$ TAMs and SPP1$^+$ TAMs gene signatures can work better than M1 and M2 signatures in other cancers, we also analyzed another single cell data of advanced basal cell carcinoma (BCC) (16). In the BCC data, C1QC$^+$ TAMs and SPP1$^+$ TAMs gene signatures, but not M1 and M2 gene signatures, can divide TAMs into two different subsets (**Figure S1**). It is worth mentioning that, in both single cell databases, both C1QC$^+$ TAMs and SPP1$^+$ TAMs gene signatures had the highest expression only in TAMs but not in other cell types (**Figures 1** and **S1**). These data indicated that at least in colon cancer and advanced basal cell carcinoma, C1QC$^+$ TAMs and SPP1$^+$ TAMs gene signatures are better separators than M1 and M2 gene signatures to divide TAMs into different subsets, which may represent different immune functions.

C1QC$^+$ TAMs and SPP1$^+$ TAMs Gene Signatures Can Divide Cervical Patients Into Different Prognostic and Clinical Subgroups

Because there is no single-cell database of cervical patients, it is unknown of separation of TAMs from cervical patients into two distinct subgroups based on the TAMs gene signatures. We speculate that if C1QC$^+$ TAMs and SPP1$^+$ TAMs gene signatures can divide TAMs of cervical cancer patients into two distinct functional subsets, patients with different levels of C1QC$^+$ TAMs and SPP1$^+$ TAMs gene signatures may have different clinical features. We calculated C1QC$^+$ TAMs and SPP1$^+$ TAMs gene signatures in cervical cancer patients and normal cervical tissue from TCGA and GTEX, respectively, using their transcriptome data (*Materials and Methods*). Consistent with results in single-cell level data (10), cervical cancer samples showed higher C1QC$^+$ TAMs gene signature than normal cervical tissues (**Figure 2A**). However, we did not find significant difference of SPP1$^+$ TAMs gene signature between normal cervical tissues and cervical cancer samples (**Figure 2B**). Besides, we found that patients with locally advanced cervical cancer (LACC, Stage IB2-IVA) have lower C1QC$^+$ TAMs signature and higher SPP1$^+$ TAMs gene signature compared with patients with early stage (stage I-IB1) cervical cancer (**Figures 2C, D**). Although patients with locally advanced cervical cancer and those with early stage cervical cancer have similar M1 and M2 gene signature levels (**Figures S2A, B**).

Next, we divided cervical patients into high and low groups by the 55th and 45th quantile values of C1QC$^+$ TAMs and SPP1$^+$ TAMs gene signatures, respectively, and further separated patients into four subgroups according to the C1QC$^+$ and SPP1$^+$ TAMs gene signatures levels. We found patients with C1QC^{high} and SPP1^{low} TAMs gene signatures have the best overall survival (OS) and disease specific survival (DSS) (**Figures 2E, F**), whereas patients with C1QC^{low} and SPP1^{high} TAMs gene signatures have the worst OS and DSS (**Figures 2E, F**). However, M1 and M2 gene signatures could not divide patients into distinct prognosis subgroups (**Figures S2C, D**). We also found that patients with C1QC^{high} and SPP1^{low} TAMs gene signatures have the lowest proportion (34.21%) of LACC, whereas patients with C1QC^{low}

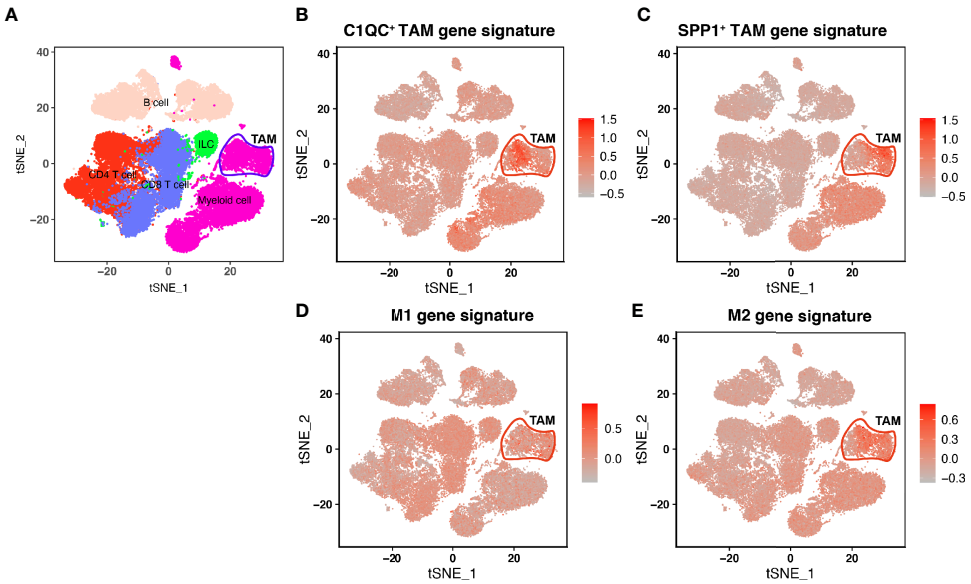

FIGURE 1 | Single-cell transcriptome profiling and TAM gene signatures of the Human CRC TME. **(A)** tSNE plot showing major immune cell subsets in human CRC TME. **(B)** tSNE plot of all immune cells colored by enrichment of C1QC^{+} TAM gene signatures. **(C)** tSNE plot of all immune cells colored by enrichment of SPP1^{+} TAM gene signatures. **(D)** tSNE plot of all immune cells colored by enrichment of M1 gene signatures. **(E)** tSNE plot of all immune cells colored by enrichment of M2 gene signatures.

and SPP1^{high} TAMs gene signature have the highest proportion (71.79%) of LACC (**Figure 2G**). When comparing clinical features between these two groups, patients with C1QC^{low} and SPP1^{high} TAMs gene signatures had later FIGO stages, more positive pathologic lymph node, higher mortality, and higher proportion of patients developed with disease (**Table 1**). There was no significant difference of histological grade, lymphovascular invasion indicator, tumor status, and metastasis between patients with C1QC^{high} and SPP1^{low} TAMs gene signatures and those with C1QC^{low} and SPP1^{high} TAMs gene signatures (**Table 1**). Besides, after adjusting by age and FIGO stage, the C1QC^{low} and SPP1^{high} TAMs gene signatures showed as an independent predict factor to worse OS (**Table 2**). Although advanced FIGO stage (IB2-IVA) is correlated with C1QC^{low} and SPP1^{high} TAMs gene signatures (**Table 1**), it was not associated with worse prognosis (P = 0.793, **Table 2**). These results suggested that C1QC^{+} and SPP1^{+} TAMs gene signatures could provide additional information besides clinicopathological factors to find cervical patients with different clinical outcome and prognosis.

C1QC^{+} TAMs and SPP1^{+} TAMs Gene Signatures Divide Cervical Patients Into Subgroups With Different Immune States

The abundance of different TAM subtypes could have an impact on other immune cells infiltration and disease outcome in patients (6). We compared the immune cell infiltration by using cell type scores calculated by TIMER. Patients with C1QC^{high} and SPP1^{low} TAMs gene signatures had the highest immune cell infiltration, whereas patients with C1QC^{low} and SPP1^{high} TAMs gene signatures had the lowest immune cell infiltration (**Figure 3A**). Also, we found patients with C1QC^{high} and SPP1^{low} TAMs gene signatures had significantly higher CD8 T cell and CD4 T cell infiltration level than patients with C1QC^{low} and SPP1^{high} TAMs gene signatures (**Figure 3B**). The macrophages infiltration level did not show significant difference between patients with C1QC^{high} and SPP1^{low} TAMs gene signatures and patients with C1QC^{low} and SPP1^{high} TAMs gene signatures (**Figure 3B**). This may suggest that it is the different ratio of C1QC^{+} and SPP1^{+} TAMs, but not the TAMs amount, impacts the TME. We also used immune cells infiltration scores calculated by XCELL and CIBERSORT to perform the same analysis, and we found similar results (**Figures S3A, B**). "Hot tumors" which had higher T-cell immune infiltration was reported to have higher response rates to immune checkpoint inhibitors (ICIs) immunotherapies compared with "cold tumors," which had lower T-cell immune infiltration (23). PD1, PD-L, and tumor mutational burden (TMB) were also reported to be associated with response to ICIs immunotherapy (24). We found that patients with C1QC^{high} TAMs gene signatures had higher PD1 and PD-L1 expression than those with C1QC^{low} TAMs gene signatures (**Figures 3C, D**), and patients with C1QC^{high} and SPP1^{low} TAMs gene signature had the highest PD1 expression compared with the other three subgroups (**Figure 3C**). Also, we found that patients with C1QC^{high} and SPP1^{low} TAMs gene signatures had lowest TMB, whereas patients with C1QC^{low} and SPP1^{high} TAMs gene signatures had highest TMB, although the difference was not significant (**Figure 3E**). Microsatellite instability (MSI) is genetic instability in short nucleotide repeats (microsatellites) because of a high mutation rate resulted in abnormal DNA mismatch repair (25).

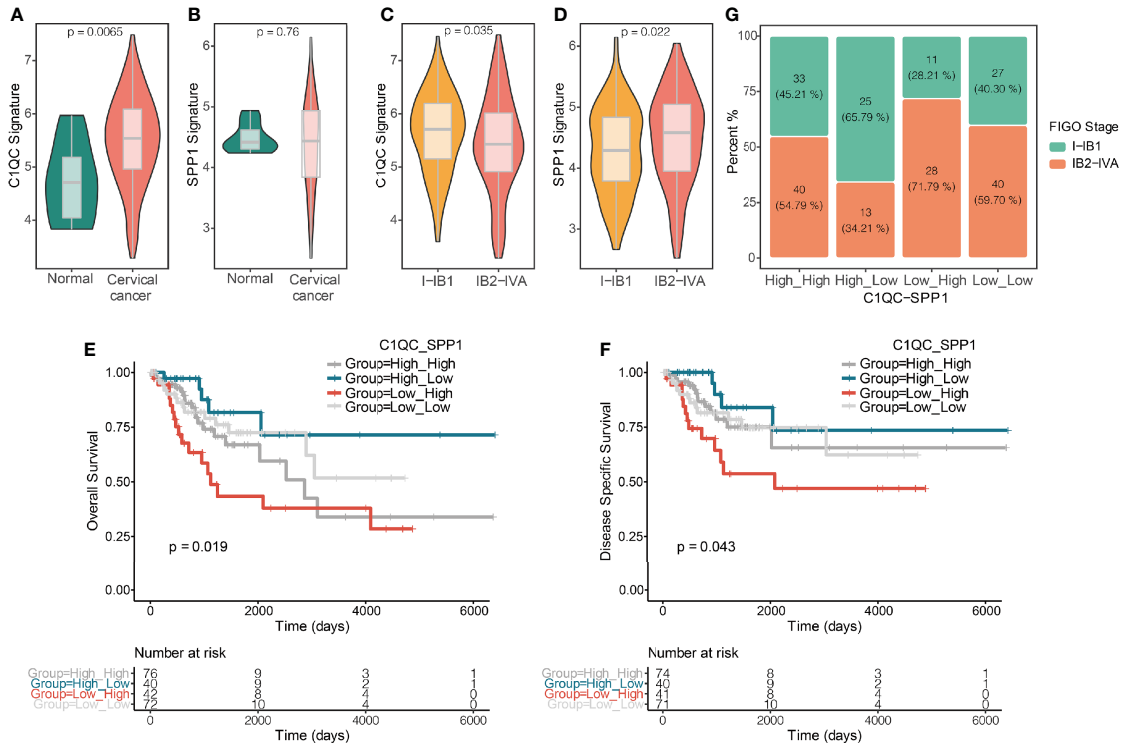

FIGURE 2 | C1QC+ and SPP1+ TAMs gene signatures in TCGA cervical cancer patients. **(A)** Violin plots showing comparison of C1QC$^+$ TAM gene signatures levels between normal and cervical cancer samples in TCGA. Two-sided Wilcoxon test. **(B)** Violin plots showing comparison of SPP1$^+$ TAM gene signatures levels between normal and cervical cancer samples in TCGA. Two-sided Wilcoxon test. **(C)** Violin plots showing comparison of C1QC$^+$ TAM gene signatures levels between patients with FIGO stage 1-IB1 and patients with FIGO stage IB2-IVA in TCGA. Two-sided Wilcoxon test. **(D)** Violin plots showing comparison of SPP1$^+$ TAM gene signatures levels between patients with FIGO stage 1-IB1 and patients with FIGO stage IB2-IVA in TCGA. Two-sided Wilcoxon test. **(E)** The Kaplan-Meier overall survival curves of TCGA cervical cancer patients grouped by the gene signature expression of C1QC$^+$ TAM and SPP1$^+$ TAM. **(F)** The Kaplan-Meier Disease specific survival curves of TCGA cervical cancer patients grouped by the gene signature expression of C1QC$^+$ TAM and SPP1$^+$ TAM. **(G)** Proportions of patients with FIGO stage I-IB1 and IB2-IVA in cervical cancer patients grouped by the gene signature expression of C1QC$^+$ TAM and SPP1$^+$ TAM.

Tumors with MSI-H exhibit a high mutation rate and neoantigen load that is positively associated with overall lymphocytic infiltration. The tumor-infiltrating lymphocytes, T helper 1 cells and memory T cells, will ultimately trigger an effective antitumor immune response (26–28). MSI only exists in a small subset of cervical cancer patients (29). We found that patients with C1QC^{high} and SPP1^{low} TAMs gene signatures had higher proportion of MSI-H than patients with C1QC^{low} and SPP1^{high} TAMs gene signatures (**Figure 3F**). All these results suggest that patients could be divided into subgroups based on the C1QC$^+$ and SPP1$^+$ TAMs gene signatures. This distinction is associated with different genomic status, immune cell infiltration, and finally different prognosis, which implies that different ratios of C1QC$^+$ and SPP1$^+$ TAMs subsets may impact TME state.

Different Pathways Involved in Different C1QC$^+$ and SPP1$^+$ TAMs Gene Signatures Subgroups

To figure out if some special pathways involved in different subsets divided by C1QC$^+$ and SPP1$^+$ TAMs gene signatures, we compared transcriptome data of patients with C1QC^{high} and SPP1^{low} TAMs gene signatures to that of patients with C1QC^{low} and SPP1^{high} TAMs gene signatures. Gene set enrichment analysis (GSEA) was used to detect pathways enriched in different groups. C1QC^{high} and SPP1^{low} TAMs gene signatures group exhibited enrichment of TCR signaling and interferon gamma signaling (**Figure 4**), suggesting the anti-tumor functions in these patients. While C1QC^{low} and SPP1^{high} TAMs gene signatures group exhibited TGFb associated pathways, extracellular matrix organization, and keratinization pathway (**Figure 4**), suggesting the pro-tumorigenic functions in these patients. The GSEA results suggested that subgroups of patients divided by C1QC$^+$ and SPP1$^+$ TAMs gene signatures showed different anti- or pro-tumor states.

Different C1QC$^+$ and SPP1$^+$ TAMs Gene Signatures Subgroups Showed Variable ICMs Expression and Immunotherapy Response

The expressions of ICMs were associated with checkpoint inhibitor immunotherapy response (30, 31). Many ICMs, such as PD1, CTLA4, IDO1, and HAVCR2, were used as the

TABLE 1 | Clinicopathological factors of cervical cancer patients from TCGA.

	Overall (N=82)	C1QC^{+}-SPP1^{+} TAMs gene signatures		P-value
		High_Low (N=40)	Low_High (N=42)	
Age, years				
Mean (SD)	46.0 (13.0)	46.9 (12.9)	45.2 (13.3)	0.567
Median [Min, Max]	44.5 [21.0, 79.0]	44.5 [25.0, 75.0]	44.5 [21.0, 79.0]	
FIGO Stage				
I-IB1	36 (43.9%)	25 (62.5%)	11 (26.2%)	0.002
IB2-IVA	41 (50.0%)	13 (32.5%)	28 (66.7%)	
Missing	5 (6.1%)	2 (5.0%)	3 (7.1%)	
Histological type				
Adenosquamous	1 (1.2%)	1 (2.5%)	0 (0%)	0.400
Cervical squamous cell carcinoma	69 (84.1%)	31 (77.5%)	38 (90.5%)	
Endocervical adenocarcinoma of the usual type	3 (3.7%)	1 (2.5%)	2 (4.8%)	
Endocervical type of adenocarcinoma	5 (6.1%)	4 (10.0%)	1 (2.4%)	
Endometrioid adenocarcinoma of endocervix	1 (1.2%)	1 (2.5%)	0 (0%)	
Mucinous adenocarcinoma of endocervical type	3 (3.7%)	2 (5.0%)	1 (2.4%)	
Histological grade				
G1	5 (6.1%)	2 (5.0%)	3 (7.1%)	0.981
G2	34 (41.5%)	17 (42.5%)	17 (40.5%)	
G3	37 (45.1%)	18 (45.0%)	19 (45.2%)	
GX	6 (7.3%)	3 (7.5%)	3 (7.1%)	
Lymphovascular invasion indicator				
Absent	20 (24.4%)	15 (37.5%)	5 (11.9%)	0.126
Present	25 (30.5%)	12 (30.0%)	13 (31.0%)	
Missing	37 (45.1%)	13 (32.5%)	24 (57.1%)	
Tumor status				
Tumor free	55 (67.1%)	31 (77.5%)	24 (57.1%)	0.112
With tumor	26 (31.7%)	9 (22.5%)	17 (40.5%)	
Missing	1 (1.2%)	0 (0%)	1 (2.4%)	
Metastasis				
No	76 (92.7%)	38 (95.0%)	38 (90.5%)	0.717
Yes	6 (7.3%)	2 (5.0%)	4 (9.5%)	
Pathologic M				
M0	30 (36.6%)	19 (47.5%)	11 (26.2%)	0.262
M1	2 (2.4%)	2 (5.0%)	0 (0%)	
MX	34 (41.5%)	17 (42.5%)	17 (40.5%)	
Missing	16 (19.5%)	2 (5.0%)	14 (33.3%)	
Pathologic N				
N0	40 (48.8%)	30 (75.0%)	10 (23.8%)	0.002
N1	18 (22.0%)	5 (12.5%)	13 (31.0%)	
NX	10 (12.2%)	4 (10.0%)	6 (14.3%)	
Missing	14 (17.1%)	1 (2.5%)	13 (31.0%)	
OS				
No	60 (73.2%)	35 (87.5%)	25 (59.5%)	0.009
Yes	22 (26.8%)	5 (12.5%)	17 (40.5%)	
DSS				
No	64 (78.0%)	36 (90.0%)	28 (66.7%)	0.034
Yes	17 (20.7%)	4 (10.0%)	13 (31.0%)	
Missing	1 (1.2%)	0 (0%)	1 (2.4%)	
DFI				
No	38 (46.3%)	26 (65.0%)	12 (28.6%)	0.900
Yes	10 (12.2%)	6 (15.0%)	4 (9.5%)	
Missing	34 (41.5%)	8 (20.0%)	26 (61.9%)	
PFI				
No	60 (73.2%)	31 (77.5%)	29 (69.0%)	0.539
Yes	22 (26.8%)	9 (22.5%)	13 (31.0%)	
Treatment				
Radical surgery	24 (29.3%)	14 (35.0%)	10 (23.8%)	0.771
Radical surgery and radiotherapy, or concurrent chemoradiation	23 (28.0%)	12 (30.0%)	11 (26.2%)	
Radiotherapy	17 (20.7%)	8 (20.0%)	9 (21.4%)	
Other	18 (22.0%)	6 (15.0%)	12 (28.6%)	

TAMs, tumor-associated macrophages; High_Low, C1QC^{high} and SPP1^{low} TAMs gene signatures group; Low_High, C1QC^{low} and SPP1^{high} TAMs gene signatures group; SD, standard deviation; FIGO, International Federation of Gynecology and Obstetrics; OS, overall survival; DSS, disease-specific survival; DFI, disease-free interval; PFI, progression-free interval.

TABLE 2 | Prognostic values of clinical factors and C1QC+ and SPP1+ TAMs gene signatures in cervical cancer.

	Overall	HR (univariable)		HR (multivariable)|	
	(n=75)	HR (95% CI)	P	HR (95% CI)	P
Age, years					
Mean (SD)	46	1.03 (1.00–1.07)	0.067	1.06 (0.99–1.12)	0.078
FIGO stage					
I-IB1	36				
IB2-IVA	41	1.95 (0.79–4.79)	0.146	1.20 (0.30–4.77)	0.793
Histological type					
SCC	69				
AS	1	NA	NA	NA	NA
Other	12	0.24 (0.03–1.76)	0.159	0.37 (0.03–4.03)	0.416
Histological grade					
G1	5				
G2	34	0.53 (0.07–4.33)	0.554	0.08 (0.00–1.28),	0.074
G3	37	0.90 (0.11–7.21)	0.924	0.03 (0.00–0.91)	0.044
GX	6	4.78 (0.51–45.22)	0.172	0.39 (0.01–12.22)	0.595
Pathologic M					
M0	30				
M1	2	2.88 (0.35–23.84)	0.327	NA	NA
MX	34	0.71 (0.26–1.97)	0.514	0.10 (0.01–1.10)	0.059
Pathologic N					
N0	40				
N1	18	2.76 (0.84–9.07)	0.094	0.98 (0.20–4.76)	0.981
NX	10	5.48 (1.52–19.76)	0.009	4.91 (0.35–69.22)	0.238
C1QC_SPP1					
High_Low	40				
Low_High	42	4.08 (1.50–11.09)	0.006	8.40 (1.33–52.94)	0.023

TAMs, tumor-associated macrophages; HR, hazard ratio; CI, confidence interval; SD, standard deviation; FIGO, International Federation of Gynecology and Obstetrics; SCC, squamous cell carcinoma; AS, adenosquamous cell carcinoma; C1QC_SPP1, C1QC$^+$ and SPP1$^+$ TAMs gene signatures; High_Low, C1QC^{high} and SPP1^{low} TAMs gene signatures; Low_High, C1QC^{low} and SPP1^{high} TAMs gene signatures.
NA, Not available.

immunotherapy targets in the clinical trials (30). We compared most ICM expression among different C1QC$^+$ and SPP1$^+$ TAMs gene signatures subgroups. Most (19/25) of the ICMs express higher in patients with C1QC^{high} TAMs gene signatures compared with patients with C1QC^{low} TAMs gene signatures (**Figure 5**). Also, we found that patients with C1QC^{high} and SPP1^{low} TAMs gene signatures had the highest expression of some ICMs (CD40LG, ADORA2A, CTLA4, IL2, LAG3, PDCD1, and TIGIT) compared with the other three subgroups (**Figure 5**), which means these patients may benefit more from ICI immunotherapy. Also, we also notice that the patients with C1QC^{high} and SPP1^{low} TAMs gene signatures showed best OS and DSS (**Figures 2E, F**). We used TIDE (21) to predict response to immunotherapy and found that patients with C1QC^{high} TAMs gene signatures had higher immunotherapy response ratio than those with C1QC^{low} TAMs gene signatures. Patients with C1QC^{low} and SPP1^{high} TAMs gene signatures had the lowest ratio of response to immunotherapy (**Figure S4**). These results suggest that the C1QC$^+$ and SPP1$^+$ TAMs gene signatures may be used to select cervical cancer patients who will benefit more from ICI immunotherapy.

DISCUSSION

The development of cervical cancer is reportedly associated with human papillomavirus (HPV) infection, especially HPV intergation (32, 33). On the other hand, immune system defects play a significant role in cancer progress, It is believed that HPV infection triggers a primarily cell-mediated immune response (34, 35). Macrophage percentage was reported to increase linearly with neoplasia progression (36). Some studies showed that higher FIGO stage and lymph node metastasis or lymphangiogenesis usually showed larger counts of M2 macrophages, which were usually associated with poor prognosis (34). However, TAMs are of high heterogeneity, which contain various subsets with different functions. TAMs in different tumors also show different subsets (11, 12). In this study, we evaluated the "traditional" M1/M2 gene signatures and the C1QC$^+$ and SPP1$^+$ TAMs gene signatures in cervical cancer. We found that C1QC$^+$ and SPP1$^+$ TAMs gene signatures were more suitable to divide cervical patients into subgroups with distinct clinical outcomes than M1/M2 gene signatures. Our research has three important implications for understanding the role of TAM cells in cervical cancer immunity.

First, we found that C1QC$^+$ and SPP1$^+$ TAMs gene signatures, but not M1 and M2 gene signatures, could clearly divided TAMs into two subsets in a colon cancer data set and an advanced basal cell carcinoma data set at single cell level. Although we did not have single cell level data to show subsets of TAMs in cervical cancer, we showed that, by using bulk RNA-seq data of cervical cancer from TCGA, C1QC$^+$ and SPP1$^+$ TAMs gene signatures, but not M1 and M2 gene signatures, could divide cervical cancer patients into subgroups with

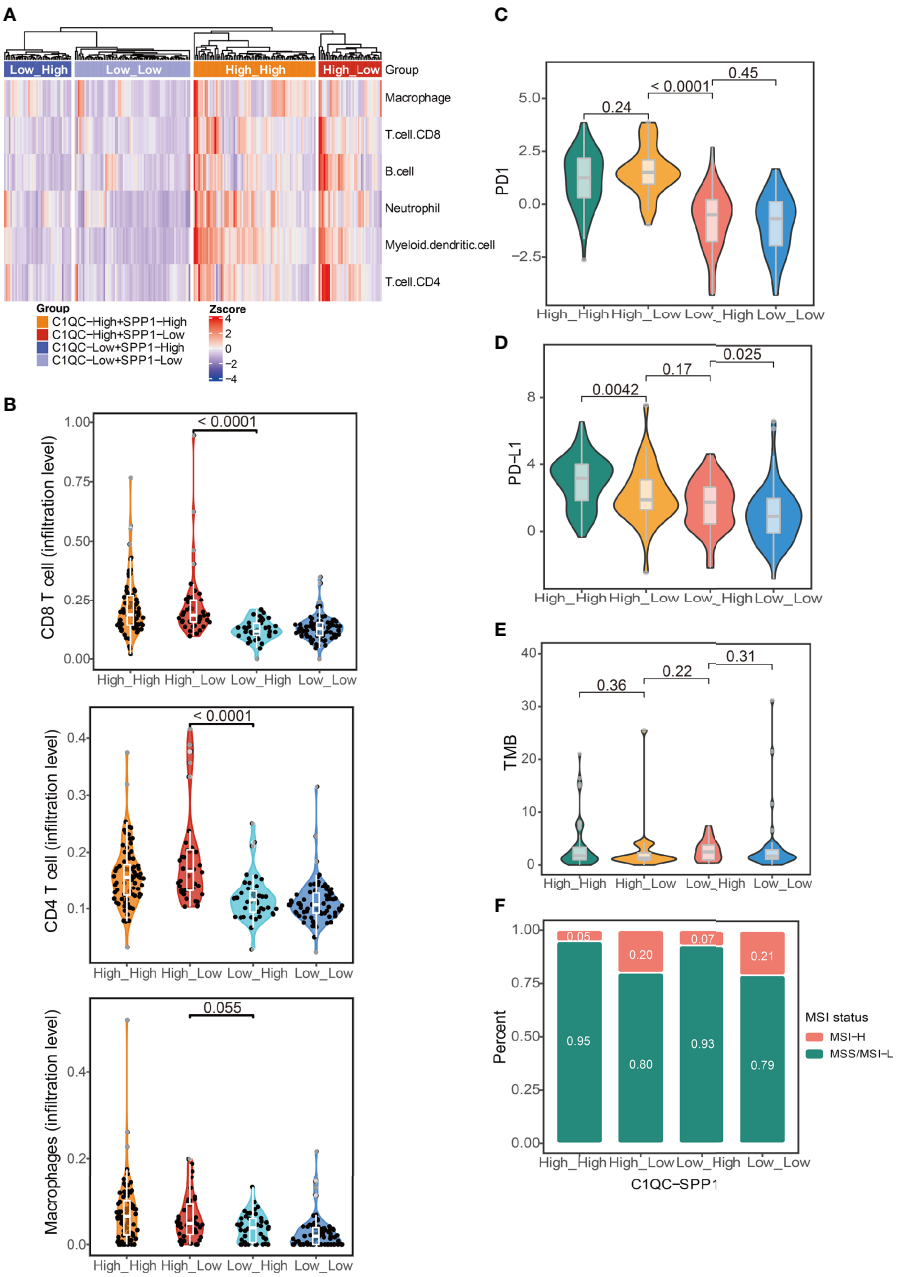

FIGURE 3 | Immune characteristics in different groups of TCGA cervical cancer patients. **(A)** Heatmap showing immune cell signatures by TIMER in cervical cancer patients grouped by the gene signature expression of C1QC$^+$ TAM and SPP1$^+$ TAM. **(B)** Violin plots showing comparison of CD8 T cell, CD4 T cell, and macrophages gene signatures among cervical cancer patients grouped by the gene signature expression of C1QC$^+$ TAM and SPP1$^+$ TAM. Two-sided Wilcoxon test. **(C)** Violin plots showing comparison of PD1 gene expression among cervical cancer patients grouped by the gene signature expression of C1QC$^+$ TAM and SPP1$^+$ TAM. Two-sided Wilcoxon test. **(D)** Violin plots showing comparison of PD-L1 gene expression among cervical cancer patients grouped by the gene signature expression of C1QC$^+$ TAM and SPP1$^+$ TAM. Two-sided Wilcoxon test. **(E)** Violin plots showing comparison of TMB among cervical cancer patients grouped by the gene signature expression of C1QC$^+$ TAM and SPP1$^+$ TAM. Two-sided Wilcoxon test. **(F)** Proportions of patients with MSI-H and MSS/MSI-L state in cervical cancer patients grouped by the gene signature expression of C1QC$^+$ TAM and SPP1$^+$ TAM.

different prognosis and different tumor stages. Patients with the C1QC^{high} and SPP1^{low} TAMs gene signatures had the lowest ratio of local advanced FIGO stages, whereas patients with the C1QC^{low} and SPP1^{high} TAMs gene signatures had the highest ratio of local advanced FIGO stages. C1QC$^+$ and SPP1$^+$ TAMs gene signatures were obtained from TAMs; however, they could significantly divide patients into subgroups with distinct clinical outcomes, implying the importance of TAMs in the development

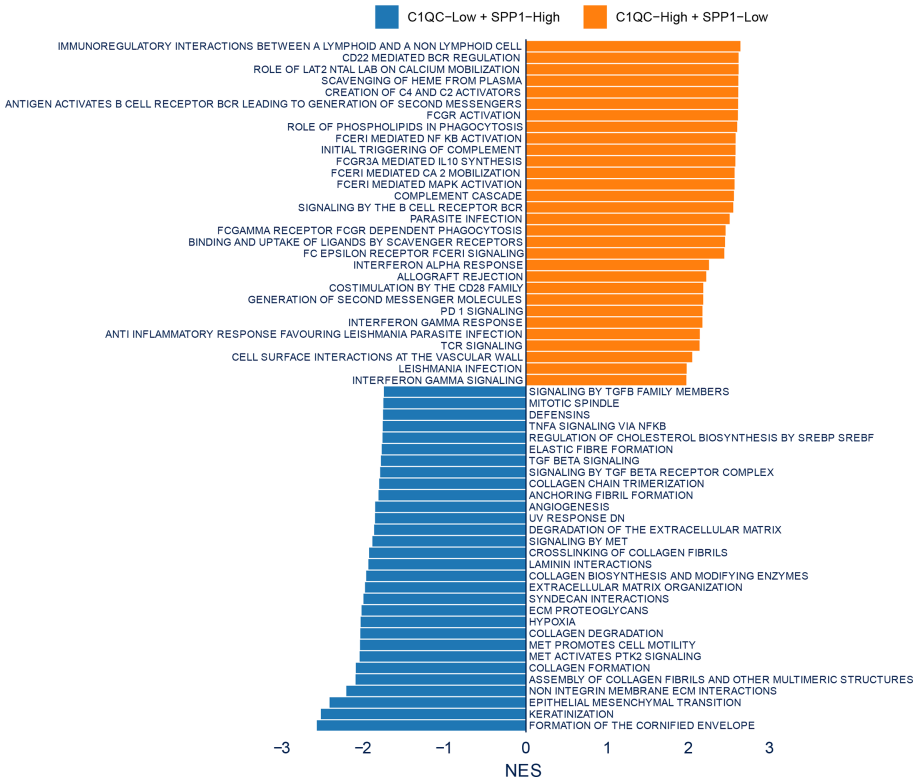

FIGURE 4 | Enrichment plots from gene set enrichment analysis (GSEA). Differential pathway enriched in C1QC^{low} + SPP1^{high} TAMs gene signatures group and C1QC^{high} + SPP1^{low} TAMs gene signatures group.

of cervical cancer. Further studies are needed to figure out how the TAMs affect cervical cancer development.

Second, cervical cancer subgroups divided by C1QC^{+} and SPP1^{+} TAMs gene signatures showed different immune cell infiltration, with the C1QC^{high} and SPP1^{low} groups have the highest immune cell infiltration, whereas the C1QC^{low} and SPP1^{high} groups had the lowest immune cell infiltration. It was reported that "hot tumors" (with more T cell infiltration) had higher antitumor ability and were more responsive to immunotherapy than "cold tumors" (with none or few T cell infiltration) (37). In our study, we found that patients of the C1QC^{high} and SPP1^{low} group, which had the highest T-cell infiltration, showed the best prognosis, whereas patients of the C1QC^{low} and SPP1^{high} group, which had the lowest T cell infiltration, showed the worst prognosis. Patients with different C1QC^{+} and SPP1^{+} TAMs gene signature patterns showed different T-cell infiltration, implying the effect of TAMs to T cell infiltration. The mechanism behind this phenomenon needs further research.

Finally, we found that many of the immune checkpoint molecules (ICMs) expressed differently in different C1QC^{+} and SPP1^{+} TAMs gene signature subgroups. Generally, patients with C1QC^{high} TAMs gene signatures have higher immunotherapy checkpoint genes expression than those with C1QC^{low} TAMs gene signatures. Since 2015, Clinical trials on different ICIs have been carried out for cervical cancer (38). However, the evidence is still limited to prove the correlation between ICMs and effects of immunotherapy (39, 40). With more clinical research conducted for cervical cancer, our findings may provide valuable information for them.

As mentioned above, our current study is based on TCGA bulk RNA-seq data, which inevitably has some limitations and needs further verification. Therefore, we are now working to verify the gene signatures of C1QC^{+} and SPP1^{+} TAMs in the clinical specimens of patients with cervical cancer at different clinical stages by utilizing single-cell sequencing technology. We believe that the combination of bulk RNA-seq and single-cell sequencing data will help us confirm the gene signatures of C1QC^{+} and SPP1^{+} TAMs in the cervical cancer microenvironment and signaling pathways, which may activate or inactivate in different TAMs subsets. RT-qPCR, FACS, and even IHC could also be used to identify the gene signatures in a large scale of clinical or animal model specimens. It is important to determine the role of C1QC^{+} and SPP1^{+} TAMs subsets in cervical cancer evolution and progression, and some ongoing experiments are in process. It is reported that there are crosstalks between TAMs and T cells, TAMs, and tumor cells. TAMs may interact with CD8^{+} T cells and tumor cells through receptor-ligand pairs, such as SPP1-CD44 (41). The crosstalks between TAMs and CD8^{+} T cells/tumor cells may be validated by using multiplex imaging analysis (41).

In conclusion, C1QC^{+} and SPP1^{+} TAMs gene signatures derived from TAMs can divide cervical patients into subgroups

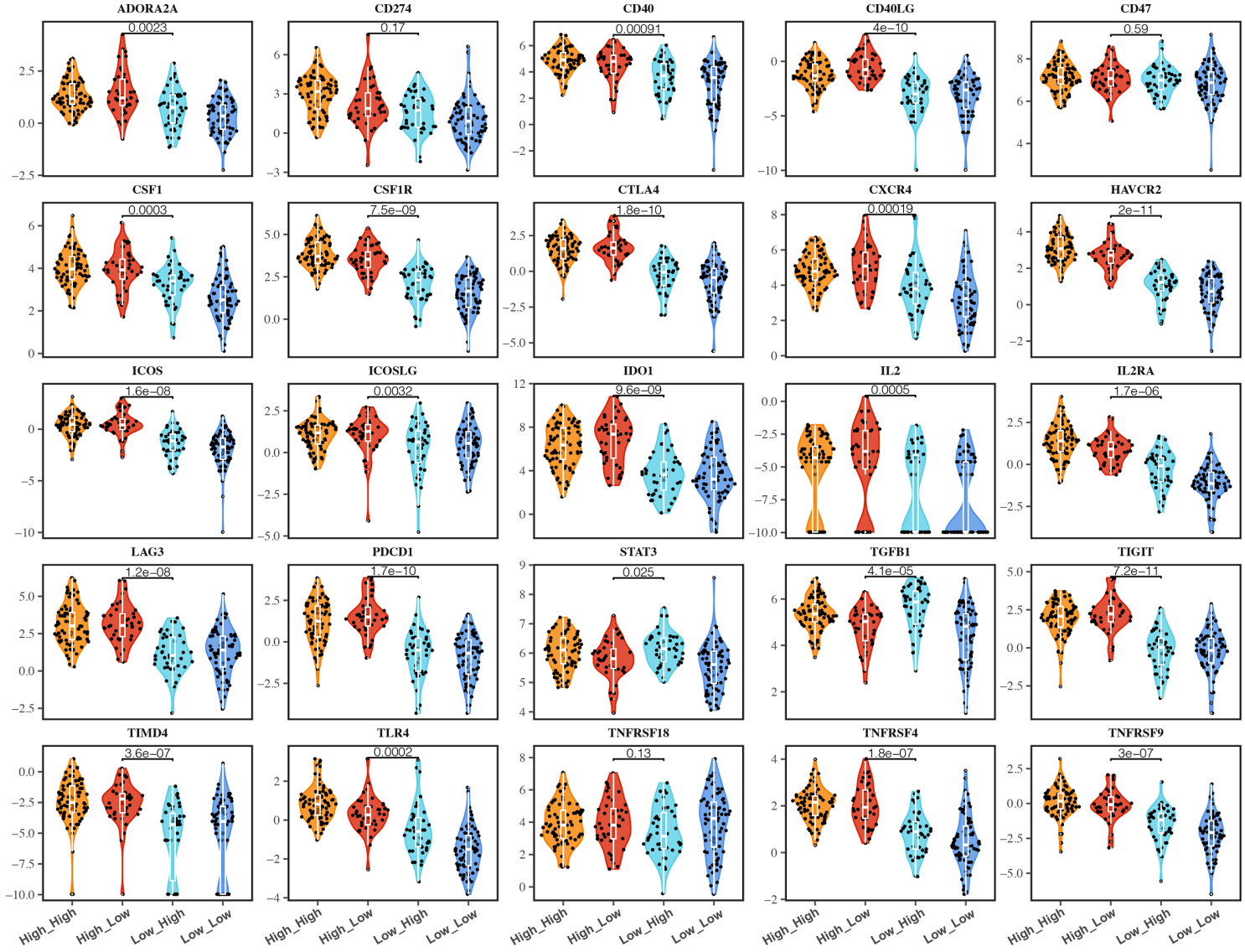

FIGURE 5 | Immune checkpoint molecules (ICMs) expressions in different groups of TCGA cervical cancer patients. Violin plots showing comparison of ICMs expressions among cervical cancer patients grouped by the gene signature expression of C1QC^{+} TAM and SPP1^{+} TAM.

with different prognosis and tumor stage, which may due to different immune cell infiltration. Our findings may help to find suitable treatment strategy for different subgroups of cervical cancer patients.

DATA AVAILABILITY STATEMENT

The original contributions presented in the study are included in the article/**Supplementary Material**. Further inquiries can be directed to the corresponding author.

AUTHOR CONTRIBUTIONS

XL, QZ, GC, and DL designed the study. XL and DL analyzed, interpreted data, and wrote the paper. All authors contributed to the article and approved the submitted version.

FUNDING

This work was supported by the National Natural Science Foundation of China (81902653, 81472783, 81472444, 81202061), and Wuhan Municipal health Commission (WX18Q16).

ACKNOWLEDGMENTS

We thank all participants recruited for this study.

SUPPLEMENTARY MATERIAL

The Supplementary Material for this article can be found online at: https://www.frontiersin.org/articles/10.3389/fimmu.2021.694801/full#supplementary-material

Supplementary Figure 1 | Single-cell transcriptome profiling and TAM gene signatures of the Human BCC TME. **(A)** UMAP plot showing major immune cell subsets in human BCC TME. **(B)** UMAP plot of all immune cells colored by enrichment of C1QC$^+$ TAM gene signatures. **(C)** UMAP plot of all immune cells colored by enrichment of SPP1$^+$ TAM gene signatures. **(D)** UMAP plot of all immune cells colored by enrichment of M1 gene signatures. **(E)** UMAP plot of all immune cells colored by enrichment of M2 gene signatures.

Supplementary Figure 2 | M1 and M2 gene signatures in TCGA cervical cancer patients. **(A)** Violin plots showing comparison of M1 gene signatures levels between patients with FIGO stage 1-IB1 and patients with FIGO stage IB2-IVA in TCGA. Two-sided Wilcoxon test. **(B)** Violin plots showing comparison of M2 gene signatures levels between patients with FIGO stage 1-IB1 and patients with FIGO stage IB2-IVA in TCGA. Two-sided Wilcoxon test. **(C)** The Kaplan-Meier overall survival curves of TCGA cervical cancer patients grouped by the gene signature expression of M1 and M2. **(D)** The Kaplan-Meier Disease specific survival curves of TCGA cervical cancer patients grouped by the gene signature expression of M1 and M2.

Supplementary Figure 3 | Heatmaps of immune cell infiltration in different groups of TCGA cervical cancer patients. **(A)** Heatmap showing immune cell signatures by XCELL in cervical cancer patients grouped by the gene signature expression of C1QC$^+$ TAM and SPP1$^+$ TAM. **(B)** Heatmap showing immune cell signatures by CIBERSORT in cervical cancer patients grouped by the gene signature expression of C1QC$^+$ TAM and SPP1$^+$ TAM.

Supplementary Figure 4 | Immunotherapy responses predicted by TIDE in TCGA cervical cancer patients. Immunotherapy responses were predicted by TIDE in cervical cancer patients grouped by the gene signature expression of C1QC$^+$ TAM and SPP1$^+$ TAM.

REFERENCES

1. Torre LA, Bray F, Siegel RL, Ferlay J, Lortet-Tieulent J, Jemal A. Global Cancer Statistics, 2012. *CA Cancer J Clin* (2015) 65:87–108. doi: 10.3322/caac.21262
2. Fokdal L, Sturdza A, Mazeron R, Haie-Meder C, Tan LT, Gillham C, et al. Image Guided Adaptive Brachytherapy With Combined Intracavitary and Interstitial Technique Improves the Therapeutic Ratio in Locally Advanced Cervical Cancer: Analysis From the retroEMBRACE Study. *Radiother Oncol* (2016) 120:434–40. doi: 10.1016/j.radonc.2016.03.020
3. Rosen VM, Guerra I, McCormack M, Nogueira-Rodrigues A, Sasse A, Munk VC, et al. Systematic Review and Network Meta-Analysis of Bevacizumab Plus First-Line Topotecan-Paclitaxel or Cisplatin-Paclitaxel Versus Non-Bevacizumab-Containing Therapies in Persistent, Recurrent, or Metastatic Cervical Cancer. *Int J Gynecol Cancer* (2017) 27:1237–46. doi: 10.1097/IGC.0000000000001000
4. Alley EW, Lopez J, Santoro A, Morosky A, Saraf S, Piperdi B, et al. Clinical Safety and Activity of Pembrolizumab in Patients With Malignant Pleural Mesothelioma (KEYNOTE-028): Preliminary Results From a Non-Randomised, Open-Label, Phase 1b Trial. *Lancet Oncol* (2017) 18:623–30. doi: 10.1016/S1470-2045(17)30169-9
5. Borcoman E, Le Tourneau C. Keynote-158 Study, FDA Granted Accelerated Approval of Pembrolizumab for the Treatment of Patients With Advanced PD-L1-Positive Cervical Cancer. *Ann Transl Med* (2020) 8:1611. doi: 10.21037/atm-20-2656
6. Vitale I, Manic G, Coussens LM, Kroemer G, Galluzzi L. Macrophages and Metabolism in the Tumor Microenvironment. *Cell Metab* (2019) 30:36–50. doi: 10.1016/j.cmet.2019.06.001
7. Salmaninejad A, Valilou SF, Soltani A, Ahmadi S, Abarghan YJ, Rosengren RJ, et al. Tumor-Associated Macrophages: Role in Cancer Development and Therapeutic Implications. *Cell Oncol (Dordr)* (2019) 42:591–608. doi: 10.1007/s13402-019-00453-z
8. Cassetta L, Fragkogianni S, Sims AH, Swierczak A, Forrester LM, Zhang H, et al. Human Tumor-Associated Macrophage and Monocyte Transcriptional Landscapes Reveal Cancer-Specific Reprogramming, Biomarkers, and Therapeutic Targets. *Cancer Cell* (2019) 35:588–602.e510. doi: 10.1016/j.ccell.2019.02.009
9. Chevrier S, Levine JH, Zanotelli VRT, Silina K, Schulz D, Bacac M, et al. An Immune Atlas of Clear Cell Renal Cell Carcinoma. *Cell* (2017) 169:736–49.e718. doi: 10.1016/j.cell.2017.04.016
10. Zhang L, Li Z, Skrzypczynska KM, Fang Q, Zhang W, O'Brien SA, et al. Single-Cell Analyses Inform Mechanisms of Myeloid-Targeted Therapies in Colon Cancer. *Cell* (2020) 181:442–59.e429. doi: 10.1016/j.cell.2020.03.048
11. Azizi E, Carr AJ, Plitas G, Cornish AE, Konopacki C, Prabhakaran S, et al. Single-Cell Map of Diverse Immune Phenotypes in the Breast Tumor Microenvironment. *Cell* (2018) 174:1293–308.e1236. doi: 10.1016/j.cell.2018.05.060
12. Lambrechts D, Wauters E, Boeckx B, Aibar S, Nittner D, Burton O, et al. Phenotype Molding of Stromal Cells in the Lung Tumor Microenvironment. *Nat Med* (2018) 24:1277–89. doi: 10.1038/s41591-018-0096-5
13. Cassetta L, Pollard JW. Targeting Macrophages: Therapeutic Approaches in Cancer. *Nat Rev Drug Discov* (2018) 17:887–904. doi: 10.1038/nrd.2018.169
14. Liu Y, Li L, Li Y, Zhao X. Research Progress on Tumor-Associated Macrophages and Inflammation in Cervical Cancer. *BioMed Res Int* (2020) 2020:6842963. doi: 10.1155/2020/6842963
15. Ding H, Cai J, Mao M, Fang Y, Huang Z, Jia J, et al. Tumor-Associated Macrophages Induce Lymphangiogenesis in Cervical Cancer *via* Interaction With Tumor Cells. *APMIS* (2014) 122:1059–69. doi: 10.1111/apm.12257

16. Yost KE, Satpathy AT, Wells DK, Qi Y, Wang C, Kageyama R, et al. Clonal Replacement of Tumor-Specific T Cells Following PD-1 Blockade. *Nat Med* (2019) 25:1251–9. doi: 10.1038/s41591-019-0522-3
17. Sturm G, Finotello F, Petitprez F, Zhang JD, Baumbach J, Fridman WH, et al. Comprehensive Evaluation of Transcriptome-Based Cell-Type Quantification Methods for Immuno-Oncology. *Bioinformatics* (2019) 35:i436–45. doi: 10.1093/bioinformatics/btz363
18. Thorsson V, Gibbs DL, Brown SD, Wolf D, Bortone DS, Ou Yang TH, et al. The Immune Landscape of Cancer. *Immunity* (2018) 48:812–30.e814. doi: 10.1016/j.immuni.2018.03.023
19. Butler A, Hoffman P, Smibert P, Papalexi E, Satija R. Integrating Single-Cell Transcriptomic Data Across Different Conditions, Technologies, and Species. *Nat Biotechnol* (2018) 36:411–20. doi: 10.1038/nbt.4096
20. Gu Z, Eils R, Schlesner M. Complex Heatmaps Reveal Patterns and Correlations in Multidimensional Genomic Data. *Bioinformatics* (2016) 32:2847–9. doi: 10.1093/bioinformatics/btw313
21. Jiang P, Gu S, Pan D, Fu J, Sahu A, Hu X, et al. Signatures of T Cell Dysfunction and Exclusion Predict Cancer Immunotherapy Response. *Nat Med* (2018) 24:1550–8. doi: 10.1038/s41591-018-0136-1
22. Yu G, Wang LG, Han Y, He QY. Clusterprofiler: An R Package for Comparing Biological Themes Among Gene Clusters. *Omics* (2012) 16:284–7. doi: 10.1089/omi.2011.0118
23. Maleki Vareki S. High and Low Mutational Burden Tumors Versus Immunologically Hot and Cold Tumors and Response to Immune Checkpoint Inhibitors. *J Immunother Cancer* (2018) 6:157. doi: 10.1186/s40425-018-0479-7
24. Chan TA, Yarchoan M, Jaffee E, Swanton C, Quezada SA, Stenzinger A, et al. Development of Tumor Mutation Burden as an Immunotherapy Biomarker: Utility for the Oncology Clinic. *Ann Oncol* (2019) 30:44–56. doi: 10.1093/annonc/mdy495
25. Cabel L, Proudhon C, Romano E, Girard N, Lantz O, Stern MH, et al. Clinical Potential of Circulating Tumour DNA in Patients Receiving Anticancer Immunotherapy. *Nat Rev Clin Oncol* (2018) 15:639–50. doi: 10.1038/s41571-018-0074-3
26. Dudley JC, Lin MT, Le DT, Eshleman JR. Microsatellite Instability as a Biomarker for PD-1 Blockade. *Clin Cancer Res* (2016) 22:813–20. doi: 10.1158/1078-0432.CCR-15-1678
27. Giannakis M, Mu XJ, Shukla SA, Qian ZR, Cohen O, Nishihara R, et al. Genomic Correlates of Immune-Cell Infiltrates in Colorectal Carcinoma. *Cell Rep* (2016) 15:857–65. doi: 10.1016/j.celrep.2016.03.075
28. Llosa NJ, Cruise M, Tam A, Wicks EC, Hechenbleikner EM, Taube JM, et al. The Vigorous Immune Microenvironment of Microsatellite Instable Colon Cancer Is Balanced by Multiple Counter-Inhibitory Checkpoints. *Cancer Discov* (2015) 5:43–51. doi: 10.1158/2159-8290.CD-14-0863
29. Wong YF, Cheung TH, Poon KY, Wang VW, Li JC, Lo KW, et al. The Role of Microsatellite Instability in Cervical Intraepithelial Neoplasia and Squamous Cell Carcinoma of the Cervix. *Gynecol Oncol* (2003) 89:434–9. doi: 10.1016/s0090-8258(03)00134-3
30. Litchfield K, Reading JL, Puttick C, Thakkar K, Abbosh C, Bentham R, et al. Meta-Analysis of Tumor- and T Cell-Intrinsic Mechanisms of Sensitization to Checkpoint Inhibition. *Cell* (2021) 84(3):596–614.e14. doi: 10.1016/j.cell.2021.01.002
31. Topalian SL, Taube JM, Pardoll DM. Neoadjuvant Checkpoint Blockade for Cancer Immunotherapy. *Science* (2020) 367(6477):eaax0182. doi: 10.1126/science.aax0182
32. Gagliardi A, Porter VL, Zong Z, Bowlby R, Titmuss E, Namirembe C, et al. Analysis of Ugandan Cervical Carcinomas Identifies Human Papillomavirus Clade-Specific Epigenome and Transcriptome Landscapes. *Nat Genet* (2020) 52:800–10. doi: 10.1038/s41588-020-0673-7
33. Hu Z, Zhu D, Wang W, Li W, Jia W, Zeng X, et al. Genome-Wide Profiling of HPV Integration in Cervical Cancer Identifies Clustered Genomic Hot Spots and a Potential Microhomology-Mediated Integration Mechanism. *Nat Genet* (2015) 47:158–63. doi: 10.1038/ng.3178
34. Guo L, Hua K. Cervical Cancer: Emerging Immune Landscape and Treatment. *Onco Targets Ther* (2020) 13:8037–47. doi: 10.2147/OTT.S264312
35. Burd EM. Human Papillomavirus and Cervical Cancer. *Clin Microbiol Rev* (2003) 16:1–17. doi: 10.1128/cmr.16.1.1-17.2003
36. Hammes LS, Tekmal RR, Naud P, Edelweiss MI, Kirma N, Valente PT, et al. Macrophages, Inflammation and Risk of Cervical Intraepithelial Neoplasia (CIN) Progression–Clinicopathological Correlation. *Gynecol Oncol* (2007) 105:157–65. doi: 10.1016/j.ygyno.2006.11.023
37. Ott PA, Bang YJ, Piha-Paul SA, Razak ARA, Bennouna J, Soria JC, et al. T-Cell-Inflamed Gene-Expression Profile, Programmed Death Ligand 1 Expression, and Tumor Mutational Burden Predict Efficacy in Patients Treated With Pembrolizumab Across 20 Cancers: KEYNOTE-028. *J Clin Oncol* (2019) 37:318–27. doi: 10.1200/JCO.2018.78.2276
38. Kagabu M, Nagasawa T, Sato C, Fukagawa Y, Kawamura H, Tomabechi H, et al. Immunotherapy for Uterine Cervical Cancer Using Checkpoint Inhibitors: Future Directions. *Int J Mol Sci* (2020) 21:2335. doi: 10.3390/ijms21072335
39. Frenel JS, Le Tourneau C, O'Neil B, Ott PA, Piha-Paul SA, Gomez-Roca C, et al. Safety and Efficacy of Pembrolizumab in Advanced, Programmed Death Ligand 1-Positive Cervical Cancer: Results From the Phase Ib KEYNOTE-028 Trial. *J Clin Oncol* (2017) 35:4035–41. doi: 10.1200/JCO.2017.74.5471
40. Chung HC, Ros W, Delord JP, Perets R, Italiano A, Shapira-Frommer R, et al. Efficacy and Safety of Pembrolizumab in Previously Treated Advanced Cervical Cancer: Results From the Phase II KEYNOTE-158 Study. *J Clin Oncol* (2019) 37:1470–8. doi: 10.1200/JCO.18.01265
41. Bi K, He MX, Bakouny Z, Kanodia A, Napolitano S, Wu J, et al. Tumor and Immune Reprogramming During Immunotherapy in Advanced Renal Cell Carcinoma. *Cancer Cell* (2021) 39(5):649–61.e5. doi: 10.1016/j.ccell.2021.02.015

Conflict of Interest: The authors declare that the research was conducted in the absence of any commercial or financial relationships that could be construed as a potential conflict of interest.

frontiers in Immunology

ORIGINAL RESEARCH
published: 12 July 2021
doi: 10.3389/fimmu.2021.702615

Identification and Validation of the Immune Regulator CXCR4 as a Novel Promising Target for Gastric Cancer

Shuai Xue[1†], Ming Ma[2†], Songhua Bei[1†], Fan Li[1], Chenqu Wu[1], Huanqing Li[1], Yanling Hu[3], Xiaohong Zhang[1], YanQing Qian[1], Zhe Qin[1], Jun Jiang[1] and Li Feng[1*]*

[1] Endoscopy Center, Minhang Hospital, Fudan University, Shanghai, China, [2] Department of Gastroenterology, Minhang Hospital, Fudan University, Shanghai, China, [3] Institute of Fudan Minhang Academic Health System, Minhang Hospital, Fudan University, Shanghai, China

OPEN ACCESS

Edited by:
Ziming Li,
Shanghai Jiaotong University, China

Reviewed by:
Xin Hong,
Anhui University, China
Ruidong Zhang,
Inner Mongolia Agricultural University, China

***Correspondence:**
Jun Jiang
15110700028@fudan.edu.cn
Li Feng
feng_li@fudan.edu.cn

†These authors have contributed equally to this work

Specialty section:
This article was submitted to Cancer Immunity and Immunotherapy, a section of the journal Frontiers in Immunology

Received: *29 April 2021*
Accepted: *10 June 2021*
Published: *12 July 2021*

Citation:
Xue S, Ma M, Bei S, Li F, Wu C, Li H, Hu Y, Zhang X, Qian Y, Qin Z, Jiang J and Feng L (2021) Identification and Validation of the Immune Regulator CXCR4 as a Novel Promising Target for Gastric Cancer. Front. Immunol. 12:702615. doi: 10.3389/fimmu.2021.702615

Immune checkpoint blockade has attracted a lot of attention in the treatment of human malignant tumors. We are trying to establish a prognostic model of gastric cancer (GC) based on the expression profile of immunoregulatory factor-related genes. Based on the TCGA database, we identified 234 differentially expressed immunoregulatory factors. Gene Ontology (GO) and Kyoto Encyclopedia of Genes and Genomes (KEGG) conducted enrichment analysis to clarify the biological functions of differential expression of immunoregulatory factors. STRING database predicted the interaction network between 234 differently expressed immune regulatory factors. The expression of 11 immunoregulatory factors was significantly related to the overall survival of gastric cancer patients. Univariate Cox regression analysis, Kaplan–Meier analysis and multivariate Cox regression analysis found that immunomodulatory factors were involved in the progression of gastric cancer and promising biomarkers for predicting prognosis. Among them, CXCR4 was related to the low survival of GC patients and a key immunomodulatory factor in GC. Based on TCGA data, the high expression of CXCR4 in GC was positively correlated with the advanced stage and grade of gastric cancer and related to poor prognosis. Univariate analysis and multivariate analysis indicated that CXCR4 was an independent prognostic indicator for TCGA gastric cancer patients. *In vitro* functional studies had shown that CXCR4 promoted the proliferation, migration, and invasion of gastric cancer cells. In summary, this study has determined the prognostic value of 11 immunomodulatory factors in gastric cancer. CXCR4 is an independent prognostic indicator for gastric cancer patients, which may help to improve the individualized prognostic prediction of GC and provide candidates for the diagnosis and treatment of GC.

Keywords: gastric cancer, immunoregulatory factors, bioinformatics analysis, CXCR4, prognosis

INTRODUCTION

As one of the widely occurred carcinomas, gastric cancer (GC) is the third primary inducer of mortality amid cancers worldwide (1). Despite the occurrence rate of GC has fallen sharply in western countries, it remains high in East Asian countries (2, 3). Nevertheless, this increasing trend of GC has decreased recently, especially the proportion of early GC cases. Currently, surgical resection is the possibly available strategy for GC, whereas it is only applied in stage I of early GC cases. Clinical stage II or stage III patients require multidisciplinary adjunctive approaches (4, 5). The primary contributor to the failure of GC treatment is drug resistance (6, 7). In the past few decades, several pivotal regulators are reported to participate in GC's pathogenesis (8, 9). For example, METTL3-mediated m^6A methylation of SPHK2 targets KLF2, thus promoting advanced GC (10). Human CCR4 and CAF1 deacetylase mediate the regulation of human GC cell proliferation and tumorigenicity *via* modulating the cell cycle process (11). Understanding the regulatory mechanism of GC will offer new insights into treating GC (12).

In the past decade, immune checkpoint blockade has attracted a lot of attention in the human malignant neoplasms treatment, lung carcinoma, breast carcinoma and stomach carcinoma included (13–15). In GC, several anti-PD1 therapies have been approved for GC treatment. For instance, pembrolizumab largely extends the over survival (OS) and presents increasing benefits in GC patients as the PD-L1 score increased (16–18). Herein, pembrolizumab is approved for the third-line therapy of PDL1- positive (CPS ≥1) GC (19, 20). In addition, regarding the first-line therapy of HER2-negative GC patients with PD-L1 CPS no less than 5, chemotherapy along with nivolumab becomes a newly produced treatment. Nevertheless, the regulatory mechanism of immunoregulatory factors on GC still stays unclear. Previously, several immunoregulatory factors are reported to exhibit importance in GC (21–23). For example, BICC1 is shown to be a split-new prognostic indicator for GC related to immune infiltration (24).

Researches have revealed that immune regulatory factors exhibit a relationship with the poorly prognostic status of GC patients, and promote the malignant phenotype of GC cells (25, 26). Here, our purpose is to comprehensively study the expression features and clinicopathological parameters of immunomodulatory factors, so as to uncover prospective targets in treating GC. Besides, we perform loss of function tests to confirm our bioinformatics findings. We hope that this study can provide new therapeutic targets for GC.

MATERIALS AND METHOD

Data Collection

The RNA-Seq transcriptome data cohort (STAD) and clinical or prognostic details of GC were derived from TCGA (https://cancergenome.nih.gov/). CBIORTAL (www.cbioportal.org) was employed to detect the changes in the CXCR4 genome. We acquired CXCR4 mRNA expression profile from the International Cancer Genome Collaboration Group (ICGC) and Genome-wide Pan Cancer Analysis (PCAWG).

Selection of Immunomodulators

Currently, 10 genes (NRP1, CXCR4, METTL14, BCL11B, ZC3H13, HNMT, ASGR2, EZH2, ANXA5 and CDH2) are considered as classic immunomodulators. Here, we discovered three new immunomodulatory genes (BASP1, OsbPL1A and CD59). We further obtained the expression profiles of these identified genes from the TCGA STAD cohort with clinical details. The differential expressions of these genes in GC were shown by the Violet curve.

Consistent Cluster Analysis

In order to further explore the immunomodulatory factors, we applied consensus cluster analysis in the STAD cohort based on immunomodulatory factors. We identified two subgroups in this cohort. Besides, we carried out gene ontology (GO) and Kyoto Encyclopedia of Genes and Genomes (KEGG) analysis to evaluate their involved functions and pathways in the light of the gene profiles in the two subgroups.

Predictive Signature Generation

We employed the univariate Cox regression model to determine the correlation of immunoregulatory genes with the OS of GC patients. We defined it as the protection and hazard of these genes with a hazard ratio HRs <1 and HRs >1, respectively. Five genetic risk signals (NRP1, ZC3H13, CXCR4, ASGR2 and CXCR4) were determined according to the minimum standard. Besides, we calculated the risk score in view of the coefficients in the Lasso algorithm. On the basis of the average value of the risk score, we classified the TCGA STAD cohort into high-risk and low-risk groups.

Genome Changes and Identification of Co-Expressed Genes

We applied the CBioPortal tool (http://cbioportal.org) to analyze the mutations, copy number variation (CNV) and CXCR4 mRNA changes in GC. Oncoprint provided an overall outline of the changes of CXCR4 in STAD samples. The Linkedomics platform (27) was utilized to conduct co-expression analysis. We predicted potential functions through overexpression enrichment analysis (ORA) on the basis of GO, KEGG with Reactome pathways.

The Prognostic Value Assessment of Genetic Markers

We employed chi-square test and heat map analysis to determine clinicopathological features (age, gender, grade and stage, and survival status) in high-risk and low-risk groups. We utilized

Kaplan–Meier analysis and the Log-Rank test to calculate risk scores in high-risk groups and patients with low score group OS of distinct groups. Receiving the operating characteristic (ROC) and a curve were taken to investigate the prognostic value of the patient's survival prediction. We conducted univariate and multivariate Cox regression analysis to determine the impacts of risk score on GC prognosis.

Cell Culture and Transfection

HFE-145, MGC-803, HGC-27, AGS, SGC-7901 and BGC-823 were acquired from the Cell Bank of the Chinese Academy of Sciences (Shanghai, China). All cells were cultured in DMEM (Gibco, USA) with 10% FBS (Gibco, USA) and 1% penicillin/streptomycin. CXCR4 knockout plasmid was ordered from Dharmacon (CA, USA). The small interference RNA (siRNA) sequence was listed below: si-CXCR4-1, GATGCCGTGGCAAACTGGTACTTTG; si-CXCR4-2, TGGTTGGCCTTATCCTGCCTGGTAT; si-NC, UUCUC CGAACGUGUCACGUTT. The full-length CXCR4 cDNA was inserted into the pcDNA3.1 vector (Invitrogen, USA). About 2 μg of overexpression plasmid or 1.5 μg of siRNA was separately transfected into 1×10^6 cells in a 6 cm petri dish using 12 μl of Lipofectamine®2000 reagent (Invitrogen) as instruction described.

Cell Proliferation Assay

The ability of cells to proliferate in GC cells was determined using the CCK-8 kit (Dojindo, Japan). Specified GC cells were inoculated in a 96-well plate and then treated differently at the specified time. The OD values of 450 nm were detected after incubation with CCK-8 solution on a Fluoroskan Ascent fluorometer (Thermo Fisher, Finland).

Transwell Assay

An 8 μm Transwell chamber (Corning, USA) was set in a 24-well plate to perform the invasion assay. We plated 200 μl of GC cells in the upper chamber pre-coated with Matrigel (BD, USA). The lower chamber was filled with a complete medium. At 24 h post-incubation, we fixed the chamber with 4% paraformaldehyde and stained it in 0.1% crystal violet solution. Then, we calculated the number of samples in each group under a microscope. We conducted three independent experiments in triplicate one time. The Transwell migration assay was performed as described above but without the Matrigel.

RNA Extraction and RT-qPCR

We employed RNeasy reagent (Qiagen, Germany) to harvest the whole RNA. RT-qPCR was conducted with SYBR Premix ex TAG Mastermix kit (Takara, Japan) on the ICycler real-time system (Bio-Rad Laboratories, USA) as manual described. Glyceraldehyde-3-phosphate dehydrogenase was an internal control. The relative RNA expression was analyzed by the $2^{-\Delta\Delta Ct}$ approach and presented as the target gene/internal control ratio [$2^{-\Delta\Delta Ct\ (\text{target gene-internal control})}$] (28). The data were obtained from three independent experiments in triplicate one time. The primers of CXCR4 are 5'-ACTACACCGAGGAAATGGGCT-3' (F) and 5'-CCCACAATGCCAGTTAAGAAGA-3' (R). The primers of GAPDH are 5'-CTGGGCTACACTGAGCACC-3' (F) and 5'-CTGGGCTACACTGAGCACC-3' (R).

Statistical Analysis

All derived data were analyzed by GraphPad Prism 8.0 (GraphPad, Inc., USA) and Image-Pro Plus 6.0 and shown as the mean ± standard deviation (SD). We employed Student's t-test and one-way analysis of variance (ANOVA) to analyze the differences existing in two groups and more groups, respectively. Kaplan–Meier method and Log-rank test were taken to plot the survival curve. $P < 0.05$ meant that there was significant difference in compared groups.

RESULTS

Immunoregulatory Factors Expression Features

In this study, by analyzing the TCGA database, the gene expression profiles of 782 immune regulatory factors were identified. We identified 234 differentially expressed immunoregulatory factors with the criteria of the absolute logarithmic 2-fold change (FC) >1and the adjusted *P*-value of LIMMA <0.05 in GC compared to normal gastric samples, including 132 immunoregulatory factors with up-regulation and 111 immunoregulatory factors with down-regulation (**Figure 1**).

Bioinformatics Analysis of Differential Expression of Immunoregulatory Factors

Except for the regulation of immune response, we conducted GO and KEGG pathway analysis to evaluate the biological functions of these differently expressed immune regulatory factors. Enrichment of the KEGG pathway indicated that these differentially expressed immunoregulatory factors primarily took part in MAPK signaling pathway, endocytosis and proteoglycans in cancer (**Figure 2A**). GO CC analysis showed that these differentially expressed immunoregulatory factors were significantly enriched in endosome membrane, nuclear envelope, cell-substrate junction and focal adhesion (**Figure 2B**). For GO MF analysis, the first four significantly enriched terms are small GTPase binding, Ras GTPase binding, protein serine/threonine kinase activity, and ubiquitin-like protein transeferase activity (**Figure 2C**). The first four significantly richer BP terms included autophagy, a process utilizing autophagic mechanism, regulation of GTPase activity and regulation of cell morphogenesis (**Figure 2D**).

The Prognostic Significance of Immunomodulatory Factors

Then, we evaluated the significance of immunoregulatory factors on the prognosis of patients with GC. Univariate Cox regression and Kaplan–Meier analysis showed that higher expression of nine regulatory factors, including OsBPL1a, CD59, CDH2, NRP1,

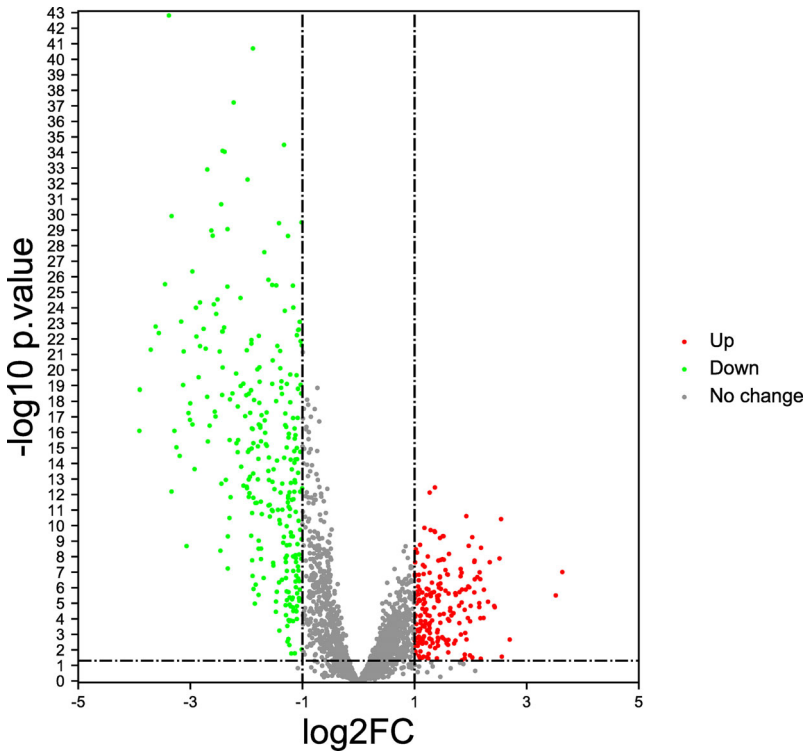

FIGURE 1 | Immunoregulatory factors expression features (Volcano plot). The red dots represent significantly up-regulated, the green dots represent significantly down-regulated, and the gray dots represent no difference change.

ANXA5, ASGR2, HNMT, BASP1, CXCR4, and were associated with lower survival rates of GC patients (**Figures 3A–I**). On the contrary, higher expression of EZH2 and BCL11B were associated with longer survival rates of GC patients (**Figures 3J, K**). We established a prognostic signal based on the multivariate Cox regression of ABCB6, FLVCR1, SLC48A1 and SLC7A11. Risk Score = (−0.028) ∗ of EZH2 + (0.06. 4) ∗ NRPl + (0.1308) ∗ CD59 + (0.15. 3) ∗ OsBPL1a + (−0.2268) ∗ BCL11B + (0.09 22 is) ∗ BASP1 + (0.0989) ∗ HNMT + (.0954) ∗ of CXCR4 + (0.0702) ∗ ASGR2+ (0.09 15) ∗ ANXA5+ (0.0168) ∗ CDH2. LASSO regression with tenfold cross-validation was performed to get the optimal lambda value that came from the minimum partial likelihood deviance, which was related to 11 genes that were significantly associated with OS (**Figures 4A, B**). **Figure 4C** shows that the survival of GC patients could be significantly predicted by the Signature risk score. Kaplan–Meier analysis revealed that the high-risk group presented dramatically shorter OS than the low-risk group (**Figure 4D**). Time-dependent ROC at 1, 3 and 5-year area (middle curve of the AUC) were 0.64, 0.696, and 0.68, respectively (**Figure 4E**).

Analysis of the Correlation Between CXCR4 and Clinical Characteristics

The above analysis revealed that CXCR4 was a key immunoregulatory factor in GC, so CXCR4 was selected for further analysis. According to the TCGA database, we found CXCR4 in GC was dramatically up-regulated in comparison with that in normal samples (**Figure 5A**). According to nodal metastasis status, stage, grade, stage and age, CXCR4 in GC was further analyzed. The results showed that CXCR4 was up-regulated in all N-stages of GC, with the strongest expression in N1 stage gastric cancer (**Figure 5B**). CXCR4 expression was positively related to the advanced stage and grade of GC. CXCR4 had the highest expression level in grade 3 and stage 4 samples, respectively (**Figures 5C, D**). Very interestingly, the CXCR4 expression level was negatively correlated to the age of patients with GC (**Figure 5E**).

In addition, univariate analysis (**Figure 6A**) and multivariate analysis (**Figure 6B**) indicated that CXCR4 was an independent prognostic indicator for GC patients in TCGA. Then, we based on AJCC stage and CXCR4 multivariate expressed Cox coefficient regression model constructed nomogram, and 1 year by AJCC calculated a score for each patient stage variable value, so as to arrive GC. The patient's 3- and 5-year survival probability and risk score (**Figure 7A**). Next, through the evaluation of the C index and AUC value, as well as the evaluation of the discriminant efficiency and prediction accuracy of the nomogram in the training set. Our results show that the nomogram is well-calibrated because the curve is close to the diagonal (**Figure 7B**).

Survival analysis showed that STAD patients with higher levels of CXCR4 had lower survival (**Figure 8A**). Compared with Caucasians with a higher level of CXCR4, Asians with a higher level of CXCR4 had lower survival (**Figure 8B**).

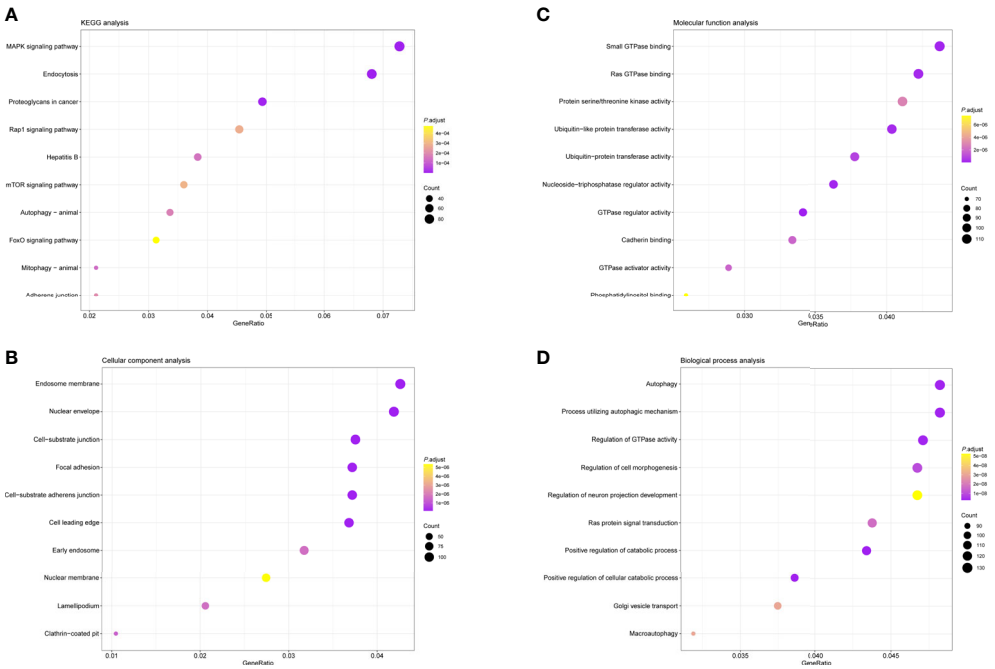

FIGURE 2 | Bubble diagrams showing the enrichment analysis and signal pathway analysis results of Differential Expression of Immunoregulatory Factors. The top 10 enriched terms covering **(A)** BP, **(B)** MF and **(C)** CC are presented. **(D)** The top 10 enriched pathways of Differential Expression of Immunoregulatory Factors in KEGG analysis are introduced. GO, Gene Ontology; BP, biological processes; MF, molecular functions; CC, cellular components; KEGG, Kyoto Encyclopedia of Genes and Genomes.

Compared with females with lower levels of CXCR4, males with lower levels of CXCR4 had lower survival (**Figure 8C**). In general, up-regulated CXCR4 in GC exhibits a close relationship to GC occurrence and development.

CXCR4 Promoted GC Cells Proliferation

We analyzed the expression level of CXCR4 in five GC cell lines, and the results showed that CXCR4 was significantly up-regulated in GC cell lines, especially SGC-7901 and BGC-823 (**Figure 9A**). We designed CXCR4 siRNA to further investigate CXCR4 function in GC cells. We established the CXCR4 knockdown cell line in SGC7901 and AGS cells, and its knockdown efficiency was detected by RT-qPCR (**Figure 9B**). RT-qPCR showed that in infected SNHG16 cells, the expression of SNHG16 in SGC-7901 cells was significantly increased (**Figure 9C**). Compared to control cells, two siRNAs could effectively knock down CXCR4 in two cells. Overexpression of CXCR4 significantly promoted GC cell proliferation (**Figure 9D**). Abated CXCR4 dramatically inhibited GC cell proliferation (**Figures 9E, F**). Collectively, CXCR4 was a promoter in facilitating GC cell proliferation.

CXCR4 Facilitated Cell Migration and Invasion of GC

Since GC is highly malignant, it is prone to multiple metastases in the early stage and the survival rate is extremely low. Here, we studied the metastasis of GC. Because CXCR4 exerted an effect on GC cell proliferation, we will explore the influence of CXCR4 on GC cell invasion. We conducted Transwell analysis to detect cell invasion capability. Overexpression of CXCR4 in SGC7901 cells the invasion ability was greatly promoted (**Figure 10A**). After knocking down CXCR4 in SGC7901 and AGS cells, the invasion ability was greatly inhibited (**Figure 10B**).

DISCUSSION

Abnormally expressed immunoregulatory factors are associated with a variety of malignant behaviors in multiple types of carcinoma. A series of immunoregulatory factors are shown to play vital parts in GC. For example, a higher level of soluble PD-L1 (sPD-L1) in plasma predicts shorter overall survival for GC patients (29, 30). Wang et al. showed that signals including 8-immune-related genes (IRG) could function as a predictor of the OS rate of GC patients and their response to immune checkpoint inhibitors (28). Additionally, a prognostic model with three immune-related genes (SEMA6A, LTBP1 and BACH2) could predict the OS rate of GC patients with different microsatellite instability states. Here, we evaluated the expression patterns of 782 immune regulatory factors in GC and determined that 234 immune regulatory factors were significantly dysregulated in GC compared to the normal sample. In addition, except for immune regulation, we also found that these dysregulated immune regulatory factors were related to the MAPK

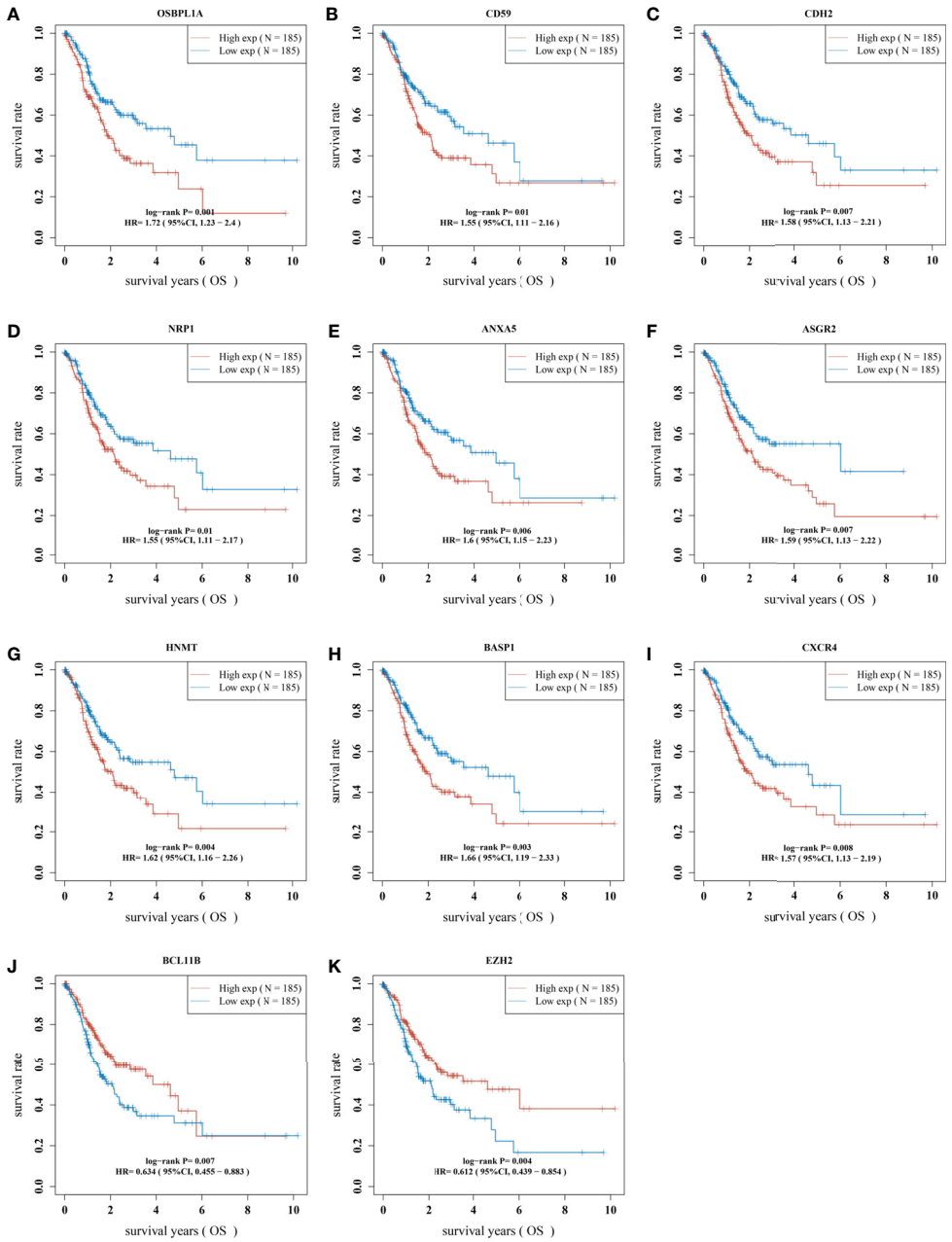

FIGURE 3 | The prognostic value of immunomodulatory factors in GC. The correlation analysis between the expression levels of 11 immune regulatory factors and the OS of gastric cancer patients was analyzed, including **(A)** OSBPL1A, **(B)** CD59, **(C)**CDH2, **(D)** NRP1, **(E)** ANXA5, **(F)** ASGR2, **(G)** HNMT, **(H)** BASP1, **(I)** CXCR4, **(J)** BCL11B and **(K)** EZH2. OS, overall survival.

signaling pathway, endosome membrane, small GTPase binding and autophagy. This indicated that they may have multiple key roles in GC. Finally, we found that the imbalance of 11 immune regulatory factors could predict the overall survival time of gastric cancer, including EZH2, NRP1, CD59, OsBPL1aBCL11B, BASP1, HNMT, CXCR4, ASGR2, ANXA5, CDH2. This study shows for the first time that immunomodulatory factors might be utilized as potential biomarkers for GC prognosis.

In the past few decades, people have made a lot of efforts to uncover potential indicators for GC's prognosis. For instance, PFKFB4 is a promising biomarker for predicting the poorly prognostic status of GC patients (31). Overexpressed CLC-3 is an indicator for poorly prognostic status of GC. The overexpression of CLC-3 is regulated by XRCC5, which is a biomarker for the poor prognosis of GC (32). Nevertheless, the 5-year survival rate of distant GC is still as low as 6%. Therefore, there is an urgent

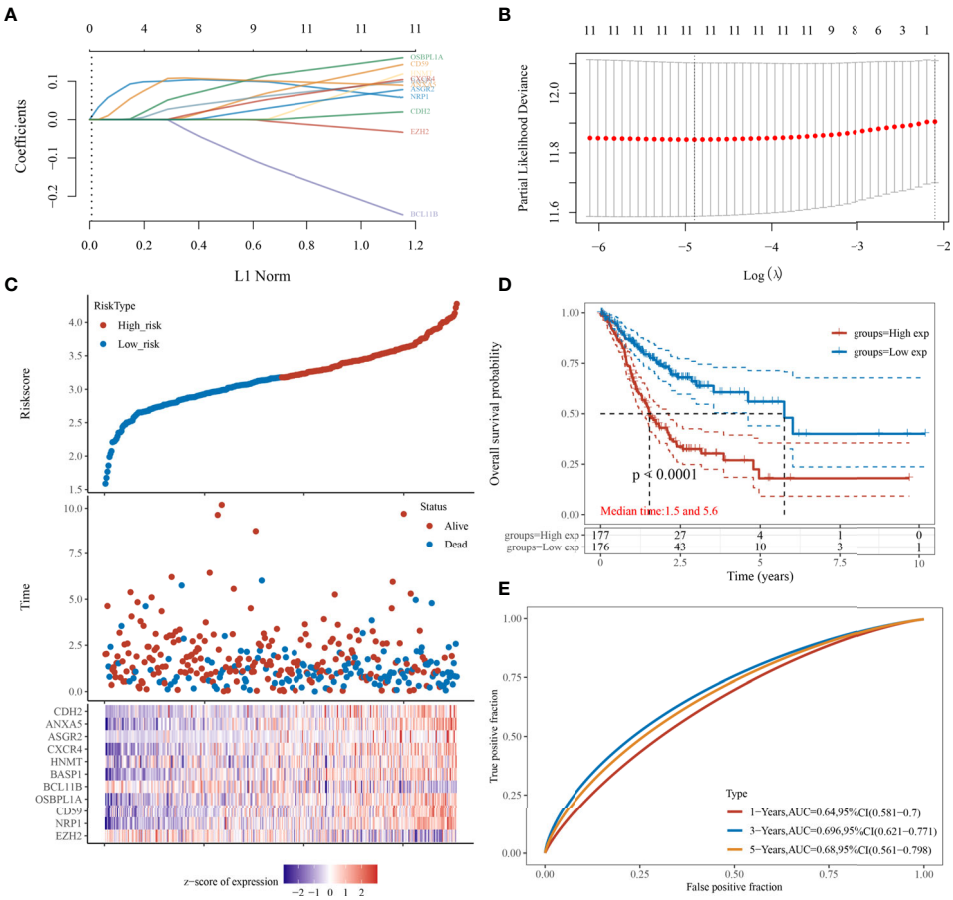

FIGURE 4 | Prognostic significance analysis of immunomodulatory factor markers. **(A, B)** LASSO regression with tenfold cross-validation of 11. **(C)** survival of GC patients by the Signature risk score. **(D)** Kaplan–Meier analysis of high-risk group and low-risk group. **(E)** Time-dependent ROC at 1, 3 and 5-year area (middle curve of the AUC).

need to find new biomarkers. Here, we are trying to construct a signal based on immune regulatory factors to make predictions. We made a distinction between the prognostic risk signals with 11 genes, including EZH2, NRP1, CD59, OsBPL1A, BCL11B, BASP1, HNMT, CXCR4, ASGR2, ANXA5CDH2. It is worth noting that compared to previously reported prognostic indicators (T, N, M clinical stage), our prognostic risk characteristics present higher accuracy, with AUC value >0.8. To sum up, our findings show that the risk signal could be utilized as potential biomarkers, providing more clinical applications and effective treatment guidelines.

Immune regulatory factors may also be related to tumor progression except for the prognostic value of risk signals. EZH2 (Enhancer of Zeste homolog 2) belongs to a member of the Polycomb gene family and is an important class of epigenetic modulators in inhibiting transcription (33). Polycomb suppression complex 2 (PRC2) is one core complex of PCG, mediating gene silencing mainly *via* modulating chromatin structure (34). As the enzymatic subunit of PRC2, EZH2 alters gene expression *via* trimethylating Lys-27 in histone 3 (H3K27me3) (33, 35). H3K27Me3 is reported to be related to the inhibition of gene expression and is considered to be a key epigenetic event in the development of tissues and the determination of stem cell fate. In GC, inhibiting EZH2 and EGFR exerts a synergistic effect on cell apoptosis *via* raising autophagy in GC cells (36). EZH2 mediates the promotion of 5-FU resistance in GC by epigenetically inhibiting FBXO32 expression (37). EZH2 induces the transition of epithelial–mesenchymal and pluripotency phenotype of GC cells *via* combination with the PTEN promoter (38). CD59 is a glycosylphosphatidylinositol-anchored membrane protein, acting as a suppressor of membrane attack complex to modulate complement activation (39). Current reports have revealed high expression of CD59 in various cell lines and tissues of cancer. It is found that CD59 is necessary for the epithelial cancer stem cells to evade complement monitoring. In breast cancer, CD59 could promote the growth of neoplasm and predict the poorly prognostic status (40). The transcription factor BCL11B is an important immunoregulatory factor that can promote the typical and adaptive differentiation of NK cells (41). Emerging reports have shown that BASP1 could modulate multiple biological behaviors,

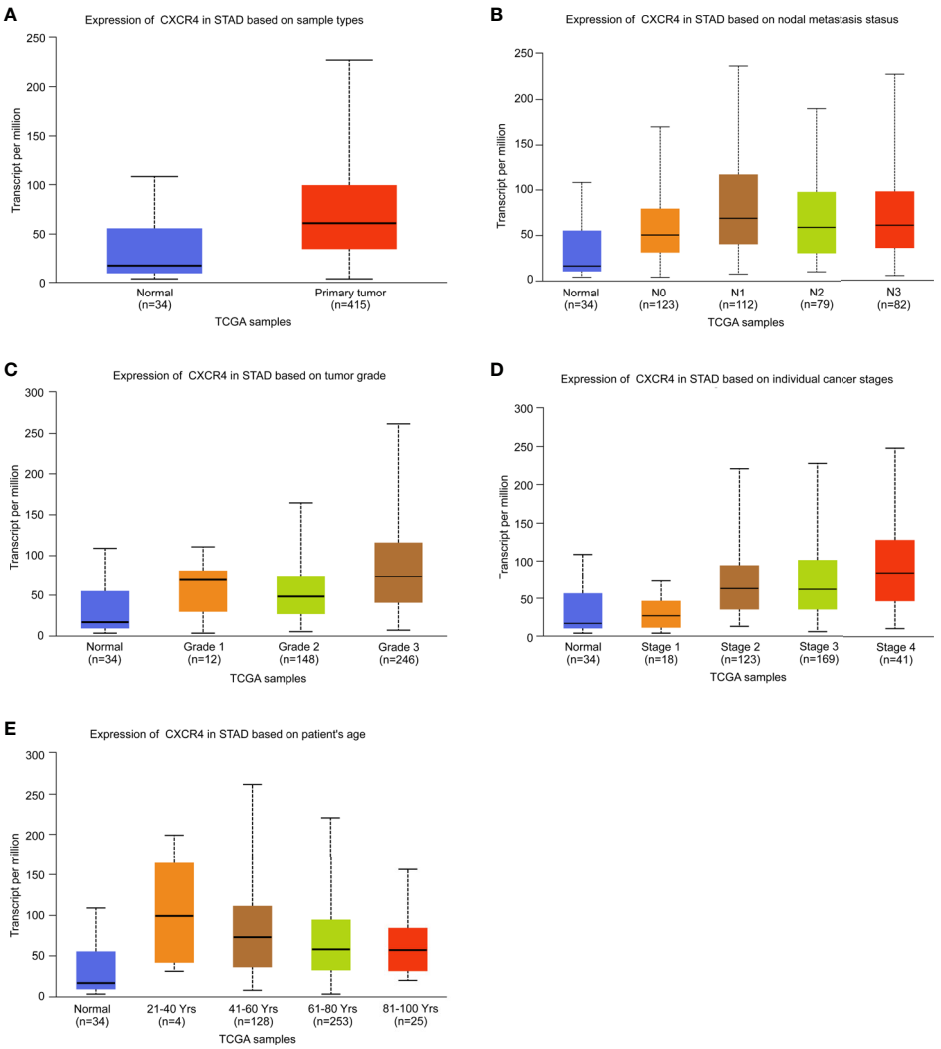

FIGURE 5 | Analysis of the expression level of CXCR4 in GC. The expression level of CXCR4 was analyzed based on **(A)** sample type, **(B)** nodal metastasis status, **(C)** tumor grade, **(D)** individual cancer stage, and **(E)** patient age.

such as cell proliferation, apoptosis, and differentiation (42, 43). More and more pieces of evidence confirm that BASP1 plays as a potential suppressor of tumor and functions importantly in various carcinomas, including thyroid carcinoma (44), stomach carcinoma (45) and lung carcinoma (46). Nevertheless, it is unclear the influence of BASP1 on GC. In GC, BASP1 suppressed cell growth and metastasis *via* inhibiting the Wnt/β-catenin pathway (45). This study confirms for the first time that the imbalance of these immune regulatory factors is associated with the survival time of GC patients.

CXCR4 displays a key role in a variety of cancers. CXCR4 expression in cancer cells is negatively related to the prognosis of the disease and serves as an independent factor of other prognostic parameters. The discovery involves tumor-initiating cancer stem cells (CSC) of CXCR4 expression which is conducive to CXCR4 in resistance to treatment, recurrence, metastasis and poor clinical outcome. The CXCR4/RhoA signaling pathway participates in miR-128-modulated human thyroid carcinoma cells proliferation and apoptosis (47). In endometrial cancer, the CXCL12/CXCR4 axis induces proliferation and invasion (48). Recently, some studies have revealed the function of CXCR4 in GC. For example, the block of CXCR4/mTOR signaling pathway induces anti-metastatic properties and autophagic cell death of CER cells in disseminated peritoneal GC (49). Here, we systematically investigate the expression features, possible effects and mechanisms of CXCR4 in GC. We discover CXCR4 is highly expressed in GC and closely related to the prognosis of GC. Reducing CXCR4 largely hinders GC cells proliferation, migration and invasion *in vitro*. These results demonstrated that CXCR4 acted as an oncogene and is a potential biomarker for GC treatment.

There are several limitations that should be taken into consideration. First of all, this is a bioinformatics analysis based on public databases. Therefore, the functions of the three

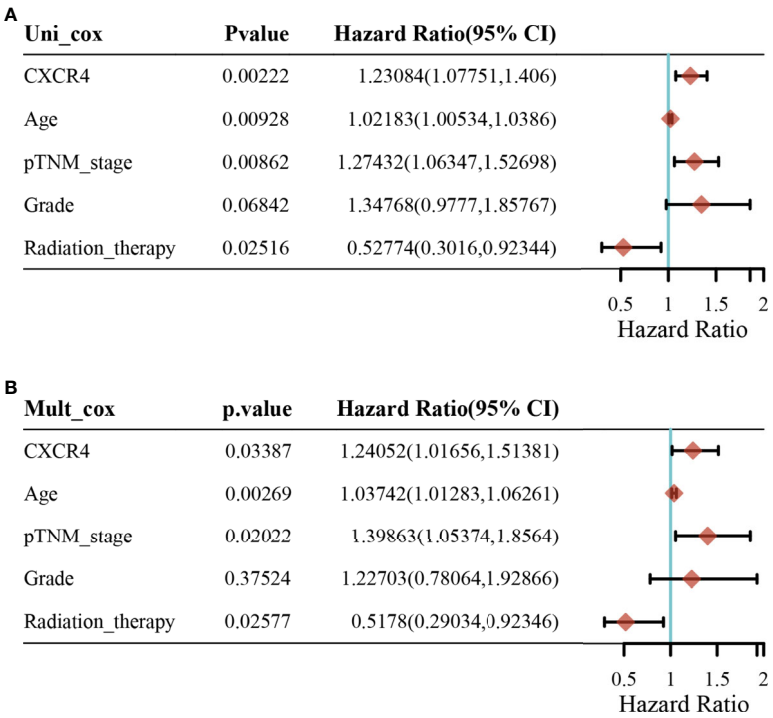

FIGURE 6 | Univariate analysis and multivariate analysis for patients with gastric cancer. **(A)** Univariate analysis and **(B)** multivariate analysis.

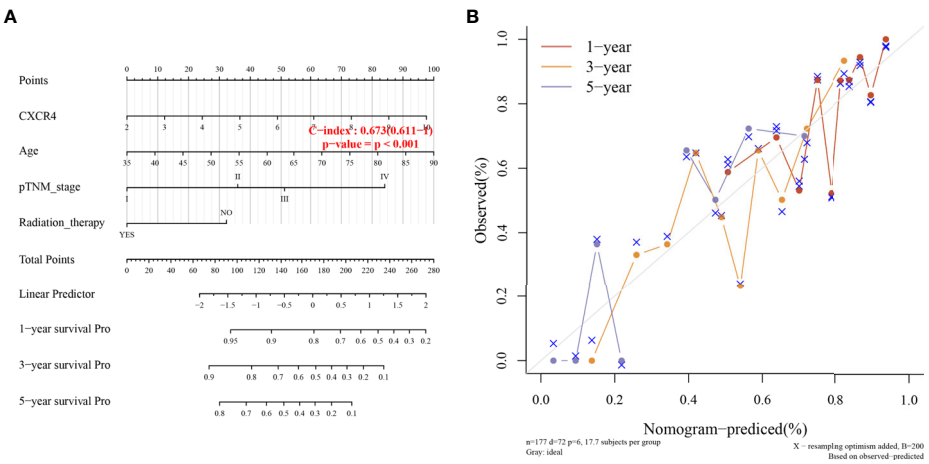

FIGURE 7 | Clinical association analysis and Fitting analysis**. (A)** Association Analysis between survival probability and risk score. **(B)** Time Fitting analysis.

new immunomodulatory genes (BASP1, OsbPL1A and CD59) need to be further explored. At the same time, we have not verified the expression of key immune regulatory genes in clinical samples. Therefore, we plan to continue to collect patient and clinical data to further verify this issue in the future. Finally, we will further verify the results of CXCR4 *in vitro* studies through an animal model assay.

CONCLUSION

In conclusion, this study analyzed and constructed a gastric cancer prognosis model based on the expression profile of immunoregulatory factor-related genes, which provided new information for gastric cancer research. We identified 234 differently expressed immunoregulatory factors and established

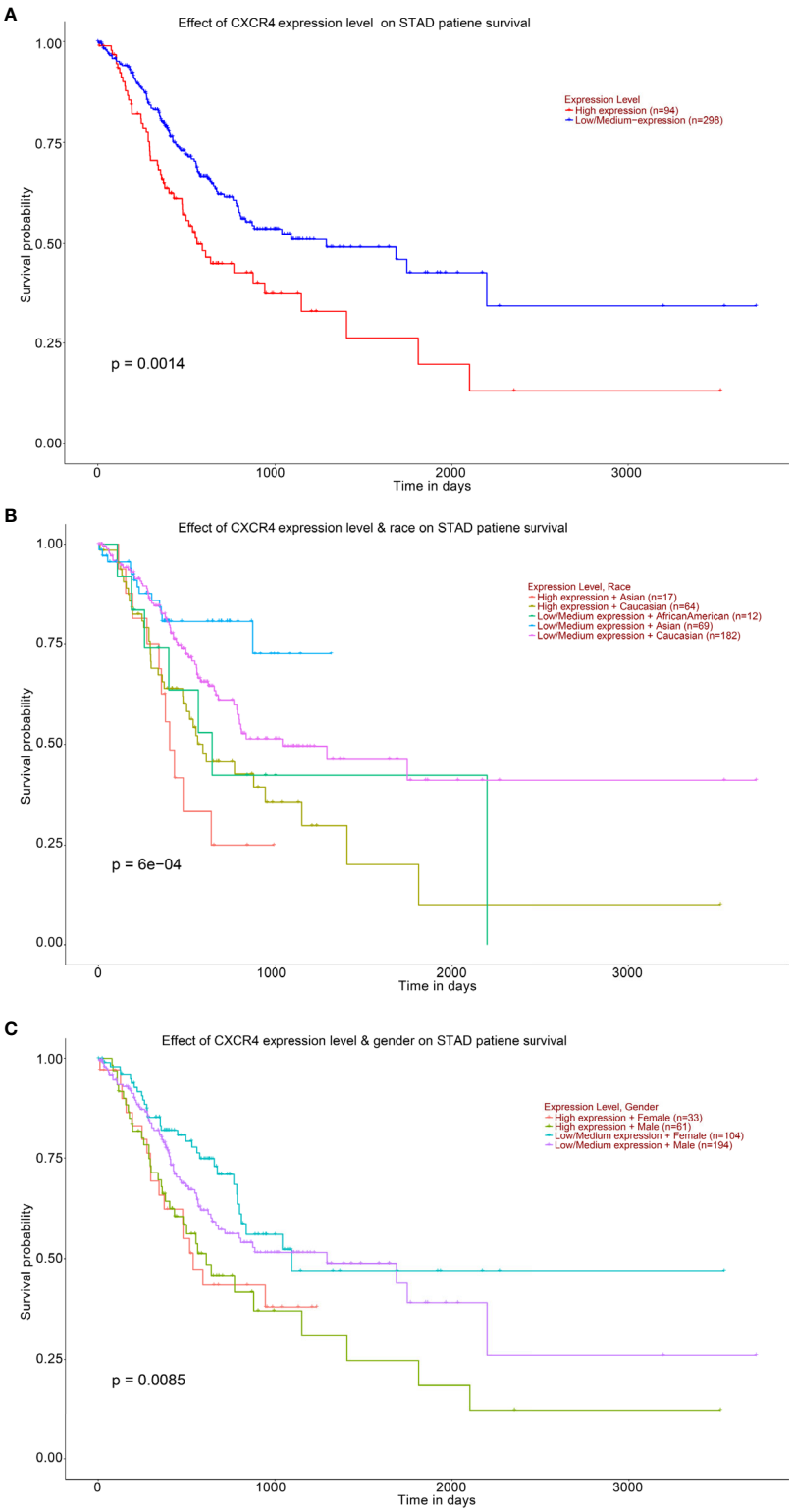

FIGURE 8 | Analysis of the expression level of CXCR4 and the ten-year survival of STAD patients. Kaplan–Meier based on **(A)** STAD patient, **(B)** STAD patient's race, **(C)** STAD patient's gender.

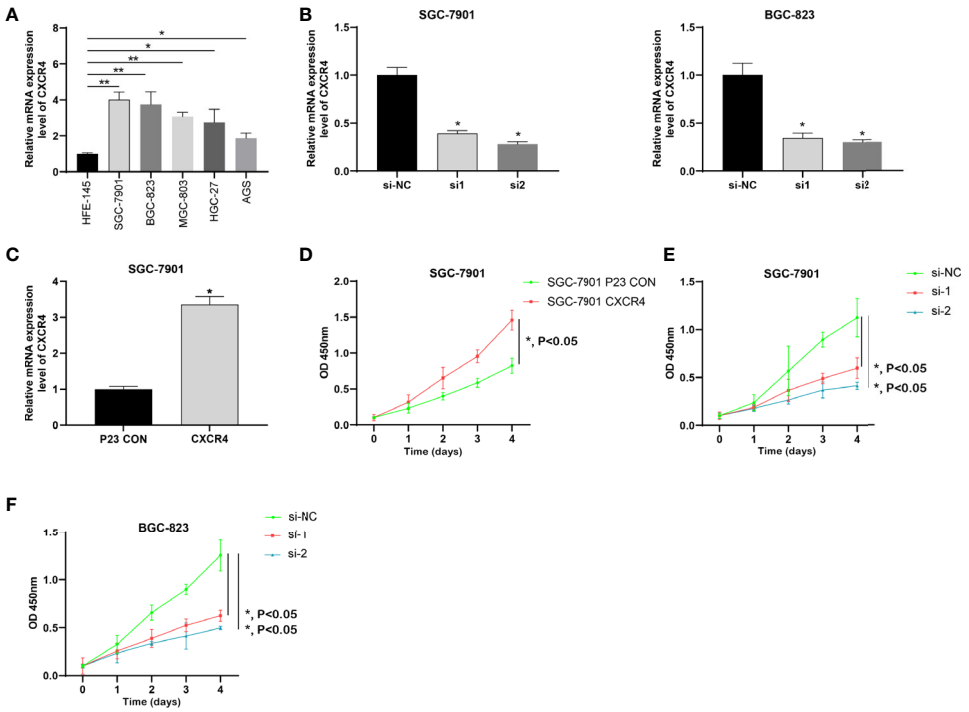

FIGURE 9 | CXCR4 was up-regulated in GC and promoted the proliferation of GC cells. **(A)** The expression of CXCR4 in GC cells was determined by RT-qPCR. **(B)** The specific siRNA knockdown the expression of CXCR4 in the GC cell line. **(C)** The CXCR4 overexpression vector increase the expression of CXCR4 in the GC cell line. **(D)** Overexpression of CXCR4 promoted the proliferation of the SGC-7910 cell line. Knockdown of CXCR4 inhibited the proliferation of SGC-7910 **(E)** and BGX-823 **(F)** cell lines. * means $P < 0.05$; ** means $P < 0.01$.

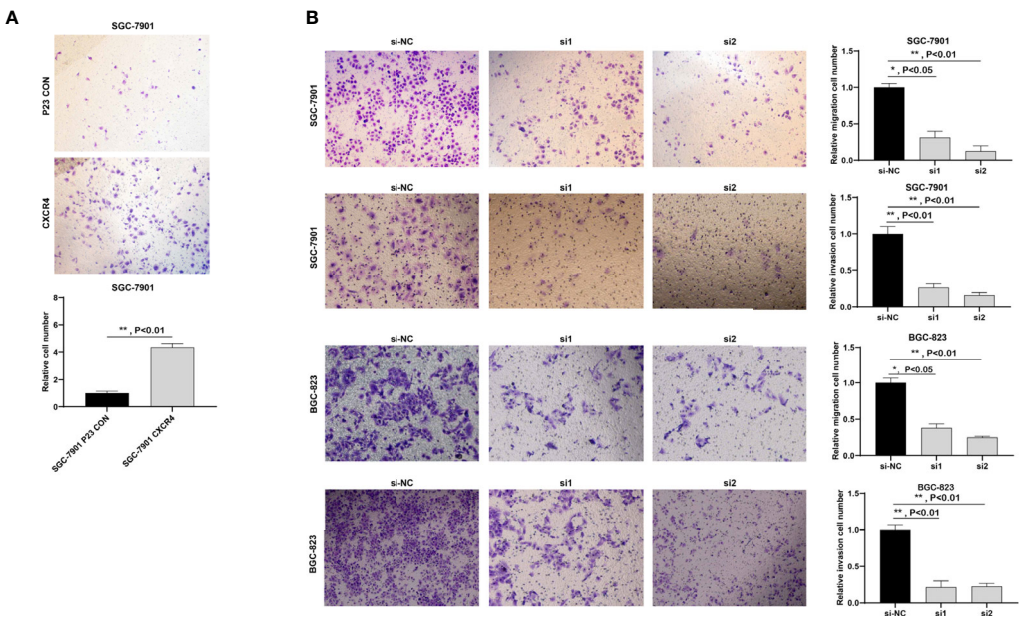

FIGURE 10 | CXCR4 promoted the migration and invasion of GC cells. **(A)** Overexpression of CXCR4 promoted metastasis of the SGC-7901 cell line. **(B)** Knockdown of CXCR4 inhibited the migration and invasion of SGC-7901 and BGC-823 cell lines.

risk signals formed by 11immunoregulatory factors for prognostic evaluation of gastric cancer. SED was performed on the TCGA data set. Finally, we focus on CXCR4 expression and find that CXCR4 is greatly up-regulated in GC. Additionally, we discover CXCR4 is an oncogene of GC cell proliferation, migration and invasion. Our research provides a new biomarker-based on immunomodulatory factor analysis for GC prognosis and treatment.

DATA AVAILABILITY STATEMENT

The datasets presented in this study can be found in online repositories. The names of the repository/repositories and accession number(s) can be found below: https://cancergenome.nih.gov/, TCGA.

AUTHOR CONTRIBUTIONS

Conception and design: SX and FL. Development of methodology: SX, CW, HL and YH. Sample collection: FL, XZ and LF. Analysis and interpretation of data: YQ, JJ and ZQ. Writing, review, and/or revision of the manuscript: MM, SB, SX, JJ, and LF.

REFERENCES

1. Smyth EC, Nilsson M, Grabsch HI, van Grieken NC, Lordick F. Gastric Cancer. *Lancet* (2020) 396(10251):635–48. doi: 10.1016/S0140-6736(20)31288-5
2. Sano T. Gastric Cancer: Asia and the World. *Gastric Cancer* (2017) 20(Suppl 1):1–2. doi: 10.1007/s10120-017-0694-9
3. Bray F, Ferlay J, Soerjomataram I, Siegel RL, Torre LA, Jemal A. Global Cancer Statistics 2018: GLOBOCAN Estimates of Incidence and Mortality Worldwide for 36 Cancers in 185 Countries. *CA Cancer J Clin* (2018) 68 (6):394–424. doi: 10.3322/caac.21492
4. Ajani JA, Lee J, Sano T, Janjigian YY, Fan D, Song S. Gastric Adenocarcinoma. *Nat Rev Dis Primers* (2017) 3:17036. doi: 10.1038/nrdp.2017.36
5. Digklia A, Wagner AD. Advanced Gastric Cancer: Current Treatment Landscape and Future Perspectives. *World J Gastroenterol* (2016) 22 (8):2403–14. doi: 10.3748/wjg.v22.i8.2403
6. Chen Z, Li Y, Tan B, Zhao Q, Fan L, Li F, et al. Progress and Current Status of Molecule-Targeted Therapy and Drug Resistance in Gastric Cancer. *Drugs Today (Barc)* (2020) 56(7):469–82. doi: 10.1358/dot.2020.56.7.3112071
7. Choi SJ, Jung SW, Huh S, Chung YS, Cho H, Kang H. Alteration of DNA Methylation in Gastric Cancer With Chemotherapy. *J Microbiol Biotechnol* (2017) 27(8):1367–78. doi: 10.4014/jmb.1704.04035
8. Shan C, Zhang Y, Hao X, Gao J, Chen X, Wang K. Biogenesis, Functions and Clinical Significance of circRNAs in Gastric Cancer. *Mol Cancer* (2019) 18 (1):136. doi: 10.1186/s12943-019-1069-0
9. Yuan L, Xu ZY, Ruan SM, Mo S, Qin JJ, Cheng XD. Long non-Coding RNAs Towards Precision Medicine in Gastric Cancer: Early Diagnosis, Treatment, and Drug Resistance. *Mol Cancer* (2020) 19(1):96. doi: 10.1186/s12943-020-01219-0
10. Huo FC, Zhu ZM, Zhu WT, Du QY, Liang J, Mou J. METTL3-Mediated M(6) a Methylation of SPHK2 Promotes Gastric Cancer Progression by Targeting KLF2. *Oncogene* (2021) 40(16):2968–81. doi: 10.1038/s41388-021-01753-1
11. Chalabi Hagkarim N, Grand RJ. The Regulatory Properties of the Ccr4-Not Complex. *Cells* (2020) 9(11):2379. doi: 10.3390/cells9112379
12. Song XH, Liao XY, Zheng XY, Liu JQ, Zhang ZW, Zhang LN, et al. Human Ccr4 and Caf1 Deadenylases Regulate Proliferation and Tumorigenicity of Human Gastric Cancer Cells Via Modulating Cell Cycle Progression. *Cancers (Basel)* (2021) 13(4):834. doi: 10.3390/cancers13040834
13. Filin IY, Solovyeva VV, Kitaeva KV, Rutland CS, Rizvanov AA. Current Trends in Cancer Immunotherapy. *Biomedicines* (2020) 8(12):621. doi: 10.3390/biomedicines8120621
14. Osipov A, Murphy A, Zheng L. From Immune Checkpoints to Vaccines: The Past, Present and Future of Cancer Immunotherapy. *Adv Cancer Res* (2019) 143:63–144. doi: 10.1016/bs.acr.2019.03.002
15. Wilky BA. Immune Checkpoint Inhibitors: The Linchpins of Modern Immunotherapy. *Immunol Rev* (2019) 290(1):6–23. doi: 10.1111/imr.12766
16. Muro K, Chung HC, Shankaran V, Geva R, Catenacci D, Gupta S, et al. Pembrolizumab for Patients With PD-L1-positive Advanced Gastric Cancer (KEYNOTE-012): A Multicentre, Open-Label, Phase 1b Trial. *Lancet Oncol* (2016) 17(6):717–26. doi: 10.1016/S1470-2045(16)00175-3
17. Shitara K, Özgüroğlu M, Bang YJ, Di Bartolomeo M, Mandalà M, Ryu MH, et al. Pembrolizumab Versus Paclitaxel for Previously Treated, Advanced Gastric or Gastro-Oesophageal Junction Cancer (KEYNOTE-061): A Randomised, Open-Label, Controlled, Phase 3 Trial. *Lancet* (2018) 392 (10142):123–33. doi: 10.1016/S0140-6736(18)31257-1
18. Wainberg ZA, Fuchs CS, Tabernero J, Shitara K, Muro K, Van Cutsem E, et al. Efficacy of Pembrolizumab Monotherapy for Advanced Gastric/Gastroesophageal Junction Cancer With Programmed Death Ligand 1 Combined Positive Score ≥10. *Clin Cancer Res* (2021) 27(7):1923–31. doi: 10.1158/1078-0432
19. Taieb J, Moehler M, Boku N, Ajani JA, Yañez Ruiz E, Ryu MH, et al. Evolution of Checkpoint Inhibitors for the Treatment of Metastatic Gastric Cancers: Current Status and Future Perspectives. *Cancer Treat Rev* (2018) 66:104–13. doi: 10.1016/j.ctrv.2018.04.004
20. Rosenbaum MW, Gonzalez RS. Targeted Therapy for Upper Gastrointestinal Tract Cancer: Current and Future Prospects. *Histopathology* (2021) 78 (1):148–61. doi: 10.1111/his.14244
21. Ji L, Qian W, Gui L, Ji Z, Yin P, Lin GN, et al. Blockade of β-Catenin-Induced CCL28 Suppresses Gastric Cancer Progression Via Inhibition of Treg Cell Infiltration. *Cancer Res* (2020) 80(10):2004–16. doi: 10.1158/0008-5472.CAN-19-3074
22. Yoshii M, Tanaka H, Ohira M, Muguruma K, Iwauchi T, Lee T, et al. Expression of Forkhead Box P3 in Tumour Cells Causes Immunoregulatory Function of Signet Ring Cell Carcinoma of the Stomach. *Br J Cancer* (2012) 106(10):1668–74. doi: 10.1038/bjc.2012.141
23. Lin C, He H, Liu H, Li R, Chen Y, Qi Y, et al. Tumour-Associated Macrophages-Derived CXCL8 Determines Immune Evasion Through Autonomous PD-L1 Expression in Gastric Cancer. *Gut* (2019) 68(10):1764–73. doi: 10.1136/gutjnl-2018-316324
24. Zhao R, Peng C, Song C, Zhao Q, Rong J, Wang H, et al. BICC1 as a Novel Prognostic Biomarker in Gastric Cancer Correlating With Immune Infiltrates. *Int Immunopharmacol* (2020) 87:106828. doi: 10.1016/j.intimp.2020.106828
25. Park HS, Kwon WS, Park S, Jo E, Lim SJ, Lee CK, et al. Comprehensive Immune Profiling and Immune-Monitoring Using Body Fluid of Patients With Metastatic Gastric Cancer. *J Immunother Cancer* (2019) 7(1):268. doi: 10.1186/s40425-019-0708-8
26. Kashimura S, Saze Z, Terashima M, Soeta N, Ohtani S, Osuka F, et al. CD83(+) Dendritic Cells and Foxp3(+) Regulatory T Cells in Primary Lesions and Regional Lymph Nodes Are Inversely Correlated With Prognosis of Gastric Cancer. *Gastric Cancer* (2012) 15(2):144–53. doi: 10.1007/s10120-011-0090-9
27. Vasaikar SV, Straub P, Wang J, Zhang B. LinkedOmics: Analyzing Multi-Omics Data Within and Across 32 Cancer Types. *Nucleic Acids Res* (2018) 46 (D1):D956–d963. doi: 10.1093/nar/gkx1090
28. Wang Z, Li X, Xu Y. Prediction of Overall Survival and Response to Immune Checkpoint Inhibitors: An Immune-Related Signature for Gastric Cancer. *Transl Oncol* (2021) 14(6):101082. doi: 10.1016/j.tranon.2021.101082
29. Shigemori T, Toiyama Y, Okugawa Y, Yamamoto A, Yin C, Narumi A, et al. Soluble PD-L1 Expression in Circulation as a Predictive Marker for Recurrence and Prognosis in Gastric Cancer: Direct Comparison of the

Clinical Burden Between Tissue and Serum PD-L1 Expression. *Ann Surg Oncol* (2019) 26(3):876–83. doi: 10.1245/s10434-018-07112-x
30. Takahashi N, Iwasa S, Sasaki Y, Shoji H, Honma Y, Takashima A, et al. Serum Levels of Soluble Programmed Cell Death Ligand 1 as a Prognostic Factor on the First-Line Treatment of Metastatic or Recurrent Gastric Cancer. *J Cancer Res Clin Oncol* (2016) 142(8):1727–38. doi: 10.1007/s00432-016-2184-6
31. Wang F, Wu X, Li Y, Cao X, Zhang C, Gao Y. PFKFB4 as a Promising Biomarker to Predict a Poor Prognosis in Patients With Gastric Cancer. *Oncol Lett* (2021) 21(4):296. doi: 10.3892/ol.2021.12557
32. Gu Z, Li Y, Yang X, Yu M, Chen Z, Zhao C, et al. Overexpression of CLC-3 Is Regulated by XRCC5 and Is a Poor Prognostic Biomarker for Gastric Cancer. *J Hematol Oncol* (2018) 11(1):115. doi: 10.1186/s13045-018-0660-y
33. Duan R, Du W, Guo W. EZH2: A Novel Target for Cancer Treatment. *J Hematol Oncol* (2020) 13(1):104. doi: 10.1186/s13045-020-00937-8
34. Chammas P, Mocavini I, Di Croce L. Engaging Chromatin: PRC2 Structure Meets Function. *Br J Cancer* (2020) 122(3):315–28. doi: 10.1038/s41416-019-0615-2
35. Gan L, Yang Y, Li Q, Feng Y, Liu T, Guo W. Epigenetic Regulation of Cancer Progression by EZH2: From Biological Insights to Therapeutic Potential. *Biomark Res* (2018) 6:10. doi: 10.1186/s40364-018-0122-2
36. Yang Y, Zhu F, Wang Q, Ding Y, Ying R, Zeng L. Inhibition of EZH2 and EGFR Produces a Synergistic Effect on Cell Apoptosis by Increasing Autophagy in Gastric Cancer Cells. *Onco Targets Ther* (2018) 11:8455–63. doi: 10.2147/OTT.S186498
37. Wang C, Li X, Zhang J, Ge Z, Chen H, Hu J. EZH2 Contributes to 5-FU Resistance in Gastric Cancer by Epigenetically Suppressing FBXO32 Expression. *Onco Targets Ther* (2018) 11:7853–64. doi: 10.2147/OTT.S180131
38. Gan L, Xu M, Hua R, Tan C, Zhang J, Gong Y, et al. The Polycomb Group Protein EZH2 Induces Epithelial-Mesenchymal Transition and Pluripotent Phenotype of Gastric Cancer Cells by Binding to PTEN Promoter. *J Hematol Oncol* (2018) 11(1):9. doi: 10.1186/s13045-017-0547-3
39. Blom AM. The Role of Complement Inhibitors Beyond Controlling Inflammation. *J Intern Med* (2017) 282(2):116–28. doi: 10.1111/joim.12606
40. Ouyang Q, Zhang L, Jiang Y, Ni X, Chen S, Ye F, et al. The Membrane Complement Regulatory Protein CD59 Promotes Tumor Growth and Predicts Poor Prognosis in Breast Cancer. *Int J Oncol* (2016) 48(5):2015–24. doi: 10.3892/ijo.2016.3408
41. Holmes TD, Pandey RV, Helm EY, Schlums H, Han H, Campbell TM, et al. The Transcription Factor Bcl11b Promotes Both Canonical and Adaptive NK Cell Differentiation. *Sci Immunol* (2021) 6(57):eabc9801. doi: 10.1126/sciimmunol.abc9801
42. Gao Y, Dutta Banik D, Muna MM, Roberts SG, Medler KF. The WT1-BASP1 Complex Is Required to Maintain the Differentiated State of Taste Receptor Cells. *Life Sci Alliance* (2019) 2(3):3. doi: 10.26508/lsa.201800287
43. Sanchez-Niño MD, Fernandez-Fernandez B, Perez-Gomez MV, Poveda J, Sanz AB, Cannata-Ortiz P, et al. Albumin-Induced Apoptosis of Tubular Cells Is Modulated by BASP1. *Cell Death Dis* (2015) 6(2):e1644. doi: 10.1038/cddis.2015.1
44. Guo RS, Yu Y, Chen J, Chen YY, Shen N, Qiu M. Restoration of Brain Acid Soluble Protein 1 Inhibits Proliferation and Migration of Thyroid Cancer Cells. *Chin Med J (Engl)* (2016) 129(12):1439–46. doi: 10.4103/0366-6999.183434
45. Li L, Meng Q, Li G, Zhao L. Basp1 Suppresses Cell Growth and Metastasis Through Inhibiting Wnt/β-Catenin Pathway in Gastric Cancer. *BioMed Res Int* (2020) 2020:8628695. doi: 10.1155/2020/8628695
46. Wang X, Cao Y, BoPan B, Meng Q, Yu Y. High BASP1 Expression Is Associated With Poor Prognosis and Promotes Tumor Progression in Human Lung Adenocarcinoma. *Cancer Invest* (2021) 2021:1–14. doi: 10.1080/07357907.2021.1910290
47. Zheng X, Wang S, Hong S, Liu S, Chen G, Tang W, et al. CXCR4/Rhoa Signaling Pathway Is Involved in miR-128-Regulated Proliferation and Apoptosis of Human Thyroid Cancer Cells. *Int J Clin Exp Pathol* (2017) 10 (9):9213–22.
48. Liu P, Long P, Huang Y, Sun F, Wang Z. CXCL12/CXCR4 Axis Induces Proliferation and Invasion in Human Endometrial Cancer. *Am J Transl Res* (2016) 8(4):1719–29.
49. Hashimoto I, Koizumi K, Tatematsu M, Minami T, Cho S, Takeno N, et al. Blocking on the CXCR4/mTOR Signalling Pathway Induces the Anti-Metastatic Properties and Autophagic Cell Death in Peritoneal Disseminated Gastric Cancer Cells. *Eur J Cancer* (2008) 44(7):1022–9. doi: 10.1016/j.ejca.2008.02.043

Conflict of Interest: The authors declare that the research was conducted in the absence of any commercial or financial relationships that could be construed as a potential conflict of interest.

frontiers in Oncology

REVIEW
published: 03 January 2022
doi: 10.3389/fonc.2021.716042

Deciphering the Immune–Tumor Interplay During Early-Stage Lung Cancer Development *via* Single-Cell Technology

Wei-Wei Chen[1†], Wei Liu[2†], Yingze Li[3†], Jun Wang[2†], Yijiu Ren[3], Guangsuo Wang[4], Chang Chen[3*] and Hanjie Li[2*]*

[1] Department of Clinical Oncology, University of Hong Kong, Hong Kong, Hong Kong SAR, China, [2] CAS Key Laboratory of Quantitative Engineering Biology, Shenzhen Institute of Synthetic Biology, Shenzhen Institutes of Advanced Technology, Chinese Academy of Sciences, Shenzhen, China, [3] Department of Thoracic Surgery, Shanghai Pulmonary Hospital, Tongji University School of Medicine, Shanghai, China, [4] Department of Thoracic Surgery, Shenzhen People's Hospital, The Second Clinical Medical College, Jinan University, The First Affiliated Hospital, Southern University of Science and Technology, Shenzhen, China

OPEN ACCESS

Edited by:
Peter Brossart, University of Bonn, Germany

Reviewed by:
Hyun-Sung Lee, Baylor College of Medicine, United States
Farrah Kheradmand, Baylor College of Medicine, United States
Sebastian Marwitz, Research Center Borstel (LG), Germany

***Correspondence:**
Guangsuo Wang
wgswy01@163.com
Chang Chen
chenthoracic@163.com
Hanjie Li
hj.li@siat.ac.cn

†These authors have contributed equally to this work

Specialty section:
This article was submitted to Cancer Immunity and Immunotherapy, a section of the journal Frontiers in Oncology

Received: *14 June 2021*
Accepted: *08 November 2021*
Published: *03 January 2022*

Citation:
Chen W-W, Liu W, Li Y, Wang J, Ren Y, Wang G, Chen C and Li H (2022) Deciphering the Immune–Tumor Interplay During Early-Stage Lung Cancer Development via Single-Cell Technology. Front. Oncol. 11:716042. doi: 10.3389/fonc.2021.716042

Lung cancer is the leading cause of cancer-related death worldwide. Cancer immunotherapy has shown great success in treating advanced-stage lung cancer but has yet been used to treat early-stage lung cancer, mostly due to lack of understanding of the tumor immune microenvironment in early-stage lung cancer. The immune system could both constrain and promote tumorigenesis in a process termed immune editing that can be divided into three phases, namely, elimination, equilibrium, and escape. Current understanding of the immune response toward tumor is mainly on the "escape" phase when the tumor is clinically detectable. The detailed mechanism by which tumor progenitor lesions was modulated by the immune system during early stage of lung cancer development remains elusive. The advent of single-cell sequencing technology enables tumor immunologists to address those fundamental questions. In this perspective, we will summarize our current understanding and big gaps about the immune response during early lung tumorigenesis. We will then present the state of the art of single-cell technology and then envision how single-cell technology could be used to address those questions. Advances in the understanding of the immune response and its dynamics during malignant transformation of pre-malignant lesion will shed light on how malignant cells interact with the immune system and evolve under immune selection. Such knowledge could then contribute to the development of precision and early intervention strategies toward lung malignancy.

Keywords: tumorigenesis, early-stage lung cancer, single-cell sequencing technology, immune-editing, immune evasion, tumor immunology

INTRODUCTION

As a life-threatening disease, lung cancer was estimated to cause more than 1.8 million deaths per year all over the world, with a 5-year survival rate of less than 20% (1). Based on the pathological type, lung cancer is divided into small cell lung cancer and non-small cell lung cancer (NSCLC), with the latter accounting for approximately 85% of the cases (1, 2). The histological subtypes of lung cancer are complex and highly various, which makes it challenging for the early diagnosis and treatment of lung cancer. Thus, accurate and comprehensive clinicopathological classification is critical in guiding the clinical treatment and predicting the prognosis of lung cancer (3–5). In 2016, the International Association for the Study of Lung Cancer (IASLC) proposed the 8th edition of TNM staging. Lung adenocarcinoma (LUAD) and its precursors range from atypical adenomatous hyperplasia, invasive adenocarcinoma *in situ*, micro-invasive adenocarcinoma, to eventually invasive lung adenocarcinoma (6). If lung cancer can be identified and treated at an early stage, before angiogenesis and invasion, patients have a greater chance of better disease control rate and survival rate.

Although many therapies, including chemotherapy, radiosurgery, targeted therapy, and immunotherapy, have been applied for lung cancer treatment, the 5-year survival rate is only 50% for patients with early-stage lung cancer (7). Surgery accounts for the primary first-line treatment for patients with early-stage lung cancer (8). However, patients with early-stage lung cancer may be diagnosed as multiple lesions, which occurs in 30%–50% of early-stage lung cancer (9). Besides, multiple lesions may occur simultaneously or successively in patients with lung cancer (10). There are great limitations in the radical and surgical treatment for multifocal early lung adenocarcinoma, while chemotherapy and targeted therapy cannot ameliorate the dilemmas, either. Thus, it is urgent to develop a novel therapy regimen for patients with early-stage lung cancer. With the recent development of tumor immunology, immunotherapy has provided new options for lung cancer patients (11–13). The emergence of immune checkpoint inhibitors has opened a new era of cancer therapy. Anti-PD-1/PD-L1 immunotherapy, an immune normalization therapy, selectively reinvigorates the anti-tumor immune responses in the tumor microenvironment (TME) with fewer immune-related adverse events (14, 15). Immunotherapy combined with surgery shows impressive clinical benefits in early-stage resectable NSCLC (16). Numerous ongoing clinical trials of immunotherapies and the novel combination therapies suggest that immunotherapies can be an optimal treatment strategy for unresectable early-stage NSCLC (14). However, the 5-year survival rate in NSCLC patients after combined surgery with immunotherapy treatment is still not ideal (17, 18). On the other hand, patients with the same TNM stage showed different prognosis outcomes after immunotherapy (19). Therefore, despite its success, it is still pressing to disentangle the complicated interactions between the immune system and tumor progression for developing novel and more effective strategies for the immune diagnosis and immunotherapies of lung cancer (20–22).

Profiling of the molecular states of all cell types within the lung tissue is currently revolutionizing the discovery of the mechanisms of lung cancer development (23) and can provide plentiful novel insights into the immune–tumor interplay in the early stage of lung cancer (24). The single-cell sequencing technologies in transcriptomics, genomics, epigenomics, proteomics, metabolomics, and spatial information have revolutionized biomedical research. The application of these tools enables the multidimensional study of organs, from cell atlas profiling, cell fate determination, cell–cell interaction to spatial construction (25, 26). Single-cell multi-omics have also emerged in recent years. All aspects of the cell, including a full history of its molecular states, spatial positions, and environmental interactions can be examined at the level of single cell by multimodal technologies and integrated computational methods (27). These methods demonstrated the power of simultaneously characterizing multiple levels of the immune response, which may boost our understanding of the underlying molecular mechanisms on how tumor evolves, and therefore contribute to the early detection and treatment of lung cancer by aiding the rational design of innovative diagnostic and personalized management approaches for patients (28, 29) (**Table 1**). Here, we discuss recent progress in employing multidimensional single-cell sequencing technologies to investigate the initiation and development processes of the pre-malignant lesion into lung cancer.

GENERAL TUMOR EVOLUTION PROCESS AND UNIQUE CHARACTERISTICS IN THE EARLY STAGE OF LUNG CANCER

The development of lung cancer is a multistep process defined by spatiotemporal interactions between heterogeneous cell types, including the malignant, immune, and stromal cells in a complex ecosystem (48). The functional diversity of immune cells is especially critical for the generation of the different regulator and effector responses required to safeguard the host against cancer, while survived tumor cells evolve to actively evade immune surveillance (49). The innate and adaptive arms of our immune system act as a complementary network of self-defense against the early progression from normal to malignant (50). Despite the fact that the immune system can identify and destroy nascent tumor cells, it can also be hijacked to promote tumor initiation and progression (51, 52). The dual anti-tumor and pro-tumor roles of immunity are referred to as cancer immunoediting (50). Immunoediting consists of three processes that function to control and shape cancer development either independently or in sequence. In the elimination phase, innate and the adaptive immune systems recognize transformed cells and destroy them, resulting in a return to normal physiological tissue (53). However, if antitumor immunity fails to eliminate transformed cells (also known as immunoselection), survived tumor cells may enter into the equilibrium phase, when the adaptive immunity prevents tumor outgrowth (53). Then, these cell variants may eventually

TABLE 1 | Important discoveries of single-cell technology in the evolution of early-stage lung cancer.

Fields of Lung Cancer	Years	Pathological Type	Conclusions	Reference
Tumor Heterogeneity	2015	LUAD	Identified intratumoral and intertumoral heterogeneity and the correlation with prognosis	(30)
	2017	SCLC	Proposed a novel mutation profile and expression characteristics of SCLC	(31)
	2020	LUAD	Detected heterogeneity at the molecular level in each tumor and stromal cells of GGN more effectively	(32)
	2021	LUAD	Characterized the heterogenetic of tumor cells, immune cells, and stromal cells in SSN lesions	(33)
Evolution and Metastasis	2014	NSCLC	Detected the differential expression in metastasis-associated cancer initiation cells	(34)
	2020	LUAD	Revealed the progression of lung adenocarcinoma mainly depends on tumor cell reprogramming	(35)
	2020	LUAD	Discovered a cluster of tumor cells with high plasticity and the potential to transform into different states	(36)
	2021	LUAD	Analyzed unravel cell populations, states, and phenotypes in the spatial and ecologic evolution	(37)
Tumor Metabolic	2017	LUAD	Found a new metabolic phenotype of lung cancer and provide a theoretical framework	(38)
	2019	LUAD	Analyzed different expressed genes of single malignant cells with different metabolic phenotypes	(39)
Lung Cancer Treatment	2015	LUAD (cell line)	Revealed different expression patterns of individual cells induced by molecular targeted drug therapy resistance	(40)
	2021	LUAD	Characterized the different tumor microenvironment and provided prognostic information	(41)
Tumor Microenvironment	2017	LUAD	Analyzed the early immune cells, especially the innate immune cells and their molecular profiles	(42)
	2018	NSCLC	Showed the landscape of stroma and immune cells of NSCLC	(43)
	2018	NSCLC	Explored the heterogeneity and characteristics of T cells in TME	(44)
	2020	NSCLC	Reveals the diversity of B cells in the early stage of non-small cell lung cancer	(45)
	2021	NSCLC	Verified the enrichment of different macrophage subtypes in lung cancer	(46)
	2021	LUAD	Characterize shifts in the TME from early to advanced lung cancer	(47)

LUAD, lung cancer adenocarcinoma; NSCLC, non-small cell lung cancer; SCLC, small cell lung cancer; GGN, ground glass nodule; SSN, subsolid nodule; CNV, copy number variation.

acquire further mutations that help them evade immune surveillance, and progress to clinically detectable malignancies in the escape phase (54).

The immune responses in the process of lung cancer evolution gradually transit from immune activation to immunosuppression, characterized by decreased T-cell clonotypes, increased infiltration of regulatory T cells, and the reduced infiltration of cytotoxic T cells and anti-tumor helper T cells (55). Meanwhile, the driver mutations, chromosomal copy number aberrations, and abnormal epigenetic events in tumor cells work together to influence host immune responses (56). These results reveal that the early development of lung cancer is a continuous and gradual process modulated by the immune-editing mechanism (**Figure 1**). However, it was demonstrated that the precancerous mutated cells in some early-stage lung cancer patients were already able to suppress the immune system and escape the immune surveillance before the invasive stage, which is contradictive to the supposed elimination phase of immune-editing theory (57, 58). Thus, the developmental process in the early stage of lung cancer does not have to go through the three immune-editing phases in sequence. Some early mutations can confer the tumor cells with strong immunosuppressive capability, paralyzing anti-tumor immune responses to early tumor development (59). Consequently, those tumor cells might skip the elimination and equilibrium phase and jump into the "escape" phase. Besides, the highly heterogeneous tumor immune microenvironments of individual patients also limit the wide applicability of the immune-editing theory. Furthermore, the detailed regulatory pathways that determine the phase transition during the

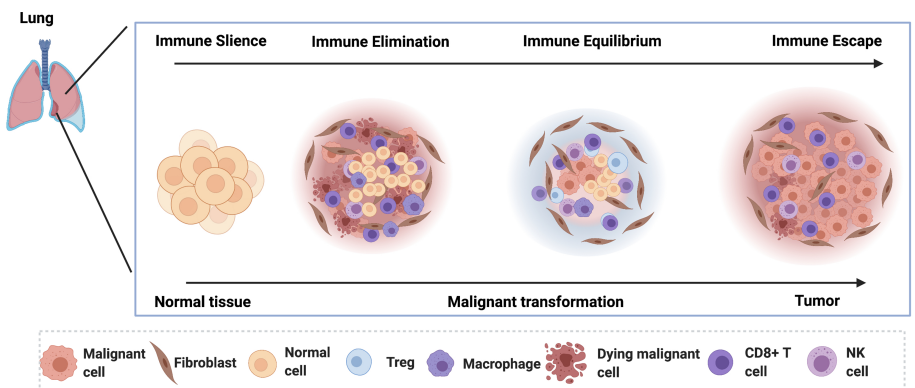

FIGURE 1 | The lung cancer tumorigenesis in the early stage of lung cancer is depicted. In the pre-lesion, the immune cells dominate the microenvironment and eliminate the malignant cells by inducing the cell death. In the immune equilibrium phase, the malignant cells become quiescent under the control of the activated immune cells. As the disease progress, the malignant cells escape the immune surveillance.

immune-editing process remain elusive. Conventional strategies using bulk cell populations are unable to fully delineate the various cell types and states engaged in the immune process toward malignancy, impeding further the investigation and precise interventional therapy (60). By contrast, single-cell techniques can classify the individual cells, gain into the multi-dimensional interactions between the tumor and the immune system, characterize the variations in their molecular profiles and developmental processes, and then contribute to the development of novel and practical strategies for the immune diagnosis and intervention of early-stage lung cancer (61) (**Table 2**). Here, we will highlight current findings and the potential application of single-cell technology in deciphering the evolution process of early stage of lung cancer.

APPLICATION OF SINGLE-CELL TECHNOLOGIES IN THE EARLY STAGE OF LUNG CANCER

Single-Cell RNA Sequencing in the Early Stage of Lung Cancer

Single-cell RNA sequencing (ScRNA-seq) technologies allow the dissection of the gene expression at single-cell resolution, revolutionizing transcriptomic studies from various aspects such as cell clustering, trajectory inference, differential expression calling, alternative splicing, allelic expression, and gene regulatory network reconstruction (64). These techniques have paved the way for the discovery of previously unknown cell types and subtypes in the normal and diseased lung, especially facilitating the study of rare cells (65). Furthermore, scRNA-seq can characterize immune cells and tumor cells in an unbiased manner at the same time (66).

The analysis of the single-cell transcriptomes of the seven stages of the mouse lung tumors, from pre-neoplastic hyperplasia to adenocarcinoma, found that the diversity of transcriptional states in the tumor and immune cells increased over time (36). In human subjects, a scRNA-seq study of 16 subsolid nodules samples and 6 adjacent normal lung tissues revealed that the cytotoxic natural killer T cells were dominant in the TME of subsolid nodules, and the malignant cells in the subsolid nodules underwent strong metabolic reprogramming and immune stress (67). Besides, a scRNA-seq analysis of ground-glass nodules (GGNs) demonstrated that the proliferation of the cancer cells was inhibited, and the immune cells were more activated in the GGN, compared with the activated proliferation of the cancer cells and the suppressive immune cells in the solid adenocarcinoma (32). A study of a total of 16 subsolid nodules (SSNs) samples from 16 treatment-naive patients provided single-cell transcriptomic profiling of SSN and their TME and indicated that SSNs exhibited more indolent biological behaviors than solid LUAD, that cytotoxic natural killer/T cells dominated in the TME of SSN, that malignant cells in SSN underwent enhanced immune stress, and that the subtype composition of endothelial cells

TABLE 2 | Summary of advantages and disadvantages of current single-cell sequencing platforms in studying the evolution of early-stage LUAD.

Molecular level	mRNA		mRNA+ Protemoics	Genome	Epigenome
Method	**Smart-seq2**	**Droplet-based scRNA-seq**	**CITE-seq, Mars-seq**	**SNS, SCI-seq**	**sciATAC-seq; scATAC-seq**
Indications	Alternative splicing of genes	Differential gene expression calling Allelic expression of genes Gene regulatory network reconstruction dynamic changes and heterogeneity cell percentage and subtypes Cell trajectory inference	Analysis of targeted populations;phenotypic classifications based on surface protein and transcriptomic	Recording of the interaction between mutant tumor cells and the immune cells' behaviors The cell clonal evolution	Epigenetic biomarkers for early cancer diagonstic and epigentic regulation of genes
Advantages	Full-length transrcpit to find the mutation and splicing alteration of tumor cell	Available commercial kits High content to identify different types and heterogeneity Sufficient quantity and quality of gene detections	Rare cell-type dicovery and more presice in cell phenotype identification	Genetic deterministic genes in governing the emergence and maintenance of heterogeneity and colonel evolution	Investigation of regulatory state transitions and chromatin- modifying proteins in malignant transformation
Disadvantages	Pathology misdiagnosis in early stage of lung cancer Hard to identify the lineage tracing of cell phenotypes and rare cell types Hard to characterize the clonality, inter-patient ITH, and initiation tumor site Require live cells and high sample quality		High cost; difficult to standarized in different labs	Missing information about transcriptional heterogeneity during tumor progression	Difficult to determine how cells navigate these regulatory transitions toward malignant
Reference	Marjanovic, N.D., et al. (36)	(33, 43, 45, 47, 62)	Lavin, Y., et al. (35); LaFave, L.M., et al. (42); Leader, Grout et al. (62)	Rooney, Shukla et al. (63)	LaFave, L.M., et al. (35); Marjanovic, N.D., et al. (36)

NSCLC, non-small cell lung cancer; Smart-seq2, Switching Mechanism At the end of the 5'-end of the RNA Transcript; scRNA, single-cell RNA sequencing; SNS, single-nucleus sequencing; SCI-seq, single-cell combinatorial indexed sequencing; scATAC-seq, Single-cell sequencing assay for transposase- accessible chromatin; ITH, intratumor heterogeneity; CITE-seq, cellular Indexing of Transcriptomes and Epitopes by Sequencing; Mars-seq, massively parallel single-cell RNA-Seq.

was more like that in normal lung samples in SSN (62). ScRNA-seq has unmasked the complexity and heterogeneity of tumor–immune interplay during the transformation from pre-malignant lesions to cancerous damage.

ScRNA-seq analysis also helps elucidate the detailed interactions between tumor cells and immune cells in the early stage of lung cancer. A multiscale single-cell profiling of 35 early-stage NSCLC lesions found that a key cellular module consisting of *PDCD1*$^+$ *CXCL13*$^+$ activated T cells, IgG$^+$ plasma cells, and *SPP1*$^+$ macrophages, closely associated with evasion of lung cancer cells (62). A scRNA-seq analysis of human and mouse lung tumors unveiled that tissue-resident macrophages accumulated close to tumor cells promoted epithelial–mesenchymal transition and invasiveness, and induced a potent regulatory T cell response that protected tumor cells from adaptive immunity during early tumor formation (46). Consistently, Lavin et al. also demonstrated that Treg and non-functional T cells were enriched but cytolytic natural killer cells were excluded in the early LUAD lesions (42). Furthermore, Guo, Zhang et al. showed that there was a significant proportion of inter-tissue effector T cells with a highly migratory nature and that a high ratio of "pre-exhausted" to exhausted T cells was associated with a better prognosis of lung adenocarcinoma (42, 44). In addition, a study of seven stage-I/II LUAD samples harboring *EGFR* mutations and five tumor-adjacent lung tissues revealed that the adenocarcinoma cells were characterized by activated cell proliferation and antigen presentation to immune cells (68).

By comparing malignant lung samples with the non-malignant counterparts, scRNA-seq also uncovered the different and plastic interaction patterns between immune cells and normal cells or malignant cells. Lambrechts et al. identified some heterogeneous sub-subpopulations in stromal cells and the transcription factors that regulate their heterogeneity in the early LUAD patients by scRNA-seq (43). ScRNA-seq analysis of 10 normal lung tissues and 10 fresh LUAD tissues found that the TME was composed of cancer-associated myofibroblasts, exhausted CD8$^+$ T cells, proinflammatory monocyte-derived macrophages, plasmacytoid dendritic cells, myeloid dendritic cells, anti-inflammatory monocyte-derived macrophages, normal-like myofibroblasts, NK cells, and conventional T cells (69). Multi-region of five early-stage LUADs and 14 multi-region normal lung tissues found that the Treg$^+$ cells are increased in normal tissues with proximity to LUAD and the signatures and fractions of cytotoxic CD8+ T cells, antigen-presenting macrophages, and inflammatory dendritic cells were decreased (37).

ScRNA also unveiled the different characteristics of tumor–immune interplays between early-stage and advanced-stage LUAD. Compared with the early-stage LUAD, scRNA-seq demonstrated the naïve-like B cells decreased in advanced NSCLC, and their lower number was associated with poor prognosis (45). Based on scRNA-seq data of 29 lung samples of different developmental stages, Chen, Huang et al. found that advanced malignant cells exhibited a remarkably more complex TME and higher intratumor heterogeneity level than early malignant cells. In terms of immune cells, the proportions of CD8$^+$/cytotoxic T cells, Treg+ T cells, and follicular B cells remarkedly differed in early and advanced LUAD. Notably, the ligand-receptor analysis found that the GNAI2-DRD2 and C4B-CD46 pairs were only detected in advanced LUAD, while COL3A1-MAG, HLA-C-SLC9C2, and COL2A1-MAG were uniquely expressed in early LUAD (47).

Collectively, scRNA-seq has helped characterize the cellular phenotypes of various immune and tumor cell types and reveal their interactions within the TME during the development of lung cancer. However, there are many limitations by now. One of the major challenges is the paucity of human patient samples available for scRNA-seq in the early stage of lung cancer. Further validation by alternative methods or larger patient cohorts is required (70). Furthermore, sample quality is a big issue because it is impossible to separate the LUAD featured with ground glass nodules from solid adenocarcinoma by pathological methods when studying the initiation of LUAD (45). Moreover, the scRNA-seq lacks the power to distinguish the ground glass opacification part and the solid part in the same LUAD, which is vital to identify the initiation site of the cellular activation module. Furthermore, it is difficult to interpret the evolution process of specific cells, identify cell phenotypes for lineage tracing, acquire cell surface antigens information, characterize the intratumor clonal heterogeneity and inter-patient clonal heterogeneity, and identify genomic alterations by scRNA-seq. Therefore, we will further discuss other single-cell techniques and their potential applications in the investigation of early-stage lung cancer development.

Single-Cell Genome Sequencing in the Early Stage of Lung Cancer

In the initiation of lung cancer, a single normal cell gradually evolves into a malignant tumor cell and forms distinct subpopulations, which then lead to intratumoral heterogeneity and clonal diversity by genomic alterations (71). Copy number variations or single-nucleotide variations in *EGFR, RBM10*, *MET, BRAF, K-Ras*, and *TP53* were found to be functionally important in the evolution of lung cancer (72). The genome doubling and ongoing dynamic chromosomal instability in *CDK4, FOXA1*, and *BCL11A* also resulted in the progression of lung cancer (73, 74). These genomic alterations are also present in early-stage lung cancer cells, determining their sensitivity to the immune cells and associating with immune cells' phenotypes (75). For example, patients harboring *KRAS* mutations displayed significantly lower levels of dysfunctional immune T-cell markers: PD-1 and TIM-3, in the tumors than those with wild-type *KRAS*, which indicated a suppressive immune microenvironment in *EGFR*-mutated tumors (76). Furthermore, it was found that the *ADCY8*, *PIK3CA*, and *CDKN2A* mutations were associated with remarkedly decreased expression of the immune-inhibitory ligand: PD-L1 (77), which indicated an upregulated immune response in early-stage lung cancer patients with these gene mutations. McGranahan et al. demonstrated the positive association of high tumor mutation burdens with more activated CD8$^+$ T cells and higher levels of PD-L1 expression in early-stage NSCLC (78).

Although these results revealed the important roles of gene mutations in the early stage of lung cancer by interacting with

the immune system, most of the results derived from the sequencing data of bulk tumor cells, which is difficult to unmask the deeper underlying genotypic and phenotypic heterogeneity that exists inter- and intra-tumors. Furthermore, the number of cells harboring the mutations and the zygosity of these mutations cannot be accurately assessed by bulk genome sequencing (79). Moreover, current findings were insufficient to clarify the interactions between the individual mutant tumor cells and the immune cells when the normal epithelial cells transformed to malignant cells (63). Meanwhile, it remains unclear how the components of adaptive immune system individually respond to the transformation at the genome level (80). Single-cell DNA sequencing may overcome these obstacles by detecting the founder mutations and sub-clonal mutations in tumor cells at a single-cell level (81). Further application of the newly developed single-genome technique, such as SNS-seq (single-nucleus sequencing), LIANT (single-cell whole-genome analyses by linear amplification *via* transposon insertion), and SCI-seq (single-cell combinatorial indexed sequencing) (82) may unravel the clonal relationship between different malignant cells and dissect the immune responses contributed by the genomic elements of the individual cells during the progression from pre-malignant lesion to advanced oncogenesis (83).

Single-Cell Epigenome Sequencing in the Early Stage of Lung Cancer

Cellular heterogeneity of individual cells within the tumor–immune ecosystem is displayed not only in the genome and transcriptome, but also in the epigenome. Epigenetic alterations, including DNA methylation, histone modifications, and non-coding RNA expression, have been reported to play an important role in the tumorigenesis of lung cancer (84, 85). At the epigenetic level, the histone H3 lysine 36 methyltransferase NSD3 could promote the development of lung squamous cell carcinoma (86). The DNA methyltransferase inhibitors and histone deacetylase inhibitors could reverse tumor immune evasion in NSCLC by modulating the T-cell exhaustion state towards the memory and effector T-cell phenotypes (87, 88). Besides, the antigen presentations of the immune cells are also altered by epigenetic modulations with the hypomethylating agents or histone deacetylase inhibitors (89). These findings demonstrated the vital roles of epigenetic regulation in cancer evolution. However, the detailed mechanisms of how these epigenetic events modulate the immunoediting process in specific cell types remain unclear during lung cancer early development.

Single-cell epigenome profiling methods include scATAC-seq (assay for transposase-accessible chromatin in single cells with sequencing), scCHIP-seq (single-cell chromatin immune-precipitation followed by sequencing), sciHi-C (single-cell combinatorial indexed Hi-C), and scCUT&Tag (single-cell cleavage under targets & tagmentation) (90–93). ScATAC-seq can reveal the chromatin accessibility landscape that governs the transcriptional regulation in different cell populations (94). Sn-m3C-seq (single-nucleus methyl-3C sequencing) can give information about chromatin organization and DNA methylation and distinguish the heterogeneous cell types (95). Smart-RRBS (single-cell methylome and transcriptome analysis) can detect the methylation status in the promoters of specific tumor suppressor genes and the overall number of hypermethylated genes, which increases with the neoplastic progression from hyperplasia to adenocarcinoma (96). A scATAC-seq analysis of the K-Ras+/LSLG12D;p53frt/frt (KP) mouse model found that the cancer cells were tightly regulated by the smarca4, which regulated the activity of the lung lineage SWI/SNF transcription factor and ultimately accelerated tumor progression (35). Using the KP mice and sciATAC-seq (combinatorial indexing to identify single cells without single-cell isolation for chromatin accessibility), LaFave, Kartha et al. also defined co-accessible regulatory programs and inferred key activating and repressive chromatin regulators of epigenetic changes in the tumor cells, including RUNX transcription factors (which are predictive biomarkers for the survival of LUAD patients) (35).

Together, these results demonstrated the power of single-cell epigenomics to identify regulatory programs and key biomarkers during tumor progression. Combined single-cell methods have also emerged to allow analyses of epigenetic–transcriptional correlations, thereby enabling detailed investigations of how epigenetic states modulate cell phenotypes and the immune editing process.

Single-Cell Proteomics in the Early Stage of Lung Cancer

Although single-cell transcriptomic, genomic, and epigenomic methods have been informative about gene expression and genome landscapes and have demonstrated vital basic research and clinical value in lung cancer, information on proteins is also important and necessary since proteins are the cellular workhorses (97). Methods of protein detection at the single-cell level include flow cytometry, Sc-MS (liquid chromatography mass spectrometry-based single-cell proteomics), ScoPE (isobaric labeling for single-cell proteomics), CyTOF (cytometry by time-of-flight), SCITO-seq (single-cell combinatorial indexed cytometry sequencing), CITE-seq (cellular indexing of transcriptomes and epitopes by sequencing), Mars-seq (massively parallel single-cell RNA-Seq), and SCPFC (single-cell phospho-specific flow cytometry) (98–100). Some of these methods can simultaneously measure multiple cellular proteins and RNA at the single-cell level.

Leader Grout et al. applied CITE-seq combining phenotypic classifications based on surface protein expression and transcriptomic profile, to characterize the cellular classification and increase our understanding of the immune cellular landscape in the mouse model of early-stage lung cancer (62). Lin et al. utilized SCPFC in the investigation of signaling network interactions and unraveled the dynamic changes of tyrosine phospho-Stat1 (pStat1) in lung cancer cells in a mouse model (101). More recently, Rahman et al. performed a CyTOF analysis of cell suspensions derived from tissues of early-stage LUAD

after surgical resection. They found that high levels of cerium were specifically associated with a phenotypically distinct subset of lung macrophages that were most prevalent in noninvolved lung tissue, whereas tumor-associated macrophages had lower levels of cerium (99). The CyTOF combined with mars-seq2 fully characterized the immune landscape of early-stage LUAD and distinguished the immune changes driven by the tumor lesion from those driven by the lung tissue (42).

In sum, single-cell proteomics can add another dimension to clarify the substantial heterogeneity and complicated interaction among seemingly identical cells at the genome level, significantly contributing to the quantitative understanding of the developmental mechanisms of early-stage lung cancer.

Single-Cell Metabolic Profiling in the Early Stage of Lung Cancer

The metabolic reprogramming is fundamental to both cancer cells and responding immune cells during cancer development (102, 103). Moreover, metabolic heterogeneity and plasticity exist in diverse cells, especially in the immune cells responding to cancer cells (104–106). A recent finding indicated that lactate acid secreted by the glycolytic cancer cells favored the activation of the immune cells toward an immunosuppressive phenotype (107). In addition, the cancer cells could harness the metabolic by-products to induce the immune suppressive microenvironment (108).

The single-cell metabolomics field is at its very early stage at this moment. The sc-MS (single-cell metabolic profiling by mass cytometry) (109, 110) and the SCENITH (Flow Cytometry-Based Method to Functionally Profile Energy Metabolism with Single-Cell Resolution) were recently developed (111). These technologies could reveal global metabolic functions and determine complex and linked immune phenotypes in rare cell subpopulations (112, 113).

Lineage Tracing Combined With Single-Cell Sequencing in the Early Stage of Lung Cancer

Another long-standing quest is to understand the developmental origin and the cell fate determination of each cell within a tissue (114). Cell states are highly flexible and present multipotent characteristics before reaching differentiation destination. A comprehensive study of the molecular alterations during cell fate determination would be useful to better clarify those steps involved in the precancerous stage of lung tumor. Using the methods of lineage tracing with single-cell technology such as CellTaging (a combinatorial cell indexing approach), TracerSeq (transposon-based barcoding sequencing), scGESTALT (single-cell genome editing of synthetic target arrays for lineage tracing), and MEMOIR (memory by engineered mutagenesis with optical *in situ* readout), we can investigate an individual cell early and track the states of its clonal progeny at a later time point *via* sequencing of the inherited DNA sequences, or "barcodes" (115–117). These methods offer an opportunity to integrate complementary information about both cell lineage and cell states into synthetical views of cell a differentiation destination and dynamic interactions between the tumor and immune cells (118, 119). ScRNA-seq combined with lineage tracing allows simultaneous measurement of cell identity and developmental origin at single-cell resolution (119). Zepp et al. revealed that the transformation from the alveolar type 1 progenitor cells to alveolar type 2 cells in the mesenchymal alveolar niche of the lung is important for the tissue injury response by combining scRNA-seq and signaling lineage reporter system (58, 120). Furthermore, Wellenstein et al. tracked the fate determination process of immune cells in response to the antigens expressed specifically on the surface of nearby tumor cells during the immune editing process (121). Labeling cell subpopulations across the lung region by the Dre-Rox or Cre-LoxP recombination system together with single-cell sequencing technology has potential to be used for simultaneously investigating the reciprocal evolution of tumor cells and immune cells as well as their fate determinations in the lesion at the initial stage (122, 123).

Together, parallel advances in single-cell sequencing techniques and lineage tracing methods facilitate the mapping of the clonal relationships onto the tumor immune landscape and help decipher the crosstalk between the tumor and immune cells during the whole developmental process.

Single-Cell Spatial Omics in the Early Stage of Lung Cancer

Recent advances in spatially resolved methods allow us to achieve transcriptional cell-type classifications, map cellular spatial distributions in tissues, and reveal the intracellular and intercellular networks in lung tumors (124). Genome sequencing analyses of 25 spatially distinct regions of early-stage NSCLC found that the driver mutations displayed sub-clonal diversification in different regions, embodying the value of combining spatial information with sequencing data in deciphering the mechanism of the evolution of lung cancer cells (125). Many single-cell spatial transcriptomics combines spatial barcoding-based methods (ST, Visium, HDST, Slidesee, Naostring, GeoMx, DBiT-seq, and Zipcode) and imaging-based methods (osm-FISH, MERFISH, SeqFish, STARMAP, and FISSEQ) (126–128). These technologies may deepen our understanding of the functional organization of the tissue and the cellular and molecular mechanism on how cancer cells modify their surroundings to generate an immune suppressive microenvironment in the early-stage lung cancer (126–128). Indeed, single-cell spatial transcriptomics has already started to be used to delineate the precise landscape of the TME and the crosstalk between the tumor and immune cells at both cellular and sub-cellular levels (129). A spatial transcriptomics analysis of LUAD and LUSC samples has demonstrated the spatial gene expression atlas and spatial heterogeneity variation between LUAD and LUSC as well as differences in normal and cancerous regions (130).

The immune responses occurring in the early stage of lung cancer are mediated by not only the cell–cell interaction, but also the coordinated actions of a diverse set of cytokines (131). In the early stage of lung cancer, the majority of the cytokines consists

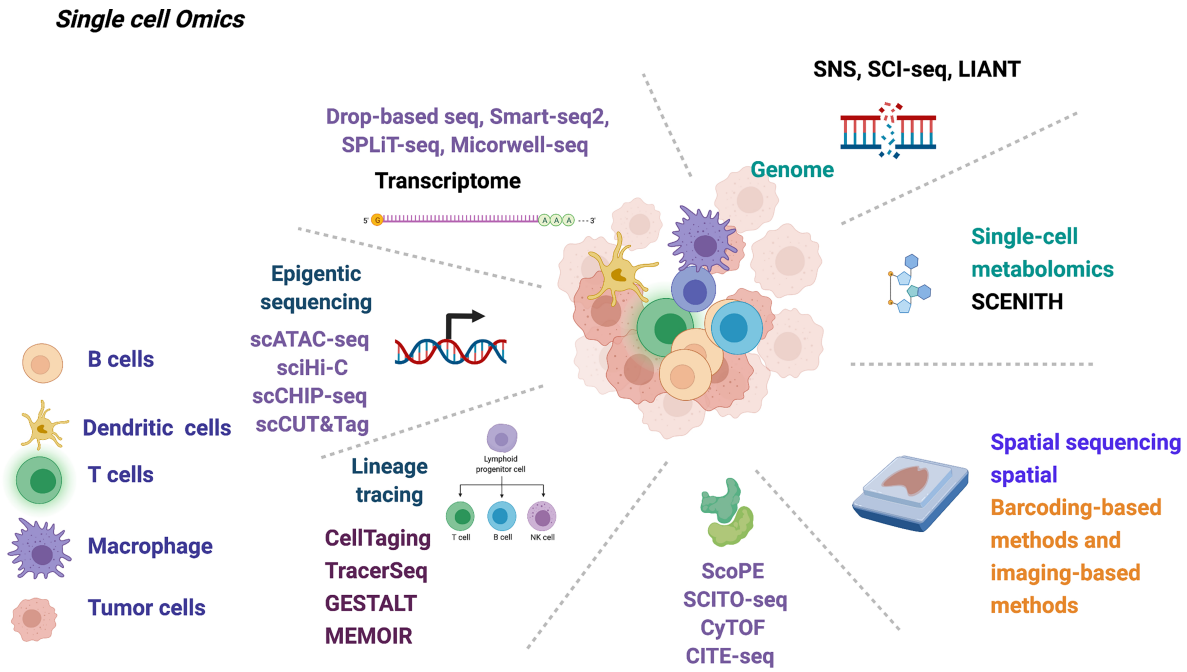

FIGURE 2 | Summary of current single-cell multi-omics technology that may be used in deciphering the early-stage lung cancer evolution.

of IFN-γ, IL-12, and TNF-α, whereas the concentration of the pro-angiogenic cytokine VEGF is extremely low (132, 133). These cytokines are crucial for regulating the immune equilibrium. However, the spatial localization of tissue-resident immune or tumor cells producing specific modulatory cytokines remains elusive. The application of the spatial genomic sequencing method at the single-cell level can specifically identify the signaling interactions and communications between the immune and tumor cells in the early stage of lung cancer (115, 127). Together, analyzing single-cell gene expression in a spatially resolved context is critical for understanding the heterotypic interactions among the cells in the TME in the early stage of lung cancer.

CONCLUSION AND PERSPECTIVE

A comprehensive understanding of the tumor immune microenvironment is vital to treatment options and prognosis of lung cancer. Multi-omics simultaneous profiling of gene expression, genetic variation, epigenetic change, cell surface proteins, metabolic activities, and spatial information from the same single cell allows full and robust delineation of the developmental plasticity and immune-mediated pruning of the tumor cells from multiple dimensions during the early development of lung cancer (**Figure 2**).

The goal of tumor immunology research is to be able to manipulate the immune cells/molecules to prevent and treat cancer (134). A deeper understanding of the immune–tumor interplay during early-stage lung cancer by single-cell sequencing technology can help identify novel immunotherapy targets, determine which patients may benefit most from immunotherapy, and discover new mechanisms of resistance to immunotherapy (135).

In sum, our views of the applications of the multi-omics single-cell techniques in the early stage of lung cancer will contribute to broadening their application in relevant basic research and boosting the development of immunotherapy for early-stage lung cancer.

AUTHOR CONTRIBUTIONS

All authors critically wrote and revised the manuscript. All authors contributed to the article and approved the submitted version.

FUNDING

The research was supported by the National Key R&D Program of China (2019YFA0906100 and 2020YFA0804100); the National Natural Science Foundation of China (32170919 and 92042305); Shanghai Pulmonary Hospital Innovation Team (FKCX1906); Shanghai Science and Technology Committee (20YF1441100, 20XD1403000, 18DZ2293400); Shenzhen Science and Technology Program (KQTD2016113015442590) and Natural Science Foundation of Guangdong (2021A1515010919).

REFERENCES

1. Siegel RL, Miller KD, Jemal A. Cancer Statistics, 2020. *CA Cancer J Clin* (2020) 70(1):7–30. doi: 10.3322/caac.21590
2. Wei W, Zeng H, Zheng R, Zhang S, An L, Chen R, et al. Cancer Registration in China and its Role in Cancer Prevention and Control. *Lancet Oncol* (2020) 21(7):e342–9. doi: 10.1016/S1470-2045(20)30073-5
3. Owada-Ozaki Y, Muto S, Takagi H, Inoue T, Watanabe Y, Fukuhara M, et al. Prognostic Impact of Tumor Mutation Burden in Patients With Completely Resected Non-Small Cell Lung Cancer: Brief Report. *J Thorac Oncol* (2018) 13(8):1217–21. doi: 10.1016/j.jtho.2018.04.003
4. Tavernari D, Battistello E, Dheilly E, Petruzzella AS, Mina M, Sordet-Dessimoz J, et al. Non-Genetic Evolution Drives Lung Adenocarcinoma Spatial Heterogeneity and Progression. *Cancer Discov* (2021) 11(6):1490–507. doi: 10.1158/2159-8290.CD-20-1274
5. Sharma A, Merritt E, Hu X, Cruz A, Jiang C, Sarkodie H, et al. Non-Genetic Intra-Tumor Heterogeneity Is a Major Predictor of Phenotypic Heterogeneity and Ongoing Evolutionary Dynamics in Lung Tumors. *Cell Rep* (2019) 29(8):2164–2174 e5. doi: 10.1016/j.celrep.2019.10.045
6. Detterbeck FC, Boffa DJ, Kim AW, Tanoue LT. The Eighth Edition Lung Cancer Stage Classification. *Chest* (2017) 151(1):193–203. doi: 10.1016/j.chest.2016.10.010
7. Gettinger S, Horn L, Jackman D, Spigel D, Antonia S, Hellmann M, et al. Five-Year Follow-Up of Nivolumab in Previously Treated Advanced Non-Small-Cell Lung Cancer: Results From the CA209-003 Study. *J Clin Oncol* (2018) 36(17):1675–84. doi: 10.1200/JCO.2017.77.0412
8. Manser R, Wright G, Hart D, Byrnes G, Campbell DA. Surgery for Early Stage Non-Small Cell Lung Cancer. *Cochrane Database Syst Rev* (2005) 2005 (1):Cd004699. doi: 10.1002/14651858.CD004699.pub2
9. Blandin Knight S, Crosbie PA, Balata H, Chudziak J, Hussell T, Dive C. Progress and Prospects of Early Detection in Lung Cancer. *Open Biol* (2017) 7(9):170070. doi: 10.1098/rsob.170070
10. Liu C, Li H, Xu K, Song S, He Y, Cai X, et al. Multiple Primary Lung Cancer Versus Intrapulmonary Metastatic Cancer: A Case of Multiple Pulmonary Nodules. *Thorac Cancer* (2019) 10(2):352–8. doi: 10.1111/1759-7714.12918
11. Riley RS, June CH, Langer R, Mitchell MJ. Delivery Technologies for Cancer Immunotherapy. *Nat Rev Drug Discovery* (2019) 18(3):175–96. doi: 10.1038/s41573-018-0006-z
12. Yang Y. Cancer Immunotherapy: Harnessing the Immune System to Battle Cancer. *J Clin Invest* (2015) 125(9):3335–7. doi: 10.1172/JCI83871
13. Ko EC, Raben D, Formenti SC. The Integration of Radiotherapy With Immunotherapy for the Treatment of Non-Small Cell Lung Cancer. *Clin Cancer Res* (2018) 24(23):5792–806. doi: 10.1158/1078-0432.CCR-17-3620
14. Rosner S, Reuss JE, Forde PM. PD-1 Blockade in Early-Stage Lung Cancer. *Annu Rev Med* (2019) 70:425–35. doi: 10.1146/annurev-med-050217-025205
15. Liu SY, Wu YL. Ongoing Clinical Trials of PD-1 and PD-L1 Inhibitors for Lung Cancer in China. *J Hematol Oncol* (2017) 10(1):136. doi: 10.1186/s13045-017-0506-z
16. Forde PM, Chaft JE, Smith KN, Anagnostou V, Cottrell TR, Hellmann MD, et al. Neoadjuvant PD-1 Blockade in Resectable Lung Cancer. *N Engl J Med* (2018) 378(21):1976–86. doi: 10.1056/NEJMoa1716078
17. Hoy H, Lynch T, Beck M. Surgical Treatment of Lung Cancer. *Crit Care Nurs Clin North Am* (2019) 31(3):303–13. doi: 10.1016/j.cnc.2019.05.002
18. Ghysen K, Vansteenkiste J. Immunotherapy in Patients With Early Stage Resectable Nonsmall Cell Lung Cancer. *Curr Opin Oncol* (2019) 31(1):13–7. doi: 10.1097/CCO.0000000000000497
19. Walk EE, Yohe SL, Beckman A, Schade A, Zutter MM, Pfeifer J, et al. The Cancer Immunotherapy Biomarker Testing Landscape. *Arch Pathol Lab Med* (2020) 144(6):706–24. doi: 10.5858/arpa.2018-0584-CP
20. Gonzalez H, Hagerling C, Werb Z. Roles of the Immune System in Cancer: From Tumor Initiation to Metastatic Progression. *Genes Dev* (2018) 32(19-20):1267–84. doi: 10.1101/gad.314617.118
21. O'Donnell JS, Teng MWL, Smyth MJ. Cancer Immunoediting and Resistance to T Cell-Based Immunotherapy. *Nat Rev Clin Oncol* (2019) 16 (3):151–67. doi: 10.1038/s41571-018-0142-8
22. Bruni D, Angell HK, Galon J. The Immune Contexture and Immunoscore in Cancer Prognosis and Therapeutic Efficacy. *Nat Rev Cancer* (2020) 20 (11):662–80. doi: 10.1038/s41568-020-0285-7
23. Zhang Y, Liu F. Multidimensional Single-Cell Analyses in Organ Development and Maintenance. *Trends Cell Biol* (2019) 29(6):477–86. doi: 10.1016/j.tcb.2019.02.006
24. Wu F, Fan J, He Y, Xiong A, Yu J, Li Y, et al. Single-Cell Profiling of Tumor Heterogeneity and the Microenvironment in Advanced Non-Small Cell Lung Cancer. *Nat Commun* (2021) 12(1):2540. doi: 10.1038/s41467-021-22801-0
25. Baslan T, Hicks J. Unravelling Biology and Shifting Paradigms in Cancer With Single-Cell Sequencing. *Nat Rev Cancer* (2017) 17(9):557–69. doi: 10.1038/nrc.2017.58
26. Gawad C, Koh W, Quake SR. Single-Cell Genome Sequencing: Current State of the Science. *Nat Rev Genet* (2016) 17(3):175–88. doi: 10.1038/nrg.2015.16
27. Hedlund E, Deng Q. Single-Cell RNA Sequencing: Technical Advancements and Biological Applications. *Mol Aspects Med* (2018) 59:36–46. doi: 10.1016/j.mam.2017.07.003
28. Greenberg AK, Yee H, Rom WN. Preneoplastic Lesions of the Lung. *Respir Res* (2002) 3(1):20–0. doi: 10.1186/rr170
29. Klebe S, Henderson DW. Facts and Fiction: Premalignant Lesions of Lung Tissues. *Pathology* (2013) 45(3):305–15. doi: 10.1097/PAT.0b013e32835f45fd
30. Min JW, Kim WJ, Han JA, Jung YJ, Kim KT, Park WY, et al. Identification of Distinct Tumor Subpopulations in Lung Adenocarcinoma *via* Single-Cell RNA-Seq. *PloS One* (2015) 10(8):e0135817. doi: 10.1371/journal.pone.0135817
31. Xiong D, Pan J, Yin Y, Jiang H, Szabo E, Lubet RA, et al. Novel Mutational Landscapes and Expression Signatures of Lung Squamous Cell Carcinoma. *Oncotarget* (2018) 9(7):7424–41. doi: 10.18632/oncotarget.23716
32. Lu T, Yang X, Shi Y, Zhao M, Bi G, Liang J, et al. Single-Cell Transcriptome Atlas of Lung Adenocarcinoma Featured With Ground Glass Nodules. *Cell Discov* (2020) 6:69. doi: 10.1038/s41421-020-00200-x
33. Xing X, Yang F, Huang Q, Guo H, Li J, Qiu M, et al. Decoding the Multicellular Ecosystem of Lung Adenocarcinoma Manifested as Pulmonary Subsolid Nodules by Single-Cell RNA Sequencing. *Sci Adv* (2021) 7(5):eabd9738. doi: 10.1126/sciadv.abd9738
34. Rothwell DG, Li Y, Ayub M, Tate C, Newton G, Hey Y, et al. Evaluation and Validation of a Robust Single Cell RNA-Amplification Protocol Through Transcriptional Profiling of Enriched Lung Cancer Initiating Cells. *BMC Genomics* (2014) 15:1129. doi: 10.1186/1471-2164-15-1129
35. LaFave LM, Kartha VK, Ma S, Meli K, Del Priore I, Lareau C, et al. Epigenomic State Transitions Characterize Tumor Progression in Mouse Lung Adenocarcinoma. *Cancer Cell* (2020) 38(2):212–.e13. doi: 10.1016/j.ccell.2020.06.006
36. Marjanovic ND, Hofree M, Chan JE, Canner D, Wu K, Trakala M, et al. Emergence of a High-Plasticity Cell State During Lung Cancer Evolution. *Cancer Cell* (2020) 38(2):229–46.e13. doi: 10.1016/j.ccell.2020.06.012
37. Sinjab A, Han G, Treekitkarnmongkol W, Hara K, Brennan PM, Dang M, et al. Resolving the Spatial and Cellular Architecture of Lung Adenocarcinoma by Multiregion Single-Cell Sequencing. *Cancer Discov* (2021) 11(10):2506–23. doi: 10.1158/2159-8290.CD-20-1285
38. Yu L, Lu M, Jia D, Ma J, Ben-Jacob E, Levine H, et al. Modeling the Genetic Regulation of Cancer Metabolism: Interplay Between Glycolysis and Oxidative Phosphorylation. *Cancer Res* (2017) 77(7):1564–74. doi: 10.1158/0008-5472.CAN-16-2074
39. Li Z, Wang Z, Tang Y, Lu X, Chen J, Dong Y, et al. Liquid Biopsy-Based Single-Cell Metabolic Phenotyping of Lung Cancer Patients for Informative Diagnostics. *Nat Commun* (2019) 10(1):3856. doi: 10.1038/s41467-019-11808-3
40. Suzuki A, Matsushima K, Makinoshima H, Sugano S, Kohno T, Tsuchihara K, et al. Single-Cell Analysis of Lung Adenocarcinoma Cell Lines Reveals Diverse Expression Patterns of Individual Cells Invoked by a Molecular Target Drug Treatment. *Genome Biol* (2015) 16:66. doi: 10.1186/s13059-015-0636-y
41. Kim M, Min YK, Jang J, Park H, Lee S, Lee CH. Single-Cell RNA Sequencing Reveals Distinct Cellular Factors for Response to Immunotherapy Targeting CD73 and PD-1 in Colorectal Cancer. *J Immunother Cancer* (2021) 9(7): e002503. doi: 10.1136/jitc-2021-002503
42. Lavin Y, Kobayashi S, Leader A, Amir E-AD, Elefant N, Bigenwald C, et al. Innate Immune Landscape in Early Lung Adenocarcinoma by Paired Single-Cell Analyses. *Cell* (2017) 169(4):750–65.e17. doi: 10.1016/j.cell.2017.04.014
43. Lambrechts D, Wauters E, Boeckx B, Aibar S, Nittner D, Burton O, et al. Phenotype Molding of Stromal Cells in the Lung Tumor Microenvironment. *Nat Med* (2018) 24(8):1277–89. doi: 10.1038/s41591-018-0096-5

44. Guo X, Zhang Y, Zheng L, Zheng C, Song J, Zhang Q, et al. Global Characterization of T Cells in Non-Small-Cell Lung Cancer by Single-Cell Sequencing. *Nat Med* (2018) 24(7):978–85. doi: 10.1038/s41591-018-0045-3
45. Chen J, Tan Y, Sun F, Hou L, Zhang C, Ge T, et al. Single-Cell Transcriptome and Antigen-Immunoglobin Analysis Reveals the Diversity of B Cells in Non-Small Cell Lung Cancer. *Genome Biol* (2020) 21(1):152. doi: 10.1186/s13059-020-02064-6
46. Casanova-Acebes M, Dalla E, Leader AM, LeBerichel J, Nikolic J, Morales BM, et al. Tissue-Resident Macrophages Provide a Pro-Tumorigenic Niche to Early NSCLC Cells. *Nature* (2021) 595(7868):578–84. doi: 10.1038/s41586-021-03651-8
47. Chen Z, Huang Y, Hu Z, Zhao M, Li M, Bi G, et al. Landscape and Dynamics of Single Tumor and Immune Cells in Early and Advanced-Stage Lung Adenocarcinoma. *Clin Transl Med* (2021) 11(3):e350. doi: 10.1002/ctm2.350
48. Nasim F, Sabath BF, Eapen GA. Lung Cancer. *Med Clin North Am* (2019) 103(3):463–73. doi: 10.1016/j.mcna.2018.12.006
49. Schreiber RD, Old LJ, Smyth MJ. Cancer Immunoediting: Integrating Immunity's Roles in Cancer Suppression and Promotion. *Science* (2011) 331(6024):1565–70. doi: 10.1126/science.1203486
50. Rosenthal R, Cadieux EL, Salgado R, Bakir MA, Moore DA, Hiley CT, et al. Neoantigen-Directed Immune Escape in Lung Cancer Evolution. *Nature* (2019) 567(7749):479–85. doi: 10.1038/s41586-019-1032-7
51. Vesely MD, Kershaw MH, Schreiber RD, Smyth MJ. Natural Innate and Adaptive Immunity to Cancer. *Annu Rev Immunol* (2011) 29:235–71. doi: 10.1146/annurev-immunol-031210-101324
52. Dunn GP, Old LJ, Schreiber RD. The Immunobiology of Cancer Immunosurveillance and Immunoediting. *Immunity* (2004) 21(2):137–48. doi: 10.1016/j.immuni.2004.07.017
53. Dunn GP, Bruce AT, Ikeda H, Old LJ, Schreiber RD. Cancer Immunoediting: From Immunosurveillance to Tumor Escape. *Nat Immunol* (2002) 3(11):991–8. doi: 10.1038/ni1102-991
54. Kunimasa K, Goto T. Immunosurveillance and Immunoediting of Lung Cancer: Current Perspectives and Challenges. *Int J Mol Sci* (2020) 21(2):597. doi: 10.3390/ijms21020597
55. Saab S, Zalzale H, Rahal Z, Khalifeh Y, Sinjab A, Kadara H. Insights Into Lung Cancer Immune-Based Biology, Prevention, and Treatment. *Front Immunol* (2020) 11(159). doi: 10.3389/fimmu.2020.00159
56. Dejima H, Hu X, Chen R, Zhang J, Zhang J. Immune Evolution From Preneoplasia to Invasive Lung Adenocarcinomas and Underlying Molecular Features. *Nat Commun* (2021) 12(1):2722. doi: 10.1038/s41467-021-22890-x
57. Singhal S, Stadanlick J, Annunziata MJ, Rao AS, Bhojnagarwala PS, O'Brien S, et al. Human Tumor-Associated Monocytes/Macrophages and Their Regulation of T Cell Responses in Early-Stage Lung Cancer. *Sci Transl Med* (2019) 11(479):eaat1500. doi: 10.1126/scitranslmed.aat1500
58. Vinay DS, Ryan EP, Pawelec G, Talib WH, Stagg J, Elkord E, et al. Immune Evasion in Cancer: Mechanistic Basis and Therapeutic Strategies. *Semin Cancer Biol* (2015) 35(Suppl):S185–98. doi: 10.1016/j.semcancer.2015.03.004
59. Zitvogel L, Tesniere A, Kroemer G. Cancer Despite Immunosurveillance: Immunoselection and Immunosubversion. *Nat Rev Immunol* (2006) 6 (10):715–27. doi: 10.1038/nri1936
60. Wiel C, Le Gal K, Ibrahim MX, Jahangir CA, Kashif M, Yao H, et al. BACH1 Stabilization by Antioxidants Stimulates Lung Cancer Metastasis. *Cell* (2019) 178(2):330–45.e22. doi: 10.1016/j.cell.2019.06.005
61. Seijo LM, Peled N, Ajona D, Boeri M, Field JK, Sozzi G, et al. Biomarkers in Lung Cancer Screening: Achievements, Promises, and Challenges. *J Thorac Oncol* (2019) 14(3):343–57. doi: 10.1016/j.jtho.2018.11.023
62. Leader AM, Grout JA, Chang C, Maier B, Tabachnikova A, Walker L, et al. *CITEseq Analysis of Non-Small-Cell Lung Cancer Lesions Reveals an Axis of Immune Cell Activation Associated With Tumor Antigen Load and TP53 Mutations*. Cold Spring Harbor Laboratory (2020).
63. Rooney MS, Shukla SA, Wu CJ, Getz G, Hacohen N. Molecular and Genetic Properties of Tumors Associated With Local Immune Cytolytic Activity. *Cell* (2015) 160(1-2):48–61. doi: 10.1016/j.cell.2014.12.033
64. Chen G, Ning B, Shi T. Single-Cell RNA-Seq Technologies and Related Computational Data Analysis. *Front Genet* (2019) 10:317. doi: 10.3389/fgene.2019.00317
65. Schiller HB, Montoro DT, Simon LM, Rawlins EL, Meyer KB, Strunz M, et al. The Human Lung Cell Atlas: A High-Resolution Reference Map of the Human Lung in Health and Disease. *Am J Respir Cell Mol Biol* (2019) 61 (1):31–41. doi: 10.1165/rcmb.2018-0416TR
66. Papalexi E, Satija R. Single-Cell RNA Sequencing to Explore Immune Cell Heterogeneity. *Nat Rev Immunol* (2018) 18(1):35–45. doi: 10.1038/nri.2017.76
67. Reyfman PA, Walter JM, Joshi N, Anekalla KR, McQuattie-Pimentel AC, Chiu S, et al. Single-Cell Transcriptomic Analysis of Human Lung Provides Insights Into the Pathobiology of Pulmonary Fibrosis. *Am J Respir Crit Care Med* (2019) 199(12):1517–36. doi: 10.1164/rccm.201712-2410OC
68. He D, Wang D, Lu P, Yang N, Xue Z, Zhu X, et al. Single-Cell RNA Sequencing Reveals Heterogeneous Tumor and Immune Cell Populations in Early-Stage Lung Adenocarcinomas Harboring EGFR Mutations. *Oncogene* (2021) 40(2):355–68. doi: 10.1038/s41388-020-01528-0
69. Bischoff P, Trinks A, Obermayer B, Pett JP, Lehmann A, Jurmeister P, et al. Single-Cell RNA Sequencing Reveals Distinct Tumor Microenvironmental Patterns in Lung Adenocarcinoma. *Oncogene* (2021). doi: 10.1038/s41388-021-02054-3
70. Batson J, Royer L, Webber J. Molecular Cross-Validation for Single-Cell RNA-Seq. *bioRxiv* (2019) 786269. doi: 10.1101/786269
71. McGranahan N, Swanton C. Clonal Heterogeneity and Tumor Evolution: Past, Present, and the Future. *Cell* (2017) 168(4):613–28. doi: 10.1016/j.cell.2017.01.018
72. Reiniger L, Téglási V, Pipek O, Rojkó L, Glasz T, Vágvölgyi A, et al. Tumor Necrosis Correlates With PD-L1 and PD-1 Expression in Lung Adenocarcinoma. *Acta Oncol* (2019) 58(8):1087–94. doi: 10.1080/0284186X.2019.1598575
73. Kerr EM, Gaude E, Turrell FK, Frezza C, Martins CP. Mutant Kras Copy Number Defines Metabolic Reprogramming and Therapeutic Susceptibilities. *Nature* (2016) 531(7592):110–3. doi: 10.1038/nature16967
74. Ciabatti S, Cammelli S, Frakulli R, Arcelli A, Macchia G, Deodato F, et al. Radiotherapy of Pancreatic Cancer in Older Patients: A Systematic Review. *J Geriatr Oncol* (2019) 10(4):534–9. doi: 10.1016/j.jgo.2018.09.007
75. Schumacher TN, Schreiber RD. Neoantigens in Cancer Immunotherapy. *Science* (2015) 348(6230):69–74. doi: 10.1126/science.aaa4971
76. Datar I, Sanmamed MF, Wang J, Henick BS, Choi J, Badri T, et al. Expression Analysis and Significance of PD-1, LAG-3, and TIM-3 in Human Non–Small Cell Lung Cancer Using Spatially Resolved and Multiparametric Single-Cell Analysis. *Clin Cancer Res* (2019) 25(15):4663–73. doi: 10.1158/1078-0432.CCR-18-4142
77. Choi M, Kadara H, Zhang J, Parra ER, Rodriguez-Canales J, Gaffney SG, et al. Mutation Profiles in Early-Stage Lung Squamous Cell Carcinoma With Clinical Follow-Up and Correlation With Markers of Immune Function. *Ann Oncol* (2017) 28(1):83–9. doi: 10.1093/annonc/mdw437
78. McGranahan N, Furness AJS, Rosenthal R, Ramskov S, Lyngaa R, Saini SK, et al. Clonal Neoantigens Elicit T Cell Immunoreactivity and Sensitivity to Immune Checkpoint Blockade. *Science* (2016) 351(6280):1463–9. doi: 10.1126/science.aaf1490
79. Shi X, Chakraborty P, Chaudhuri A. Unmasking Tumor Heterogeneity and Clonal Evolution by Single-Cell Analysis. *J Cancer Metastasis Treat* (2018) 4:47. doi: 10.20517/2394-4722.2018.32
80. Turajlic S, Sottoriva A, Graham T, Swanton C. Resolving Genetic Heterogeneity in Cancer. *Nat Rev Genet* (2019) 20(7):404–16. doi: 10.1038/s41576-019-0114-6
81. Rizvi NA, Hellmann MD, Snyder A, Kvistborg P, Makarov V, Havel JJ, et al. Mutational Landscape Determines Sensitivity to PD-1 Blockade in Non–Small Cell Lung Cancer. *Science* (2015) 348(6230):124–8. doi: 10.1126/science.aaa1348
82. Leung ML, Davis A, Gao R, Casasent A, Wang Y, Sei E, et al. Single-Cell DNA Sequencing Reveals a Late-Dissemination Model in Metastatic Colorectal Cancer. *Genome Res* (2017) 27(8):1287–99. doi: 10.1101/gr.209973.116
83. Baslan T, Kendall J, Rodgers L, Cox H, Riggs M, Stepansky A, et al. Genome-Wide Copy Number Analysis of Single Cells. *Nat Protoc* (2012) 7(6):1024–41. doi: 10.1038/nprot.2012.039
84. Darılmaz Yüce G, Ortaç Ersoy E. [Lung Cancer and Epigenetic Modifications]. *Tuberk Toraks* (2016) 64(2):163–70. doi: 10.5578/tt.10231
85. Duruisseaux M, Esteller M. Lung Cancer Epigenetics: From Knowledge to Applications. *Semin Cancer Biol* (2018) 51:116–28. doi: 10.1016/j.semcancer.2017.09.005

86. Yuan G, Flores NM, Hausmann S, Lofgren SM, Kharchenko V, Angulo-Ibanez M, et al. Elevated NSD3 Histone Methylation Activity Drives Squamous Cell Lung Cancer. *Nature* (2021) 590(7846):504–8. doi: 10.1038/s41586-020-03170-y
87. Mehta A, Dobersch S, Romero-Olmedo AJ, Barreto G. Epigenetics in Lung Cancer Diagnosis and Therapy. *Cancer Metastasis Rev* (2015) 34(2):229–41. doi: 10.1007/s10555-015-9563-3
88. Franco F, Jaccard A, Romero P, Yu YR, Ho PC. Metabolic and Epigenetic Regulation of T-Cell Exhaustion. *Nat Metab* (2020) 2(10):1001–12. doi: 10.1038/s42255-020-00280-9
89. Kommalapati A, Tanvetyanon T. Epigenetic Modulation of Immunotherapy Cofactors to Enhance Tumor Response in Lung Cancer. *Hum Vaccines Immunotherapeut* (2021) 17(1):51–4. doi: 10.1080/21645515.2020.1764273
90. Cui Z, Cui Y, Gao Y, Jiang T, Zang T, Wang Y. Enhancement and Imputation of Peak Signal Enables Accurate Cell-Type Classification in scATAC-Seq. *Front Genet* (2021) 12:658352. doi: 10.3389/fgene.2021.658352
91. Ku WL, Nakamura K, Gao W, Cui K, Hu G, Tang Q, et al. Single-Cell Chromatin Immunocleavage Sequencing (Scchic-Seq) to Profile Histone Modification. *Nat Methods* (2019) 16(4):323–5. doi: 10.1038/s41592-019-0361-7
92. Ramani V, Deng X, Qiu R, Gunderson KL, Steemers FJ, Disteche CM, et al. Massively Multiplex Single-Cell Hi-C. *Nat Methods* (2017) 14(3):263–6. doi: 10.1038/nmeth.4155
93. Bartosovic M, Kabbe M, Castelo-Branco G. Single-Cell CUT&Tag Profiles Histone Modifications and Transcription Factors in Complex Tissues. *Nat Biotechnol* (2021) 39(7):825–35. doi: 10.1038/s41587-021-00869-9
94. Buenrostro JD, Wu B, Litzenburger UM, Ruff D, Gonzales ML, Snyder MP, et al. Single-Cell Chromatin Accessibility Reveals Principles of Regulatory Variation. *Nature* (2015) 523(7561):486–90. doi: 10.1038/nature14590
95. Lee D-S, Luo C, Zhou J, Chandran S, Rivkin A, Bartlett A, et al. Simultaneous Profiling of 3D Genome Structure and DNA Methylation in Single Human Cells. *Nat Methods* (2019) 16(10):999–1006. doi: 10.1038/s41592-019-0547-z
96. Gu H, Raman AT, Wang X, Gaiti F, Chaligne R, Mohammad AW, et al. Smart-RRBS for Single-Cell Methylome and Transcriptome Analysis. *Nat Protoc* (2021) 16(8):4004–30. doi: 10.1038/s41596-021-00571-9
97. Nigro E, Imperlini E, Scudiero O, Monaco ML, Polito R, Mazzarella G, et al. Differentially Expressed and Activated Proteins Associated With Non Small Cell Lung Cancer Tissues. *Respir Res* (2015) 16(1):74. doi: 10.1186/s12931-015-0234-2
98. Kelly RT. Single-Cell Proteomics: Progress and Prospects. *Mol Cell Proteomics* (2020) 19(11):1739–48. doi: 10.1074/mcp.R120.002234
99. Rahman AH, Lavin Y, Kobayashi S, Leader A, Merad M. High-Dimensional Single Cell Mapping of Cerium Distribution in the Lung Immune Microenvironment of an Active Smoker. *Cytomet B Clin Cytom* (2018) 94 (6):941–5. doi: 10.1002/cyto.b.21545
100. Dou M, Clair G, Tsai CF, Xu K, Chrisler WB, Sontag RL, et al. High-Throughput Single Cell Proteomics Enabled by Multiplex Isobaric Labeling in a Nanodroplet Sample Preparation Platform. *Anal Chem* (2019) 91 (20):13119–27. doi: 10.1021/acs.analchem.9b03349
101. Lin CC, Huang WL, Su WP, Chen HH, Lai WW, Yan JJ, et al. Single Cell Phospho-Specific Flow Cytometry can Detect Dynamic Changes of Phospho-Stat1 Level in Lung Cancer Cells. *Cytomet A* (2010) 77(11):1008–19. doi: 10.1002/cyto.a.20965
102. O'Neill LAJ, Pearce EJ. Immunometabolism Governs Dendritic Cell and Macrophage Function. *J Exp Med* (2016) 213(1):15–23. doi: 10.1084/jem.20151570
103. Weber GF. Metabolism in Cancer Metastasis. *Int J Cancer* (2016) 138 (9):2061–6. doi: 10.1002/ijc.29839
104. Schmidt DR, Patel R, Kirsch DG, Lewis CA, Vander Heiden MG, Locasale JW. Metabolomics in Cancer Research and Emerging Applications in Clinical Oncology. *CA: A Cancer J Clin* (2021) 71(4):333–58. doi: 10.3322/caac.21670
105. Bergers G, Fendt S-M. The Metabolism of Cancer Cells During Metastasis. *Nat Rev Cancer* (2021) 21:162–80. doi: 10.1038/s41568-020-00320-2
106. Leone RD, Powell JD. Metabolism of Immune Cells in Cancer. *Nat Rev Cancer* (2020) 20(9):516–31. doi: 10.1038/s41568-020-0273-y
107. Huang H, Zhou P, Wei J, Long L, Shi H, Dhungana Y, et al. *In Vivo* CRISPR Screening Reveals Nutrient Signaling Processes Underpinning CD8+ T Cell Fate Decisions. *Cell* (2021) 184(5):1245–61.e21. doi: 10.1016/j.cell.2021.02.021
108. Zappasodi R, Serganova I, Cohen IJ, Maeda M, Shindo M, Senbabaoglu Y, et al. CTLA-4 Blockade Drives Loss of Treg Stability in Glycolysis-Low Tumours. *Nature* (2021) 591(7851):652–8. doi: 10.1038/s41586-021-03326-4
109. Shrestha B. *Ten Major Future Challenges in Single-Cell Metabolomics, in Single Cell Metabolism: Methods and Protocols*. B Shrestha, editor. New York, NY: Springer New York (2020) p. 219–23.
110. Evers TMJ, Hochane M, Tans SJ, Heeren RMA, Semrau S, Nemes P, et al. Deciphering Metabolic Heterogeneity by Single-Cell Analysis. *Analytical Chem* (2019) 91(21):13314–23. doi: 10.1021/acs.analchem.9b02410
111. Arguello RJ, Combes AJ, Char R, Gigan JP, Baaziz AI, Bousiquot E, et al. SCENITH: A Flow Cytometry-Based Method to Functionally Profile Energy Metabolism With Single-Cell Resolution. *Cell Metab* (2020) 32(6):1063–.e7. doi: 10.1016/j.cmet.2020.11.007
112. Vodnala SK, Eil R, Kishton RJ, Sukumar M, Yamamoto TN, Ha NH, et al. T Cell Stemness and Dysfunction in Tumors Are Triggered by a Common Mechanism. *Science* (2019) 363(6434):eaau0135. doi: 10.1126/science.aau0135
113. Depeaux K, Delgoffe GM. Metabolic Barriers to Cancer Immunotherapy. *Nat Rev Immunol* (2021) 21:785–97. doi: 10.1038/s41577-021-00541-y
114. Sheng N, Li Y, Qian R, Li Y. The Clinical Significance and Biological Function of lncRNA RGMB-AS1 in Hepatocellular Carcinoma. *BioMed Pharmacother* (2018) 98:577–84. doi: 10.1016/j.biopha.2017.12.067
115. Hu KH, Eichorst JP, McGinnis CS, Patterson DM, Chow ED, Kersten K, et al. ZipSeq: Barcoding for Real-Time Mapping of Single Cell Transcriptomes. *Nat Methods* (2020) 17(8):833–43. doi: 10.1101/2020.02.04.932988
116. Wu SS, Lee JH, Koo BK. Lineage Tracing: Computational Reconstruction Goes Beyond the Limit of Imaging. *Mol Cells* (2019) 42(2):104–12. doi: 10.14348/molcells.2019.0006
117. Wagner DE, Weinreb C, Collins ZM, Briggs JA, Megason SG, Klein AM. Single-Cell Mapping of Gene Expression Landscapes and Lineage in the Zebrafish Embryo. *Science* (2018) 360(6392):981–7. doi: 10.1126/science.aar4362
118. Figueres-Oñate M, Sánchez-Villalón M, Sánchez-González R, López-Mascaraque L. Lineage Tracing and Cell Potential of Postnatal Single Progenitor Cells *In Vivo*. *Stem Cell Rep* (2019) 13(4):700–12. doi: 10.1016/j.stemcr.2019.08.010
119. Praktiknjo SD, Obermayer B, Zhu Q, Fang L, Liu H, Quinn H, et al. Tracing Tumorigenesis in a Solid Tumor Model at Single-Cell Resolution. *Nat Commun* (2020) 11(1):991. doi: 10.1038/s41467-020-14777-0
120. Zepp JA, Zacharias WJ, Frank DB, Cavanaugh CA, Zhou S, Morley MP, et al. Distinct Mesenchymal Lineages and Niches Promote Epithelial Self-Renewal and Myofibrogenesis in the Lung. *Cell* (2017) 170(6):1134–48.e10. doi: 10.1016/j.cell.2017.07.034
121. Wellenstein MD, de Visser KE. Cancer-Cell-Intrinsic Mechanisms Shaping the Tumor Immune Landscape. *Immunity* (2018) 48(3):399–416. doi: 10.1016/j.immuni.2018.03.004
122. Wagner DE, Klein AM. Lineage Tracing Meets Single-Cell Omics: Opportunities and Challenges. *Nat Rev Genet* (2020) 21(7):410–27. doi: 10.1038/s41576-020-0223-2
123. Liu Q, Liu K, Cui G, Huang X, Yao S, Guo W, et al. Lung Regeneration by Multipotent Stem Cells Residing at the Bronchioalveolar-Duct Junction. *Nat Genet* (2019) 51(4):728–38. doi: 10.1038/s41588-019-0346-6
124. Lein E, Borm LE, Linnarsson S. The Promise of Spatial Transcriptomics for Neuroscience in the Era of Molecular Cell Typing. *Science* (2017) 358 (6359):64–9. doi: 10.1126/science.aan6827
125. De Bruin EC, McGranahan N, Mitter R, Salm M, Wedge DC, Yates L, et al. Spatial and Temporal Diversity in Genomic Instability Processes Defines Lung Cancer Evolution. *Science* (2014) 346(6206):251–6. doi: 10.1126/science.1253462
126. Moor AE, Itzkovitz S. Spatial Transcriptomics: Paving the Way for Tissue-Level Systems Biology. *Curr Opin Biotechnol* (2017) 46:126–33. doi: 10.1016/j.copbio.2017.02.004
127. Baccin C, Al-Sabah J, Velten L, Helbling PM, Grünschläger F, Hernández-Malmierca P, et al. Combined Single-Cell and Spatial Transcriptomics Reveal the Molecular, Cellular and Spatial Bone Marrow Niche Organization. *Nat Cell Biol* (2020) 22(1):38–48. doi: 10.1038/s41556-019-0439-6
128. Wang X, Allen WE, Wright MA, Sylwestrak EL, Samusik N, Vesuna S, et al. Three-Dimensional Intact-Tissue Sequencing of Single-Cell Transcriptional States. *Science* (2018) 361(6400):eaat5691. doi: 10.1126/science.aat5691
129. Kumar MP, Du J, Lagoudas G, Jiao Y, Sawyer A, Drummond DC, et al. Analysis of Single-Cell RNA-Seq Identifies Cell-Cell Communication

Associated With Tumor Characteristics. *Cell Rep* (2018) 25(6):1458–68.e4. doi: 10.1016/j.celrep.2018.10.047
130. Zhang L, Mao S, Yao M, Chao N, Yang Y, Ni Y, et al. Spatial transcriptome sequencing revealed spatial trajectory in the Non-Small Cell Lung Carcinoma. *bioRxiv* (2021) 2021.04.26.441394. doi: 10.1101/2021.04.26.441394
131. Mascaux C, Angelova M, Vasaturo A, Beane J, Hijazi K, Anthoine G, et al. Immune Evasion Before Tumour Invasion in Early Lung Squamous Carcinogenesis. *Nature* (2019) 571(7766):570–5. doi: 10.1038/s41586-019-1330-0
132. Meng L, Jiang X, Liang J, Pan Y, Pan F, Liu D. Postoperative Psychological Stress and Expression of Stress-Related Factors HSP70 and IFN-γ in Patients With Early Lung Cancer. *Minerva Med* (2020). doi: 10.23736/S0026-4806.20.06658-6
133. Eruslanov EB, Bhojnagarwala PS, Quatromoni JG, Stephen TL, Ranganathan A, Deshpande C, et al. Tumor-Associated Neutrophils Stimulate T Cell Responses in Early-Stage Human Lung Cancer. *J Clin Invest* (2014) 124 (12):5466–80. doi: 10.1172/JCI77053
134. Laughney AM, Hu J, Campbell NR, Bakhoum SF, Setty M, Lavallee VP, et al. Regenerative Lineages and Immune-Mediated Pruning in Lung Cancer Metastasis. *Nat Med* (2020) 26(2):259–69. doi: 10.1038/s41591-019-0750-6
135. Beaumont KG, Beaumont MA, Sebra R. Application of Single-Cell Sequencing to Immunotherapy. *Urol Clin North Am* (2020) 47(4):475–85. doi: 10.1016/j.ucl.2020.07.005

Conflict of Interest: The authors declare that the research was conducted in the absence of any commercial or financial relationships that could be construed as a potential conflict of interest.

Publisher's Note: All claims expressed in this article are solely those of the authors and do not necessarily represent those of their affiliated organizations, or those of the publisher, the editors and the reviewers. Any product that may be evaluated in this article, or claim that may be made by its manufacturer, is not guaranteed or endorsed by the publisher.

Advantages of publishing in Frontiers

OPEN ACCESS
Articles are free to read for greatest visibility and readership

FAST PUBLICATION
Around 90 days from submission to decision

HIGH QUALITY PEER-REVIEW
Rigorous, collaborative, and constructive peer-review

TRANSPARENT PEER-REVIEW
Editors and reviewers acknowledged by name on published articles

Frontiers
Avenue du Tribunal-Fédéral 34
1005 Lausanne | Switzerland

Visit us: www.frontiersin.org
Contact us: frontiersin.org/about/contact

REPRODUCIBILITY OF RESEARCH
Support open data and methods to enhance research reproducibility

DIGITAL PUBLISHING
Articles designed for optimal readership across devices

FOLLOW US
@frontiersin

IMPACT METRICS
Advanced article metrics track visibility across digital media

EXTENSIVE PROMOTION
Marketing and promotion of impactful research

LOOP RESEARCH NETWORK
Our network increases your article's readership